Investigation into thermal adaptation mechanisms of *Streptococcus pneumoniae* and its impact on pneumococcal pathogenicity

Thesis submitted for the degree of

Doctor of Philosophy at the

University of Leicester

Ozcan Gazioglu

Department of Respiratory Sciences

University of Leicester

August 2019

Statement of originality

This accompanying thesis submitted for the degree of PhD entitled "**Investigation into thermal adaptation mechanisms of *Streptococcus pneumoniae* and its impact on pneumococcal pathogenicity**" is based on work conducted by the author in the Department of Respiratory Sciences of the University of Leicester during the period between September 2015 and September 2018.

All the work recorded in this thesis is original unless otherwise acknowledge in the text or by references.

None of this work has been submitted for another degree in this or any other University.

Signed …… Date ……

Investigation into thermal adaptation mechanisms of *Streptococcus pneumoniae* and its impact on pneumococcal pathogenicity

Ozcan Gazioglu

Abstract

Temperature is a critical and ubiquitous environmental signal that influences the growth, virulence, and survival of diverse microbial species. The human pathogen *Streptococcus pneumoniae* is a commensal microorganism, whose ecological niche is the human nasopharynx, and becomes pathogenic after spreading to other niches such as lung, blood stream, or brain. During progression from colonisation to invasion, the pneumococcus must contend with temperature fluctuations that can influence its phenotypic character. This study demonstrated that temperature has a significant impact on pneumococcal phenotype, such as growth, biofilm formation, metabolism, and virulence factor generation. To understand the thermal adaptation mechanisms employed by this microbe, the pneumococcal transcriptome was obtained by microarray analysis at 34°C, 37°C, or 40°C. The analysis showed that 6% (132) and 5% (120) of genes were differentially expressed at 34ºC and 40ºC, respectively, at mid-exponential growth phase by 2-fold relative to the expression at 37ºC. Interestingly, the genes upregulated in one temperature were downregulated at another temperature. For further analysis, I selected seven genes (*gdhA, ciaR, comD, merR*^{2}, *SPD_0132/0133, SPD_1711,* and *SPD_1651*) that were expressed differentially at different temperatures and characterized the mutants using different experimental techniques such as growth profile analysis, cell size measurement, biofilm formation, capsule synthesis, and for the production of virulence proteins. I found that loss of the selected genes led to attenuation at 40°C in all assays comparing to the wild type strain. It was particularly interesting to find that glutamate dehydrogenase (*gdhA*, SPD_1158) is highly active at 40°C rather than 34°C, suggesting that GdhA is a thermostable protein. *In vivo* analysis showed that *gdhA*-null strain grown at 40°C was less virulent in *G. mellonella* acute infection model, indicating that GdhA is required for pneumococcal virulence at high temperatures. In conclusion, temperature fluctuation has impact on transcriptional and phenotypic profiles of *S. pneumoniae.*

Acknowledgement

I would like to thank my supervisors Dr. Hasan Yesilkaya and Professor Peter Andrew for their intellectual and scientific support throughout this study. I cannot find words to thank Dr. Hasan Yesilkaya for his support, encouragement, patience, and critical reading of this thesis. Thank you for believing in me and for always pushing me. I would also like to extend my gratitude to Professor Peter Andrew for scientific suggestions, advises, and guidance throughout this study.

I would like to thank my panel members Dr. Cordula Stover and Dr. Manish Pareek for their valuable advices during my study.

I would also like to thank my colleagues Iman Abdullah, Banaz Kareem, Shamam Al-Husseini, Mohammed Imam, and Giannis Koukkidis, and the members of lab 125 and 213 for their friendship.

I dedicate this thesis to my beloved family. Words are never enough to express my sincere thanks and appreciation for your endless love, support and best wishes. Without their support, I would not be able to finish this thesis.

Table of Contents

Abstract ..... **i**
Acknowledgement ..... **ii**
Table of Contents ..... **iii**
List of Figures ..... **vii**
List of Tables ..... **ix**
Abbreviations ..... **x**
Chapter 1 Introduction **1**
1.1 Pneumococcal biology 1
1.2 Pneumococcal colonisation 2
1.3 Pneumococcal invasion 6
1.4 Host immune response to pneumococcal infection 12
1.5 Antibiotic resistance and treatment of pneumococcal diseases 14
1.6 Pneumococcal adaptation to host environment 15
1.6.1 Sugar metabolism 16
1.6.2 Oxidative stress 17
1.6.3 Metal homeostasis 18
1.6.4 Acid tolerance 19
1.7 Temperature stress 20
1.8 Microbial thermosensors 25
1.8.1 Thermosensing at DNA level 25
1.8.2 Thermosensing at RNA level 27
1.8.3 Thermosensing at protein level 29
1.8.4 Thermosensing at lipid and membrane fluidity level 31
1.9 Aims of the study 32
Chapter 2 Materials and Methods **34**
2.1 Bacterial strains and plasmids 34
2.2 Bacterial growth conditions and media 36
2.3 Preparation of frozen bacterial stocks 38
2.4 Colony forming unit counts 38
2.5 Growth studies in BHI and CDM medium 39
2.6 DNA extraction 39

2.6.1 Extraction of D39 chromosomal DNA....39
2.6.2 Extraction of plasmid DNA from *E. coli* 40
2.7 Polymerase Chain Reaction (PCR)....41
2.8 Electrophoresis....41
2.9 Restriction digestion of amplified DNA....42
2.10 DNA ligation reaction....42
2.11 Genetic transformation of DNA....43
2.11.1 Transformation into *E. coli* 43
2.11.2 Transformation into *S. pneumoniae* 43
2.12 Mutagenesis....43
2.12.1 Gene splicing overlap extension PCR (SOEing PCR)....43
2.12.2 Amplification of SOEing fragments and antibiotic resistance cassette 44
2.12.3 Fusion of SOEing fragments and transformation into *S. pneumoniae* 46
2.12.4 Confirmation of gene deletion/replacement with antibiotic cassette 47
2.13 Genetic complementation of mutant strains 48
2.13.1 Transformation of modified pCEP plasmid into *E. coli*....49
2.13.2 Transformation of modified pCEP plasmid into the mutant strain 50
2.14 Construction of *lacZ* fusions and transformation into *E. coli*....50
2.14.1 Transformation of recombinant plasmid into *S. pneumoniae* 51
2.14.2 β-galactosidase activity assay 52
2.15 Enzyme assays 53
2.15.1 Preparing cell lysates by sonication 53
2.15.2 Quantification of protein concentration-Bradford assay....54
2.15.3 Haemolytic assay 54
2.15.4 Neuraminidase assay....54
2.16 Biofilm formation assay....55
2.17 Glucuronic acid assay 55
2.18 Determination of cell size....56
2.19 Growth studies on nitrogen-source medium....56
2.20 Glutamate dehydrogenase enzyme activity assay....57
2.21 *In vitro* survival assay at different pH conditions....58
2.22 Fermentation end product analysis during growth at different temperatures 59
2.22.1 Measuring the concentration of L-lactic acid....60
2.22.2 Measuring the concentration of formic acid 61
2.22.3 Measuring the concentration of acetic acid....62

2.23 *In vivo* studies 63
2.23.1 Bacterial inoculum preparation 63
2.23.2 *Galleria mellonella* model of pneumococcal infection 64
2.24 Statistical analysis 64
Chapter 3 Results 65
3.1 Part A: Thermophysiology of *S. pneumoniae* D39 at different temperatures 65
3.2 Growth behaviour of D39 changes with temperature shifts 65
3.2.1 Growth in BHI 65
3.2.2 Growth at different temperatures in CDM supplemented with 55 mM glucose 67
3.3 Temperature has impact on pneumococcal cell size 68
3.4 Haemolysis differs at different temperatures in pneumococcus 71
3.5 Neuraminidase activity is influenced by temperature changes in pneumococcus 73
3.6 Pneumococcal biofilm formation is affected by temperature 75
3.7 Pneumococcal capsule production changes with temperature 76
3.8 Part B. Microarray analysis of pneumococcal genes 78
3.8.1 Screening of temperature-induced operons 82
3.8.2 Motif search in transcriptionally altered genes at different temperatures 86
3.9 Part C: Construction of isogenic mutants 90
3.9.1 Selection of targets to study their possible involvement for pneumococcal thermal adaptation 91
3.10 Mutagenesis by gene splicing overlap extension PCR (SOEing PCR) 97
3.11 Amplification of SOEing flanks and antibiotic cassette *aadA* 99
3.12 Fusion of SOEing fragments and transformation into D39 101
3.13 Confirmation of mutagenesis 102
3.14 Part D: Temperature-dependent phenotypic characterisation of pneumococcal mutant strains 106
3.15 Growth behaviour of pneumococcal strains in CDM medium 106
3.16 Cell size determination of pneumococcal strains in CDM medium 109
3.17 Involvement of selected genes on assessing of virulence factors 111
3.17.1 Determining the haemolytic activity 111
3.17.2 Determining the neuraminidase activity 113
3.18 Biofilm formation of pneumococcal mutant strains 115
3.19 Determination of capsule level of pneumococcal mutant strains 117
3.20 Part E: Construction of reporter strains and temperature-dependent gene expression analysis (β-galactosidase assays) 119

3.21 Construction of reporter strain in proxy of *lacZ* gene 119
3.21.1 Identification of putative promoter regions of target genes 121
3.21.2 Preparation of insert/vector fragments for reporter constructs 123
3.21.3 Transformation of transcriptional reporter strain into *S. pneumoniae* 124
3.21.4 Expression of transcriptional *lacZ*-fusions at different temperatures 126
3.22 Part F: Glutamate dehydrogenase is required at high temperature 127
3.23 Characterization of glutamate dehydrogenase 128
3.24 Regulation of glutamine/glutamate metabolism in *S. pneumoniae* 129
3.25 Genetic complementation of *gdhA* mutant strain 131
3.25.1 Preparation of pCEP for complementation 132
3.25.2 Amplification of GdhA for complementation 133
3.25.3 Integration of recombinant pCEP construct into Δ*gdhA* strain 134
3.26 Additional phenotypic characterization of Δ*gdhA* mutant strain 135
3.26.1 Growth profile of GdhA is temperature- and nitrogen source-dependent 135
3.26.2 Glutamate dehydrogenase is more active at higher temperature 140
3.26.3 Inactivation of GdhA reduces the pH homeostasis in response to temperature shift 142
3.26.4 Temperature changes the formation of fermentation end products 144
3.27 *In vivo* virulence studies 146
3.27.1 *Galleria mellonella* – a novel bacterial infection model 146
3.27.2 Determination of median lethal dose (LD_{50}) of *S. pneumoniae* 147
Chapter 4 Discussion 152
4.1 Temperature alters phenotype of *S. pneumoniae* D39 153
4.2 Temperature alters the pneumococcal transcriptome 163
4.3 GdhA is required for high temperature adaptation of *S. pneumoniae* D39 166
Final remarks 170
Future plan 171
Appendix A 173
Bibliography 178

List of Figures

Figure 1.1. Progression of pneumococcal infections. 7
Figure 1.2. Pneumococcal virulence factors. 12
Figure 1.3. Illustration of DNA-dependent thermoregulation mechanisms. 27
Figure 1.4. Illustration of RNA thermometers. 29
Figure 1.5. Illustration of protein thermometers. 31

Figure 2.1. The schematic illustration of β-galactosidase assay. 52

Figure 3.1. The growth profile of wild type D39 in BHI under micro-aerobic condition at 34°C, 37°C, or 40°C. 66
Figure 3.2. The growth of wild type D39 in CDM supplemented with 55 mM glucose under micro-aerobic condition at 34°C, 37°C, or 40°C. 67
Figure 3.3. The cell size of wild type D39 grown in BHI (A) or CDM supplemented with 55 mM glucose (B) at 34°C, 37°C, or 40°C. 70
Figure 3.4. The haemolytic activity of wild type D39 grown in BHI (A) or CDM supplemented with 55 mM glucose (B) at 34°C, 37°C, or 40°C. 72
Figure 3.5. The neuraminidase activity of wild type D39 grown in BHI (A) or CDM supplemented with 55 mM glucose (B) at 34°C, 37°C, or 40°C. 74
Figure 3.6. The biofilm formation of wild type D39 grown in THY medium at 34°C, 37°C, or 40°C 76
Figure 3.7. The glucuronic acid concentration of wild type D39 grown in BHI (A) or CDM supplemented with 55 mM glucose (B) at 34°C, 37°C, or 40°C. 77
Figure 3.8. Venn diagram highlighting relative transcript levels of genes in *S. pneumoniae* at 34ºC and 40ºC during mid- or late-exponential growth phase. 78
Figure 3.9. Functional categories of differentially expressed genes at mid- and late-exponential growth phases in response to temperature shifts. 81
Figure 3.10. Schematic representation of allelic replacement mutagenesis (SOEing PCR) and homologous recombination in *S. pneumoniae*. 98
Figure 3.11. The image of agarose gel electrophoresis analysis showing the amplified antibiotic resistance gene, and the flanking regions of each target gene. 100
Figure 3.12. The image of agarose gel electrophoresis analysis showing the fused SOEing fragments which are approximately 2758 bp. 101
Figure 3.13. Illustration of mutation confirmation strategy. 102
Figure 3.14. Successful integration of recombinant SOEing products into D39 genome. 105
Figure 3.15. Pneumococcal growth curves performed in CDM supplemented with 55 mM glucose at 34°C (A), 37°C (B), or 40°C (C). 109
Figure 3.16. Cell sizes of pneumococcal strains grown in CDM supplemented with 55 mM glucose at different temperatures. 111

Figure 3.17. Determination of haemolytic activity of pneumococcal strains using cell lysate extracted from the strains grown in CDM supplemented with 55 mM glucose at 40°C. 112
Figure 3.18. Determination of neuraminidase activity of pneumococcal strains grown in CDM supplemented with 55 mM glucose at 34°C (A), 37°C (B), or 40°C (B). 114
Figure 3.19. Biofilm formations of pneumococcal strains grown in THY medium at 34°C (A), 37°C (B), or 40°C (C). 117
Figure 3.20. The glucuronic acid concentration from capsules of pneumococcal strains grown in CDM medium supplemented with glucose at 34°C (A), 37°C (B), or 40°C (C). 119
Figure 3.21. Illustration of the integrative promoter probe plasmid pPP2. 120
Figure 3.22. Intergenic region maps and upstream sequence of *GdhA* (1), *CiaR* (2), *ComD* (3), *MerR*^{2} (4), *SPD_0132/133* (5), *SPD_1711* (6), and *SPD_1651* (7). 123
Figure 3.23. The images of agarose gel electrophoresis analysis showing the amplified promoter regions and pPP2 plasmid. 124
Figure 3.24. The images of agarose gel electrophoresis analysis confirming the successful transformation of reporter constructs into D39 wild type strain. 125
Figure 3.25. Nitrogen metabolism and the assimilation of ammonium..... 129
Figure 3.26. The pneumococcal GlnR regulon. 130
Figure 3.27. Genetic map of pCEP. 132
Figure 3.28. Agarose gel electrophoresis analysis showing the integration of *gdhA* with their putative promoter regions into pCEP. 133
Figure 3.29. Illustration showing the strategy to confirm complementation. 134
Figure 3.30. The image of agarose gel electrophoresis confirming the successful integration of insert carrying the intact copy of *gdhA* with its putative promoter within the pneumococcal genome of Δ*gdhA*. 135
Figure 3.31. Temperature- and nitrogen source-dependent growth of pneumococcal strains. 138
Figure 3.32. Glutamate dehydrogenase activity in D39, complemented mutant strain and its isogenic pneumococcal glutamate dehydrogenase mutants in D39 at 34°C, 37°C, or 40°C. 141
Figure 3.33. Acidity tolerance of D39 (wt) and Δ*gdhA* strains at 34°C, 37°C, or 40°C. 143
Figure 3.34. The specific production rate of lactate, formate, and acetate in D39 (wt), Comp*ΔgdhA* and Δ*gdhA* strains at 34°C, 37°C, or 40°C. 145
Figure 3.35. Photographic image of larvae and health score. 147
Figure 3.36. Log10 LD_{50} for *G. mellonella* after 24 hr post infection..... 149
Figure 3.37. Images of *G. mellonella* after 24 hr post infection. 150
Figure 3.38. Mortality number of *G. mellonella*..... 151

List of Tables

Table 1.1. Selected pneumococcal virulence factors and their contributions to pneumococcal infection. 11

Table 2.1. Bacterial strains and plasmids. 34
Table 2.2. Composition of CDM used for growth of pneumococcal strains. 37
Table 2.3. The list of primers used for SOEing mutagenesis. 45
Table 2.4. The list of primers used for confirmation of mutagenesis. 48
Table 2.5. The list of primers used for genetic complementation. 49
Table 2.6. The list of primers used for the construction of *lacZ*-fusions. 51
Table 2.7. The composition of buffers used to adjust culture pH. 59

Table 3.1. Growth rate (μ) and yield (maximal OD_{600nm}) of pneumococcal strain grown in BHI at 34°C, 37°C, or 40°C. 66
Table 3.2. Growth rate (μ) and yield (maximal OD_{600nm}) of pneumococcal strain grown micro-aerobically in CDM with 55 mM glucose at 34°C, 37°C, or 40°C. 68
Table 3.3. The cell size of pneumococcal strain grown micro-aerobically in BHI and CDM supplemented with glucose at 34°C, 37°C, or 40°C. 69
Table 3.4. Operons up- or downregulated at 34ºC or 40ºC relative to 37ºC. 83
Table 3.5. Fold change of target genes at 34ºC or 40ºC, relative to 37ºC. 91
Table 3.6. Growth rate (h^{-1}) and yield (OD_{600nm}) of pneumococcal strains grown in CDM supplemented with 55 mM glucose at 34°C, 37°C, or 40°C. 107
Table 3.7. Cell sizes of pneumococcal strains grown in CDM supplemented with 55 mM glucose at 34°C, 37°C, or 40°C. 110
Table 3.8. Expression levels of pneumococcal transcriptional *lacZ* fusions to the promoters of target genes grown in CDM supplemented with 55 mM of glucose at different temperatures. 127
Table 3.9. Temperature- and nitrogen source-dependent growth rate (h^{-1}) (A) and growth yield (B) of the wild type and Δ*gdhA* strains. 140

Abbreviations

BAB - Blood Agar Base	**µg -** Microgram
BHI - Brain heart infusion	**µM -** Micromolar
bp - Base pair	**mM -** Millimolar
BSA - Bovine serum albumin	**NADH-** Nicotinamide adenine dinucleotide
CDM - Chemically defined medium	**NADP -** Nicotinamide adenine dinucleotide phosphate
CFU - Colony forming unit	**NAD -** Nicotinamide adenine dinucleotide
CPS - capsule polysaccharide synthesis	**ONPG -** 2-Nitrophenyl β-D-galactopyranoside
CSP - Competence stimulating peptide	**OD -** Optical density
dNTP - Deoxynucleotide triphosphate	**PBS -** Phosphate buffered saline
EDTA - Ethylenediaminetetraacetic acid	**PCV -** Protein conjugate carriage
kb - Kilobase	**pNP-NANA -** 2-O-(p-nitrophenyl)-α-D-Nacetylneuraminic acid
LA- Luria agar	**PS -** Polysaccharide vaccine
LB- Luria broth	**ROS** – Reactive oxygen species
HSP - Heat shock protein	**TCS -** Two component system
HtrA - High temperature requirement A	**TF -** Transcriptional factor
mg - Milligram	**TE -**Tris/EDTA buffer
ml - Millilitre assay	**v/v -** Volume per volume

Chapter 1 Introduction

Streptococcus pneumoniae: Biology, carriage, epidemiology and pathogenesis

1.1 Pneumococcal biology

Streptococcus pneumoniae (pneumococcus) is a major human pathogen, being the leading cause of bacterial pneumonia and a major agent of meningitis and septicaemia as well as several less severe, but nevertheless debilitating, diseases such as otitis media, septic arthritis, keratitis and sinusitis (Mitchell and Mitchell, 2010). Currently, it is not known what leads to transition from colonisation to invasiveness but several microbial (expression of specialised virulence determinants and metabolic adaptation) and host factors (living conditions and host's immune status) have been implicated in this process (Henriques-Normark and Tuomanen, 2013).

The pneumococcus is a Gram-positive, non-motile, non-spore forming, and facultative anaerobic bacterium. It forms small, translucent, and flat colonies on blood agar plate and its morphology under microscope appears as short chains or lancet-shaped (Zhang *et al.*, 2006). The microbe is surrounded by a polysaccharide based capsule, which is one of the most important virulence determinants and the main ingredient of existing pneumococcal vaccines (Brooks and Mias, 2018). Based on the chemical composition of capsule, so far 97 different serotypes have been identified (Geno *et al.*, 2015). The microbe can be differentiated from other streptococci by being susceptible to ethylhydrocupreine-HCl (optochin), and by formation of α-haemolysis, which is due to incomplete haemolysis of haemoglobin and is characterised by a green colour formation around the colonies. The pneumococcus is unable to produce catalase, and it is bile soluble (Arbique *et al.*, 2004).

Streptococcus pneumoniae can grow at a wide temperature range of 25°C to 42°C, but 37°C is the optimal growth temperature for the microbe. In addition, it can tolerate a wide range of pH, from 6.5 to 8.3, and the optimal growth pH is 7.8. The pneumococcus is an oxygen tolerant anaerobic microorganism. It grows better in an atmosphere enriched with 5-10% CO_2 (Restrepo *et al.*, 2005). Fermentation of host-derived sugars is the only method of metabolic energy generation for *S. pneumoniae* because the complete set of genes for respiration could not be identified in its AT-rich genome (Yesilkaya *et al.*,

2009). The microbe is able to ferment at least 32 different sugars, and these sugars are transferred mainly by phosphotransferase systems (PTS) and ABC transporters (Bidossi *et al.*, 2012).

The complete pneumococcal genome was published in 2001 (Tettelin *et al.*, 2001). The sequence analysis showed that the microbe has a 2.16 Mbp genome with 2236 protein encoding genes and it has 40% mol GC content. The high percentage of the genes code for proteins involved in sugar uptake and metabolism (Tettelin *et al.*, 2001). Further analysis of pneumococcal genomes belonging to different lineages and serotypes showed that over twenty percent of the coding sequences of any single pneumococcal isolates are not present in all strains, but instead are part of an accessory genome unequally spread across different isolates (Donati *et al.*, 2010), very likely due to its ability to acquire foreign genetic material, also known as genetic competence (Salvadori *et al.*, 2019). However, certain genes, approximately 1600, were found to be universally present in different strains, and these well-preserved genes were suggested to form the core genome of *S. pneumoniae*, and were implicated in colonisation and virulence (Obert *et al.*, 2006).

1.2 Pneumococcal colonisation

Streptococcus pneumoniae is a resident of human upper respiratory tract (URT) flora and pneumococcal infections begin with the colonisation of nasopharynx (Hammerschmidt, 2006). Nasopharyngeal colonisation is also an important facet for direct transmission between individuals, therefore, it is important to understand the pneumococcal carriage. Infants and young children are the main reservoirs for carriage. The carriage rate in infants is at least ten times higher than in adults (Mehr and Wood, 2012) and ranges from 27% in developed countries to 85% in developing countries. Colonisation rate decreases with the age, especially after 2 years of age. This age coincides with the development of cell-mediated immunity (Brooks and Mias, 2018).

Studies have shown that pneumococcal serotype plays an important role for colonisation. Certain serotypes such as 6A, 6B, 9V, 14, and 19F are more common among young children (<5 yr), while serotypes 3 and 23F are shown to be more prevalent among adults.

The duration of pneumococcal colonisation can vary depending on the serotype. While serotypes 6 and 23 are more persistent in nasopharynx, the duration of colonisation with serotypes 9 and 14 were found to be shorter (Hogberg *et al.*, 2007; Song *et al.*, 2013). The duration of colonisation suggested to be linked to serotype interaction with microbiota in nasopharynx and the thickness of capsule (Weiser *et al.*, 2018). Interestingly, serotypes, which are prevalent among young children, have longer carriage time compare to the serogroups colonising adults.

Pneumococci reside in the nasopharynx within biofilm communities (Chao *et al.*, 2014). The role of biofilm formation during colonisation includes increased resistance to antimicrobial agents and exchange of genetic material to promote adaptation, and plays a crucial role in the events leading to transition from asymptomatic colonisation to dissemination into normally sterile niches (Marks *et al.*, 2012a). In biofilms, the pneumococci are reported to exist in phenotypically heterogeneous forms. Marks et al. (2012b) showed the phenotypic variation in biofilm in terms of bacterial signalling and virulence factor expression, and in binding to epithelial ligands in the murine nasopharynx (Marks *et al.*, 2012b).

The nasopharyngeal environment is challenging for pneumococci and this affects biofilm formation in this niche. The microbe is exposed to insults of host immune system, hence it needs to be able to adjust its metabolism for the use of different sugars in the presence of atmospheric oxygen at 34°C (Chao *et al.*, 2014). Nutrient availability may influence the biofilm formation. It was shown that the pneumococcus forms a poor biofilm in a complex nutrient environment, while it forms more structured biofilm in a nutrient-limited medium. In addition, at 32°C-34°C, pneumococci form biofilm with high biomass compared to at 37°C (Chao *et al.*, 2014).

The role of several pneumococcal factors have been shown to be important for pneumococcal colonisation. The notable ones include glycosidases, capsule, pneumolysin and surface proteins (King, 2010; Ogunniyi *et al.*, 2007). The pneumococcus has a large repertoire of glycosidases including three neuraminidases, two galactosidases, N-acetyl hexosaminidase, glycanase and hyaluronidase (Singh *et al.*, 2014). Among these,

neuraminidases play a critical role. Neuraminidases are a family of enzymes that cleave the terminal sialic acid residues from host glycans including mucin, glycolipids, and glycoproteins on the cell surface or in body fluids (Gualdi *et al.*, 2012). The neuraminidases have distinct roles on enabling exposure of the host cell-surface to mediate pneumococcal adhesion. They interfere with the process of opsonophagocytosis by desialyation of the host innate factors, initiate the release of sugars to be used as a bacterial nutrient source, and consequently are involved in biofilm formation and pathogenicity (Trappetti *et al.*, 2009; Wren *et al.*, 2017). Initial removal of terminal sialic acid is essential for further cleavage of glycans by other pneumococcal glycosidases. The pneumococcus has three neuraminidase genes, *nanA*, *nanB* and *nanC*. While *nanA* is found universally in all pneumococcal strains, *nanB* is present in 90%, and *nanC* is found in 51% of strains mainly associated with meningitis (Pettigrew *et al.*, 2006). The major pneumococcal neuraminidase activity originates from *nanA*. NanA has been shown to expose galactose and this promotes pneumococcal biofilm formation in nasopharynx (Blanchette *et al.*, 2016). *In vivo* studies reported that NanA has a major role on incidence of otitis media by degrading the sialic acid in chinchilla infection model (Tong *et al.*, 2005), and also it was shown to be important in pneumococcal survival in upper respiratory tract in a mouse model of pneumonia (Manco *et al.*, 2006). The other gene that is responsible for total pneumococcal neuraminidase activity is *nanB*. The studies done in Leicester established that NanB is also crucial for pneumococcal survival in upper respiratory tract and sepsis (Manco *et al.*, 2006). While NanC is found in just over 50% of pneumococcal strains, it is believed that the presence of this enzyme allows pneumococcal access to a wider spectrum of glycoconjugates because the substrate specificity of each neuraminidase differs, and this enhances the invasive capability of *S. pneumoniae* synergistically with NanA and NanB (Janesch *et al.*, 2018).

Streptococcus pneumoniae encodes two surface-associated β-galactosidases, BgaA and BgaC, both of which are shown to be important for the adherence of pneumococci to human epithelial cells (King *et al.*, 2006), and the colonisation of nasopharynx, respectively (Terra *et al.*, 2010). BgaA is highly specific for terminal galactose β (1-4) linked to N-acetylglucosamine (GlcNAc) (Ramakrishnan *et al.*, 2012). Unlike other microbial β-galactosidases, pneumococcal BgaA does not involve in lactose fermentation. On the other hand, BgaC has a high substrate specificity to galactose β (1-

3) linked to *N*-acetylglucosamine (GlcNAc). Both BgaA and BgaC catalyse the hydrolysis of β-galactosides of host cells to promote pneumococcal colonisation (Terra *et al.*, 2010). It has been shown that inactivation of both galactosidases diminish the total activity but did not abolish it altogether, suggesting that there may be other additional enzymes encoding β-galactosidase. Having a multiplicity of galactosidases implies that galactose is an important sugar for pneumococcal colonisation (Terra *et al.*, 2010; Yesilkaya *et al.*, 2009).

Pneumococcus also encodes several other surface-associated enzymes. β-N-acetylglucosaminidase (StrH) has been shown to cleave terminal β1-linked N-acetylglucosamine (GlNAc) to expose mannose, and glycanase (Endo-α-N-acetylgalactosaminidase) is required for cleavage of sialylated core-1-*O* linked glycans (Marion *et al.*, 2009). *Ex-vivo* studies showed that StrH also contributes to the pneumococcal adherence and colonisation by deglycosylating complex host glycans (Marion *et al.*, 2011).

Pneumolysin (Ply) is probably the most-studied virulence factor of all pneumococcal clinical isolates. It is a 53 kDA intracellular pore-forming cholesterol-dependent cytolysin (Hirst *et al.*, 2004). Although, Ply is thought to have an intracellular location, recent studies have shown that the toxin can also be detected in the cell wall of microbe. It is not known exactly how the toxin is released because it lacks the signal peptide and all known cell wall anchoring motifs in Gram-positive bacteria (Price and Camilli, 2009). Shak et al. (2013) showed that Ply is expressed during initial formation of biofilms. Inactivation of Ply in D39 and TIGR4 strains was shown to attenuate pneumococcal biofilm generation significantly compared to the wild type strains *in vitro* and *ex vivo* (Shak *et al.*, 2013).

The polysaccharide capsule surrounding the cell wall is one of the most important virulence factors required for asymptomatic pneumococcal colonisation (Brooks and Mias, 2018). It has been reported that there is an inverse correlation between the capsule expression and colonisation (Nelson *et al.*, 2007). Low level of capsule facilitates adherence to epithelial cells and promotes biofilm formation. In the oxygenated

environment of nasopharynx, the amount of capsule produced is downregulated. This downregulation has been suggested to be due to the activity of pyruvate oxidase (SpxB), which dissimilates pyruvate into acetyl-CoA and its activity requires oxygen. A SpxB mutant of the pneumococcus has been shown to be attenuated in adherence and colonisation (Blanchette *et al.,* 2016). Another line of evidence regarding the level of capsule and colonisation comes from the studies of opaque and transparent colonies, a phenomenon known as the phase variation. While the transparent colonies producing less capsule displays strong pneumococcal attachment to epithelial cells, the opaque colonies possess high level of capsule and are associated with invasiveness (Shainheit *et al.*, 2014).

Pneumococcal surface proteins have also been implicated in the colonisation process. Among these, pneumococcal surface protein C (PspC), also known as choline-binding protein A (CbpA), plays a role in colonisation (Voss *et al.*, 2013). It has been shown that a deficiency in PspC significantly reduces the nasopharyngeal colonisation compare to the wild type strain in a mouse model of asymptomatic colonisation (Rosenow *et al.*, 1997). PspA is another abundant surface protein in *S. pneumoniae,* and it has been reported that it contributes to the nasopharyngeal colonisation because PspA-deficient strain was less able to colonise mouse nasopharynx than the wild type strain (Ogunniyi *et al.*, 2007). King *et al.* (2009) also found that the growth of PspA mutant was approximately 1800 fold lower than the wild type in the mouse nasopharynx, indicating that in addition to promoting colonisation, PspA may have some other metabolic roles required for pneumococcal survival in nasopharynx (King *et al.*, 2009). The mechanism by which PspA mediates adherence and colonisation has been linked to its positive charge, which promotes the surface exposure by reducing electrostatic repulsion (Swiatlo *et al.*, 2002).

1.3 Pneumococcal invasion

Colonisation of pneumococcus within nasal cavity is often asymptomatic. By the age of 5, the colonisation rate drops from >95% to 25-40%, while it is much lower among adults, 8-15% (Millar *et al.*, 2008). Despite a low invasive disease rate, *S. pneumoniae* can disseminate from upper respiratory tract to other niches (lung, ear, blood and brain),

which leads to the development of serious pneumococcal diseases including otitis media, pneumonia, bacteraemia, and meningitis (Figure 1.1).

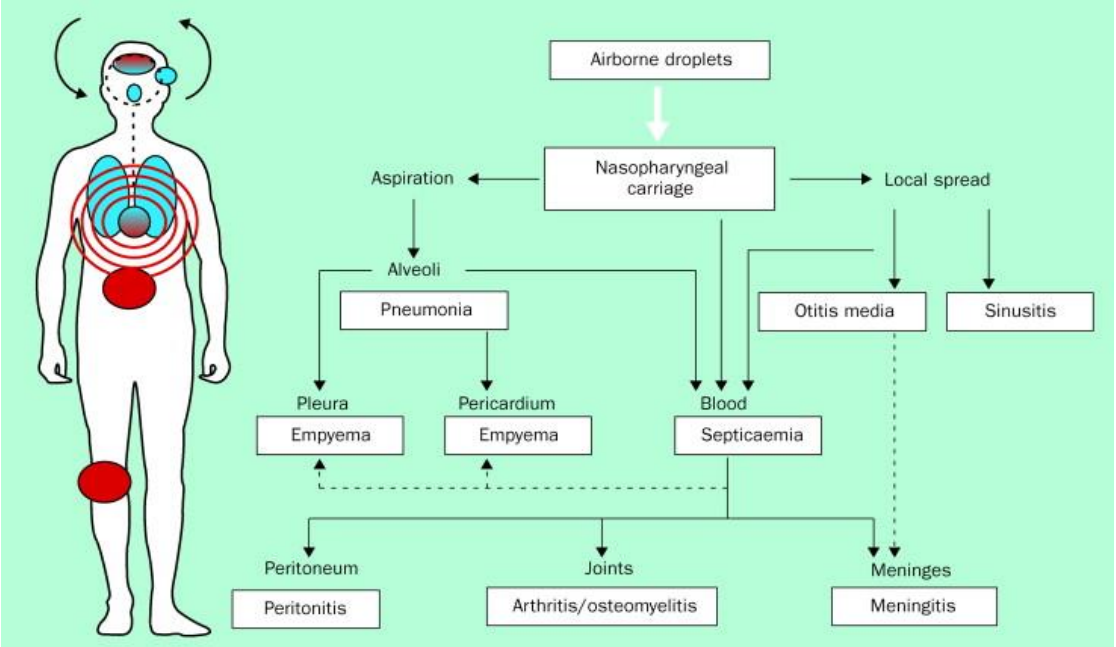

Figure 1.1. Progression of pneumococcal infections.
The diagram shows the systematic dissemination of pneumococci through the host tissues. The figure is adapted from Bogaert *et al.* (2004).

The risk of having invasive pneumococcal diseases is influenced by the socio-economic status of individuals, the living conditions, vaccination status, and lifestyle (being a smoker or alcoholic) (Backhaus *et al.*, 2016). In addition, individuals at extreme ages, children below 5 years and elderly, those suffering from serious medical conditions such as HIV, AIDS, and chronic lung disease, and persons who have undergone cardiac transplantation are considered to be high-risk groups for invasive pneumococcal infections (Backhaus *et al.*, 2016; Kyaw *et al.*, 2005). The time of year and viral diseases are also influence acquisition of pneumococcal infections (Weinberger *et al.*, 2014). The pneumococcal diseases are more frequent during winter months than spring and summer (Dowell *et al.*, 2003). This is believed to be due to high rates of viral diseases and especially respiratory syncytial virus (RSV) and influenza, which are known to predispose individuals to secondary pneumococcal infections (Dowell *et al.*, 2003).

The capsule type is known to be an important determinant of invasiveness. It has been reported that serotypes 1, 4, 5, 7F, 8, 12F, 14, 18C, and 19A are highly invasive, while 6A/B, 11A, 15B/C, and 23F are less invasive (Brueggemann *et al.*, 2003; Yildirim *et al.*, 2010). Serotype distribution of pneumococci vary depending on geography. For example, the serotypes 6A/B, 14, 19F, and 23F, were shown to be the main sources of pneumococcal infections in Africa (Usuf *et al.*, 2014), while serotypes 8, 15A, 22F, and 24F are more prevalent in Europe (Tin Tin Htar *et al.*, 2015). In addition, the available data also suggest that capsule type is associated with the strains' tissue preference. Serotypes 1 and 19A are commonly linked to pneumonia, while serotypes 6B, 9V, 14, 19A/F, and 23F are frequently isolated from children with otitis media (Rodgers *et al.*, 2009). In addition, serotypes 1, 3, and 19A are prevalent for haemolytic uremic syndrome (Song *et al.*, 2013).

Several pneumococcal determinants of virulence have been identified in last few decades. Most of these studies have attributed a function to a given pneumococcal product through characterisation of isogenic mutant strains in *in vitro*, *ex-vivo*, and *in vivo* models. There are a large number of pneumococcal virulence determinants, some of which have been listed in Table 1.1 and illustrated in Figure 1.2, and these can be grouped in several categories, those responsible for protecting *S. pneumoniae* against host immune system, such as capsule, PspC, and pneumolysin, those that are important for adhesion and nutrient metabolism, glysosidases, and those that are linked to oxidative stress resistance, such as superoxide dismutase and thiol peroxidase. I will cover some of these in detail below.

The polysaccharide capsule is a major pneumococcal virulence factor and plays a major role in meningitis, pneumonia, and bacteraemia (Hathaway *et al.*, 2012). The function of the capsule in virulence derives from its anti-phagocytic activity. The capsule inhibits phagocytosis by innate immune cells, limits the interaction of binding with complement molecules and receptors on the host cells (Hyams *et al.*, 2010). It was reported that complement system plays a crucial role for host immunity against pneumococcus. The capsule protects the pneumococcus by inhibiting the deposition of opsonins (C3b and iC3b) mediated by the complement receptors CR1 and CR3. In this pathway, a C3

convertase enzyme is formed and cleaves the complement component C3 followed by the deposition of C3b and iC3b on the pneumococcal surface (Hyams *et al.*, 2010). The same study also found that the capsule type is also important for the extension of complement-mediated phagocytosis. It has been shown that serotypes 4 and 7F are more resistant to complement deposition and phagocytosis than serotypes 6A and 23F in a mouse model of sepsis (Andre *et al.*, 2017). Pneumococcal phase variation, which is linked to the amount of capsule produced, is important attribute of pneumococcal pathogenicity. Transparent colonies are found to be more virulent *in vivo* compare to their opaque variants and they have increased ability to bind complement system to protect the pneumococcus (Hyams *et al.*, 2010).

Pneumolysin is one of the most crucial virulence determinants of *S. pneumoniae* (Jedrzejas, 2001). The main role of pneumolysin in pneumococcal pathogenicity during infection is to form pores in cholesterol-rich membranes, which causes severe tissue damage and inhibits ciliary beating of epithelial cells (Hirst *et al.*, 2004). It is also expressed in early stage of biofilms. Shak *et al.* (2013) reported that biofilm formation in pneumolysin-deficient D39 and TIGR4 strains reduced compare to their parent strains on plastic surface and human cell substrates under static or continuous flow conditions (Shak *et al.*, 2013). The involvement of pneumolysin in pneumococcal virulence have been demonstrated by several independent studies. Berry *et al.* (1999) reported that pneumolysin is able to disseminate between host tissues (Berry *et al.*, 1999). Kadioglu *et al.* (2002) showed that the deletion of pneumolysin reduced the pneumococcal survival in a mouse model of acute pneumonia (Kadioglu *et al.*, 2002). One of the main reasons why pneumolysin contributes to the pathophysiology of pneumococcal infections is linked to its ability to interfere with immune system cell function, for example, the inhibition of respiratory burst of phagocytes at sublytic concentrations and stimulation of chemokine and cytokine release (Kadioglu *et al.*, 2004). Pneumolysin was shown to activate the inflammatory response, and influence the release of chemokines such as tumor necrosis factor alpha (TNF-α) and interleukin-1β (Cockeran *et al.*, 2002). Furthermore, it also inhibits the complement pathways (Yuste *et al.*, 2005).

Pneumococcal surface protein C, PspC, plays an important role in pneumococcal virulence (Kerr *et al.*, 2006). It has been shown that PspC enhances pneumococcal invasion of epithelial cells *in vitro* (Quin *et al.*, 2007). The role of PspC on infection was also supported by *in vivo* studies. In a mouse pneumonia model, PspC mutant strain had reduced virulence compared to the wild type strain (Ogunniyi *et al.*, 2007). The same study also found that the mutant PspC strain was as infectious as the wild type in the bacteraemia model, however, double deletion of PspC and PspA caused clearance of pneumococcus (Ogunniyi *et al.*, 2007). The contribution of PspC on pneumococcal virulence is attributed to its interaction with complement system and complement pathway regulator factor H (Dave *et al.*, 2001), and its binding ability to human secretory immunoglobulin A and Ig receptor (pIgR), which enhances the pneumococcal invasion (Balachandran *et al.*, 2002).

Table 1.1. Selected pneumococcal virulence factors and their contributions to pneumococcal infection.

Virulence factors	Functions
Neuraminidase	• Degrades mucus • Promotes growth and survival • Aids in with cell adherence
Autolysin (lytic amidase)	• Cell lysis • Break down peptidoglycan • Exposes hosts cell to pneumolysin • Aids with bacterial colonisation
Pneumococcal surface adhesin A (PsaA)	• Aids with pneumococcal adhesion
Other choline-binding proteins: LytB, LytC, CbpC, CbpG	• Modify proteins on cell surfaces and allows for binding to host cell receptors • Important for host cell recognition
Non-classical surface proteins	• Act as adhesins • Promote immune system evasion by inhibiting complement • Controls inflammation and affects cytokine production
Pili	• Inhibits phagocytosis by immune cells
Bacteriocin	• Inhibits the growth of competing bacterial cells
Biofilm	• Helps to reduce bacterial recognition by the host immune system • Reduces the impact of antimicrobial agents on bacteria
IgA protease	• Breaks down IgA
Lipoteichoic acid	• Causes inflammation

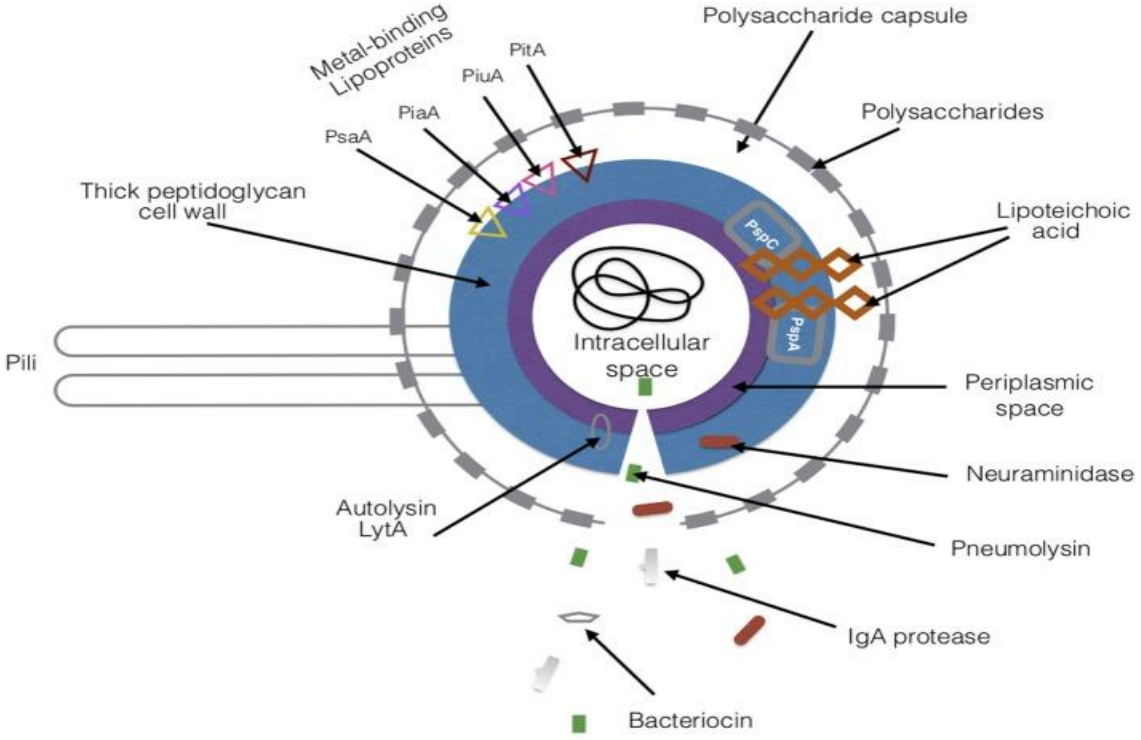

Figure 1.2. Pneumococcal virulence factors.
Polysaccharide capsule, cell wall, neuraminidase, pneumolysin, surface proteins (PspA and PspC), autolysin A (LytA), surface antigen A (PspA), iron acquisition A (PiaA), iron uptake A (PiuA), iron transporter (PitA), and pili. The figure is adapted from Brooks and Mias (2018).

1.4 Host immune response to pneumococcal infection

The host immune system is capable of preventing pneumococcal colonisation. This is influenced by host age and capsular serotypes (Brooks and Mias, 2018). Immune response to colonisation is complex and occurs by cooperation between two components of immunity, innate and adaptive immunities (Paterson and Orihuela, 2010). Innate immunity is stimulated by the introduction of bacteria, and is therefore, non-specific, is mediated by phagocytosis and complement system as well as the activation of pattern recognition receptors (PRRs) consisting of the Toll-like receptors (TLRs) and the cytosolic NOD-like receptors (NLRs) (Paterson and Orihuela, 2010). Human phagocytes are able to recognise pneumococcal patterns and bind them via TLRs. This causes the ingestion of the microbe into a phagosome and digestion process mediated by cytokines

such as TNF-α, IL-6, and pro-IL-1β (Zhang *et al.*, 2015). However, the capsular polysaccharide can inhibit phagocytosis (Hyams *et al.*, 2010).

Another innate immune system is the complement system, which relies on the activation of C3 by a series of complex reactions involving antigen-antibody complexes or binding to pneumococcal surface (Hyams *et al.*, 2010). This initiates the amplified response against the pathogen intrusion, cleavage of component C3 enzyme by production of C3 convertase, deposition of C3b, and migration of immune cells to the site of infection. This process is called opsonophagocytosis (Yuste *et al.*, 2008). However, pneumococcal choline-binding surface proteins, PspA and PspC, were shown to inhibit the complement activation by preventing the deposition of C3b on the surface of the bacteria (Yuste *et al.*, 2008). Moreover, capsule plays a role on prevention of C3b opsonisation (Hyams *et al.*, 2010). The pivotal role of pneumolysin on complement system was also studied *in vivo*. Yuste *et al.* (2005) showed that pneumolysin prevents the opsonisation of bacteria as deletion of *ply* increased the complement deposition on pneumococcus. This study also found that there is a synergistic effect between pneumolysin and PspA on prevention of phagocytosis through complement system and both genes are essential for *S. pneumoniae* to cause septicaemia in mice (Yuste *et al.*, 2005).

The adaptive immune system relies on the serotype/antigen specificity. Serotype-specific IgA antibody is responsive to capsular polysaccharide and pneumococcal proteins. IgA initiates immune response by activating the B cells and T cells at the site of infection (Bogaert *et al.*, 2009). Furthermore, $CD4^+$ T17 cells play a crucial role on resistance to pneumococcal infection. These cells are important for clearance of pathogens, especially in upper respiratory tract via their role in migration of neutrophils to the infection site. Then, neutrophils break the epithelial barrier and secrete antimicrobial peptides (Ramos-Sevillano *et al.*, 2019). Host defences do not always succeed to clear the bacteria from the body. To combat with pneumococcal colonisation and diseases, serotype-specific vaccines have been produced, which are discussed in section 1.5.

1.5 Antibiotic resistance and treatment of pneumococcal diseases

Early diagnosis and therapy are vital to control invasive pneumococcal infections. Broad-range antibiotics have been used for a number of decades to treat pneumococcal diseases, however, pneumococcal strains display increased resistance to available antimicrobials (Reinert, 2009). The antibiotic-resistant bacterial infections are becoming more ubiquitous and turning into a global health problem (Clatworthy *et al.*, 2007). Pneumococcal infections were treated with penicillin and other β-lactam antibiotics in 1940s (Kim *et al.*, 2016). From the beginning of the antibiotic era to 1980s, the pneumococci rapidly developed resistance to penicillin, erythromycin, and trimethoprim-sulfamethoxazole (TMP-SMX). Unfortunately, antibiotic-resistant pneumococci disseminated around the world (Henderson *et al.*, 1988). The susceptibility of *S. pneumoniae* to macrolides, fluoroquinolones, and other non-β-lactam antibiotics were also reported (Cornick and Bentley, 2012). The isolation rate of macrolide-resistant pneumococci (commonly to erythromycin) is considerably higher relative to penicillin-resistant isolates in 21st century (Felmingham *et al.*, 2002). Fluoroquinolones have also had a major impact on the treatment of pneumococcal infections (LaPlante *et al.*, 2007). The resistance of *S. pneumoniae* to a wide range of antibiotics including tetracycline, rifampicin, and trimethoprim-sulfamethoxazole has also been reported (Kim *et al.*, 2016).

Pneumococcal infections have been treated with two types of vaccines, the 23-valent capsular polysaccharide vaccine (PS) and a 7-valent protein-PS conjugate vaccine (PCV-7). The PS vaccine consists of 23 polysaccharides (1, 2, 3, 4, 5, 6B, 7F, 8, 9N, 9V, 10A, 11A, 12F, 14, 15B, 17F, 18C, 19A, 19F, 20, 22F, 23F and 33F), which may induce the immune response against invasive pneumococcal diseases (Russell *et al.*, 2010). PS vaccination for below 2 years of age is not as effective as in elder people as the infants do not have T-cell immunity. Thus, PS is relatively poor antigen to prevent pneumococcal disease in this age group (Bogaert *et al.*, 2004). In the following years, seven-valent pneumococcal conjugate vaccine (PCV-7 or *Prevenar*™, Wyeth Vaccines) was introduced in the United States. PCV-7 was developed for 7 common serotypes (4, 6B, 9V, 14, 18C, 19F, and 23F), and it is very effective on immunised infants and immune-deficient individuals (Bryant *et al.*, 2010). PCV-7 contains polysaccharide antigens, which are conjugated to protein carriers. This conjugation creates a T-cell dependent

immunity that induces immune response with higher affinity of antibodies, produces immunoglobulin G (IgG) and memory B-cell pool (Clutterbuck *et al.*, 2012). However, PCV-7 was serotype-dependent (Munoz-Almagro *et al.*, 2008), therefore, PCV-10 and then PCV-13 were introduced to vaccine-market. It has been reported that PCV-13 induces the memory B- and T-cell immune responses in infants and the elderly (Namkoong *et al.*, 2016), and has managed to reduce pneumococcal infections by 42% (Kaplan *et al.*, 2013). But, PCV-13 is also limited as the non-vaccine serotypes can still cause pneumococcal disease due to serotype replacement, which means that the incidence of infections caused by serotypes not represented in the vaccine formulation increases (Dirmesropian *et al.*, 2015).

1.6 Pneumococcal adaptation to host environment

S. pneumoniae is an infectious agent that is responsible for life-threatening diseases with high morbidity and mortality worldwide. Extending knowledge of pneumococcal biology is important to improve the understanding of pathogenesis, diagnosis, and treatment of pneumococcal infections (Brooks and Mias, 2018). So far, most of the pneumococcal studies have focused on the host-pathogen interactions, but adaptation mechanisms to different host niches is also important for pneumococcal virulence. The pneumococcus can colonise, invade, survive in host, and cause an array of diseases in various anatomical sites, which may be restricted in nutrients required for bacterial growth, and have different concentration of oxygen, pH, and a range of temperature (Charpentier *et al.*, 2000). Although adaptation to these fluctuating environments *in vivo* is crucial for pneumococcal virulence, the knowledge on these pneumococcal traits is still relatively limited. Some of *in vivo* environmental factors encountered by the pneumococcus and its adaptation mechanism have been covered below. Moreover, the main subject of this study, the impact of temperature on pneumococcal metabolism and thermal adaptation mechanisms, has been discussed in detail in sections 1.7 and 1.8.

1.6.1 Sugar metabolism

Streptococcus pneumoniae is a strict fermentative microbe obtaining its energy via glycolysis as it lacks the complete set of genes for respiration (Paixao *et al.*, 2015a). During progression from colonisation to disease, the pneumococcus is subjected to changing sugars available in the host environments (Paixao *et al.*, 2015a). It has been reported that pneumococcus can utilise at least 32 different carbohydrates using mainly phosphotransferase systems (PTS) and ATP-binding cassette (ABC) transporters (Bidossi *et al.*, 2012). In the nasopharynx, glucose is the preferred sugar for pneumococcal growth, although it is poor in the environment (<1 mM), it is enriched during infection (4-6 mM in blood and lung) (Shelburne *et al.*, 2008). On the other hand, the nasopharynx is rich in O- and N-linked glycans, which are derived from glycoproteins and glycosaminoglycans (Burnaugh *et al.*, 2008). To increase the colonisation rate in the human airway epithelial cells, the pneumococcus deglycosylates the glycans which generates free sugar mixture (Marion *et al.*, 2012). Mucins are major components of the mucus that cover the epithelial surfaces and composed of N-acetylglucosamine (GlcNAc), N-acetylgalactosamine (GalNAc), N-acetylneuraminic acid (NeuNAc), galactose (Gal), fucose (Fuc) and sulphated sugars. However, the most abundant sugar in mucin is known to be galactose and galactosamines (Terra *et al.*, 2010). In such a mixed sugar environment, the pneumococcus activates the carbon catabolite repression (CCR), a regulatory network that upregulate the expression of genes involve in the utilisation of preferred sugars, while downregulates the other genes involved in the use of less-preferred sugars (Gorke and Stulke, 2008).

In the respiratory tract, galactose is a key carbon source for pneumococcal growth. Galactose is metabolized by two catabolic pathways, Leloir or tagatose 6-phosphate (T6P). It has been reported that the inactivation of both pathways lead to impaired pneumococcal growth and colonisation in the nasopharynx and reduced virulence (Paixao *et al.*, 2015b). Blanchette *et al.* (2016) showed that galactose promotes biofilm formation during nasopharyngeal colonisation (Blanchette *et al.*, 2016). Thus, it seems that galactose is one of the main carbon sources for pneumococcal energy requirement in the respiratory tract. Although, galactose is not a preferential sugar for pneumococcus compare to glucose or N-acetylglucosamine, galactose catabolism has been shown to

trigger mixed acid fermentation (Paixao *et al.*, 2015b). It has been shown by our research group that pyruvate formate-lyase (PFL), which is active when galactose is provided as the nutrient source for dissimilation of pyruvate to acetyl-CoA and formate, plays an important role on pneumococcal virulence (Yesilkaya *et al.*, 2009). Furthermore, Al-Bayati *et al.* (2017), also from our research group, investigated that PFL synthesis is controlled by two transcriptional regulators (CcpA and GlnR), which involve in pneumococcal metabolism and virulence (Al-Bayati *et al.*, 2017).

As summarised above, *S. pneumoniae* is exposed to different carbohydrates in host tissues. This suggests that preference of sugar is essential to promote pneumococcal fitness and virulence.

1.6.2 Oxidative stress

Streptococcus pneumoniae has to cope with variant levels of oxygen during progression from colonisation to infection (Yesilkaya *et al.*, 2013). In the human airway, the pneumococcus is exposed to 21% oxygen, while it is 10-15% in the alveoli and 5% in the tissues of lower respiratory tract (Burghout *et al.*, 2010). The pneumococcus employs enzymatic mechanisms to remove reactive oxygen species (ROS) in anaerobic tissues such as bloodstream and brain (Burghout *et al.*, 2010). ROS, including hydrogen peroxide (H_2O_2), hydroxyl radical ($OH^{\bullet}$) and superoxide anion ($O_2^{\cdot -}$), are produced in the presence of oxygen (Fenton reaction). Our research group has reported that these species are harmful for the microbe and the host (Najmuldeen *et al.*, 2019). $O_2^{\cdot -}$ and H_2O_2 are known to damage proteins and cause mutations on DNA (Andisi *et al.*, 2012). During aerobic metabolism, the pneumococcus produces millimolar concentrations of H_2O_2 from pyruvate, which is mediated by the pyruvate oxidase (SpxB) (Najmuldeen *et al.*, 2019). In the upper respiratory tract, the concentration of H_2O_2 produced by *S. pneumoniae* is high enough to compete with other inhabitants such as *Haemophilus influenza* and *Neisseria meningitidis* (Pericone *et al.*, 2000). However, the H_2O_2 activity of pneumococci is not effective to compete with the colonisation of *Staphylococcus aureus* in neonatal rat model (Margolis, 2009).

S. pneumoniae has no major H_2O_2-degrading enzyme, such as catalase, or oxidative-stress response sensors such as OxyR, SoxRS, PerR, or AhpC (Yesilkaya *et al.*, 2013). However, it has the other enzymes that can use ROS as substrate. For example, manganese-dependent SOD (MnSOD) converts superoxide radicals to H_2O_2 and O_2. It has been shown that pneumococcal growth was restricted in aerobic environments in the absence of MnSOD (SodA) (Yesilkaya *et al.*, 2000). Ahp, an alkyl hydroperoxidase, can catalyse the conversion of toxic peroxide compounds to alcohol and water by cleaving hydrogen peroxide, and is responsive to oxidative stress (Mishra and Imlay, 2012). NADH-oxidase (Nox) is a housekeeping enzyme that reduces O_2 to water (Auzat *et al.*, 1999), and it has been shown that the inactivation of *nox* decreases the virulence of *S. pneumoniae* in a murine model (Yu *et al.*, 2001). Additionally, transcriptional regulator Rgg, the serine protease HtrA, the MerR/NmlR family transcription factor, ClpP protease, and thioredoxins were found to be involved in pneumococcal oxidative-stress response (Andisi *et al.*, 2012). Recently, it was demonstrated that flavin reductase (FlaR), a Fe^{2+} binding protein, has a role in pneumococcal resistance to H_2O_2 in both O_2^- rich and limited environments and pneumococcal virulence was attenuated in a mice infection model in the absence of *flaR* (Morozov *et al.*, 2018).

Hence, the pneumococcus has ability to sense different level of oxygen and develop responses to oxidative stress, which is important for pneumococcal *in vivo* fitness.

1.6.3 Metal homeostasis

Microbes possess systems to maintain metal homeostasis as the concentration of metals needs to be finely balanced. Metals are subsets of nutrients required for bacterial growth and virulence because they are needed for the function and activity of various proteins and enzymes as co-factors or structural elements (Porcheron *et al.*, 2013).

S. pneumoniae encodes metal import and export systems to access trace metals which vary in different host tissues (Honsa *et al.*, 2013). For example, the host sequesters the essential metals such as iron and manganese, which are utilized by the pneumococcus. However, some other metals such as copper and zinc are released by the host to eliminate

the pathogen (Honsa *et al.*, 2013). The concentration of manganese recorded in mice tissues ranges from 0.4 to 1.1 μM in the blood, nasopharynx, and lungs (Ong *et al.*, 2013). The pneumococcus transports manganese by PsaBCA regulon. It has been reported that absence of PsaA restricts the uptake of manganese, which leads to attenuation of pneumococcal virulence in a murine model (Ong *et al.*, 2013). In addition, iron concentration in the blood is 138 μM and raises to 257 μM during infection (Honsa *et al.*, 2013) . Zinc concentration is ten times higher in the blood in infected than healthy tissues (Ong *et al.*, 2013). When the zinc concentration is high, SczA, encoding tetracycline resistance family regulator, controls the expression of *czcD*, which is responsible for exporting toxic zinc (Kloosterman *et al.*, 2007). The concentration of copper is 6 μM in nasopharynx, while it is 11 μM in blood. During pneumococcal infection, the host releases copper to clear the invasion of pathogen. *S. pneumoniae* encodes a copper exporter (*copA*) or a chaperon (*cupA*) which involve in copper resistance mechanism. Shafeeq *et al.* (2011) showed that the *cop* operon in wild type strain is induced in the nasopharynx and lungs in mice, while a *copA*$^{-}$ mutant strain was less virulent in a mouse model of pneumococcal pneumonia due to decreased growth of the strain in high level of copper *in vitro* (Shafeeq *et al.*, 2011).

In light of literature, *S. pneumoniae* encounters with changes in the concentration of metal ions in host tissues. Some of these metals are beneficial for pneumococcal growth at certain concentration ranges. Therefore, the pneumococcus has adaptive systems to maintain the metal ion homeostasis to provide nutrients for cellular metabolism and control the excess level of toxic metals to prevent cellular damages.

1.6.4 Acid tolerance

S. pneumoniae has to cope with changing pH conditions as pH of tissues changes during health and disease (Cortes *et al.*, 2015). It has been described that the pH values of human nasopharynx range from 6.10 to 7.92, and the average pH is 7.03 (Brunworth *et al.*, 2012). During infection, the pH of pleural fluids from the patients with pneumonia was recorded at 6.8 (Brunworth *et al.*, 2012). When the pneumococcus passes the blood-brain barrier, pH values are between 6.1 to 6.8 and 4.8 to 6, depending on the maturation of endosome

in endothelial cells. The minimum pH that pneumococcus might tolerate has been recorded to be 4.4 in phagosomal vehicles during phagocytosis (Pinas *et al.*, 2018).

In order to survive at acidic environment, bacterial pathogens possess acid tolerance response (ATR) mechanism, which allows microbes to manifest increased resistance to lethal pH after brief exposure to the sub-lethal pH (Pinas *et al.*, 2018). For example, it has been shown that when *S. pneumoniae* R6 strain was pre-incubated at pH 5.5 for 2h, the resistance of cells increased at least by ten-fold at lethal pH 4.4 (Pinas *et al.*, 2018). In addition, F_0-F_1 ATPase system has been shown to involve in ATR. The enzyme maintains the intracellular pH homeostasis via hydrolysing ATP to generate a protein gradient for pumping protons to cytosol (Martin-Galiano *et al.*, 2001). Related to this, when the concentration of the enzyme increases, pH of the medium decreases (Martin-Galiano *et al.*, 2001). Moreover, transcriptional analysis of pneumococcal genes at low pH showed that at least 126 genes were expressed during the adaptation process. Of those genes, the level of chaperonins (hrcA, grpE, dnaK, dnaJ), the HrcA repressor, and two proteases (clpL and prtA) increased. These proteins are believed to play roles on refolding of proteins or degradation of misfolded proteins during acidic shock (Martin-Galiano *et al.*, 2001).

While the impact of various *in vivo* relevant environmental conditions on *S. pneumoniae* has been studied in some detail, more research needs to be done with respect to their contribution in pneumococcal adaptation in different host tissues. One of the environmental factor that has not been studied in detail in *S. pneumoniae* is temperature. Hence, the main objective of this study is to investigate the influence of temperature changes in pneumococcal metabolism and virulence.

1.7 Temperature stress

Microbial species are evolved to sense fluctuating environmental conditions and possess the regulatory networks to respond to these stimuli. Changes in temperature is probably one of the most important environmental parameters that the microbes need to adjust as

it has fundamental impact on microbial physiology, virulence, and survival (Klinkert and Narberhaus, 2009).

Microbial species with a potential to cause disease such as *Escherichia coli*, *Yersinia pestis*, *Shigella flexnerii*, and *Salmonella typhimurium* are able to sense the interior temperature of the warm-blooded hosts where temperature varies between 37°C to 41°C (Konkel and Tilly, 2000). Microbes encounter with different temperatures at different host tissues. For example, *E. coli* survives in blood stream, where temperature is 37°C, the microbe is also able to survive in gastrointestinal tract of animals where temperature is between 25°C to 30°C (Koziolek *et al.*, 2015). During infection, on the other hand, microbes consistently experience an elevated body temperature, which is one of the host innate immune defences against microbial infection (Swaggerty *et al.*, 2018). Hence, thermally stressed microbes can develop phenotypic adaptations to survive within their hosts.

Temperature has been found to affect the growth, morphology, cell viability, and virulence of various microbial species including bacteria, fungi, parasites, and viruses (Shapiro and Cowen, 2012). Fluctuations in temperature is generally correlated with the seasonal changes in environmental temperature (abiotic) such as increasing global temperature, interactions with diverse host species, pathogen transmission, and upon febrile response linked to infection (biotic) (Shapiro and Cowen, 2012).

The replication of human viruses is temperature dependent. A highly pathogenic avian H5N1 influenza A viruses have spread around the world with a high rate of mortality (Hatta *et al.*, 2007). To investigate the molecular mechanism behind the viral infection *ex-vivo*, the position of Glu within the sequence of PB2 protein was substituted to Lys and the modified viruses were grown at 33°C, 37°C and 41°C. The viruses possessing Glu replicated less well in cells at the lower temperature. These results suggest that Lys at PB2–627 confers to avian H5N1 viruses the advantage of efficient growth and replication in the upper and lower respiratory tracts of mammals at 33°C compared to 37°C and 41°C (Hatta *et al.*, 2007).

Temperature can affect the size and shape of cells. In most bacterial species, cell shape is determined by the cell wall. The environmental conditions may force microbes to change the chemical properties of their cell wall for nutrient acquisition, dispersal to other niches, and prevention of complement killing (Yang *et al.*, 2016). A study with six fungal dimorphic pathogens of humans including *Blastomyces dermatitidis* and *Histoplasma capsulatum* reported that changes in temperature impact the virulence linked to morphological transition as these fungi were non-pathogenic at soil temperature but turned to be pathogenic yeast upon inhalation into lungs of mammalians (Klein and Tebbets, 2007). *Bordetella pertussis*, a mucosal pathogen, has a rough shape when cultured on blood agar plates at 25°C, but smooth, dome-shaped and haemolytic cells are formed at 37°C (Konkel and Tilly, 2000). Moreover, many Gram-negative pathogens such as *E. coli*, *S. enterica*, and *V. chlorea* differentiate their characteristic shapes of long-rod to small-coccoid at low temperature (Yang *et al.*, 2016).

Temperature has also a major influence on the motility of several bacterial species (Lam *et al.*, 2014). It was shown before that when temperature increases from 23°C to 37°C, *E. coli* switches its motility steeply at 37°C, which is the temperature of gastrointestinal tract of animals, where the microbe survives (Paster and Ryu, 2008). *Yersinia* is not motile at 37°C due to restricted expression of sigma factor (*fliA*) and anti-sigma factor (*flgM*) as a result of DNA supercoiling (Ding *et al.*, 2009). In addition, the activity of *fliA* and *flgM* in *Campylobacter jejuni* enabled higher motility at 42°C than 37°C (Wosten *et al.*, 2010).

Although knowledge has accumulated about the molecular mechanism for thermosensing and regulation of gene expression in various pathogenic bacteria in response to environmental temperature fluctuations, relatively little is known about the response of streptococci. Two studies have used transcriptional analysis to investigate adaptive heat-shock response of *S. mutants* (Liu *et al.*, 2015) and *S. thermophiles* (Li *et al.*, 2011). Transcriptional profiles of *S. mutants* and *S. thermophilus* were determined at different temperatures. The results indicated differential expression of several genes involved in transcriptional regulation (*vicR, ciaR, scnR, rpoE,* and *fruR*), chaperon/protease synthesis (*hrcA, groES, grpE, clpP and clpE*), signal transduction, cell wall synthesis, energy metabolism, iron homeostasis, ABC transporter, restriction-modification system, and

virulence in response to temperature shift (Li *et al.*, 2011; Liu *et al.*, 2015). In *S. pyogenes*, it was shown that capsule production is thermoregulated by the CovRS two-component regulatory system. The CovRS system is a repressor of the *hasABC* capsular biosynthetic locus in this strain. The study showed that capsule production is higher at lower temperature (25°C) in the *covRS*-null strain compare to 37°C. However, there was still basal level of capsule production at 37°C, suggesting that capsule synthesis is mediated by CovRS in a temperature-dependent manner. The study also showed that the capsule production changed the phenotype of the bacterial cells. At 25°C, the cells were mucoid, while they were non-mucoid at 37°C (Kang *et al.*, 2012).

In *S. pneumoniae*, very limited information is available to answer the question as to how the pneumococcus responds to temperature changes at different niches. A literature search showed that the pneumococcus has different transcriptional profiles at various temperatures and most of the temperature-induced genes are virulence-related (Pandya *et al.*, 2005). Thermal adaption is tremendously important because pneumococcus has to cope with different temperature ranges during progression from colonisation to infection. It has been shown that the temperature in human nasopharynx is 33°C-34°C, while it is 37°C in blood stream and central nervous system, and can go up to 40°C-42°C in response to infection (Pandya *et al.*, 2005). Given that the pneumococcus inhabits different niches each with a different temperature, it is expected that the pneumococcus has mechanisms to control its metabolism, virulence and survival at different temperatures.

How microbes actually sense the temperature changes within their hosts is the key question. There are two main ways (heat- and cold-shock response) by which microbes can respond to changes in temperature and these responses are informative, transient, and irreversible (Klinkert and Narberhaus, 2009). Heat-shock proteins (HSPs) are classified as proteolytic proteins or molecular chaperones and involved in several processes in bacterial cells including controlling the quality of newly synthesized proteins, refolding denatured or unfolded proteins, and preventing the accumulation of damaged proteins under temperature stress (Choi *et al.*, 1999). This is known as chaperone-mediated folding process (Choi *et al.*, 1999). Some chaperons such as GroEL and DnaK have elevated expression during stress conditions, which are also required during non-stressed growth

conditions. Their role is to refold the unfolded proteins by binding to their co-chaperons GroES and DnaJ-GrpE (Roncarati and Scarlato, 2017).

It has been shown that most of the heat shock proteins have been implicated in virulence of various bacteria. For example, GroEL1 of *Mycobacterium smegmatis* is involved in the synthesis of mycolates, long-chain fatty acid components of the cell wall, which modulates biofilm maturation (Ojha *et al.*, 2005). The role of DnaK-DnaJ chaperone system has been studied in many species including *Campylobacter jejuni* and *Salmonella enterica* serovar Typhimurium and it was reported that bacterial growth is compromised in macrophages and colonisation is inhibited in a mice infection model, suggesting that these proteins are also involved in bacterial survival (Konkel *et al.*, 1998; Takaya *et al.*, 2004).

Heat-shock proteins have also been studied in *S. pneumoniae*. In the pneumococcus, GroEL (Hsp60), DnaK (Hsp70), and Clp (Hsp100) (Caseinolytic-protease) proteins were identified as major heat-shock proteins (Kwon *et al.*, 2003). Of these, Clp operon, including ClpC, ClpE, ClpL and ClpX, are probably the most-studied proteolytic chaperone under stress conditions (Chastanet *et al.*, 2001). ClpP and ClpL are the main chaperones required for thermo-sensitivity, growth, competence, and induction of virulence genes such as *cbpA, cps2A, ply,* and *psaA,* while ClpC and ClpX control the growth of pneumococcus at elevated temperatures (Chastanet *et al.*, 2001). DnaK and GroEL are also important HSP proteins. Unlike their homologues in other species such as *E. coli* or *B. subtilis*, these proteins are only induced by heat-shock, but they are not active under other stress conditions such as osmotic or ethanol shock, oxidizing agents, salt, or DNA damaging agents (Choi *et al.*, 1999). Furthermore, one of the major virulence factors and chaperone of *S. pneumoniae,* HtrA (high temperature requirement A), is expressed during heat-shock and other environmental stress conditions. It was shown that the role of HtrA switches to serine protease at elevated temperature (Choi *et al.*, 1999; Ibrahim *et al.*, 2004a, 2004b).

Low temperature is another stress condition that some pathogens have to cope within their host. As a response to temperature down-shift, microbes produce cold shock proteins

(Csp) since low temperatures cause reduced enzyme activity, cell membrane fluidity, stabilization of nucleic acid structures, protein folding and refolding, and activation of transcription/translation mechanisms (Phadtare and Inouye, 2004). Csp operon has been well studied in *E. coli*. During cold shock, CspA acts as a RNA chaperone and motifs in Csp binding domain binds to stabilize the RNA and stops the development of hairpin structure (Phadtare and Inouye, 2004). In *B. subtilis*, CspB, CspC, and CspD bind to RNA and enable microbe to initiate the translation at cold environment (Graumann *et al.*, 1997). Besides acting as chaperone, Csp plays a role on non-shock bacterial fitness, the regulatory network for expression of virulence determinants, and modulation of NaCl and oxidative stress adaptation in *Listeria monocytogenes* (Eshwar *et al.*, 2017).

1.8 Microbial thermosensors

1.8.1 Thermosensing at DNA level

Bacterial pathogenicity is mediated by transcription and the translation of genetic information. Therefore, the conditions that impact the topology of DNA is important for controlling the transcription of virulence-related genes as illustrated in Figure 1.3 (Klinkert and Narberhaus, 2009).

DNA topology is affected by temperature through alterations of supercoiling or bending of bacterial or plasmid DNA (Lam *et al.*, 2014). During heat- or cold-shock, DNA supercoiling acts as a thermosensor and affects the efficiency of transcription, binding of proteins to the related promoters, and modulates the expression of virulence genes (Steinmann and Dersch, 2013). Temperature-induced supercoiling is different in mesophilic and hyperthermophilic microorganisms. Plasmid DNA of mesophiles such as *E. coli* and *Salmonella* are negatively supercoiled, which turns positive during heat stress. This leads plasmid to relax and express type I fimbriae in *E. coli* and type III secretion system (T3SS) in *Salmonella* (Roncarati and Scarlato, 2017). A switch on supercoiling provides the expression of heat-shock proteins and promotes the adaptation of bacteria to the host environment. On the other hand, cold stress causes decreased supercoiling (Lam *et al.*, 2014). Hyperthermophiles including *Sulfolobus* and *Thermococcus* have positively supercoiled DNA that can be increased by heat stress (Shapiro and Cowen, 2012). Cold

stress changes supercoiling from positive to negative. In both cases, temperature-induced genes (gyrase and topoisomerase) involve in recovery processes (Klinkert and Narberhaus, 2009). In addition, temperature may cause bending of DNA structure, which affect the expression of temperature-related genes. Supercoiling and curvature (bend) type sensing are stabilized by histone like nucleoid-structuring proteins (H-NS) (Winardhi *et al.*, 2015). H-NS is a multifunctional regulator of the bacterial genome and is widely distributed in Gram-negative microbes. By binding to AT-rich bent DNA, H-NS silences the expression of genes that may block the binding of RNA polymerase to promoter (Winardhi *et al.*, 2015). Microarray analysis showed that H-NS is able to control 69% and 77% of temperature-regulated genes including iron and nutrient acquisition systems, the general stress response, and biofilm formation in *E. coli* and *S. enterica* (Klinkert and Narberhaus, 2009). H-NS also acts as a repressor in response to fluctuating temperature. For example, activation of T3SS, an important virulence determinant in *S. enterica,* is repressed by H-NS when bacteria is grown at 30°C or below (Duong *et al.*, 2007). Moreover, the expression of Pap pili, which is required for attachment of *E. coli* to upper urinary tract, is thermoregulated by H-NS activation. Below 26°C, H-NS represses the *pap* regulatory site, but not at 37°C (White-Ziegler *et al.*, 1998). These results suggest that H-NS regulation on expression of virulence genes is restricted with host-temperature and H-NS dependent binding occurs at non-host temperature. Although, this thermosensor has been studied well in bacteria, mostly in Gram-negative, it has not been investigated in streptococcal species.

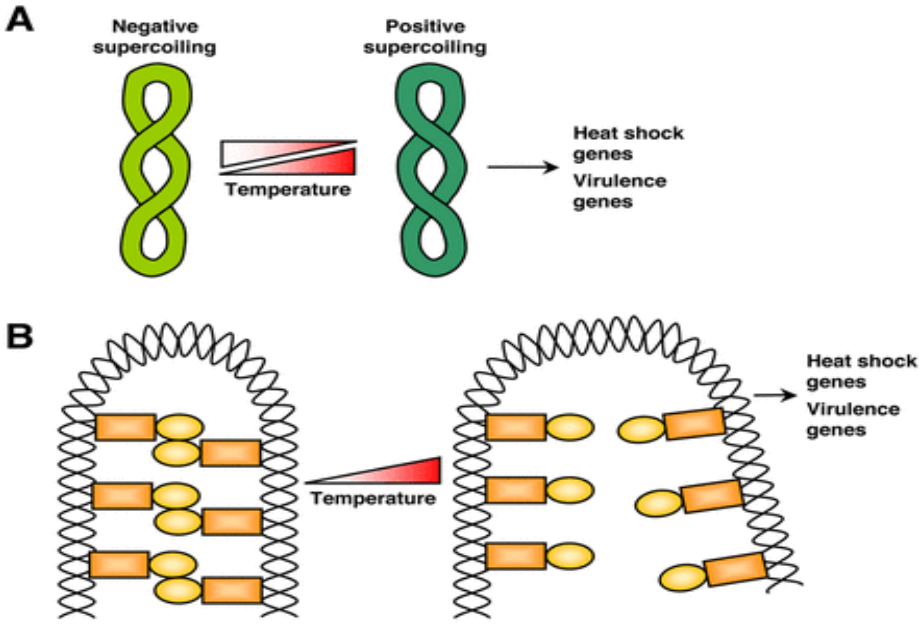

Figure 1.3. Illustration of DNA-dependent thermoregulation mechanisms.
A represents the supercoiling in mesophilic pathogens. Heat stress induces positive supercoiling and lead the transcription of virulence genes and heat-shock proteins. DNA is supercoiled positively. Decreased temperature leads to decrease in positive supercoiling and expression of those genes reduces. **B** represents the binding of H-NS to DNA that reduces relaxation of the DNA bend and leads the access of RNA polymerase to the promoter at high temperatures. These figures are adapted from Shapiro and Cowen (2012).

1.8.2 Thermosensing at RNA level

RNA is also considered as a thermometer due to its transducer role for translation. Identified RNA thermometers are found in the 5' untranslated region (UTR) of bacterial heat- and cold-shock, and virulence genes (Klinkert and Narberhaus, 2009). Principally, RNA thermometers control the initiation of translation by sequestration of the Shine-Dalgarno (SD) sequence located upstream of the AUG start codon in mRNA by forming hairpin structure. High temperature melts the secondary structure formed during cold stress and destabilizes ribosome binding to facilitate initiation of translation (Krajewski and Narberhaus, 2014). The features of RNA thermometers are illustrated in Figure 1.4.

Expression of numerous heat shock proteins in *E. coli* is mediated by alternative sigma factor σ^{32} encoded by the *rpoH* gene (Morita *et al.*, 1999). Unlike the other RNA

thermometers, which reside in 5ˈUTR, this regulatory thermometer is found in the coding region (Morita *et al.*, 1999). At high temperature (42°C), RNA structure that blocks the binding of ribosome unit to SD sequence in mRNA melts, liberating the expression of sigma factor and ignites heat-shock response (Narberhaus *et al.*, 2006).

The most abundant RNA thermometer family, repression of heat shock gene expression (ROSE), was first identified in rhizobial heat-shock genes and then found in various α- and γ-proteobacteria including *E. coli* and *Salmonella* (Narberhaus *et al.*, 2006). ROSE is formed up to 4 hairpin structure which sequester the SD sequence or AUG start codon in their 3′ hairpins, where temperature is sensed. The U(U/C)GCU motif in this hairpin obstructs binding to SD sequence due to mismatched base pairing. Increased temperature melts the hairpin allowing the binding of ribosome to SD sequence and initiates translation (Narberhaus *et al.*, 2006).

Another known RNA thermometer that has a role in the expression of heat shock genes is 'fourU' element comprising four uridines that pair with AGGA of the SD sequence resulting in blocked translation at low temperature (Rinnenthal *et al.*, 2011). For instance, translation of a small heat-shock gene (*agsA*) in *S. enterica* is initiated with increasing temperature. It was shown that the melting point of sequences is decreased by 5°C when an AU pair is exchanged for stabilizing GC pair. Moreover, the melting point is increased by 11°C with the exchange of an internal AG mismatch to a GC pair. These fluctuations effect the virulence of this microbe (Rinnenthal *et al.*, 2011). Apparently, *htrA* (high temperature requirement A) in *E. coli* is also controlled by fourU RNA thermometer as translation is induced when temperature is increased from 30°C to 42°C (Meyer *et al.*, 2017).

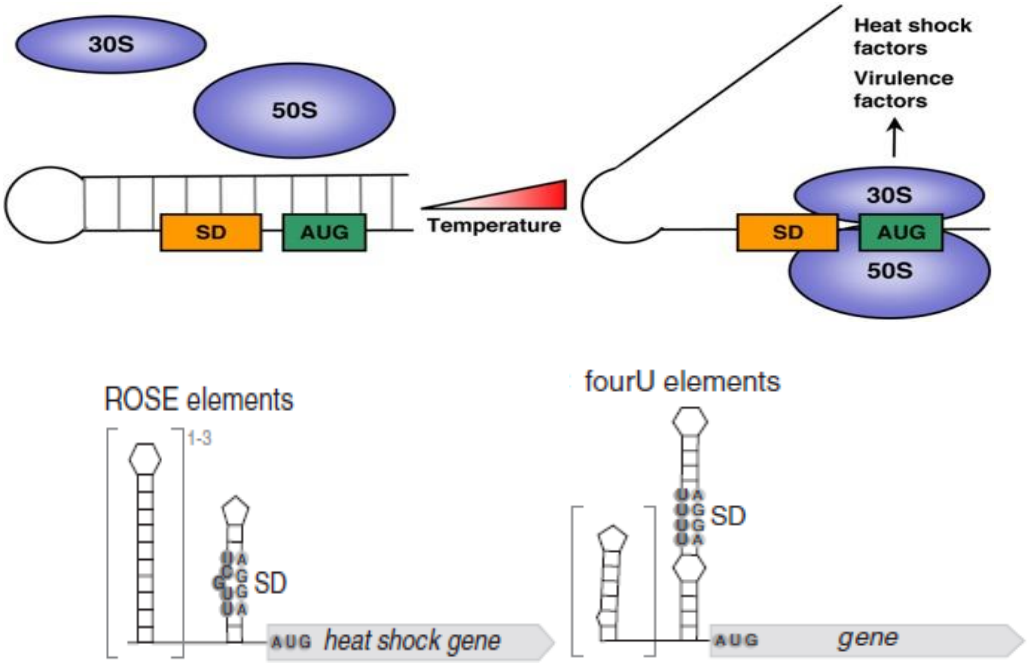

Figure 1.4. Illustration of RNA thermometers.
A hairpin structure do not allow ribosomal binding subunits (30S and 50S) to bind to SD sequence and AUG start codon to initiate the translation at low temperature. Increasing temperature destabilizes the hairpin allowing 30S and 50S ribosomal subunits to bind, and facilitating the initiation of translation. By this way, RNA is able to control the expression of genes encoding heat shock factors and virulence factors. This figure is adapted from Shapiro and Cowen (2012). ROSE elements sequester the SD sequence to be paired by U(U/C)GCU motif highlighted in gray and AUG start codon in their 3′ proximal hairpins to control the translation of heat shock genes. FourU elements form at least one hairpin structure and blocks the SD sequence for translation. This figure is adapted from Krajewski and Narberhaus (2014).

1.8.3 Thermosensing at protein level

Proteins are also known as thermosensors because their sub-structures are highly susceptible to temperature changes. The basic principles of protein thermosensors are illustrated in Figure 1.5. Conformational changes in protein structure in response to temperature shift may affect the cellular processes such as transcription and signal transduction (Sengupta and Garrity, 2013). Transcriptional regulators, kinases, and chaperons and proteases are classified as protein thermosensors (Sengupta and Garrity, 2013).

Transcriptional repressors can act as temperature sensors to regulate the heat-shock and virulence genes by dissociating from DNA in response to increasing temperature (Shapiro and Cowen, 2012). CtsR, a global repressor in Gram-positive bacteria, controls the stability of protein via sensing the heat-shock with its glycine-rich loop (Elsholz *et al.*, 2010). In *B. subtilis,* CtsR represses the transcription of heat stress response-related ATPases, ClpC, ClpE, ClpX and the peptidase ClpP (Kruger *et al.*, 2001). It was also shown that McsB inactivates the degredation activity of CtsR by the ClpCP protease during heat stress in the same microbe. Therefore, McsB is required to control the CtsR for efficient oligomerization and activity of ClpC to adapt to temperature change (Kirstein *et al.*, 2007). GmaR, first known thermosensor protein in *Listeria*, is shown to involve in flagellar motility, is down-regulated at 37°C. In addition, a conformational change in the structure of GmaR at different temperatures facilitates derepression of motility genes (Kamp and Higgins, 2011).

Sensor kinases in two-component regulatory systems (TCS) of bacteria have ability to sense temperature shift. For example, the activation of sensor kinase VirA and response regulator VirG of *A. tumefaciens* is temperature-dependent. It was shown that the virulence of the microbe is attenuated at below 32°C (Jin *et al.*, 1993).

Chaperones are also considered as proteinaceous thermosensors. In *E. coli*, the co-chaperone GrpE works co-ordinately with another chaperon DnaK and its protein sensor DnaJ. GrpE acts as a nucleotide exchange factor and converts adenosine 5′-diphosphate (ADP) from the nucleotide-binding cleft of DnaK to adenosine triphosphate (ATP). At increased temperature, GrpE controls the conformational change of unfolded polypeptides and promotes thermal adaptation (Harrison, 2003). High-temperature requirement A (HtrA) family protein (also functional in *S. pneumoniae)* has also been shown as an important chaperone/protease and thermosensor in *E. coli* (DegP) (Ortega *et al.*, 2009) and a hypothermic bacteria *Thermotoga maritima* (HtrA) (Kim *et al.*, 2003). In both bacteria, HtrA activates the proteolytic function at elevated temperature due to conformational change in the structure, and rearranges the catalytic unit and folds the protein.

The importance of protein thermosensors has been studied in detail in various bacteria. However, it has not been investigated in detail in streptococci. It has been shown that M proteins of group A streptococci are detrimental for sensing of temperature. These proteins are formed coiled-coil dimers at low temperatures, but as monomers at 37°C, suggesting that M protein can sense the temperature via the change on structure of the protein and transmit a signal through the bacterial cell wall to be avoided from human innate system during infection (Hurme and Rhen, 1998).

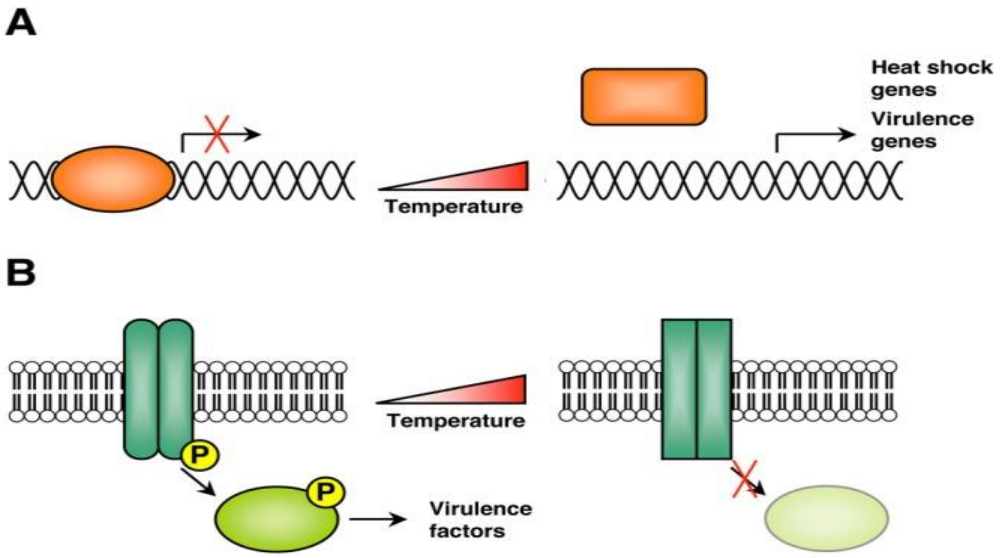

Figure 1.5. Illustration of protein thermometers.
In panel A, transcriptional repressor dissociates from binding to DNA associated with heat-shock and virulence genes at elevated temperatures. In panel B, histidine kinases of TCSs phosphorylates the response regulator to activate signalling pathways and virulence factors in response to temperature. Elevated temperature leads to changes on protein conformation that stop signalling. These figures are adapted from Shapiro and Cowen (2012).

1.8.4 Thermosensing at lipid and membrane fluidity level

Plasma membrane plays an important role in mediating microbial cells interaction with its environment. It is strongly believed that the lipid bilayers in the membrane are able to sense fluctuations of environmental temperature (Mansilla *et al.*, 2004).

In bacteria, membrane fluidity is influenced by growth temperature. As the growth temperature decreases, the fluidity is regulated by the ratio of unsaturated to saturated fatty acids (Mansilla *et al.*, 2004). It has been shown that DesKR system, a two-component regulatory system in *B. subtilis*, involves in control of membrane fluidity during temperature changes (Cybulski *et al.*, 2015). The thermosensory protein in the system is DesK. At decreased temperature, the catalytic domain of DesK (DesKC) phosphorylates the response regulator DesR, which expresses the desaturase enzyme, which mediates the level of unsaturated and saturated lipids and introduce double bonds to existing lipids. This helps bacteria to be recovered from low temperature stress (Cybulski *et al.*, 2015).

1.9 Aims of the study

The contribution of traditional pneumococcal virulence factors to colonisation and pathogenicity have been well-studied, but the impact of temperature adaptation on pneumococcal growth, physiology and gene expression need further investigation. The hypothesis of this study is that the pneumococcus has capacity to adapt to different temperature shifts and its phenotype will alter depending on the environmental temperature.

The aims of this study are;

1. Elucidate how temperature shifts affect the pneumococcal growth profile, cell size, and production of proteins known to involve in pneumococcal virulence
2. Analyse the pneumococcal gene expression at different temperatures
3. Generate mutations in selected genes and study their roles in pneumococcal biology using *in vitro* and *in vivo* assays.

To achieve the aims, I determined the pneumococcal phenotypes including growth profile, cell size, and the level of virulence determinants, biofilm formation, capsule production, and pH adaptation by growing the strains in various growth media at 34°C, 37°C, or 40°C. I determined the transcriptional profile of pneumococcus at 34°C and

40°C, relative to 37°C. A possible impact of temperature shift on induction of selected genes was determined using transcriptional *lacZ*-fusions to the promoter of selected genes in the wild type and mutant backgrounds. I also tested the contribution of *gdhA* encoding glutamate dehydrogenase and its role on pneumococcal virulence at high temperature in *Galleria mellonella* insect model.

Chapter 2 Materials and Methods

2.1 Bacterial strains and plasmids

Bacterial strains and plasmids used in this study are listed in Table 2.1. All the pneumococcal mutants were constructed in *S. pneumoniae* type 2 D39 strain background.

Table 2.1. Bacterial strains and plasmids.

Strains	Description	Source
***S. pneumoniae* D39**	Serotype 2 strain	Laboratory stock
Δ*gdhA*	SPD_1158 is deleted	This study
Comp*ΔgdhA*	Complementation of Δ*gdhA*	This study
Δ*ciaR*	SPD_0701 is deleted	This study
Δ*comD*	SPD_2064 is deleted	This study
Δ*merR*^{2}	SPD_0447 is deleted	Al-Bayati *et al*, 2017
Δ*SPD_0132/0133*	SPD_0132 and SPD_0133 are deleted	This study
Δ*SPD_1711*	SPD_1711 is deleted	This study
Δ*SPD_1651*	SPD_1651 is deleted	This study
Reporter strains		
PgdhA::lacZ-wt	D39 with integrated P*gdhA::lacZ* reporter	This study
P*gdhA::lacZ-ΔgdhA*	Δ*gdhA* with integrated P*gdhA::lacZ* reporter	This study
P*ciaR::lacZ*-wt	D39 with integrated P*ciaR::lacZ* reporter	This study
P*ciaR::lacZ-ΔciaR*	Δ*ciaR* with integrated P*ciaR::lacZ* reporter	This study

P*comD::lacZ*-wt	D39 with integrated P*comD::lacZ* reporter	This study
P*comD::lacZ*-Δ*comD*	Δ*comD* with integrated P*comD::lacZ* reporter	This study
P*SPD_0132/0133::lacZ*-wt	D39 with integrated P*SPD_0132/0133::lacZ* reporter	This study
P*SPD_0132/0133::lacZ*-Δ*0132/0133*	Δ*SPD_0132/0133* with integrated P*SPD_0132/0133::lacZ* reporter	This study
P*SPD_1711::lacZ*-wt	D39 with integrated P*SPD_1711::lacZ* reporter	This study
P*SPD_1711::lacZ*-Δ*1711*	Δ*1711* with integrated P*SPD_1711::lacZ* reporter	This study
P*SPD_1651::lacZ*-wt	D39 with integrated P*SPD_1651::lacZ* reporter	This study
P*SPD_1651::lacZ*-Δ*1651*	Δ*1651* with integrated P*SPD_1651::lacZ* reporter	This study
P*merR*^{2}*::lacZ*-wt	D39 with integrated P*merR*^{2}*::lacZ* reporter	Al-Bayati *et al.*, 2017
P*merR*^{2}*::lacZ*-Δ*merR*^{2}	*ΔmerR*^{2} with integrated P*merR*^{2}*::lacZ* reporter	Al-Bayati *et al.*, 2017
P*pp2::lacZ*-wt	D39 with integrated pPP2-*lacZ* reporter	Laboratory stock
Escherichia coli		
One Shot® TOP10	**Plasmid propagation**	**Invitrogen, UK**
gdhA- ciaR- comD- merR^2- SPD_0132/0133- SPD_1711- SPD_1651- OneShot®TOP10	Plasmid propagation; *aadA* (Spectinomycin resistance cassette)	This study
Plasmids		
pDL278	Source of spectinomycin resistance cassette	Yesilkaya *et al.*, 2000

pCEP	Source of kanamycin resistance cassette for genetic complementation	Guiral *et al.*, 2006
pPP2	Source of promoterless *lacZ* gene, resistance to tetracycline and ampicillin	Halfmann *et al.*, 2007

2.2 Bacterial growth conditions and media

Streptococcus pneumoniae strains were grown in brain heart infusion broth (BHI) or in blood agar base (BAB) (Oxoid, UK) supplemented with 5% v/v defibrinated horse blood (Oxoid) in the presence of 5% CO_2 at 34°C, 37°C, or 40°C. For selection purposes, the media was supplemented with different antibiotics with specified concentrations: spectinomycin 100 μg/ml, tetracycline 3 μg/ml, or kanamycin 50 μg/ml.

Pneumococcal strains were also grown in chemically defined medium (CDM) (Table 2.2) supplemented with 55 mM glucose as a sole carbon source. CDM was prepared by mixing 870 ml sterile basal solution, 80 ml amino acids, 10 ml micronutrients, 10 ml nitrogenous bases, 10 ml vitamins, 1 ml pyruvate, and 4 ml choline-HCl as previously described (Zhi *et al.*, 2018). Finally, CDM was filter-sterilised (0.22 μm) and stored at 4°C until needed. BAB was prepared by dissolving 4.0 g in 100 ml distilled water and autoclaved at 121°C for 15 min under 100 kPa. When needed, appropriate antibiotics and 5% v/v of defibrinated horse blood were added to the medium and poured into plates at about 20 ml per plate. When required, Todd-Hewitt broth with yeast (THY) was prepared by mixing 30 g of the Todd-Hewitt (Sigma) in one liter of distilled water supplemented with 0.5% (w/v) yeast extract. Then, broth was autoclaved at 121°C for 15 min under 100 pKa and stored until needed. Luria broth (LB) (10 g/l tryptone, 10 g/l NaCl and 5 g/l yeast extract) or Luria agar (LA) (LB supplemented with 1.5 % w/v bacteriological agar) both from Oxoid, were used to grow *E. coli* for plasmid transformation and propagation. When necessary, the growth medium was supplemented with ampicillin (100 μg/mL) or kanamycin (50 μg/mL). For growth studies, the starter cultures were inoculated in fresh BHI or CDM by diluting the bacterial stock 1 in 100 in fresh medium.

Table 2.2. Composition of CDM used for growth of pneumococcal strains.

Components			
Basal solution	**g l^{-1}**	**Amino acids**	**g l^{-1}**
Na_2-β-glycerophosphate	26	Alanine	0.24
KH_2PO_4	1.0	Arginine	0.124
$(NH_4)_3$ citrate	0.6	Asparagine	0.352
Cysteine-hydrochloride	0.4	Aspartate	0.4
Na-acetate	1.0	Glutamate	0.5
Vitamins	**mg l^{-1}**	Glutamine	0.392
Na-p-aminobenzoate	5.0	Glycine	0.176
D-Biotin	2.5	Histidine	0.152
Folic acid	1.0	Isoleucine	0.212
Nicotinic acid	1.0	Leucine	0.456
Ca D^+ Pantothenate	1.0	Lysine	0.44
Pyridoxamine-hydrochloride	2.5	Methionine	0.124
Pyridoxine-hydrochloride	2.0	Phenylalanine	0.276
Riboflavin	1.0	Proline	0.676
Thiamine-hydrochloride	1.0	Serine	0.34
DL-6,8-Thioctic acid	1.5	Threonine	0.224
Vitamin B_{12}	1.0	Tryptophan	0.052
Nitrogenous bases	**mg l^{-1}**	Valine	0.324
Adenine	10	**Micronutrients**	**mg l^{-1}**
Uracil	10	$MgCl_2$	200

Xanthine	10	$CaCl_2$	38
Guanine	10	$ZnSO_4$	5.0
Others			
Choline-hydrochloride	10 mg l^{-1}	Pyruvate	0.1 g l^{-1}

2.3 Preparation of frozen bacterial stocks

Pneumococci were streaked on blood agar plates and were incubated overnight at 34, 37, or 40°C in a candle jar. A sweep of colonies was inoculated in fresh 10 ml BHI, CDM supplemented with 55 mM glucose, and the tubes were incubated at tested temperatures until they reached 0.5-0.6 at 600 nm. Bacterial cultures were centrifuged at 3500 rpm for 10 min in Allegra TM X-22 centrifuge (Beckman Coulter, USA). The pellet was then suspended in 1 ml of fresh medium containing 15% (v/v) sterile glycerol, and the suspensions were aliquoted to 1.5 ml micro-centrifuge tubes and stored at -80°C until needed.

2.4 Colony forming unit counts

The Miles and Misra method is a quantification technique to enumerate the number of colony forming units in a bacterial suspension (Miles *et al.*, 1938). 20 µl of *S. pneumoniae* cultures grown at 34°C, 37°C, or 40°C until mid- or late-exponential growth phase were inoculated in 180 µl of sterile phosphate-buffered saline (PBS, pH 7.0) in a 96-well microtiter plate. The mixture was then serially diluted down to 10^{-6}. 40 µl of dilutions were plated onto BAB plates which had been divided into 6 sections beforehand. The plates were then incubated overnight at 37°C in a candle jar. The next day, the colonies were counted from the countable sections (30-300 colonies) and the colony-forming unit per ml (CFU/ml) was calculated using the formula below:

$$\text{CFU/ml} = (\text{number of colonies}) \times (\text{dilution factor}) \times (1000/40)$$

2.5 Growth studies in BHI and CDM medium

Growth studies in BHI and CDM supplemented with 55 mM glucose at 34°C, 37°C, and 40°C were done using temperature-controllable Thermo Multiskan^{TM} GO Microplate Spectrophotometer (Thermo Scientific, UK). 197 µl medium was mixed with 3 µl of bacterial suspension containing ~1 x 10^8 CFU/ml in a flat bottom microtitre plate. The spectrophotometer was set up to desired temperature and the growth was monitored over 24 hours by taking a reading every hour at 600 nm. The bacterial growth rates (μ) were calculated from the exponential phase of growth using the following equation:

$$(\mu)\ h^{-1} = (\ln OD_2 \text{ or } CFU_2 - \ln OD_1 \text{ or } CFU_1) / t_2 - t_1$$

Where ln is the natural logarithm of a number, t= time; OD_2 and OD_1 are the cell densities and CFU_2 and CFU_1 are the colony forming unit at time points t_2 and t_1 points, respectively. Furthermore, the growth yield at each temperature was calculated by measuring the highest optical density during the bacterial growth or via measuring the highest cell-forming unit during the bacterial growth.

2.6 DNA extraction

2.6.1 Extraction of D39 chromosomal DNA

Extraction of pneumococcal DNA was done as described previously (Saito and Miura, 1963). Firstly, *S. pneumoniae* was streaked on blood agar plates (BAB) and incubated at 37°C. The next day, one single colony was picked and sub-cultured in 10 ml of BHI, and incubated overnight at 37°C. 200 µl of overnight pneumococcal culture (OD_{600} 1.2-1.5) was inoculated to fresh 10 ml BHI and was grown for 6-8 h. The pneumococcal culture was then centrifuged at 3500 rpm for 10 min, supernatant was discarded, and the pellet was re-suspended in 400 µl TE buffer (1 M Tris-HCl and 500 mM EDTA, pH 8.0) containing 25% (w/v) of sucrose, 60 µl of 500 mM EDTA, 40 µl of 10% (w/v) of SDS, and 2 µl of Proteinase K (12.5 mg/ml). To obtain clear lysate, suspension was incubated. After 2 h incubation, samples were centrifuged at 13,000 rpm for 5 min. The clear upper aqueous phase was taken and mixed with an equal volume of phenol:chloroform:isoamyl

alcohol (25:24:1, v/v, respectively) (Invitrogen, UK). After centrifugation as before, the upper aqueous phase was transferred to a fresh tube without disturbing the protein layer. This process was repeated twice. Finally, the final suspension was mixed with 5 volumes of 100% (v/v) ethanol and 0.1 (v/v) volume of sodium acetate (3 M, pH 5.2). Nucleic acids were collected by centrifugation whilst ethanol was removed. The pellet was then washed with 500 µl of 70% (v/v) of ethanol, dried at room temperature, and re-suspended in 250 µl TE buffer. DNA samples were kept at 4°C until use. Concentration of DNA was measured by using a NanoDropTM spectrophotometer at OD_{260} (Thermo Scientific, UK).

2.6.2 Extraction of plasmid DNA from *E. coli*

Plasmid DNA was extracted from *E. coli* strains for propagation of recombinant constructs. To do this, QIAprep spin Miniprep kit (Qiagen, UK) was used and manufacturer's instructions were followed. Briefly, 10 ml of bacterial cultures were incubated at 37°C overnight in LB broth with appropriate antibiotics with vigorous shaking (200 rpm). 5 ml of overnight culture was centrifuged at 13,000 rpm for 10 min at room temperature, and then supernatant was discarded. The pellet was re-suspended in 250 µL of buffer P1 (resuspension buffer) containing RNase A, and the mixture was mixed by inverting the tube 4-5 times. Then, 250 µL of buffer P2 (lysis buffer) containing 1% sodium dodecyl sulfate (SDS) (w/v) was added to lyse the cellular membranes. The suspension was mixed by inverting the tube to obtain a clear lysate. 350 µl of buffer N3 (neutralization buffer) was added to lysate and mixed by inverting the tubes at several times, and centrifuged at 13,000 rpm for 10 min. After this, 800 µl of supernatant was transferred to QIAprep spin column and re-centrifuged at 13,000 rpm for 1 min. After the process, 0.5 ml of buffer PB (clean-up buffer) was added to the column and centrifuged for 1 min at 13000 rpm. The column was then washed with 0.75 ml of buffer PE (washing buffer), and was centrifuged for 1 min. The QIAprep column was placed on to the collection tube, 50 µl of nuclease-free water was added, and was centrifuged for 1 min at 13000 rpm to elute plasmid DNA. The concentration of the plasmid DNA was measured by using a NanoDropTM spectrophotometer at OD_{260} (Thermo Scientific, UK), and was stored at -20ºC until needed.

2.7 Polymerase Chain Reaction (PCR)

Polymerase chain reaction was done for amplification of desired fragments, mutation detection and DNA modification by using a thermal cycler (Biometra, Germany). DNA fragments were amplified using the DNA polymerases HotStarTaq *Plus* Master Mix (Qiagen, UK) or PrimeSTAR HS premix (Clontech, USA). PrimeSTAR was preferred for amplification since it provides a strong proofreading activity while HotStarTaq *Plus* Master Mix was used for mutation or routine confirmation of cloning because this enzyme can generate high yield and minimises the nonspecific amplification products, primer dimers, and background of PCR mixture by inactivating the Taq polymerase at lower temperatures. A typical 50 µl PCR mixture for PrimeSTAR reaction contained 25 µl PrimeSTAR HS premix (1.25 U/25 µl PrimeSTAR HS DNA Polymerase, 2X dNTP mixture, 2X PrimeSTAR buffer including 2 mM Mg^{2+}), 2 µl DNA template (20 ng/µl), 2 µl of gene specific forward and reverse primer mix (10 pmol each/reaction), and topped up with nuclease free water. The thermocycler was set to run a programme compromising of an initial denaturation at 98°C for 10 min to activate the enzyme, then 30 cycles of amplification consisting of a cycle of denaturation at 98°C for 10 sec, annealing at 55°C or 60°C (depending on Tm of primer mix) for 15 sec, an extension at 72°C for 1 min/1000 bp, and hold at 4°C.

The PCR mixture and set up for HotStarTaq was a slightly different than PrimeSTAR. The PCR reaction was done in a total volume of 20 µl containing 2 µl of DNA (20 ng/µl), 2 µl of specific forward and reverse primer mix (10 pmol each/reaction), 10 µl HotStarTaq *Plus* Master Mix, and 6 µl of DNase-RNase free water. The thermo cycler was set to run 35 cycles of amplification using the following conditions: activation/initial denaturation: 95°C for 5 min, amplification (35 cycles): denaturation 94°C for 45 sec, annealing 55°C or 60°C (depending on Tm of primer mix) for 45 sec, extension 72°C for 1 min/1000 bp, final extension: 72°C for 10 min, and hold at 4°C.

2.8 Electrophoresis

Agarose gel electrophoresis was performed to analyse the size and integrity of nucleic acid fragments. Agarose gel was prepared using a 1% w/v of agarose (Bioline, UK)

dissolved in 100 ml 1X TAE buffer (40 mM Tris-acetate and 1 mM EDTA, pH 8.0) (Sigma). The mixture was then microwaved and cooled at room temperature. Ethidium bromide (from a stock solution of 10 mg/ml in water) was added to a concentration of 0.5 µg/ml agarose gel to stain the DNA. DNA samples were mixed with 3 µl 6X gel loading dye (New England Biolab) and carefully loaded into the wells of the agarose gel. Where appropriate, a 1 kb or 100 bp DNA ladder (New England Biolab, UK) was also loaded to measure the size of the DNA samples. Electrophoresis was carried out at 150 volts for approximately 2 h and the DNA fragments were visualized using the UV transilluminator.

2.9 Restriction digestion of amplified DNA

Restriction endonuclease analysis of DNA sample was performed as instructed by the manufacturer (New England Biolab). For restriction digestion, 1 µl (5U) of each restriction enzyme (*Sph*I-*Bam*HI for mutagenesis or *Nco*I-*Bam*HI for complementation analysis mixed with 1 µg of plasmid or insert DNA (calculated how much needed per reaction), 5 µl of 10X CutSmart™ buffer, and nuclease-free water up to 50 µl. The mixture was then incubated in incubator at 37ºC for up to 4 hours for complete digestion. The digested plasmids and inserts were purified using the DNA purification kit, and analysed by agarose gel electrophoresis (Section 2.8), and stored at -20°C until use.

2.10 DNA ligation reaction

The ligation reaction was set up in a micro-centrifuge tube, and contained 2 µl of T4 DNA Ligase (400 U/µl) (New England Biolabs), 2 µl of 10X T4 DNA ligase reaction buffer, and 1:1 vector:insert molar ratio and nuclease-free water up to 20 µl. The ligation mixture was incubated in a thermo-cycler at 16°C for 16 hours. Then, the reaction was inactivated at 65°C for 10 min. The ligated sample was kept at -20°C until use.

2.11 Genetic transformation of DNA

2.11.1 Transformation into *E. coli*

The ligation reaction was transferred to chemically competent *E. coli* One Shot® TOP10 (Invitrogen, UK) for propagation. 50 µl competent cells and 5 µl ligation products were mixed in a pre-chilled 15 ml BD Falcon polypropylene round bottom centrifuge tube and incubated on ice for 30 min. The mixture was then heat-shocked at 42°C for 45 seconds in a water bath, and transferred immediately on ice for two minutes. 500 µl of pre-warmed LB broth was added into the reaction mixture and incubated at 37°C for 90 minutes on a shaking incubator at 200 rpm. Finally, 250 µl of transformation mixture was plated on LB agar containing appropriate antibiotic for selection of transformants and incubated overnight at 37°C.

2.11.2 Transformation into *S. pneumoniae*

Transformation of ligation products into the pneumococcus was described previously (Bricker and Camilli, 1999). Firstly, *S. pneumoniae* D39 was grown in 10 ml BHI at 37°C overnight. The next day, the culture was diluted 100 fold in 10 ml BHI and incubated at 37°C until it had reached to 0.08-0.1 at 600 nm. 860 µl of culture was mixed with fresh 100 µl NaOH (100 mM), 10 µl $CaCl_2$ (10 mM), 10 µl Bovine Serum Albumin (BSA) (20% w/v), 2 µl of 50 ng/µl competence stimulating peptide (CSP) (Alloing *et al.*, 1990) and approximately 1-1.5 µg of ligation product. The mixture was incubated at 37°C for 3 h and 330 µl of culture was plated out every hour on BAB plates supplemented with appropriate antibiotic. Plates were then incubated overnight at 37°C.

2.12 Mutagenesis

2.12.1 Gene splicing overlap extension PCR (SOEing PCR)

Gene splicing overlap extension PCR (SOEing) is a two-step PCR based method to generate recombinant DNA sequences. This method relies on fusion of two DNA fragments with compatible ends by PCR (Horton, 1995). In this study, SOEing PCR

mutagenesis was used to construct insertion-deletion mutants in *S. pneumoniae*. Briefly, genetic locus representing the left- and right flanks of the target gene to be deleted and spectinomycin resistance gene cassette were amplified. The DNA fragments were then purified by using DNA purification kit (Promega). Subsequently, purified flanking fragments and antibiotic cassette were mixed at 1:1:2 molar ratios, respectively.

2.12.2 Amplification of SOEing fragments and antibiotic resistance cassette

The upstream (left flank) and downstream (right flank) regions were amplified using the proof reading high-fidelity DNA polymerase (PrimeSTAR HS Premix, Takara), and the primer pairs were listed in Table 2.3. Furthermore, spectinomycin resistance cassette (*aadA*, 1158 bp) was amplified from pDL278 (Yesilkaya *et al.*, 2000), using the Spec/F and Spec/R primers The primer sets were designed to contain homologues sequences to target gene and the *aadA* to facilitate fusion of DNA fragments. Then, amplified PCR products were purified using the QIAquick PCR purification kits by following the manufacturer`s protocol.

Table 2.3. The list of primers used for SOEing mutagenesis.
Bold typeface shows the homologous sequence with antibiotic cassette. (LF/F: Left flank forward, LF/R: Left flank reverse, RF/F: Right flank forward, and RF/R: Right flank reverse).

Primers	**Sequence (5'- 3')**
Spec/F	ATCGATTTTCGTTCGTGAAT
Spec/R	GTTATGCAAGGGTTTATTGT
*gdhA*_LF/F	GTAACAAATTCTCCTGCCTCTG
*gdhA*_LF/R	**TATTCACGAACGAAAATCGAT**CAGATGTCATATCGTT CTCC
*gdhA*_RF/F	**AACAATAAACCCTTGCATAAC**GGTATTGTTTAAGATT
*gdhA*_RF/R	ATTTGCCTTAATGGATCTTGGTGGAGAG
*ciaR*_LF/F	AGAGTCTTATCTGGTGGTTTCAGCT
*ciaR*_LF/R	**TATTCACGAACGAAAATCGAT**CTCTCTGCATTTTACAT GAGATAGC
*ciaR*_RF/F	**AACAATAAACCCTTGCAT**GTTCAGTAAACTTAAAAAA
*ciaR*_RF/R	ACATGGAGCTCCGGCTTAATCCCATCATCTC
*comD*_LF/F	ACACCAGATAAGGCCAGTGAATCAG
*comD*_LF/R	**ATTCACGAACGAAAATCGAT**AATCCATTACTCTTTCC
*comD*_RF/F	**ACAATAAACCCTTGCATAAC**GGGAATTTGAATGAAAG
*comD*_RF/R	TTTATCTTGAAATAGGACAACGATGGTC
merR^2_LF/F	TCGATAAATCCCAGTTCAAACTT
merR^2_LF/R	**TATTCACGAACGAAAATCGAT**GCGAAATTCTTTTTCCT TCATTT

merR^2_RF/F	**AACAATAAACCCTTGCATAAC**TCACCTTTTGGTCGCG
merR^2_RF/R	GTTAGGCTCCCATTTTGGTCAAGACATTCA
0132/0133_LF/F	CAACACGTTTGAGGTAATTTGGCAC
0132/0133_LF/R	**TATTCACGAACGAAAATCGAT**GAGGAAAGTTCAATGA CAAATTTTGACATTC
0132/0133_RF/F	**AACAATAAACCCTTGCATAAC**GTCATGCTAGATAAGA
0132/0133_RF/R	AACAGCATAAACAGGGCATCTAAGC
1711_LF/F	TCTGGAGCAGGGTGAGGATG
1711_LF/R	**ATTCACGAACGAAAATCGAT**ATTATACATATTTTCTTC CTCC
1711_RF/F	**ACAATAAACCCTTGCATAAC**GCCATTTTAAGAATTAA
1711_RF/R	GGATTTGCACCTGCTGTGACG
1651_LF/F	AATCGCTTCCTGACGCCTAG
1651_LF/R	**TATTCACGAACGAAAATCGAT**TTTCCAGTTTCACTGA CGAG
1651_RF/F	**AACAATAAACCCTTGCATAAC**CTATAGCTAGTAACAT
1651_RF/R	AAAAGCGAAAGAGAAACGAGATTTGGCACC

2.12.3 Fusion of SOEing fragments and transformation into *S. pneumoniae*

The left and right flanking regions were fused with amplicons for *aadA* using X_LF/F and X_RF/R primers (where X represents the gene code or name) in Table 2.3 to generate SOEing product. The mixture for PCR contained 2 µl from flanking PCR products and the *aadA* amplicons (~20 ng/µl each), 25 µl 2X PrimeSTAR HS Premix, 1 µl of each primer (1 pmol/µl), and the volume was brought up to 50 µl with nuclease free-water.

PCR condition used to fuse the fragments was mentioned in section 2.7. The fused products were visualized by agarose gel electrophoresis and purified by using the purification kit (Promega, UK). The final product was then transformed into *S. pneumoniae* as described in section 2.11.2. The next day, recombinant colonies were selected form the BAB plate containing spectinomycin (100 µg/ml).

2.12.4 Confirmation of gene deletion/replacement with antibiotic cassette

Insertion-deletion mutation was confirmed via colony PCR using HotStarTaq *Plus* Master Mix (NEB, UK) as mentioned in Section 2.7. To confirm the gene replacement, different primer sets were used. The first set was the primers used to amplify fusion of flanks with spectinomycin cassette (Table 2.3).

The second primer set was designed as X_Ext/F and X_Ext/R to amplify the entire mutated region plus approximately 400 to 600 bp away from the up- and downstream of the target genes (Table 2.4). The third set of primers were designed as X_Ext/F-Spec/R and the Spec/F-X_Ext/R to amplify the targeted flanking region including antibiotic cassette with external sequences, which is around 200 bp for each side. X_Ext primers were placed in Table 2.4, while Spec/F and Spec/R primers were placed in Table 2.3. The last primer set, Spec/F and Spec/R, was designed to amplify the spectinomycin resistance gene (*aadA*). These primer sets were generated to confirm the presence of *aadA* cassette in the genome of the mutant strains, therefore, no product was expected from the wild type. Briefly, the DNA of well-isolated colony was prepared by suspension in 100 µl of nuclease free water. The suspension was heated at 95°C for 10 min and cooled on ice for 2 min. Then, the template was obtained by centrifugation of suspensions at 13,000 rpm for 5 min. The PCR mixture contained 2 µl of DNA, 2 µl of primers (10 pmol/reaction), 10 µl HotStarTaq *Plus* Master Mix, and 6 µl of nuclease-free water. The conditions used for amplifications have been provided in section 2.7. Finally, the PCR products were analysed using gel electrophoresis (Section 2.8).

Table 2.4. The list of primers used for confirmation of mutagenesis.
(LF/F: Left flank forward, LF/R: Left flank reverse, RF/F: Right flank forward, and Ext: External).

Primers	Sequence (5'- 3')
*gdhA*_Ext/LF/F	GATTACAGTCTAAAAGCTCTATAATC
*gdhA*_Ext/RF/R	TCATGTTTTTAAGCTACTACTGTAG
*ciaR*_Ext/LF/F	AGAATCTTGCAGGACTCCCAGCAGT
*ciaR*_Ext/RF/R	TTCGGTGGACGATAAGCTTCATGGAC
*comD*_Ext/LF/F	GTTGTAACAGTTGGGAAACTGAAAG
*comD*_Ext/RF/R	GACTATTTTATCCGCCATAGCTCAG
0132/0133_Ext/LF/F	CAAGGACTGACTGGGTAAACAGC
0132/0133_Ext/RF/R	AACACGCACGCTTTACCTAGAC
1711_Ext/LF/F	GAAGACCAAGTTGTCGGAACACC
1711_Ext/RF/R	TGCAGCCGTATCTTCTCGTTC
1651_Ext/LF/F	CCATCGGAGCTTGTCTTCTCTAC
1651_Ext/RF/R	CCTCTTTGTCATCAACCGTACC

2.13 Genetic complementation of mutant strains

Mutagenesis of a gene may result in unintended effects on the expression of downstream genes, called polar effect. To eliminate this, selected mutant strain was complemented with an intact copy of the relevant gene. The method of genetic complementation was described previously (Guiral *et al.*, 2006). To do this, I used pCEP plasmid which contains homologous sequence to pneumococcal genome and does not affect the physiology of the pneumococcus as it mediates genomic integration of intact gene into a transcriptionally silent site (Alloing *et al.*, 1990). First, the plasmid was extracted using the QIAprep spin Miniprep kit as mentioned in section 2.6.2. Since only *gdhA* (SPD_1158) was selected

for detailed study for its role on thermoregulation, *gdhA* mutant copy was complemented. Briefly, using the primers *gdhA*-Comp/F and *gdhA*-Comp/R containing the restriction sites *Nco*I and *BamH*I, the coding region of the gene was amplified (Table 2.5). The amplified product was then purified and analysed by agarose gel electrophoresis. The amplified region and the pCEP plasmid were both digested with incorporated restriction enzymes (Section 2.9) and ligated as described in Section 2.10.

Table 2.5. The list of primers used for genetic complementation.
Bold typeface shows incorporated restriction sites, *Nco*I and *Bam*HI in forward and reverse primers, respectively.

Primers	Sequence (5'- 3')
gdhA-Comp/F	GCG**CCATGG**CTCTTCCTCAACTGTCAATAT
gdhA-Comp/R	GGC**GGATCC**TTAAACAATACCTTGTGC
Mal/F	GCTTGAAAAGGAGTATACTT
pCEP/R	AGGAGACATTCCTTCCGTATC

2.13.1 Transformation of modified pCEP plasmid into *E. coli*

After ligation, the new construct was transferred into *E. coli* OneShot® TOP10 chemically competent cells (Section 2.11.1) and plated on the LA medium supplemented with kanamycin (50 μg/ml). The next day, the recombinant colonies were tested by colony PCR using the HotStarTaq *Plus* Master Mix using the primers mal/F and pCEP/R to confirm successful cloning (Table 2.5). These primers amplify a 263 bp sequence of empty plasmid and the region surrounding the cloning site and cloned gene with its promoter region in the complemented mutant or recombinant plasmid.

2.13.2 Transformation of modified pCEP plasmid into the mutant strain

Transformation of a recombinant plasmid into a pneumococcal mutant strain was carried out as in Section 2.11.2. The complemented mutant strain was able to grow in a medium containing kanamycin and spectinomycin unlike the mutant strain which could grow only in the presence of spectinomycin. The recombinant colonies were tested by PCR using the HotStarTaq *Plus* Master Mix (Section 2.7) using the primers Mal/F and pCEP/R, and the primers 1158Comp/F and 1158Comp/R (Table 2.5).

2.14 Construction of *lacZ* fusions and transformation into *E. coli*

Transcriptional fusion of the selected promoters with the *lacZ* reporter gene was constructed to study gene expression in *S. pneumoniae* as previously described (Zhi *et al.*, 2018). For this, an integrative plasmid pPP2 was used (Halfmann *et al.*, 2007a). Promoter regions of target genes were determined using the bacterial promoter prediction tool called BPROM in Softberry software. BPROM has a linear discriminant function, which combines functional motifs and oligonucleotide composition of these sites. In BPROM output, the software scores with 'weights' of two conserved promoter boxes (-10 and -35) and assigns the first nucleotide of the transcript (Solovyev *et al.*, 2010). The DNA fragments containing the putative promoter regions were amplified using the primers designed to incorporate *Sph*I and *Bam*HI restriction sites (Table 2.6). The amplified promoter regions and the plasmid pPP2 were digested and ligated together to generate recombinant pPP2. The ligation products were then transformed into *E. coli* for propagation (Section 2.11.1) and the transformants were selected on LA supplemented with ampicillin (100 μg/ml). To confirm the successful cloning, colony PCR was performed using the primers Fusion-F and Fusion-R, which are designated to amplify the cloned insert (Table 2.6).

Table 2.6. The list of primers used for the construction of *lacZ*-fusions.
Bold typeface shows incorporated restriction sites, *Sph*I and *Bam*HI.

Primers	Sequence (5'- 3')
P*gdhA*-Fusion-F	GAA**GCATGC**CTCTTCCTCAACTGTCAAT
P*gdhA*-Fusion-R	GAA**GGATCC**GATATATTCTTTAGCAGA
P*ciaR*-Fusion-F	GAC**GCATGC**GTAACATCGGTATGGGAATCAAG
P*ciaR*-Fusion-R	GCG**GGATCC**GAAACTCCTCCTTATTAAA
P*comD*-Fusion-F	CC**GGATCC**TGGGAATTTTCCCGGCTTT
P*comD*-Fusion-R	CG**GCATGC**CCTGTTCCAATTTAACTGTG
P*0132/133*-Fusion-F	CG**GGATCC**AACACATTCCTATCTTTTTG
P*0132/133*-Fusion-R	CG**GCATGC**GATTGTCAAGAATGTCAAAA
P*1711*-Fusion-F	CG**GGATCC**TCAGCTTCATCCACAACC
P*1711*-Fusion-R	CG**GCATGC**CTTAGCTTTCAATACCATTCAT
P*1651*-Fusion-F	GC**GGATCC**ACAATATCTTGATTGGACGGCT
P*1651*-Fusion-R	CG**GCATGC**CGCCAATTAAATAATGAGAAAGT
Fusion-F	CTACTTGGAGCCACTATCGA
Fusion-R	AGGCGATTAAGTTGGGTAAC

2.14.1 Transformation of recombinant plasmid into *S. pneumoniae*

Recombinant reporter plasmids were extracted from *E. coli* (Section 2.6.2) and transformed into *S. pneumoniae* (Section 2.11.2). The incorporation, into the pneumococcal genome, of the fusion constructs is mediated by homologous recombination. Finally, the transformants were selected on blood agar plates containing 3 μg/ml of tetracycline and the recombinant colonies were analysed by colony PCR using Fusion-F and Fusion-R (Table 2.6) and gel electrophoresis (Section 2.8).

2.14.2 β-galactosidase activity assay

β-galactosidase activity assay is a simple, inexpensive, and basic colorimetric assay to quantify promoter strength. To do this, a previously published protocol was followed (Miller, 1972). This assay relies on the cleavage of 2-Nitrophenyl from chromogenic colourless substrate O-Nitrophenyl β-D-galactopyranoside (ONPG), by β-galactosidase, which then turns yellow, and quantification of the product spectrophotometrically (Figure 2.1).

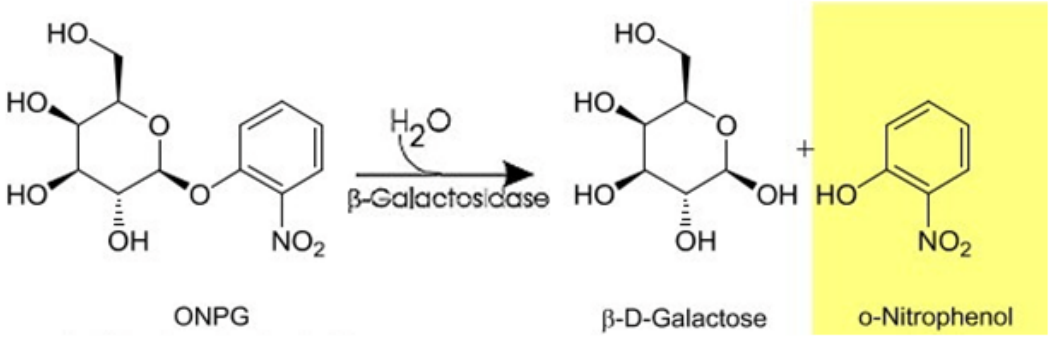

Figure 2.1. The schematic illustration of β-galactosidase assay.
The assay relies on the hydrolysis of the chromogenic substrate 2-Nitrophenyl β-D-galactopyranoside (ONPG) to galactose and 2-Nitrophenyl by β-galactosidase. The figure is adapted from (Li *et al.*, 2012).

Briefly, pneumococcal reporter strains, 1:100, were inoculated into 10 ml of fresh BHI and incubated until the OD_{600} had reached to mid-exponential phase (0.6-0.8) at 34°C, 37°C, or 40°C. Then, 10 ml CDM supplemented with 55 mM glucose as a carbon source was inoculated at a 1:100 ratio with *S. pneumoniae*, and were grown to mid-exponential phase micro-aerobically.

Afterwards, the pellets were harvested from 3 ml of bacterial culture by centrifugation at 13,000 rpm for 10 min. The supernatant was discarded, the pellets were re-suspended with 2 ml of ice-cold Z buffer (0.80 g $Na_2HPO_47H_2O$, 0.28 g $NaH_2PO_4H_2O$, 0.5 ml 1 M KCl, 0.05 ml 1 M MgSO4, 0.175 ml β-mercaptoethanol, 40 ml dH_2O, pH 7.0), and the

absorbance was measured against Z buffer as a blank at 600 nm. From remaining suspension, 500 µl of the suspensions was further diluted with 500 µl Z Buffer, added with one drop of Triton X-100 (Sigma), and incubated 10 min at 30°C. After the cells lysis, 200 µl of o-Nitrophenyl-β-galactoside (ONPG, 4 mg/ml stock) was added into the samples, vortexed and incubated at 30°C. When sufficient yellow colour developed, the reactions was stopped by adding 500 µl of 1 M Na_2CO_3, and reaction time was recorded. Samples were then centrifuged at 14,000 rpm (Microfuge, Sigma) for 5 minutes, and the OD_{420} of the sample was measured using Z buffer as a blank. The specific β-galactosidase activity was determined by the following equation:

$$\text{Miller Units} = 1000 \times (OD_{420}) / (T \times V \times OD_{600})$$

Where;

T= time of the reaction in minutes,
V= Volume of culture used in the assay (0.5 ml),
Miller unit represents nmol of *o*-nitrophenol/min/ml of cells/OD_{600}.

Finally, Miller units of reporter strains were normalized against the cfu/ml which had been counted prior to the assay.

2.15 Enzyme assays

2.15.1 Preparing cell lysates by sonication

Bacterial cell lysate was prepared according to a previous protocol (Terra *et al.*, 2010). Pneumococcal strain was grown in 10 mL of BHI or CDM supplemented with 55 mM glucose until mid-exponential growth phase at 34°C, 37°C, or 40°C and then centrifuged at 3000 g for 10 min. Then, the supernatant was discarded and the pellet was re-suspended in 1 ml of PBS. The bacterial suspension was transferred into a microcentrifuge tube and incubated on ice for 10 min. The sonicator (Soniprep 150) was adjust to an amplitude of 8 microns. Sonication was performed for 15 sec on, 45 sec off. The cells were kept on ice at all times and the sonication pulses were repeated 6 to 8 times. The cell lysate was centrifuged at 4°C for 1 min at 16,000 g, and the supernatant was collected. The lysate was filtered (0.22 µm, Thermo Scientific) and was stored at -80°C until further use.

2.15.2 Quantification of protein concentration-Bradford assay

After sonication, protein concentration in the cell extracts was measured using the Bio-Rad protein reagent (Bio-Rad Laboratories Inc., USA) following the previously described method (Bradford, 1976). Firstly, the standard curve was prepared with the known concentration of bovine serum albumin (BSA). In a 96 well microtiter plate, 190 µl of Bradford reagent was mixed with 0-0.8 mg/ml BSA and the reaction was incubated for 5 min at room temperature. Then, the concentration was measured at 595 nm in a Bio-Rad microplate reader Model 680. The standards were then plotted and the trendline was adjusted. To measure the protein concentration of unknown samples, 10 µl of clear cell lysate was mixed with 190 µl of Bradford reagent and same protocol was followed. The concentration of unknown protein determined in comparison to the standard curve prepared with the known concentration of BSA.

2.15.3 Haemolytic assay

Haemolytic activity of pneumococcal lysate was analysed to determine the production of pneumolysin as previously described (Owen *et al.*, 1994). Briefly, 5 ml PBS in one tube and 5 ml defibrinated sheep blood (Oxoid) in a second tube were centrifuged at 3000 rpm at 4°C for 15 min. Supernatant was discarded and 200 µl of blood cell pellet was mixed with 4800 µl of PBS (pH 7.0) to make 4% v/v red blood cells (RBC). 50 µl PBS was added to each well in a 96-well round bottom microtiter plate. A two-fold dilutions of 50 µl of lysate was mixed with PBS. Afterwards, 50 µl of 4% v/v RBC was added to each well and the microtiter plate was incubated at 37°C for 30 min. Haemolysis was observed directly by eye. The haemolytic unit (HU) was calculated as the highest dilution of lysate causing 50% lysis of RBC in 30 min at 37°C.

2.15.4 Neuraminidase assay

The total level of neuraminidase activity in pneumococcal cell lysates were determined by using a quantitative assay by utilising 2-O-(p-nitrophenyl)-α-D-N-acetylneuraminic acid (pNP-NANA, Sigma) as previously described (Manco *et al.*, 2006). The pNP-NANA

is cleaved by neuraminidase with the release of free p-nitrophenol (pNP), which can be assayed by its absorbance at 405 nm. Aliquots of 25 µl of cell lysate in dilution buffer (38.4 ml 100 mM citric-acid phosphate, pH 6.6, 3.12 ml 25 mg/ml BSA, 35.5 ml dH_2O, 160 µl 10% (w/v) sodium azide) was added in triplicate to each well in a flat bottom 96-well plate. Afterwards, 25 µl of pNP- NANA was added to the wells and mixed well. The reaction mixture was incubated statistically for 2 h at 37℃. The reaction was stopped by addition of 100 µl ice cold 0.5 M Na_2CO_3 (pH 9.6) and the absorbance was measured at 405 nm by ELISA plate reader (Tecan Infinitive F50). To determine the level of neuraminidase in cell lysates, a standard curve was prepared using known concentration of pNP.

2.16 Biofilm formation assay

Biofilm formation of pneumococcal strains were analysed at different temperatures using the crystal violet attachment assay (Feoktistova *et al.*, 2016). Starter cultures of pneumococcal strains were inoculated from frozen glycerol stocks into THY medium and incubated overnight at 34°C, 37°C, or 40°C. Next day, cultures were centrifuged at 13,000 rpm for 15 min, supernatants were discarded, and pellets were re-suspended in 2 ml TY. Bacterial density was measured at 600 nm. The culture was then serially diluted in the same media to an OD_{600} of 0.05–0.1. After overnight growth, the excess media was carefully aspirated, and biofilms were washed with 200 µl PBS at least three times to remove weakly or non-adherent bacteria. Attached cells were stained with 50 µl crystal violet (0.1%) for 15 min, excess stain was discarded and re-washed with distilled water three times. Subsequently, biofilm was dissolved in 200 µl of 95% ethanol and measured at OD_{595}.

2.17 Glucuronic acid assay

The method to quantify the level of capsular polysaccharide (CPS), which is composed of a polymer of sugars, was described previously (Zhi *et al.*, 2018). Samples for the determination of the capsular glucuronic acid were prepared in CDM supplemented with glucose. Cultures were grown until mid-exponential phase, OD_{600} 0.5-0.6, at 34°C, 37°C,

or 40°C. Five hundred microliters of bacterial culture was mixed with 100 µl of 1% (v/v) Zwittergent 3-14 detergent (Sigma-Aldrich) in 100 mM citric acid (pH 2.0), and then the mixture was incubated at 50°C for 20 min followed by precipitation with 1 ml of ethanol (99%). The pellet was dissolved in 200 µl of distilled water, and mixed with 1.2 ml of 12.5 mM borax (Sigma-Aldrich) in H_2SO_4. The suspension was vortexed, boiled at 100°C for 5 min, cooled down to room temperature, and mixed with 20 µl of 0.15% 3-hydroxydiphenol (Sigma-Aldrich). Absorbance was measured at a wavelength of 520 nm. Glucuronic acid standards were prepared, and the glucuronic acid concentration was calculated based on the equation obtained from a standard curve.

2.18 Determination of cell size

Bacterial cell size is firmly controlled by environmental stress (Chien *et al.*, 2012). Pneumococcal strains were grown overnight in CDM supplemented with 55 mM glucose. Bacterial suspensions were Gram-stained (Coico, 2005). Briefly, 20-30 µl of culture was taken with a sterile loop and emulsified on the surface of the microscope slide. The film was fixed by passing the slide slowly through Bunsen flame. The slide was flooded with crystal violet for 1-2 min and excess stain was discarded. Then, it was flooded by Gram`s iodine and let stand for 1-2 min and excess stain was discarded again. For 2-3 sec, the slide was washed with acetone followed by washing thoroughly with tap water. As a counter staining, the slide was flooded with safranin. After 2 min, the slide was washed with tap water and air-dried. Pneumococcal cell size was measured using Prion microscope equipped with a digital camera (Nikon) and image analysis software (Infinite).

2.19 Growth studies on nitrogen-source medium

As previously described in Section 2.5, pneumococcal strains were grown in BHI or CDM supplemented with 55 mM glucose or in blood agar base. In addition, the growth of the wild type and mutant strain Δ*gdhA* was carried out in CDM-glucose medium without or with different concentration of glutamine or glutamate. The spectrophotometer was set up on relevant temperature and the program was run for 24 hours by taking a reading

every hour at 600 nm. Optical densities at each condition were recorded and the bacterial growth rates (μ) and yields were calculated (Section 2.5).

2.20 Glutamate dehydrogenase enzyme activity assay

Glutamate dehydrogenase activity (GDH) of pneumococcal strains at different temperatures was determined using a commercial kit (Biovision, USA). Briefly, bacterial cultures were grown overnight at 34°C, 37°C, or 40°C in CDM supplemented with 55 mM glucose (Section 2.5). The next day, the cultures were centrifuged at 13,000 rpm for 10 min, re-suspended in 1 ml ice-cold PBS (pH 7.0), and sonicated to receive bacterial lysates (Section 2.15.1). The samples, 50 µl/well, were then added into 96-well plate. 100 µl of reaction mixture (82 µl assay buffer, 8 µl GDH developer and 10 µl glutamate (2 M)) were mixed with lysate suspension. The plate was incubated for 3 min at 37°C and OD_{450} nm was recorded. The plate was incubated for up to 2 h and the density was re-measured. One unit activity is the amount of enzyme to generate 1 µmol of NADH per min at pH 7.6. GdhA activity of samples was calculated using the following equation;

$$\text{GDH Activity} = B / (T \times V) \times \text{Sample Dilution Factor} = \text{nmol/min/ml} = \text{mU/ml}$$

Where,

B is the NADH amount from standard curve (in nmol),
T is the time incubated (in min).
V is the sample volume added into the reaction well (in ml).

NADH standard curve was prepared by diluting 10 µl of the 10 mM NADH stock solution with 90 µl of GDH Assay buffer to generate a 1 mM NADH standard. 0, 2, 4, 6, 8, and 10 µl of the 1 mM NADH standard were added into a 96-well plate to generate 0, 2, 4, 6, 8, and 10 nmol/well standard. The final volume was adjusted to 50 µl with assay buffer. This plate was also incubated for 3 min at 37°C and measured at 450 nm. Glutamate dehydrogenase activity was calculated by applying the enzyme activity between two

different time points to the NADH standard curve to measure the concentration of NADH produced by GDH.

2.21 *In vitro* survival assay at different pH conditions

Overnight culture in CDM supplemented with 55 mM glucose was diluted to obtain OD_{600} of 0.05 in fresh medium, and incubated at different temperatures. The pneumococcal strains were grown until mid-exponential phase (OD_{600} 0.6-0.8) at 34°C, 37°C, or 40°C, centrifuged at 13,000 rpm for 10 min, the supernatants were discarded and the pellets were re-suspended in 1 ml PBS (pH 7.0). The buffers (pH 5.0 to 8.0) were prepared as shown in Table 2.7. 180 µl buffer was mixed with 20 µl bacterial suspension in a 96-well plate and incubated at different temperatures for 30, 60, 90 and 120 min. The ability of cells to survive at different pH was monitored by measuring CFU/ml, which were determined by plating the serial dilutions of bacterial culture. For each sample, 40 µl diluted culture was plated in BAB plate, and colonies were counted after approximately 16-18 h of incubation (Section 2.4).

Table 2.7. The composition of buffers used to adjust culture pH.

pH	**Citric acid monohydrate (0.1 M)**	**Tri-sodium citrate (0.1 M)**
5.0	35 ml	65 ml
5.4	25.5 ml	74.5 ml
6.0	11.5 ml	88.5 ml
pH	**Na_2HPO_4 (0.2 M)**	**NaH_2PO_4 (0.2 M)**
6.4	13.25 ml	36.75 ml
7.0	30.5 ml	19.5 ml
7.4	40.5 ml	9.5 ml
8.0	47.35 ml	2.65 ml

2.22 Fermentation end product analysis during growth at different temperatures

Pneumococcal culture (10 ml) was grown in CDM supplemented with 55 mM glucose as the sole carbon source at 34°C, 37°C, or 40°C until they reached mid-exponential growth phase (OD 0.6-0.8 at 600 nm). From each culture, 2 ml of sample was taken out at this stage and centrifuged at 16000 x g for 2 min at 4°C. The supernatant was collected and stored at -20°C until further use. The concentration of L-lactic acid, formic acid and acetic acid were measured at tested temperatures.

2.22.1 Measuring the concentration of L-lactic acid

Lactic acid was measured following the procedure of L-Lactic Acid Assay kit supplied by Megazyme, Ireland. The method relies on two enzymatic reactions involving L-lactate dehydrogenase (L-LDH) and D-glutamate-pyruvate transaminase (D-GPT). In the first reaction, L-lactic acid is oxidised to pyruvate by nicotinamide-adenine dinucleotide (NAD^+) as shown in (**a**);

a) L-Lactic acid + NAD^+ $\xleftrightarrow[\text{L-LDH}]{}$ Pyruvate + NADH + H^+

To trap the pyruvate product, a second reaction is needed as the first reaction lies in favour of L-lactic acid and NAD^+. This reaction is done by the conversion of pyruvate to D-alanine and 2-oxoglutarate using the enzyme D-glutamate-pyruvate transaminase (D-GPT) in the presence of a large excess of D-glutamate as shown in (**b**);

b) Pyruvate + D-glutamate $\xrightarrow[\text{D-GPT}]{}$ D-alanine + 2-oxoglutarate

The amount of NADH, which is stoichiometric with the amount of L-lactic acid formed in the coupled reaction is measured by the increase in absorbance at 340 nm. For this assay, a quartz cuvette with 1 cm light path was used to measure the concentration of end products. Along with the experimental samples, a blank and a standard sample were also assayed. All samples contained 1.5 ml dH_2O, 500 µl of solution 1 (D-glutamate buffer), 100 µl solution 2 (NAD^+) and 20 µl of suspension 3 (D-GPT). Then, 100 µl of dH_2O, or 100 µl unknown sample or 100 µl standard solution (0.15 mg/ml) were added to the blank, experimental sample, or standard, respectively. The cuvettes were incubated at room temperature for 3 min and the first absorbance (A1) was recorded at 340 nm. Then, 20 µl of suspension 4 (L-LDH) was added into each cuvette and incubated again at room temperature for 10 min and the second absorbance (A2) was recorded at 340 nm. The absorbance difference (A2-A1) between the blank and sample provided the $\Delta A_{\text{L-Lactic acid}}$. Finally, the concentration of L-Lactic acid was calculated using the following formula;

$$c = (V \times MW) / (\varepsilon \times d \times v) \times \Delta A_{\text{L-Lactic acid}} \text{ [g/l]}$$

Where,

V= final volume (ml),
MW= molecular weight of L-lactic acid (g/mol),
ε=extinction coefficient of NADH at 340 nm = 6300 ($l \times mol^{-1} \times cm^{-1}$),
d= light path (cm),
v= sample volume (ml).

2.22.2 Measuring the concentration of formic acid

Formic acid was measured using the Formic Acid Assay Kit (Megazyme, Ireland). In this method, in the presence of NAD^+, formic acid is oxidised to carbon dioxide (CO_2) by the enzyme formate dehydrogenase (FDH) with the formation of NADH as illustrated in (**a**):

a) $$\text{Formic acid} + NAD^+ \xrightarrow[\text{FDH}]{} CO_2 + NADH + H^+$$

The amount of NADH, which is stoichiometric with the amount of formic acid, and is measured by the increase in absorbance at 340 nm.

The experimental sample, blank sample and standard sample were also used in this assay. The cuvettes contained 2 ml dH_2O, 200 µl of solution 1 (buffer) and 200 µl solution 2 (NAD^+). Subsequently, 100 µl of dH_2O, or 100 µl of experimental sample supernatant from section 2.22.1, or 100 µl of standard solution (0.1 g/l formic acid) was added to the blank, experimental sample or standards, respectively. The samples were then incubated at 25°C for 5 min and the first absorbance (A1) was recorded at 340 nm. Afterwards, 50 µl of suspension 3 (FDH) was added into each cuvette and incubated at 25°C for 12 min and the second absorbance (A2) was recorded at 340 nm. The absorbance difference (A2-A1) was determined for both blank and sample provided the $\Delta A_{\text{formic acid}}$. The concentration of formic acid was calculated using the following formula:

$$c = (V \times MW) / (\varepsilon \times d \times v) \times \Delta A_{\text{Formic acid}} \text{ [g/l]}$$

Where;

V= final volume (ml),
MW= molecular weight of formic acid (g/mol),
ε= extinction coefficient of NADH at 340 nm = 6300 (l x mol^{-1} x cm^{-1}),
d= light path (cm),
v= sample volume (ml).

2.22.3 Measuring the concentration of acetic acid

Acetic acid was measured using the Acetic Acid Assay Kit (Megazyme, Ireland). In this method, in the presence of ATP, acetate kinase (AK) converts acetic acid to acetyl-phosphate and adenosine-5'-diphosphate (ADP), as illustrated in (**a**):

$$\textbf{a)}\quad \text{Acetic acid} + \text{ATP} \xrightarrow{\text{AK}} \text{Acetyl-phosphate} + \text{ADP}$$

The reaction (**a**) is significantly accelerated by the action of phosphotransacetylase (PTA), which rapidly converts acetyl-phosphate to acetyl-CoA and inorganic phosphate, in the presence of coenzyme A (CoA), as described in (**b**):

$$\textbf{b)}\quad \text{Acetyl-phosphate} + \text{CoA} \xrightarrow{\text{PTA}} \text{Acetyl-CoA} + \text{Pi}$$

Afterwards, in the presence of pyruvate kinase (PK), the ADP formed in reaction (**a**) is re-converted into pyruvate and ATP and pyruvate by phosphoenolpyruvate (PEP) as described in (**c**):

$$\textbf{c)}\quad \text{ADP} + \text{PEP} \xrightarrow{\text{PK}} \text{Pyruvate} + \text{ATP}$$

Pyruvate is then reduced to D-lactic acid by reduced nicotinamide-adenine dinucleotide (NADH) and NAD^+, in the presence of D-lactate dehydrogenase (D-LDH), as shown in (**d**):

$$\textbf{d)}\quad \text{Pyruvate} + \text{NADH} \xrightarrow{\text{D-LDH}} \text{D-lactic acid} + NAD^+$$

The amount of NAD^+ formed in the above reaction is stoichiometric with the amount of acetic acid, which is measured by the increase in absorbance at 340 nm.

The experimental sample, blank sample and standard sample were included in this assay. The cuvettes contained 2 ml dH_2O, 500 µl of solution 2 (NADH/ATP/PEP/PVP buffer), 20 µl solution 3 (CoA) and 20 µl suspension 4 (D-LDH/PTA/PK). Afterwards, 100 µl of dH_2O, or 100 µl of experimental sample supernatant from section 2.22.1, or 100 µl standard solution (0.10 mg/ml) were added to the blank, the experimental sample, or standards, respectively. The cuvettes were incubated at 25°C for 2 min and the first absorbance (A1) was recorded at 340 nm. Then, 20 µl of suspension 5 (AK) was added into each cuvette and incubated at 25°C for 4 min and the second absorbance (A2) was recorded at 340 nm. The absorbance difference (A2-A1) for blank and sample provided the $\Delta A_{Acetic\ acid}$. The concentration of acetic acid was calculated using the following formula below;

$$c = (V \times MW) / (\varepsilon \times d \times v) \times \Delta A_{Acetic\ acid}\ [g/l]$$

Where;

V= final volume [ml],
MW= molecular weight of acetic acid [g/mol],
ε= extinction coefficient of NADH at 340 nm = 6300 [l x mol^{-1} x cm^{-1}],
d= light path [cm],
v= sample volume [ml].

2.23 *In vivo* studies

2.23.1 Bacterial inoculum preparation

To prepare the standard inoculum, pneumococcal strains were grown in BHI overnight at 34°C, 37°C, or 40°C. Next day, cultures were centrifuged at 3000 rpm for 15 min and the pellet was resuspended in 1 ml of BHI supplemented with 20% (v/v) filter sterilised fetal calm serum. 800-1000 µl of re-suspended culture was used to re-inoculate fresh 10 ml BHI serum broth to bring the OD 0.8-1.0 at 600 nm. The tubes were then incubated until

OD 1.5-1.6 at 600 nm at different temperatures. Finally, aliquots were made, and stored at -80°C until needed.

2.23.2 *Galleria mellonella* model of pneumococcal infection

In recent years, *G. mellonella* has been introduced as an alternative model to study the microbial pathogenicity. The virulence of pneumococcal strains at different temperatures was tested on larvae of this insect. Larvae were acquired from Livefood, UK, and those weighing 25-30 mg with white, milky appearance were used for infection. To calculate the LD_{50}, $1x10^4$, $1x10^5$, $5x10^5$, and $1x10^6$ CFU pneumococci prepared in 10 µl of PBS were administered second pro-leg of the larvae. For each strain at each temperature, 10 larvae were injected. In addition, a control group of larvae was injected with 10 µl of PBS as technical control. Infected larvae were incubated at the respective growth temperature of bacterial inoculum in dark for up to 4 days. The larvae were regularly monitored, and the survival time was recorded.

2.24 Statistical analysis

GraphPad prism version 7 (Graphpad, California, USA) was used for data analysis. The experimental results were described as mean ± standard error of the mean (SEM). One- or two-way analysis of variance (ANOVA) followed by Tukey multiple comparison test were used to compare the groups for growth studies, cell size determination, enzyme assays, and β-galactosidase assay. Less than 0.05 of *p* value was regarded statistically significant. Significance was defined as * $p<0.05$, ** $p<0.01$, *** $p<0.001$ and **** $p<0.0001$. If there was no significance, it was shown as “ns”.

Chapter 3 Results

3.1 Part A: Thermophysiology of *S. pneumoniae* D39 at different temperatures

Streptococcus pneumoniae resides asymptomatically in the nasopharynx of individuals, but under certain circumstances, it disseminates to the lower respiratory tract and converts its state from a commensal to pathogen, leading to severe diseases such as pneumonia, meningitis, and bacteraemia (Marks *et al.*, 2012a). Pneumococcus encounters varying temperatures at different human tissues, hence it is important to have mechanisms to adapt to ensure optimal survival. To determine if temperature would have any influence on pneumococcal biology, initially, I assessed the impact of different temperatures on the selected phenotypic properties of the wild type strain D39, such as growth, cell size, production of glycosidases, capsule, and pneumolysin, and biofilm biogenesis.

3.2 Growth behaviour of D39 changes with temperature shifts

To determine the impact of temperature on pneumococcal growth, the wild type strain was grown micro-aerobically in BHI or CDM supplemented with 55 mM glucose as the sole carbon source as previously described in section 2.5. Glucose was used for growth analysis of wild type because it was determined that pneumococcus use glucose as preferential substrate over other sugars such as galactose or mannose (Paixao *et al.*, 2015b).

3.2.1 Growth in BHI

In BHI, no significant differences were observed in growth properties of wild type grown at 34°C, 37°C, or 40°C (Figure 3.1) (p>0.05). The growth rate and yield were calculated as detailed in section 2.5 (Table 3.1). The growth rates (μ) ranged from 0.27 to 0.30 (h^{-1}). Bacterial yield (maximal OD_{600nm}) for wild type ranged from 1.57 to 1.58. The results suggested that the wild type growth profile in rich medium is not adversely affected by differences in temperature.

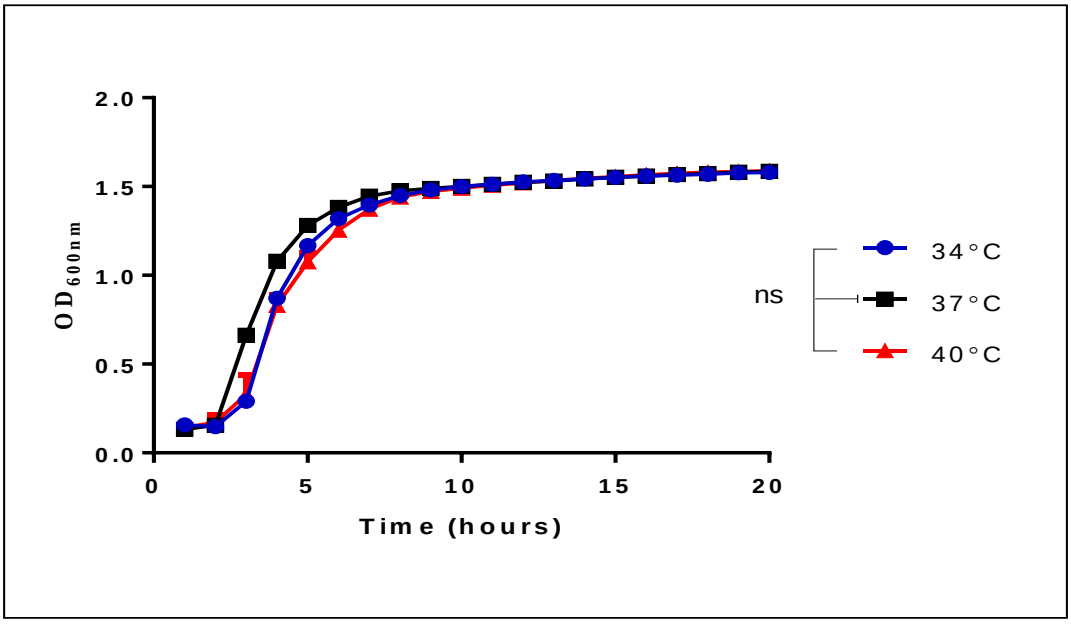

Figure 3.1. The growth profile of wild type D39 in BHI under micro-aerobic condition at 34°C, 37°C, or 40°C.
There was no significant difference in the growth rate and yield of D39 strain at different temperatures using two-way ANOVA and Dunnett's multiple comparisons test (p>0.05, ns: not significant). Experiment was repeated using 3 replicates of 3 independent biological samples.

Temperature	Growth rate (μ (h^{-1}))	Growth yield (OD_{600nm})
34°C	0.29 ± 0.002	1.57 ± 0.005
37°C	0.30 ± 0.001	1.58 ± 0.008
40°C	0.27 ± 0.005	1.58 ± 0.009

Table 3.1. Growth rate (μ) and yield (maximal OD_{600nm}) of pneumococcal strain grown in BHI at 34°C, 37°C, or 40°C.
Experiment was repeated using 3 replicates of 3 independent biological samples, '±' indicates standard error of means (SEM).

3.2.2 Growth at different temperatures in CDM supplemented with 55 mM glucose

The impact of temperature on growth of pneumococcus was tested by incubating the wild type strain in CDM supplemented with 55 mM glucose. The growth rate and yield of the wild type are presented in Table 3.2 and Figure 3.2. There was no significant difference in growth of wild type between at 34°C and 37°C. On the other hand, at 40°C, D39 wild type strain displayed slower growth rates (0.21 ± 0.004) compared to at 34°C and 37°C (0.24 ± 0.005 and 0.26 ± 0.001, respectively) (p<0.0001).

As for growth yield, D39 had similar growth yield at 34°C (1.38 ± 0.001) relative to 37°C (1.48 ± 0.006). However, the growth yield was significantly reduced at 40°C (1.16 ± 0.005) (p<0.0001).

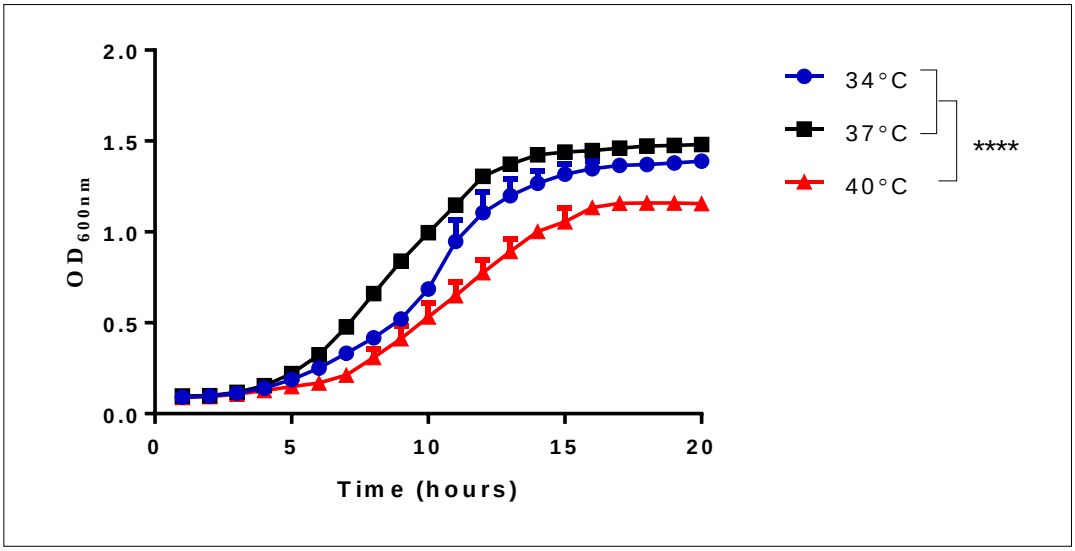

Figure 3.2. The growth of wild type D39 in CDM supplemented with 55 mM glucose under micro-aerobic condition at 34°C, 37°C, or 40°C.
Error bars show the standard error of the mean for three individual measurements each with three replicates. Significant differences were seen comparing the growth rates at 40°C to 34°C or 37°C using two-way ANOVA and Dunnett's multiple comparisons test. (**** p<0.0001). No difference was seen between the growth rate at 34°C and 37°C (0.24 ± 0.005 and 0.26 ± 0.001 h^{-1} respectively).

Temperature	Growth rate (μ (h^{-1}))	Growth yield (OD_{600nm})
34°C	0.24 ± 0.005	1.38 ± 0.001
37°C	0.26 ± 0.001	1.48 ± 0.006
40°C	0.21 ± 0.004	1.16 ± 0.005

Table 3.2. Growth rate (μ) and yield (maximal OD_{600nm}) of pneumococcal strain grown micro-aerobically in CDM with 55 mM glucose at 34°C, 37°C, or 40°C.
Experiment was repeated thrice each with triplicates, '±' indicates standard error of means (SEM).

The results suggested that the wild type growth profile on glucose is affected by increased temperature at 40°C compared to 37°C. This is likely due to inability of strain to utilize glucose in minimal nutrient environment of CDM at this temperature.

3.3 Temperature has impact on pneumococcal cell size

Microorganisms have adaptation systems to ensure their survival in non-optimal growth conditions. These include induction of stress proteins, expression of starvation genes, conversion to dormant state, or formation of spores. Changes in temperature can induce stress for microbes. To survive, microbes may reduce their size, reduce membrane polysaccharide concentration, or alter their fatty acid or phospholipid structure (Price and Sowers, 2004).

The impact of temperature on pneumococcal cell size was determined at mid-exponential phase growth (OD 0.6-0.8 at 600 nm) in BHI or CDM supplemented with glucose. Pneumococci were Gram-stained and cells were measured using a light microscope. The cell size of pneumococcus in different mediums at tested temperatures is presented in table 3.3. In BHI, no significant difference on cell size was recorded between all temperatures (0.49 ± 0.002 μm, 0.50 ± 0.006 μm, 0.47 ± 0.001 μm at 34°C, 37°C, and 40°C, respectively, p>0.05) (Figure 3.3 A).

On glucose in CDM, D39 had slightly bigger size at 37°C (0.48 ± 0.014 µm) than 34°C (0.44 ± 0.017 µm) (p<0.05). Furthermore, pneumococcus reduced its size significantly when incubated at 40°C (0.36 ± 0.003 µm) (Figure 3.3 B).

Temperature has a significant impact on the cell size of pneumococci when grown on glucose in CDM at 34°C or 40°C compare to 37°C. This is very likely due to additional stress the microbe is exposed in minimal nutrient environment of CDM.

Table 3.3. The cell size of pneumococcal strain grown micro-aerobically in BHI and CDM supplemented with glucose at 34°C, 37°C, or 40°C.
Experiment was repeated using 3 replicates of 10 independent single cells. '±' indicates standard error of means (SEM).

	Cell size (µm)	
Temperature	**BHI**	**CDM+Glucose**
34°C	0.49 ± 0.002	0.44 ± 0.017
37°C	0.50 ± 0.006	0.48 ± 0.014
40°C	0.47 ± 0.001	0.36 ± 0.003

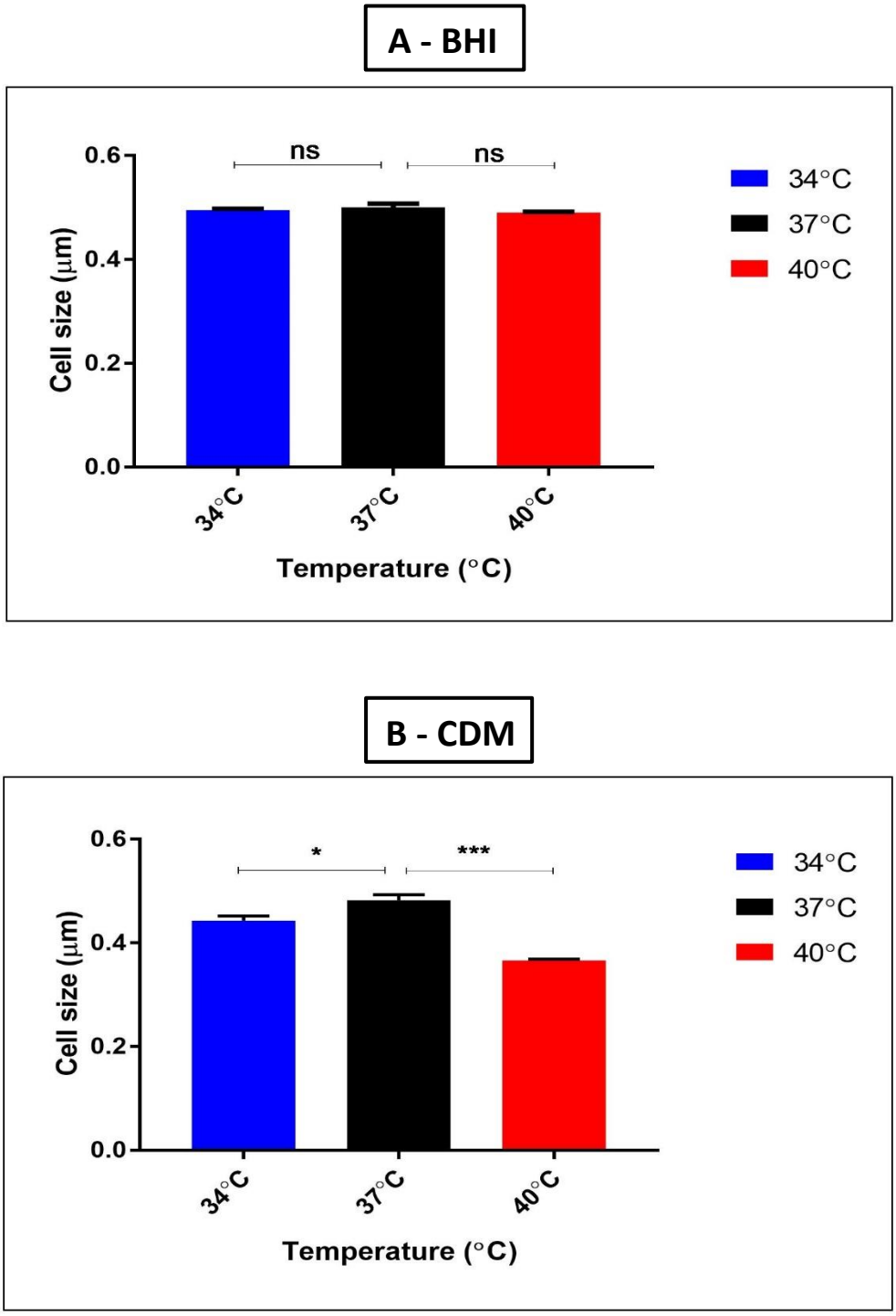

Figure 3.3. The cell size of wild type D39 grown in BHI (A) or CDM supplemented with 55 mM glucose (B) at 34°C, 37°C, or 40°C.

Error bars show the standard error of the mean for three individual measurements each with three replicates. No significant differences were seen when comparing the cell size of wild type D39 in BHI. Cell size of D39 reduced when grown at 34°C (0.44 ± 0.017 µm) or 40°C (0.36 ± 0.003 µm) compared to 37°C (0.48 ± 0.014 µm). Significant differences were seen using one-way ANOVA (* p<0.05, *** p<0.001, ns: not significant).

3.4 Haemolysis differs at different temperatures in pneumococcus

S. pneumoniae is α-haemolytic microbe and the haemolytic activity has been attributed to the production of cytotoxin pneumolysin, which is known to be one of the most important virulence determinants of pneumococcus due to its effect on immune cell function (Shak *et al.*, 2013). The effect of temperature shift on haemolytic activity was tested using 4% (v/v) RBC mixed with the cell lysates of pneumococcal strain grown in either BHI or CDM supplemented with 55 mM glucose at different temperatures as described in section 2.5. There was no difference in the haemolytic activity of the pneumococcus when using the cell lysate of bacteria grown in BHI at different temperatures ($p>0.05$) (Figure 3.4 A). Indeed, the results showed that the wild type strain had similar haemolytic activity at 34°C, 37°C, or 40°C (13.03 ± 0.85, 13.85 ± 1.21, 12.24 ± 0.36 HU/µg of protein, respectively). Furthermore, when using the cell lysate of bacteria grown on glucose in CDM at 40°C, the haemolytic activity of the wild type D39 (9.44 ± 0.74 HU/µg of protein) significantly reduced compared to activity at 37°C (12.56 ± 1.21 HU/µg of protein) ($p<0.05$), while no significant change was recorded at 34°C (11.16 ± 0.95 HU/µg of protein) ($p>0.05$) (Figure 3.4 B).

The results demonstrated that lower temperature (34°C) has no effect on haemolytic activity of pneumococcus regardless of growth medium, however, high temperature (40°C) reduces haemolytic activity in minimal medium relative to 37°C.

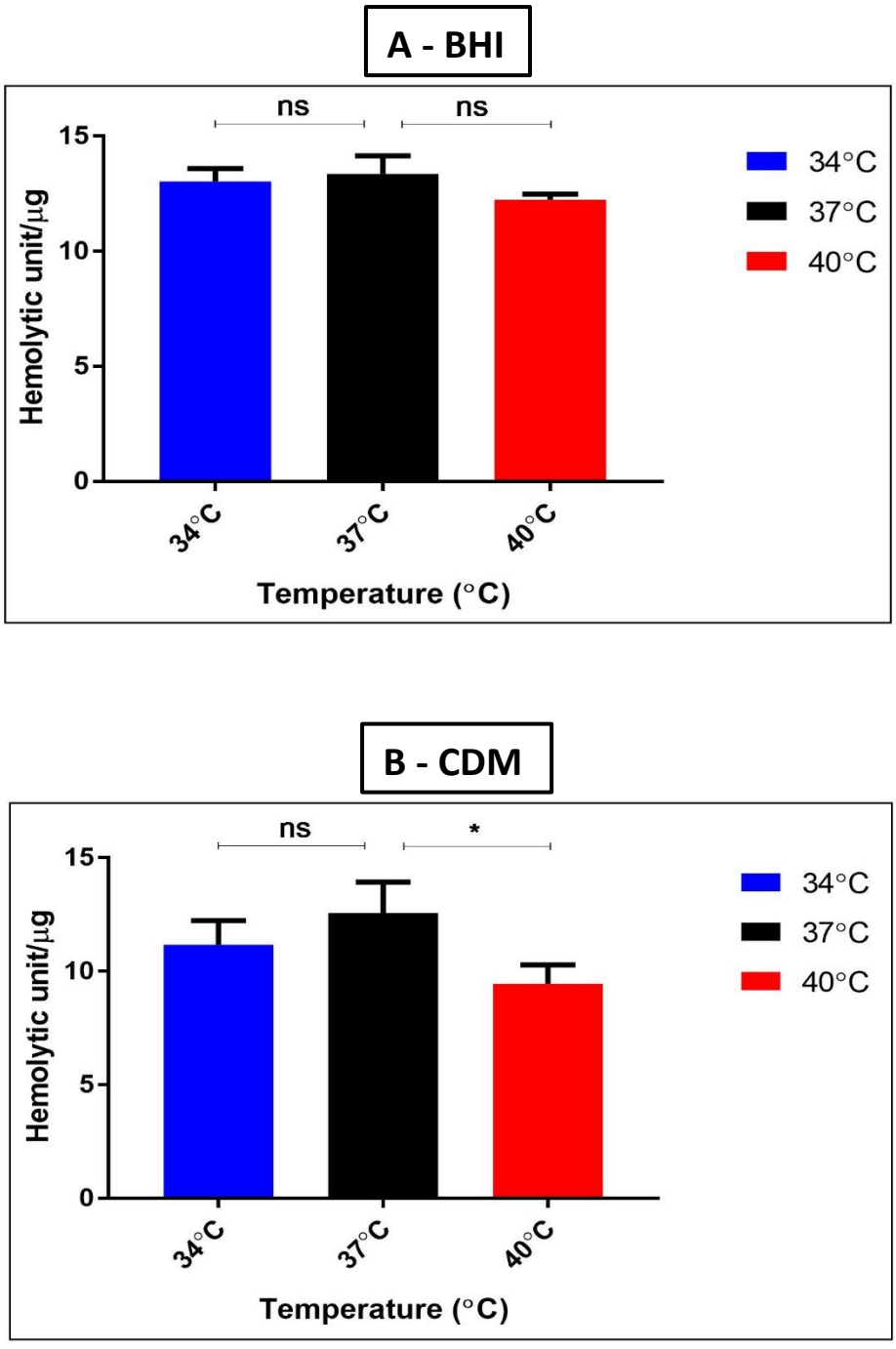

Figure 3.4. The haemolytic activity of wild type D39 grown in BHI (A) or CDM supplemented with 55 mM glucose (B) at 34°C, 37°C, or 40°C.
Haemolytic activity assay was done using 4% v/v defibrinated sheep blood. Error bars show the standard error of the mean for three individual measurements each with three independent biological samples. No significant differences were seen when comparing haemolytic activity of wild type D39 in BHI. The activity was significantly reduced at 40°C compared to 37°C while reduction was not significant at 34°C. Significant difference was obtained using one-way ANOVA and Dunnett's multiple comparisons test (* p<0.05, ns: not significant).

3.5 Neuraminidase activity is influenced by temperature changes in pneumococcus

Neuraminidases catalyse the cleavage of sialic acid residues from cell surface glycoconjugates and mucin (Parker *et al.*, 2009), which aid in pneumococci to colonize the upper respiratory tract (Manco *et al.*, 2006). The cleavage of sialic acid by neuraminidase is required to allow sequential degradation of glycoconjugates by exo-glycosidases such as by galactosidases (Kahya *et al.*, 2017; Terra *et al.*, 2010). Pneumococcal neuraminidases are encoded by three genes, *nanA*, *nanB*, and *nanC*, and their role on pneumococcal colonisation on upper respiratory tract have been studied (Manco *et al.*, 2006), and involvement in biofilm formation have been shown (Parker *et al.*, 2009).

To determine the impact of temperature on neuraminidase activity, pneumococcal cell extracts were prepared in BHI or CDM supplemented with glucose. The results showed that there was no significant change in neuraminidase activity in BHI at different temperatures ($p>0.05$) (Figure 3.5 A). On the contrary, the neuraminidase activity was significantly decreased at 34°C (214.1 ± 11.70 U) or 40°C (162.2 ± 3.21 U) compared to 37°C (252.1 ± 11.20 U) in CDM with glucose (Figure 3.5 B). In addition, reduction was more pronounced at 40°C. These results suggested that additional stress the microbe exposed in minimal nutrient environment of CDM effects the neuraminidase activity at different temperature.

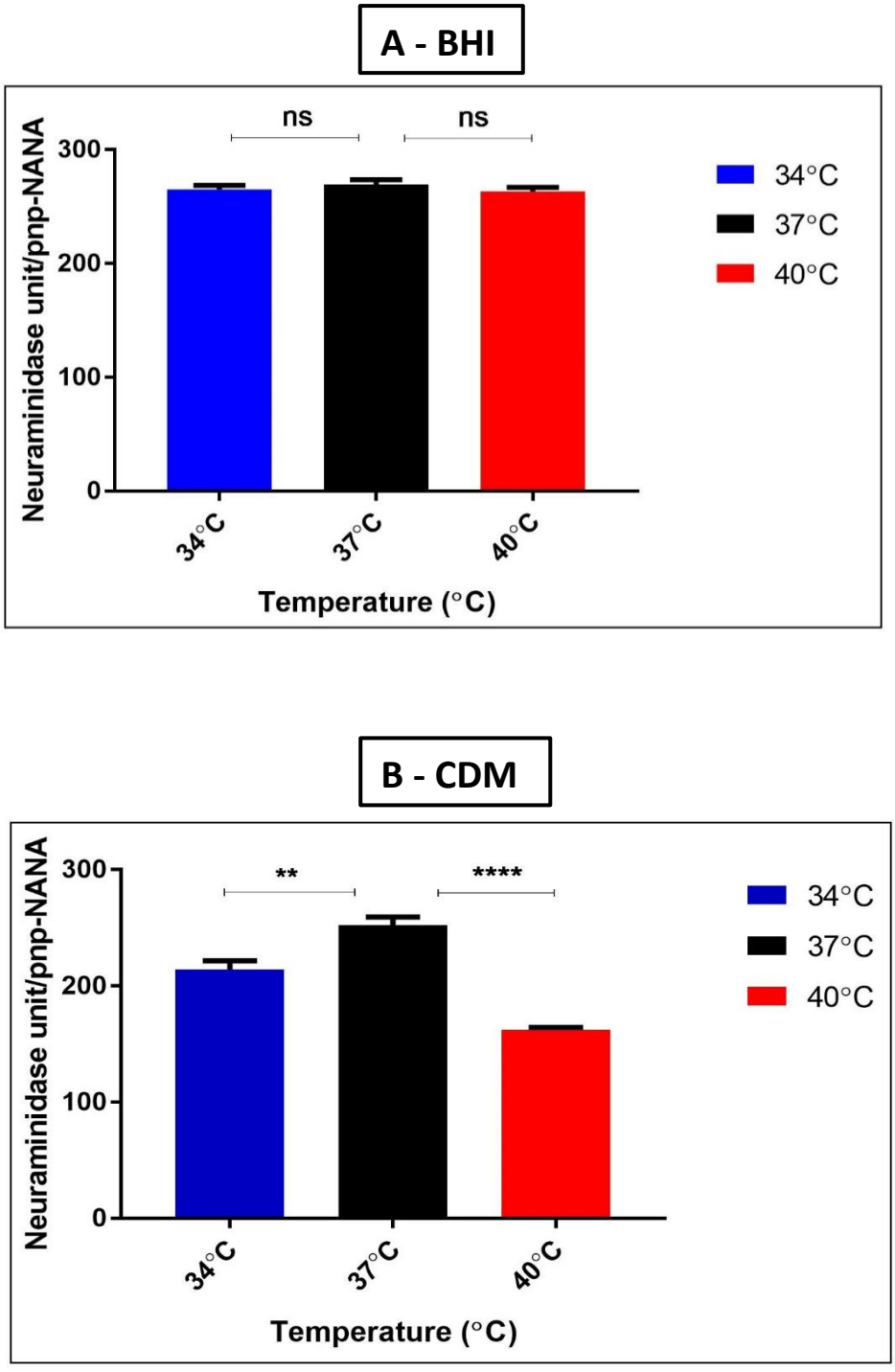

Figure 3.5. The neuraminidase activity of wild type D39 grown in BHI (A) or CDM supplemented with 55 mM glucose (B) at 34°C, 37°C, or 40°C.

The assay was done using 2-O-(p-Nitrophenyl)-α-D-N-acetylneuraminic acid (pNP-NANA) as the substrate. All values are expressed as nmol pNP released/min/μg of total protein and are means ± standard errors of the means (SEM) of triplicate samples. No significant differences were seen when comparing neuraminidase activity of wild type D39 in BHI. The activity was significantly decreased at 34°C or 40°C compared to 37°C. Significant difference was obtained using one-way ANOVA and Dunnett's multiple comparisons test. (** p<0.01, **** p<0.0001, ns: not significant).

3.6 Pneumococcal biofilm formation is affected by temperature

The first step of pneumococcal infections is formation of well-structured biofilm, which occurs during colonisation of the nasopharynx (Domenech *et al.*, 2012). It has been reported that pneumococcal biofilms show increased resistance to antimicrobial agents (Chao *et al.*, 2014), and the resistance is more challenging in nasopharyngeal environment.

As temperature is extremely important factor for pneumococcal biofilm formation (Marks *et al.*, 2012b), the impact of temperature on pneumococcal biofilm formation was determined. Overnight-grown adherent cells in THY medium were stained with crystal violet (CV) and the colour intensity as a factor of biofilm biogenesis was recorded at 595 nm as described in section 2.16. The results are shown in Figure 3.6. Compared to the wild type strain at 37°C (0.22 ± 0.003), pneumococci formed similar amount of biofilm at 34°C (0.20 ± 0.016), however, it was significantly decreased at 40°C (0.18 ± 0.015) (p<0.05).

These results suggest that the physiological temperature of the nasopharyngeal niche (34°C) and human body (37°C) provides optimal conditions to support biofilm formation. In addition, high temperature (40°C) showed additive effect during biofilm formation as it reduced significantly likely due to restricted growth of pneumococcus as nutrient-rich media (THY) did not support biofilm development.

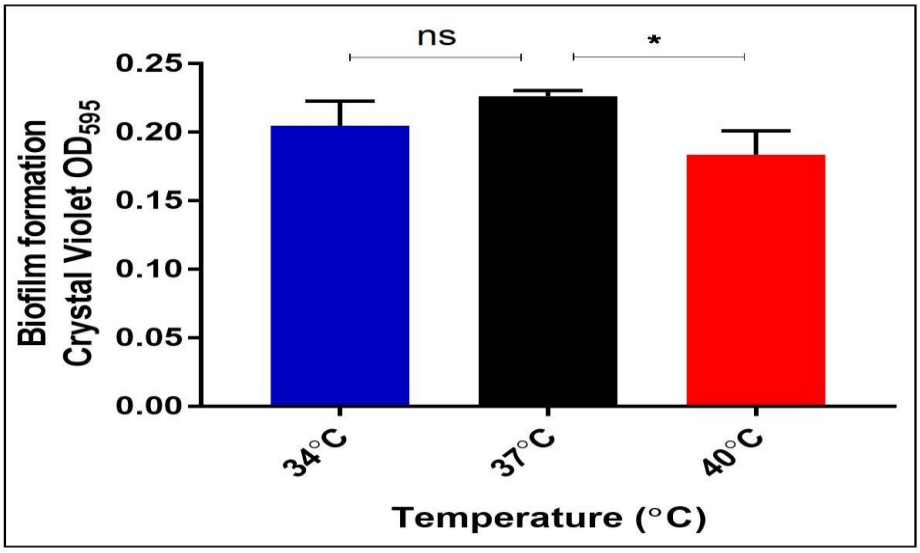

Figure 3.6. The biofilm formation of wild type D39 grown in THY medium at 34°C, 37°C, or 40°C.

All values are expressed as optical density of stained adherent cells. Error bars show the standard error of the mean for three individual measurements each with three independent experiments. The wild type D39 formed significantly less biofilm at 40°C, not at 34°C compared to 37°C. Significant difference was obtained using one-way ANOVA and Dunnett's multiple comparisons test. (* p<0.05, ns: not significant).

3.7 Pneumococcal capsule production changes with temperature

Capsular polysaccharide (CPS) is the most important trait of pneumococcal virulence, and is also required for adhesion, biofilm formation, and protection from opsonophagocytosis (Kadioglu *et al.*, 2008). Pneumococcal CPS is also the main target of drug discovery (Yang *et al.*, 2014). Thus, knowledge of the impact of temperature on CPS production may be critical to develop new anti-infective. Isolation and quantification of capsular polysaccharide of D39 wild type strain at different temperatures were described in Section 2.17. As shown in Figure 3.7 A, the wild type strain produced similar amount of glucuronic acid, which is found in type 2 capsule, at different temperatures (p>0.05). However, on glucose in CDM, pneumococcus produced more glucuronic acid at 34°C (33.81 ± 2.30 μg/ml) than at 37°C (29.20 ± 1.22 μg/ml), but the levels was significantly reduced at 40°C (23.79 ± 0.63 μg/ml) (p<0.05) (Figure 3.7 B). The results indicated that the concentration of glucuronic acid in wild type strain is temperature-dependent in the minimal medium only.

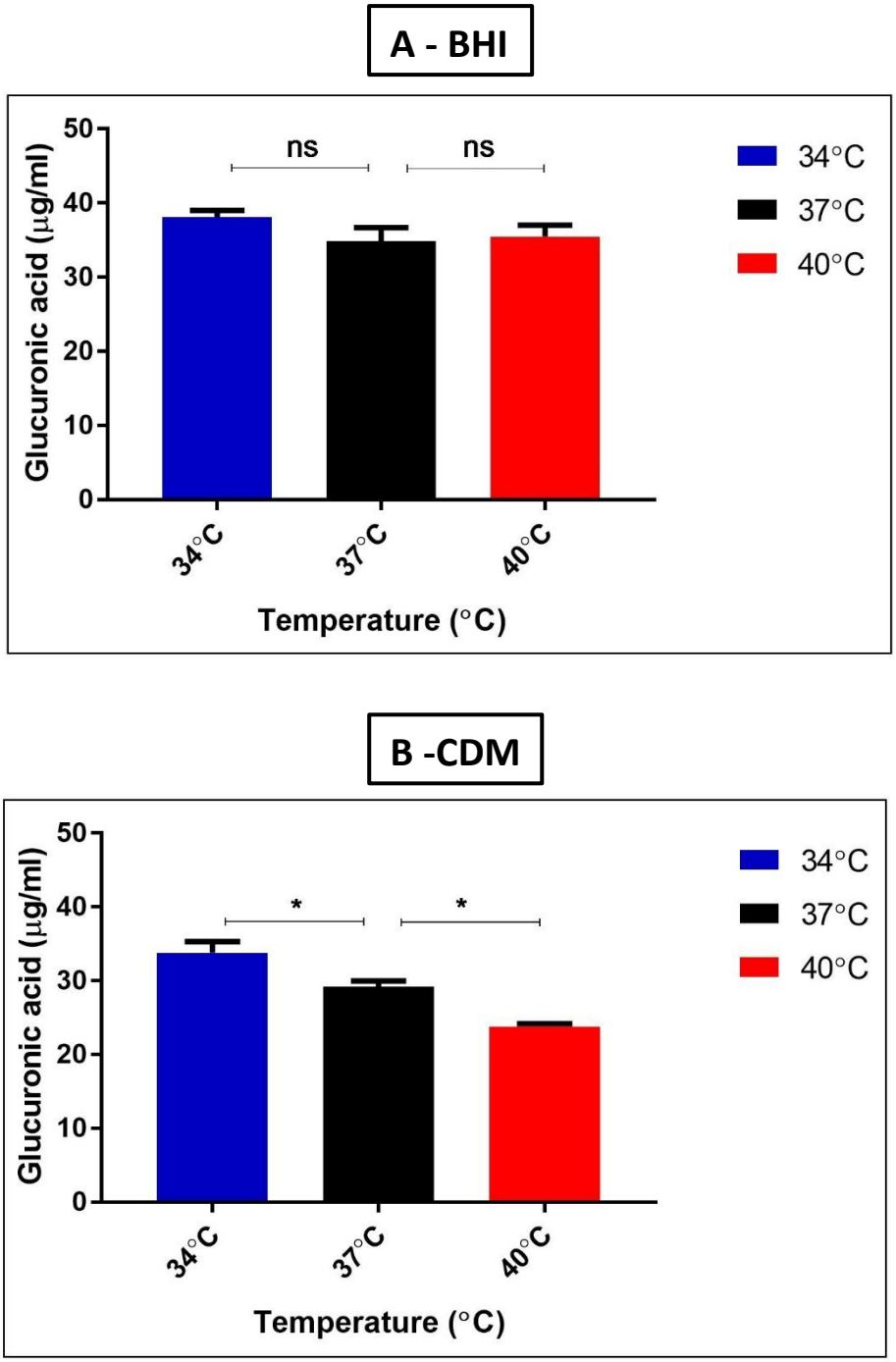

Figure 3.7. The glucuronic acid concentration of wild type D39 grown in BHI (A) or CDM supplemented with 55 mM glucose (B) at 34°C, 37°C, or 40°C.
Error bars show the standard error of the mean for three individual measurements each with three independent experiments. No significant differences were seen when comparing amount of capsule of wild type D39 in BHI. The capsule was significantly higher at 34°C than 37°C or 40°C. Significant difference was obtained using one-way ANOVA and Dunnett's multiple comparisons test. (* $p<0.05$, ns: not significant).

3.8 Part B. Microarray analysis of pneumococcal genes

Microarray analysis of pneumococcal transcriptome exposed to different temperature was done using the data, which was kindly provided by Dr Sulman Shafeeq (Karolinska Institute, Sweden). On the array, a total of 2084 genes were transcribed at 34ºC or 40ºC, relative to 37ºC. Transcripts associated with ≥2-fold expression differences represented nearly 6% (131) and 17% (360) at 34ºC, 5% (119) and 3% (70) at 40ºC during mid- or late-exponential growth phase, respectively. Interestingly, the genes differentially regulated in one temperature were also differentially regulated at another temperature, but the levels of expression were different. The Venn diagram in Figure 3.8 shows the relative transcript levels at 34ºC and 40ºC at mid- and late-exponential growth phases. The lists of up- and downregulated genes at mid-exponential phase are shown in the Appendix A.

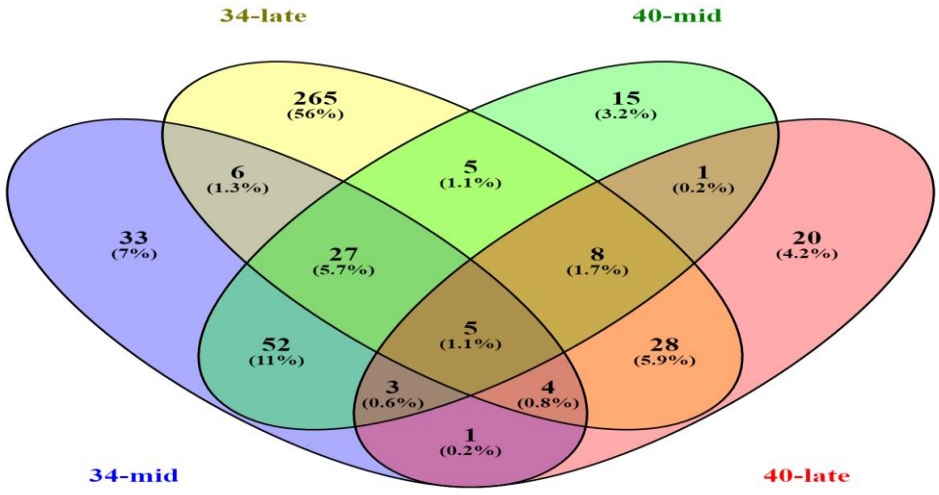

Figure 3.8. Venn diagram highlighting relative transcript levels of genes in *S. pneumoniae* at 34ºC and 40ºC during mid- or late-exponential growth phase.
For all intersections, which are not drawn to scale, the numbers of genes are indicated.

At 34ºC, 97 and 155 genes were upregulated, while 35 and 205 genes were downregulated during mid- or late-exponential growth phase, respectively. On the other hand, fewer number of genes were differentially regulated at 40ºC. In mid-exponential phase, 43

genes were upregulated and 76 genes were downregulated and 34 genes were upregulated and 36 genes were downregulated in late-exponential growth. The lower growth temperature (34ºC) had the higher number of differentially expressed genes compared to those observed at 40ºC, which is likely due to major re-orientation of bacterial metabolism.

To analyse the differentially expressed genes in detail, I clustered them into 8 functional categories as annotated by Kyoto Encyclopedia of Genes and Genomes (KEGG) (Kanehisa *et al.*, 2016), and shown in Figure 3.9. The highest number of differentially expressed genes belongs to the hypothetical gene category in at least one temperature. The functional roles of hypothetical genes are not known, but the annotation data suggests that these genes play role on pneumococcal metabolism and survival. For example, SPD_0132 and SPD_0133 locus is upregulated at 34ºC, while downregulated at 40ºC. This locus was reported to be involved in bacteriocin synthesis for protection (Kanehisa *et al.*, 2016). The second and fourth largest gene categories that were differentially expressed, were those involved in genetic information processing and nucleotide metabolism. Carbohydrate metabolism genes formed the third largest differentially expressed gene category. This is also in line with the requirement for additional ATP to adapt to changing environmental condition. On the other hand, the expression of lipid metabolism genes was the least affected.

The expression of genes encoding proteins involved in fundamental processes such as purine and pyrimidine metabolism, transport and binding functional groups, glycolysis, and sugar metabolism were primarily upregulated during mid-exponential growth at 34ºC relative to 37ºC.

Genes encoding regulatory proteins are of special interest because alteration on transcriptional activation may have pleiotropic effects. For example, two-component response regulators of *S. pneumoniae*, SPD_0701/702 (CiaR and CiaH) and SPD_2063/2064 (ComE and ComD), are present in an operon and upregulated at 34ºC. CiaR/H regulates several virulence genes and required for the development of stress-response mechanism (Ibrahim *et al.*, 2004a). ComE and ComD are required for

transcription of competence and virulence genes in pneumococcus (Kowalko and Sebert, 2008). ComX (SPD_0014), which was also upregulated, also has a role in the regulatory mechanism of Com operon. In addition, the genes of another operon, which is also involved in competence (Cgl operon), were regulated in a temperature dependent manner. On the other hand, CiaRH and competence-related operons were downregulated at 40ºC. In addition, genes involved in the bacteriocin synthesis also showed temperature-dependent regulation. BlpR (SPD_468) is a transcriptional regulator and coordinates the secretion of exotoxin protein with the other members of Blp operon including BlpS (SPD_0467) and BlpC (SPD_0470) (Dawid *et al.*, 2007). These genes were upregulated at 34ºC, while downregulated at 40ºC during mid-exponential phase. Moreover, the global nutritional repressor CodY, which regulates the genes involved in amino acid metabolism, biosynthesis, and uptake (Hendriksen *et al.*, 2008), was upregulated at 34ºC, while no change in expression was observed at 40ºC. It was also observed that several other genes with diverse functions, choline-binding protein (SPD_2028), serine protease (SPD_2068), and chromosome partitioning protein SpoJ (SPD_2069), were also upregulated at 34ºC, while downregulated at 40ºC.

On the other hand, the microarray data showed that certain transcriptional regulators were downregulated at 34ºC including SPD_0447 ($MerR^2$), SPD_1524 (GntR), SPD_1645 (MarR). $MerR^2$ is a transcriptional repressor and was found to be controlling the transcription of pyruvate and galactose metabolism (Al-Bayati *et al.*, 2017). SPD_1524 is a member of GntR family of transcriptional regulators, which act as a repressor on various metabolism including polysaccharide synthesis, and governs pneumococcal virulence (Wu *et al.*, 2016). In addition, MarR is another repressor encoding protein involved in aromatic catabolism, and antimicrobial and oxidative stress response (Reyes-Caballero *et al.*, 2010). All these proteins have been reported to play a role in virulence.

In late-exponential growth phase at 34ºC, a cluster of genetic information processing genes encoding 30S and 50S ribosomal proteins, RNA polymerase subunits, tRNA-synthesis, cell division proteins, elongation factor, and translation initiation factor were upregulated (Appendix A). Through analysis of the data, it was found that nine genes including stress response proteases and chaperones were downregulated at 34ºC. Seven

of them were more notable as they were annotated as chaperonin or heat-shock protein. For example, SPD_0458 (HrcA) and SPD_0459 (GrpE) are heat-shock proteins and they are neighbour to chaperonins SPD_0460 (DnaK) and SPD_0461 (DnaJ). Another chaperon operon GroESL encoding SPD_1709 (GroEL) and SPD_1710 (GroES) were also differentially expressed. This operon is crucial for refolding of proteins under stress environments (Kwon *et al.*, 2004). All mentioned chaperonins are required to keep protein structure stable by preventing degradation or refolding those damaged proteins. Clp protease (SPD_0308), which was also downregulated, degrades unstable protein structure (Kwon *et al.*, 2004).

Furthermore, there were certain genes that were differently regulated between growth phases at the same temperature. The cluster of SPD_1098 and SPD_1099 coding for amino acid transporter ATP-binding protein, SPD_1158 (GdhA) coding for glutamate dehydrogenase, and SPD_0447 (MerR^2) coding for glutamine synthetase were downregulated during mid-exponential growth at 34ºC, but upregulated at late-exponential growth. Moreover, all these proteins were also upregulated at mid-exponential phase at 40ºC, while downregulated during late-exponential growth.

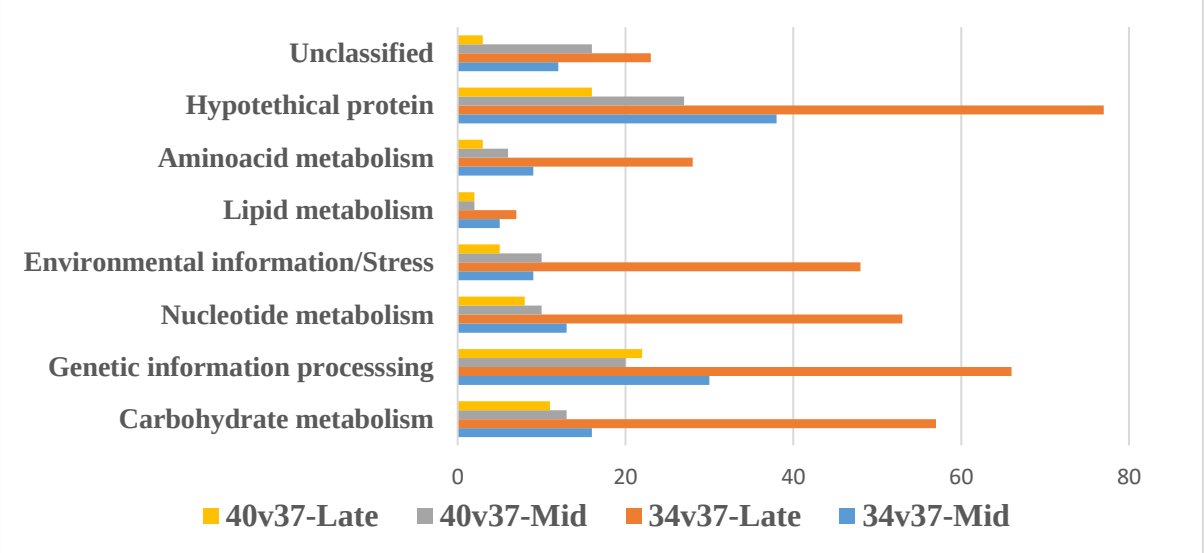

Figure 3.9. Functional categories of differentially expressed genes at mid- and late-exponential growth phases in response to temperature shifts.

3.8.1 Screening of temperature-induced operons

While the microarray analysis has been done for both mid- and late-exponential phases, the hypothesis relating to the involvement of selected genes in thermoregulation was done using the microarray data from the mid-exponential phase as at this stage transcripts are more stable, hence, more producible data can be obtained. In addition, the use of late-exponential data can be confounded due to the fact that at this stage of growth, there are other additional stress factors involved (Laakso *et al.*, 2011). Hence, some overview of differentially expressed genes at mid-exponential phase has been provided below.

At 34ºC, 20 operons were upregulated, while 7 operons were downregulated (Table 3.4 A). Of these, certain operons were highly upregulated at 34ºC whereas downregulated at 40ºC. These are Com/Pur operon including competence-related and purine metabolism genes (SPD_0049 to SPD_0057), a hypothetical operon with unknown function (SPD_0132 and SPD_0133), two bacteriocin-related operons (SPD_0046 and SPD_0047, and SPD_0466 and SPD_0468), Cgl/hypotethical operon comprising competence-related genes and hypothetical genes (SPD_1857 to SPD_1862), one other Com operon (SPD_2063 to SPD_2065), and the operon including the transcriptional regulators serine protease and spoJ (SPD_2068 and SPD_2069).

On the other hand, a hypothetical operon (SPD_0113 to SPD_0116) and the operon comprising *merR*^{2} and *glnA*, which involve in nitrogen metabolism (SPD_0447 and SPD_0448), was highly upregulated at 40ºC whereas downregulated at 34ºC (Table 3.4 B).

Table 3.4. Operons up- or downregulated at 34ºC or 40ºC relative to 37ºC.
Only genes whose transcript level showed significant fold variations (2-fold) are shown. The product names were classified based on the KEGG pathway. The operons were identified by the promoter regions shared by the surrounding genes. Blue numbers represent the upregulation while reds represent downregulation of the genes. Empty columns in fold section shows that those single genes were not induced at given condition. **A** represents the operons upregulated at 34ºC, while downregulated at 40ºC. **B** represents the operons downregulated at 34ºC, while upregulated at 40ºC. Operons are separated with a row in between.

A

		34ºC	40ºC	
Tags	**Name**	**Fold**		**Product**
SPD_0035		3	-1.93	hypothetical protein
SPD_0036		2.32	-2.18	hypothetical protein
SPD_0046	*blpU*	9.33	-7.89	bacteriocin BlpU
SPD_0047		9.35	-7.69	hypothetical protein
SPD_0049	*comA*	14.81	-9.74	competence factor transporting ATP-binding protein/permease ComA
SPD_0050	*comB*	7.92	-5.97	competence factor transport protein ComB
SPD_0051	*purC*	4.73	-4.41	phosphoribosylaminoimidazole-succinocarboxamide synthase
SPD_0052		2.58	-1.95	phosphoribosylformylglycinamidine synthase
SPD_0053	*purF*	3.05	-2.36	amidophosphoribosyltransferase
SPD_0054	*purM*	3.42	-2.26	phosphoribosylaminoimidazole synthetase
SPD_0055	*purN*	3.22	-2.5	phosphoribosylglycinamide formyltransferase
SPD_0056		4.45	-3.42	vanZ protein
SPD_0057	*purH*	2.51		phosphoribosylaminoimidazolecarboxamide formyltransferase/IMP cyclohydrolase
SPD_0059	*purE*	1.92		phosphoribosylaminoimidazole carboxylase catalytic subunit
SPD_0060	*purK*	2.79		phosphoribosylaminoimidazole carboxylase ATPase subunit
SPD_0132		6.23	-5.8	hypothetical protein
SPD_0133		52.94	-31.81	hypothetical protein
SPD_0466		7.01	-6.49	hypothetical protein
SPD_0467	*blpS*	3.21	-2.84	BlpS protein
SPD_0468	*blpR*	2.49	-2.41	response regulator BlpR

SPD_0470	*blpC*	**3.38**	**-2.02**	peptide pheromone BlpC
SPD_0471	*blpB*	**6.85**	**-4.88**	pseudogene
SPD_0472	*blpA*	**7.53**	**-5.72**	pseudogene
SPD_0473	*blpY*	**16.54**	**-9.59**	immunity protein BlpY
SPD_0474		**10.44**	**-7.41**	hypothetical protein
SPD_0701	*ciaR*	**2.06**	**-2.59**	DNA-binding response regulator CiaR
SPD_0702	*ciaH*	**1.96**	**-2.24**	sensor histidine kinase CiaH
SPD_0723	*rpiA*		**-1.99**	ribose-5-phosphate isomerase A
SPD_0724	*deoB*		**-1.9**	phosphopentomutase
SPD_0771	*lacR1*	**2.02**	**-3.04**	lactose phosphotransferase system repressor
SPD_0772		**1.91**	**-3.01**	1-phosphofructokinase
SPD_0773		**2.12**	**-2.46**	PTS system fructose specific transporter subunit IIABC
SPD_1380		**1.98**		hypothetical protein
SPD_1381	*def-2*	**2.35**		peptide deformylase
SPD_1527		**2.9**	**-2.29**	hypothetical protein
SPD_1528		**2.06**	**-2.02**	ABC transporter ATP-binding protein
SPD_1650		**2.61**		iron-compound ABC transporter permease
SPD_1651		**3.83**	**-1.96**	iron-compound ABC transporter ATP-binding protein
SPD_1652		**4.01**		iron-compound ABC transporter iron-compound-binding protein
SPD_1740	*cinA*	**5.84**	**-5.37**	competence damage-inducible protein A
SPD_1744		**3.1**	**-3.22**	hypothetical protein
SPD_1830		**1.97**		glycosyl hydrolase family protein
SPD_1831		**2.21**		PTS system transporter subunit IIC
SPD_1855		**3.71**	**-2.42**	hypothetical protein
SPD_1856		**6.18**	**-5.38**	hypothetical protein
SPD_1857		**7.65**	**-5.64**	hypothetical protein
SPD_1858		**20.86**	**-13.85**	hypothetical protein
SPD_1859		**16.21**	**-9.63**	hypothetical protein
SPD_1860	*clgD*	**20.13**	**-16.37**	competence protein CglD
SPD_1861	*cglC*	**22.59**	**-20.39**	competence protein CglC
SPD_1862	*cglB*	**37.39**	**-19.58**	competence protein CglB
SPD_2033	*yfiA*	**3.55**		ribosomal subunit interface protein
SPD_2034		**3.31**		competence protein ComF

SPD_2035		**2.82**		helicase
SPD_2063	*comE*	**39.75**	**-25.36**	response regulator
SPD_2064	*comD*	**53.65**	**-44.92**	sensor histidine kinase ComD
SPD_2065	*comC1*	**35.18**	**-23.95**	competence-stimulating peptide type 1
SPD_2068		**6.38**	**-3.73**	serine protease
SPD_2069		**4.4**	**-3.5**	SpoJ protein

B

		34°C	**40°C**	
Tags	**Name**	**Fold**		**Product**
SPD_0093		**-2.07**		hypothetical protein
SPD_0094		**-3.02**		hypothetical protein
SPD_0095		**-2.93**		hypothetical protein
SPD_0096		**-2.54**		hypothetical protein
SPD_0113		**-4.01**	**23.88**	hypothetical protein
SPD_0114		**-3.58**	**19.9**	hypothetical protein
SPD_0115		**-3.46**	**21.52**	hypothetical protein
SPD_0116		**-2.9**	**32.51**	hypothetical protein
SPD_0447	*merR*[2]	**-3.66**	**2.96**	transcriptional regulator, MerR family protein
SPD_0448	*glnA*	**-4.66**	**4.12**	glutamine synthetase, type I
SPD_0452		**-2.35**		phage integrase family protein
SPD_0453	*hsds*	**-2.37**	**2.14**	type I restriction-modification system subunit
SPD_1098		**-3.44**	**2.79**	amino acid ABC transporter amino acid-binding protein/permease
SPD_1099		**-2.9**	**2.68**	amino acid ABC transporter ATP-binding protein
SPD_1175			**2.48**	hypothetical protein
SPD_1176			**2.16**	ABC transporter ATP-binding protein
SPD_1177			**2.19**	drug efflux ABC transporter ATP-binding protein/permease
SPD_1179			**1.97**	hypothetical protein
SPD_1514			**2.74**	ABC transporter ATP-binding protein
SPD_1515			**2.86**	hypothetical protein

SPD_1516			**2.99**	hypothetical protein
SPD_1517			**3.99**	hypothetical protein
SPD_1682		**-3.49**		Not found
SPD_1683			**2.41**	Not found
SPD_1685			**2.63**	Not found
SPD_1690		**-2.01**	**2.15**	Not found
SPD_1691		**-2.22**	**2.21**	Not found
SPD_1694		**-2.83**	**2.57**	Not found
SPD_1695		**-2.04**	**2.79**	Not found
SPD_1696		**-2.42**	**2.62**	Not found
SPD_1697		**-2.58**	**3.41**	Not found
SPD_1698		**-2.58**	**2.77**	Not found

3.8.2 Motif search in transcriptionally altered genes at different temperatures

The regions located upstream of the start codon of differentially expressed operons were analysed to search for regulatory motifs. To do this, 25 differentially expressed operons (19 upregulated and 6 downregulated) at 34ºC, and 22 (15 upregulated and 7 downregulated) operons at 40ºC were screened using the bacterial promoter prediction tool (BPROM) and Motif-based sequence analysis tool (MEME) (http://meme.nbcr.net/meme/tools/meme) to detect the putative promoter regions and identify the putative binding motifs, respectively. Upregulated operons are blue coloured and downregulated operons are red coloured in Table 3.4. An illustration of binding motifs represented as sequence logos is shown below. Sequence logos consists of stacks of letters, one stack for each position in the sequence (Zambelli *et al.*, 2013). The height of different letters at the same position reflects the relative frequency of the corresponding amino or nucleic acid. Amino acids have be differentiated by colours according to their chemical properties (Crooks *et al.*, 2004).

A – Motif for upregulated genes at 34ºC

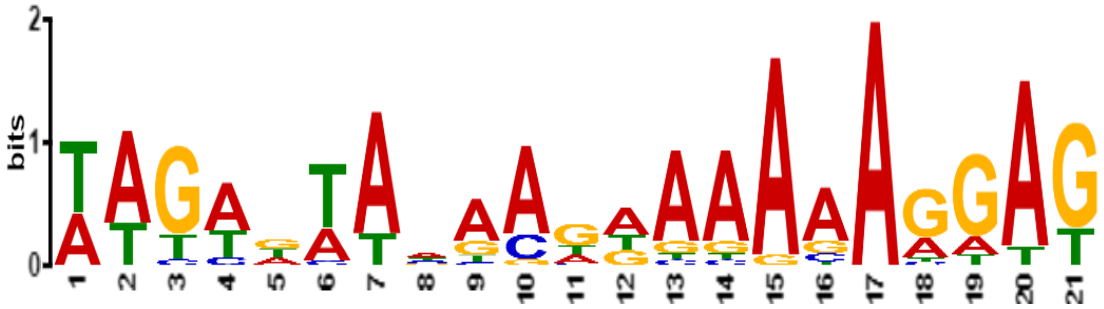

Motif: <u>WAGWDWAHAAGDAAAAAGGAG</u>

Where; W= T or A; D= A or T or G; H= A or C

This consensus sequence is present in all promoter regions of the upregulated operons at 34ºC. Motif elicitation also revealed that LexA of *Vibrio parahaemolyticus*, OmpR of *Yersinia pestis*, and MogR of *Listeria monocytogenes* have a similar motif in their sequence. LexA is a repressor of a number of genes involved in the response to DNA damage (SOS response), which links to stress-induced mutagenesis, virulence and propagation of antibiotic resistance factors in *Vibrio* species (Sanchez-Alberola *et al.*, 2012). OmpR is an important transcriptional regulator, which involves in the osmotic stress response and resistance to phagocytosis in various stress conditions in macrophages (Gao *et al.*, 2011), and MogR regulates the motility and involves in the virulence of *Listeria* (Shen and Higgins, 2006).

B – Motif for downregulated genes at 34ºC

Motif: <u>VGAAAAGGAKR</u>

Where; V= G, C, or A; K=G or T; R= G or A

This motif is present in the all promoter regions of downregulated operons at 34ºC. The analysis also showed that the motif is similar to CcpA binding site *cre*, which is also found in *S. pneumoniae*, and Fur in various species. CcpA (catabolite control protein) regulates orderly use of available carbon sources (Al-Bayati *et al.*, 2017). Fur (ferric uptake regulator) is an important transcriptional factor regulates the iron homeostasis and triggers oxidative stress response mechanism (da Silva Neto *et al.*, 2009).

C – Motif for upregulated genes at 40ºC

Motif: AGTKAKGGATG

Where; K= G or T

This consensus sequence is also similar in binding sites of CRP (Cyclic AMP receptor protein) of *E. coli* and *V. vilnificus*, and H-NS gene of *V. cholera*. CRP acts as both activator and repressor, and regulates many genes involved in energy metabolism (Basak and Jiang, 2012). It was also mentioned that CRP regulates redox-sensing regulators, SoxR and OxyR, which increase the tolerance against oxidative stress in *E. coli* (Tsai *et al.*, 2018). H-NS (histone-like nucleoide structuring protein) in *Vibrio* is a global repressor and was found to be important for adaptation to fluctuating environmental conditions by countering the transcription factors (Ayala *et al.*, 2017).

D – Motif for downregulated genes at 40ºC

Motif: AARWAAAAAGGAG

Where; R= G or A; W= T or A

The binding site of this motif is present in all promoter regions of downregulated genes at 40ºC. Motif elicitation also showed that LexA of *V. parahaemolyticus* and OmpR of *Y. pestis* share similar sequence of the motif.

E – Motif for up- or downregulated genes at 34ºC and 40ºC

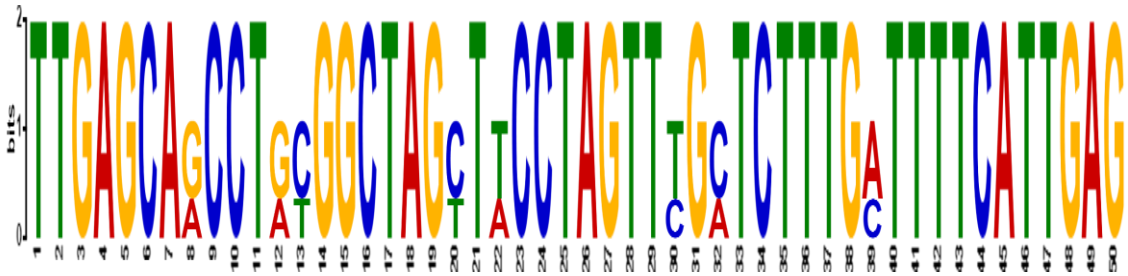

Motif: TTGAGCARCCTRYGGCTAGYTWCCTAGTTTGMTCTTTGATTTTCATTGAG

Where; R= G or A; Y=C or T; W= T or A; M= A or C

This motif is present in the all promoter regions of up- and downregulated operons at 34ºC and 40ºC. Motif analysis also showed that PvdS of *Pseudomonas aeruginosa* PAO1, ToxT and RpoN of *V. cholerae*, and LexA of *Caulobacter crescentus* have a similar binding site in their sequences. PvdS is an iron starvation sigma factor of *P. aeruginosa* and activates the regulation of genes encoding biosynthesis or uptake of siderophores

(Leoni *et al.*, 2000). ToxT is the major virulence transcription activator and regulates virulence factors toxin (CT) and toxin-coregulated pilus of *V. cholera* (Plecha and Withey, 2015), whereas RpoN is an alternative sigma factor that facilitates the regulation of motility and type VI secretion (T6SS) (Dong and Mekalanos, 2012). LexA is a transcriptional repressor, which is induced during DNA damage, and induces SOS genes such as cell division inhibitor in *C. crescentus* (Modell *et al.*, 2014).

3.9 Part C: Construction of isogenic mutants

Seven differentially regulated genes at different temperatures were selected to study the thermoregulation mechanism of *S. pneumoniae* D39 and their impact on pneumococcal physiology and virulence in detail (Table 3.5). In the light of literature, it has been shown that all selected genes involve in pneumococcal metabolism, virulence, or stress-response mechanisms. These genes were covered in below (Section 3.9.1). The notable up-regulated genes at 34ºC, while down-regulated at 40ºC, included SPD_0132/0133 coding for hypothetical proteins of unknown function, *ciaR* (*SPD_0701*) coding for DNA binding regulator protein, SPD_1651 coding for iron-compound ABC transporter ATP-binding protein, SPD_1711 coding for single-stranded DNA-binding protein, and *comD* (SPD_2064) coding for putative sensor histidine kinase. In contrast, *merR*^{2} (SPD_0447) encoding glutamine synthetase repressor protein and *gdhA* (SPD_1158) coding for glutamate dehydrogenase are downregulated at 34ºC, while upregulated at 40ºC, relative to 37ºC. The relative expression of studied genes is shown in Table 3.5.

Table 3.5. Fold change of target genes at 34ºC or 40ºC, relative to 37ºC.

Gene name	34ºC	40ºC
SPD_0132/0133	6.23/52.94	-5.81/-31.81
ciaR (SPD_0701)	2.06	-2.59
comD (SPD_2064)	53.65	-44.92
SPD_1651	3.83	-1.96
SPD_1711	59.26	-36.28
gdhA (SPD_1158)	-2.21	2.11
merR² (SPD_0447)	-3.66	2.96

3.9.1 Selection of targets to study their possible involvement for pneumococcal thermal adaptation

SPD_0132/0133 are hypothetical proteins, which are annotated as bacteriocin class II with double-glycine leader peptide (Kanehisa *et al.*, 2016). Bacteriocins are naturally produced antimicrobial peptides (Yang *et al.*, 2014). These peptides have significant potency and exhibit narrow or broad spectrum range and particularly lethal against other bacteria (Cotter *et al.*, 2013).

S. pneumoniae is a coloniser of nasopharynx, and it is reasonable to assume that bacteriocin activity might play an important role in the fluctuating environment in the host and during competition with other inhabiting bacteria in the same niche, therefore it involves the pneumococcal virulence (Lux *et al.*, 2007). It has been reported that pH, temperature and culture medium composition, and inhibitory compounds are influential

conditions on bacteriocin activity (Ben Belgacem *et al.*, 2012). Lux et al. (2007) reported that the bacteriocin is linked to biofilm formation as it was active at nasopharyngeal temperature (35°C), but not at growth temperature (37°C) (Lux *et al.*, 2007). A study with genetic analysis of bacteriocin clusters in pneumococcus showed that bacteriocin genes are differentially expressed in response to environmental stress conditions (Rezaei Javan *et al.*, 2018). Therefore, it is beneficial to study SPD_0132/133 under different temperatures to figure out its role on thermo-adaptive mechanisms of *S. pneumoniae*.

CiaR (SPD_0701) is a part of CiaRH operon, which is one of TCS in streptococci (Geno *et al.*, 2015). CiaH is a sensor of histidine kinase produced in the bacterial cell membrane and transfers environmental signals to CiaR, which is a DNA-binding response regulator (Wu *et al.*, 2010). The CiaRH system is responsible for various roles in streptococci. In *S. mutants*, CiaRH is involved in bacterial competence, tolerance to oxidative stress, and bacteriocin production (Levesque *et al.*, 2007; Qi *et al.*, 2004). In *S. gordonii*, CiaRH is induced when SdbA, encoding disulfide oxidoreductase, which represses bacteriocin production (Davey *et al.*, 2016), and maintains pH homeostasis and oxidative stress (Liu and Burne, 2009).

The CiaRH regulon is distributed in 18 different genomic regions in *S. pneumoniae*, and 26 genes involving pneumococcal colonisation and virulence were shown to be controlled by CiaR (Mascher *et al.*, 2003). It has been shown that CiaRH system directly regulates the competence-related Cia-regulated virulence gene, *htrA* encoding serine protease, which enables *S. pneumoniae* to colonise at various host tissues, to survive at high temperatures, and enhances resistance to oxidative stress (Ibrahim *et al.*, 2004b). Therefore, the importance of CiaR in various environmental signals in pneumococcus made this gene a good candidate for this study.

ComD (SPD_2064) is a histidine kinase of ComDE TCS and controls the development of genetic transformation and competence in *S. pneumoniae* (Johnsborg and Havarstein, 2009). DNA transformation in pneumococcus is induced by competence stimulating peptide (CSP) (Salvadori *et al.*, 2019). The binding of CSP to ComD (SPD_2064) initiates the competence. Phosphorylated ComD transfers phosphoryl group to ComE (response

regulator), and ComE regulates ComX (alternative sigma factor), which plays role on the regulation of late competence genes, secretion of DNA binding proteins, DNA binding-uptake, and transcriptional activation of competence (Steinmoen *et al.*, 2003). Zhu and Lau (2011) has reported that pneumococcal genes encoding virulence and antibiotic resistance are important for uptaking exogenous DNA and competence (Zhu and Lau, 2011). It has been shown that ComDE system is crucial for pneumococcal colonisation and virulence, and absence of the genes leads enhanced colonisation fitness and reduced expression of virulence factors required for infection (Kowalko and Sebert, 2008). Furthermore, Bartilson *et al.* (2001) found that the inactivation of ComD resulted in attenuated colonisation in pneumonia and bacteraemia infection models in mice (Bartilson *et al.*, 2001). Claverys *et al.* (2006) also reviewed that competent pneumococcal cells are more responsive to stress conditions such as DNA-damage and antibiotic treatments (Claverys *et al.*, 2006). A transcriptional analysis also showed that CSP-ComDE cascade positively regulates some stress response genes such as GroEL, HrcA, DnaK, and SpoJ, which are important heat-shock proteins or chaperonins, during development of competence (Peterson *et al.*, 2004). In addition, its massive expression at different temperatures (Table 3.5) made ComD a feasible candidate in my study. While characterization and regulation of ComD has been studied in detail in *S. pneumoniae*, there is more research needs to be done with respect to its contribution in thermal adaptation.

SPD_1711 was another target to test my hypothesis. *SsbB* gene is annotated to be coding for single-stranded DNA binding proteins (SSBs) (Kanehisa *et al.*, 2016), which are required for DNA replication, homologous recombination or genomic maintenance such as repair mismatches by binding to ssDNA and triggers targeted proteins during DNA metabolism in eukaryotes, prokaryotes, or archaea (Dickey *et al.*, 2013). It has been known that SSBs binding partners bind to the well-conserved C-terminal region of SSBs and activates DNA replication stress (Shereda *et al.*, 2008). The binding of SSB proteins under temperature stress has been studied in various species. Lu and Keck (2008) reported that Pro-176 sequence is mutated to a Ser in sequence of *ssb113* protein when *E. coli* is exposed to temperature-stress. The change in amino acid sequence of binding protein affected DNA replication (Lu and Keck, 2008). Olszewski *et al.* (2010) studied the SSB protein in thermophilic *Thermotoga maritima* (*Tma*SSB) and *Thermotoga neapolitana*

(*Tne*SSB). *Tma*SSB and *Tne*SSB were identified as the most thermostable single-stranded DNA binding proteins and they can be alternative to other temperature-related binding proteins, which are used in various applications requiring high temperatures such as PCR (Olszewski *et al.*, 2010). In addition, Biswas-Fiss *et al.* (2012) showed the thermodynamic activation of SSB protein in *Bacillus anthracis* (SSB_{BA}) and investigated that the binding of SSB_{BA} to ssDNA is temperature-dependent. The binding analysis showed that the segregation of binding partners increased at higher temperatures (37°C) compared to lower temperature (20°C), likely due to increased K_D value (Biswas-Fiss *et al.*, 2012).

In *S. pneumoniae*, two SSbs are present, SsbA and SsbB (Grove *et al.*, 2005). The expression studies suggested that SsbA carries the general roles of SSBs, while SsbB is functional during competency and DNA transformation in pneumococcus (Salerno *et al.*, 2011). The importance of SsbB in protection of internal ssDNA was further studied at 25°C and 30°C in the mutant and wild type strains. Interestingly, the disintegration of ssDNA during DNA transformation increased at 30°C (Attaiech *et al.*, 2011), suggesting that SsbB is a temperature-dependent protein and further analysis is required. Therefore, I hypothesized that this gene has a role on creating new phenotype at different temperatures. In addition, it had very high expression levels at different temperatures (Table 3.5).

SPD_1651 is annotated to be coding for iron-compound ABC transporter ATP-binding protein (Kanehisa *et al.*, 2016). Bacterial transport systems have been evolved for nutrient uptake regarding host-pathogen interaction (Tanaka *et al.*, 2018). ATP-binding cassette (ABC) transporters are classified as membrane proteins involved in signal transduction between membrane and environment, protein secretion, antibiotic resistance, nutrient acquisition, adhesion, environmental sensing, and growth under stress conditions (Tanaka *et al.*, 2018). Iron is an important trace element as a cofactor in TCA cycle, a catalyst in electron transportation, and also required for other biological processes such as superoxide metabolism (Davidson *et al.*, 2008). Therefore, transfer of iron from erythrocytes or other sources is vital for visibility, virulence, and survival of pathogen.

In *S. pneumoniae*, three gene clusters *pit*, *pia*, and *piu*, are identified to be involved in iron uptake (Tai *et al.*, 2003). These ABC transporters are crucial for pneumococcal virulence and effect on micronutrient acquisition under stress conditions such as iron depletion. It can be predicted that micronutrients, iron in this case, can influence gene regulation, which could affect pneumococcal adaptation to the host environment. The influence of temperature on iron uptake has not been studied well. Worsham and Konisky (1984) studied the role of growth temperature on iron uptake in *S. typhimurium* and *E. coli*. It was found that these species synthesize the siderophores (enterochelin) and generate transport system in the absence of iron. However, the transportation of ferric enterochelin attenuated 50% in Fur-null strain at 42°C compared to 37°C, whilst no difference was observed in wild type strains at these temperatures (Worsham and Konisky, 1984). On the other hand, the synergy between pyoverdin and pyochelin (siderophores) of *P. aeruginosa* PAO1 is negative as pyoverdin production decreased at 42°C, while pyochelin increased at 42°C and 25°C (Dumas *et al.*, 2013). These results confirmed that the activity of transporters are affected by temperature shift.

Iron uptake in *S. pneumoniae* has been studied in detail, however, the impact of temperature on acquisition is still unknown. Hence, its importance on pneumococcal nutrient metabolism and virulence made this gene a good candidate for my study.

MerR^2 (SPD_0447) was the next candidate gene for further analysis, which is a member of MerR transcriptional regulators, and mostly act as an activator on promoters. The MerR-like regulators are well-known in bacteria. They activate the transcription of genes involved in metal ion detoxification, efflux, or micronutrient metal homeostasis such as copper, zinc, and cobalt salts and oxidative stress (Brown *et al.*, 2003), nitrosative and carbonyl stress (McEwan *et al.*, 2011), heat-shock (Roncarati and Scarlato, 2017), and biofilm formation (Liao and Sauer, 2012) in numerous species. Kaspar *et al.* (2014) studied the growth of *L. monocytogenes* in different nitrogen sources at 24°C and 37°C, and revealed that the microbe grows better with ammonium at 24°C compare to glutamine, while no difference in both sources was observed at 37°C. This is possibly due to the strong expression of GlnR (known as MerR^2 in pneumococcus), GlnA, and GlnK

at 24°C. These result suggested that utilization of nitrogen sources is temperature-dependent (Kaspar *et al.*, 2014) .

In *S. pneumoniae*, $MerR^2$ was shown to mediate transcriptional repression (as opposite to being an activator for many other genes) of genes in GlnR regulon involved in glutamine and glutamate synthesis (GdhA), transportation of these N-sources (GlnPQ), and pentose uptake encoded by *glnPQ-zwf* in the presence of glutamine synthetase (GS) (Kloosterman *et al.*, 2006). The contribution of $MerR^2$ on regulation of pneumococcal nitrogen metabolism has been well studied, however, the impact of temperature is still unknown. Interestingly, unlike to the genes selected above, $MerR^2$ was downregulated at 34°C, while upregulated at 40°C (Table 3.5). Therefore, I hypothesized that this gene has a potential role on thermal adaptation of *S. pneumoniae*.

GdhA (SPD_1158) was my last candidate gene for this study. Glutamate dehydrogenases (GDHs) are a group of enzymes that involve in carbon and nitrogen metabolism (Gunka *et al.*, 2013), which catalyse the reversible oxidative deamination of glutamate to α-ketoglutarate and ammonia while reducing $NADP^+$ to NADPH (Plaitakis *et al.*, 2017). Glutamate plays a key role in central amino acid metabolism and biosynthesis of many other amino acids (Walker and van der Donk, 2016), and a wide range of metabolic processes such as glycolysis in cells (Feehily and Karatzas, 2013).

The importance of GdhA has been studied in many different organisms (Girinathan *et al.*, 2016), however, its involvement into temperature adaptation has not been studied in detail, particularly in mesophiles. Temperature-dependent GdhA activity has been investigated in hyperthermophiles, and it was reported that GdhA is a thermostable protein (Bhuiya *et al.*, 2002). Moreover, the microarray data in this study showed that GdhA was downregulated at 34°C, while upregulated at 40°C. Therefore, I hypothesized that the GdhA is also an individual thermosensing protein for *S. pneumoniae.*

3.10 Mutagenesis by gene splicing overlap extension PCR (SOEing PCR)

Gene splicing by overlap extension PCR (SOEing) was used to generate desired modification in pneumococcal genome. This method provides an easy, rapid and robust way of recombining sequences without depending on restriction/ligation or plasmid propagation to perform site-directed mutagenesis *in vitro* (Horton, 1995). *S. pneumoniae* is naturally competent bacteria which makes SOEing method ideal to incorporate recombinant DNA into pneumococcal genome (Steinmoen *et al.*, 2003). The main steps of SOEing PCR is illustrated in Figure 3.10. The main idea of this method is to delete the target gene and replace it with the *aadA* gene that encodes aminoglycoside-3-adenylyltransferase (Aad), which confers resistance to spectinomycin. As shown in Figure 3.10, SOEing is formed of two-step PCR. In the first PCR, two fragments (left flank (LF) and right flank (RF)) which have their ends modified to introduce a region of homology, were generated. As mentioned, the antibiotic cassette (*aadA*) was also amplified in this step. In the second PCR, these three fragments are fused to generate the SOEing construct, which is then introduced into *S. pneumoniae* by transformation, and incorporated into its genome via homologous recombination, replacing the target gene with *aadA* cassette.

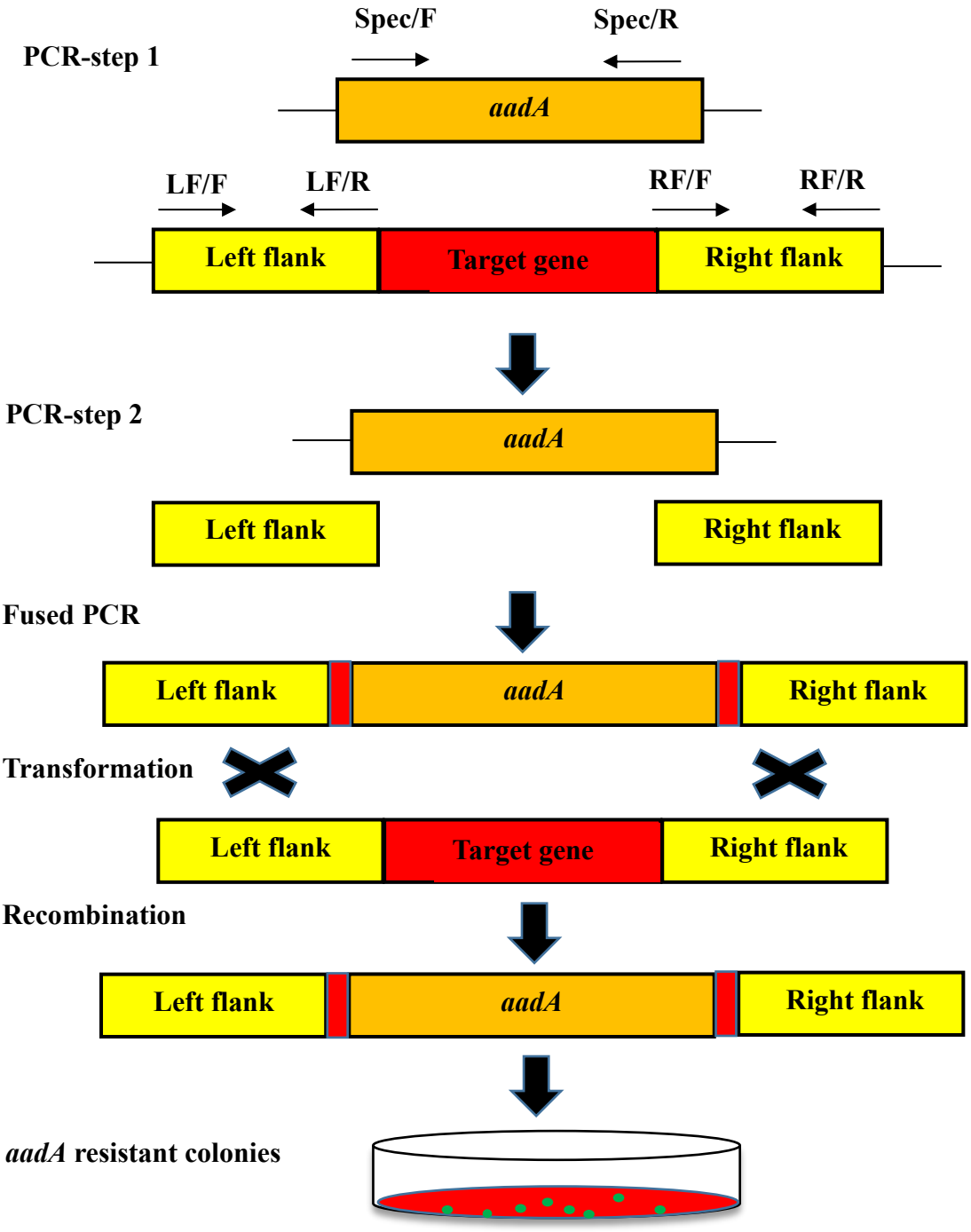

Figure 3.10. Schematic representation of allelic replacement mutagenesis (SOEing PCR) and homologous recombination in *S. pneumoniae*.
The target gene is deleted and replaced with *aadA* antibiotic resistance cassette. The figure is constructed based on Song *et al.* (2005).

3.11 Amplification of SOEing flanks and antibiotic cassette *aadA*

The left and right flanking regions of target genes (~800 bp each) and *aadA* resistance cassette (1158 bp) were amplified as described previously in section 2.12.2. Amplified products were analysed on agarose gel electrophoresis and the amplicons were confirmed by the size of the bands. Figure 3.11 represents the successful amplification of left and right flanks of each target gene and *aadA* antibiotic resistance cassette. In the figure, Lane 7 in panel A and lane 5 in panel C show the amplicon for *aadA* (1158 bp) amplified form pDL278 (Yesilkaya *et al.*, 2000). In panel A, lanes 1, 3, 5 illustrate the amplicons for left flanking and lane 2, 4, and 6 illustrate the amplicons for right flanking regions of *gdhA* (SPD_1158), *ciaR* (SPD_0701), *comD* (SPD_2064), respectively. In panel B, lane 1 and 2 represents the left and right flanking regions of SPD_0132/0133 locus. In panel C, lane 1 and 3 represent left flanking and lane 2 and 4 right flanking regions of DNA-binding protein (SPD_1711) and iron-compound transporter gene (SPD_1651), respectively. The amplicons of *merR*^{2} were not analysed in agarose gel as this mutant strain was obtained from Dr. Firas Al-Bayati (Al-Bayati *et al.*, 2017), as mentioned in section C. The successful amplicons were required to construct spectinomycin resistant mutant strains to test the hypothesis of this study.

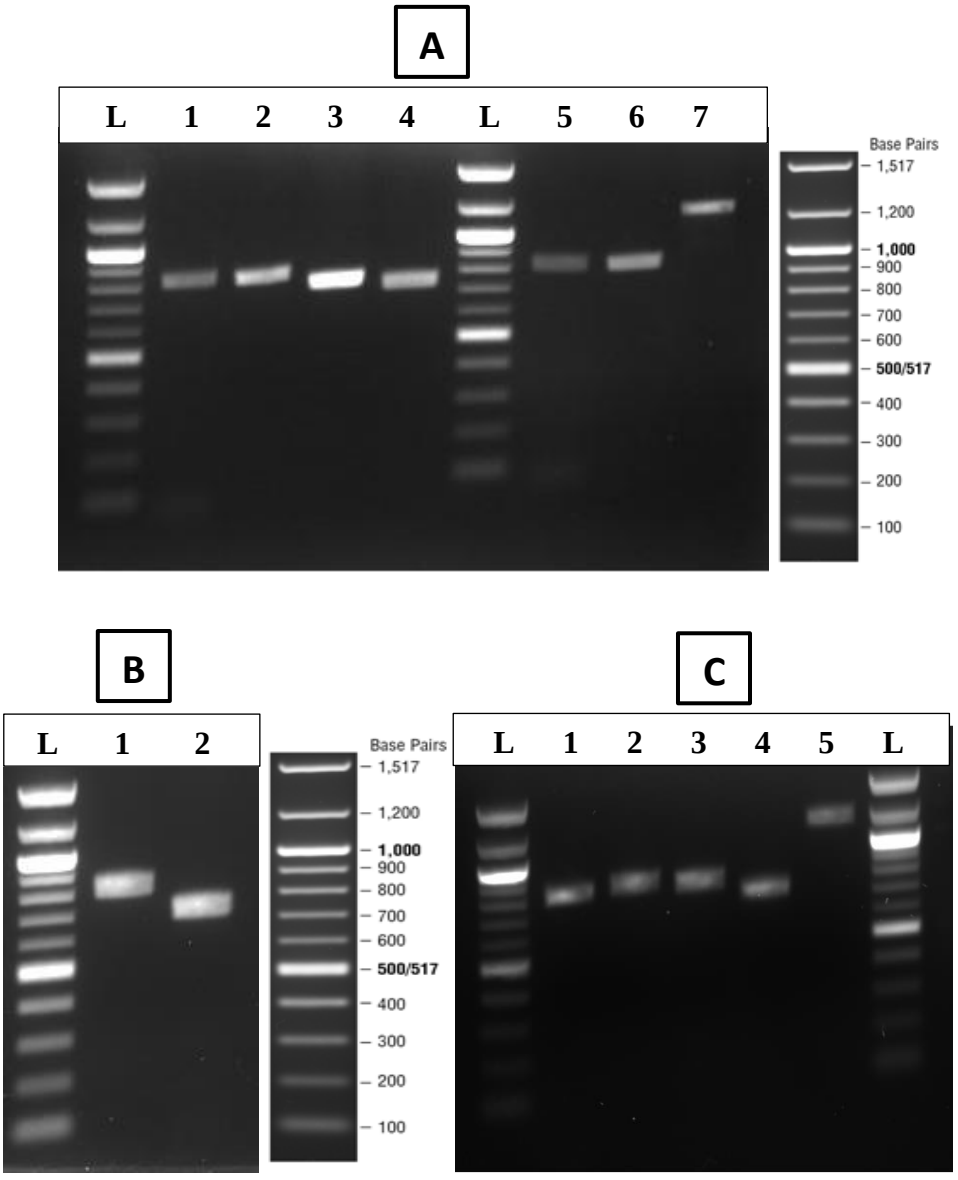

Figure 3.11. The image of agarose gel electrophoresis analysis showing the amplified antibiotic resistance gene, and the flanking regions of each target gene.
A: L - 500 ng of 100 bp DNA ladder (NEB); Lanes 1, 3, 5 are left flanking and lanes 2, 4, 6 are right flanking regions of gdhA, ciaR, and comD, respectively; Lane 7 is *aadA* cassette amplified from the plasmid pDL278. **B**: L - 500 ng of 100 bp DNA ladder; Lane 1 is left flanking and lane 2 is right flanking region of SPD_0132/133. **C**: L - 500 ng of 100 bp DNA ladder; Lanes 1 and 3 are left flanking and lanes 2 and 4 are right flanking regions of SPD_1711 and SPD_1651, respectively; Lane 5 is *aadA* cassette.

3.12 Fusion of SOEing fragments and transformation into D39

The flanking regions of each target genes were fused with the amplicons of spectinomycin resistance cassette using the primers X_LF/F and X_RF/R (where X refers to code of the target gene) as previously described in section 2.12.3. The fusion products were analysed on the agarose gel electrophoresis and specific fusion products were gel-cut, purified and re-visualized on agarose gel (Figure 3.12). The size of PCR products were the total size of left-right flanks (~800 bp each) of target gene and the *aadA* (1158 bp) which equals to approximately 2758 bp. The linear SOEing products were transformed into *S. pneumoniae* D39 strain as mentioned in section 2.12.3, and the transformants were selected on BAB plates supplemented with spectinomycin (100 mg/ml).

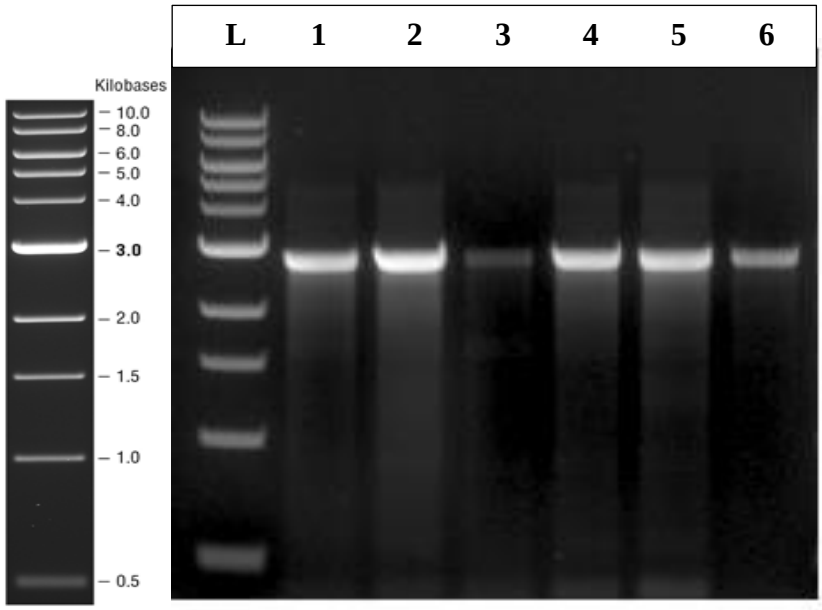

Figure 3.12. The image of agarose gel electrophoresis analysis showing the fused SOEing fragments which are approximately 2758 bp.
L- 500 ng of 1 kb DNA ladder (NEB); Lanes 1 to 6 representing the fusion of flanking regions of gdhA, ciaR, comD, SPD_0132/133, SPD_1711 and SPD_1651, respectively, with *aadA* antibiotic cassette.

3.13 Confirmation of mutagenesis

The successful construction of pneumococcal mutants was confirmed by PCR. To do this, different primer combinations were used to confirm the replacement of target genes with the antibiotic cassette as shown in Figure 3.13. The primer sets amplified larger PCR products from the mutant strains Δ*ciaR* (741 bp), Δ*SPD_0132/0133* (339 bp), Δ*SPD_1711* (396 bp), Δ*SPD_1651* (753 bp), and Δ*merR*^{2} (357 bp) compared to wild type since replacement gene *aadA* (1158 bp) is larger than the deleted target genes. In addition, Δ*gdhA* (1347 bp) and Δ*comD* (1326 bp) are slightly larger than the *aadA* gene, hence smaller amplicons were obtained compared to the wild type. The first primer set was designed as Ext/F and Ext/R to amplify approximately 800 bp from the up- and downstream of the target genes and *aadA* (spectinomycin) cassette from the mutant strains. Secondly, Ext/F-Spec/R and the Spec/F-Ext/R primers were used to amplify the targeted flanking region and the *aadA* cassette. Finally, Spec/F and Spec/R primers were designed to confirm whether the target gene was replaced by the *aadA* cassette. This primer set was generated to confirm the presence of *aadA* cassette in the genome of the mutant strains, therefore, no product was expected from the wild type DNA due to absence of *aadA* in the D39 genome.

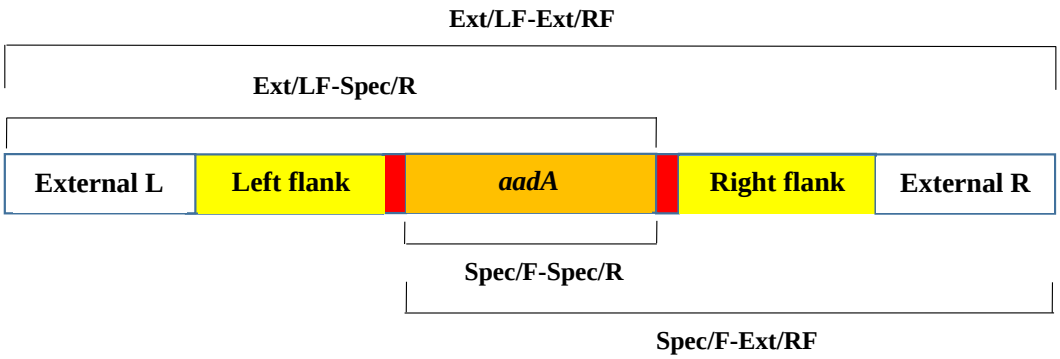

Figure 3.13. Illustration of mutation confirmation strategy.
Ext/LF indicates the forward primer of external left flank and Ext/RF is for the reverse primer of external right flank. All primers are shown in Table 2.3 and 2.4.

The insertion/deletion mutagenesis was confirmed by PCR using the genomic DNA from the putative mutant strains as templates. The wild type DNA was also used as a control. The PCR products were visualized by agarose gel electrophoresis in Figure 3.14. All the amplified products had the expected size (1158 bp) for the *aadA* cassette (Panel A: Lane 5 and 8 for Δ*gdhA* and Δ*ciaR*, respectively. Panel B: Lane 1 for Δ*comD* and Δ*SPD_0132/0133*. Panel C: Lane 1 for Δ*SPD_1711* and Δ*SPD_1651*). Lane 2 shows the amplified products using the mixture of upstream external forward primers (Ext/F) and the spectinomycin reverse primer (Spec/R) whilst lane 3 illustrates the PCR products using the primers of spectinomycin forward primer (Spec/F) and the downstream external reverse primers (Ext/R). External primers were designed as approximately 200-300 bp away from the upstream and downstream regions of each target gene, therefore, the size of PCR products vary for each target gene. Lane 4 and 5 contain PCR products that amplified using the Ext/F and Ext/R primers.

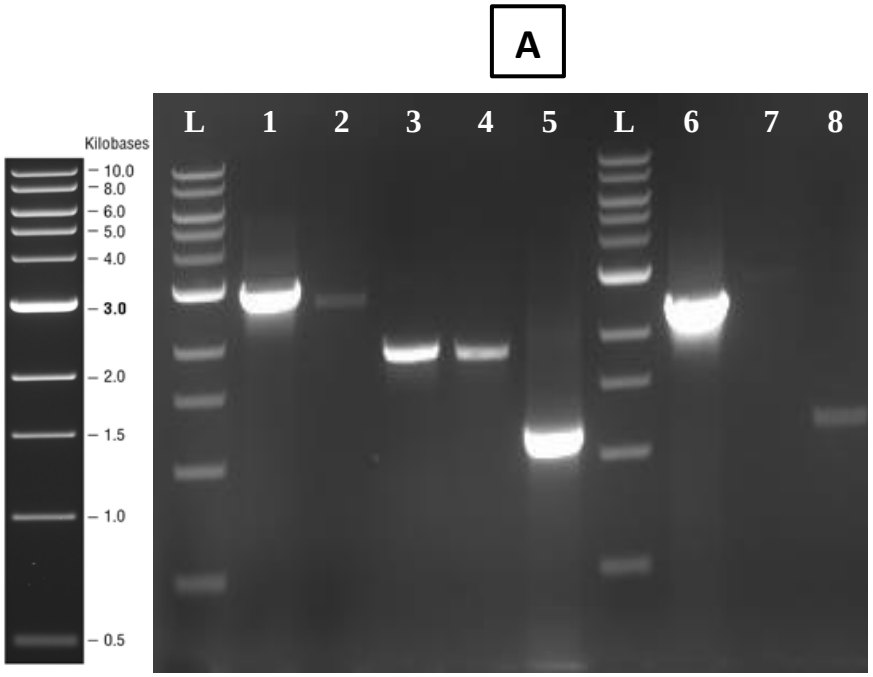

Δ*gdhA* (Left, 1-5)

Lane 1: 2877 bp
Lane 2: 2668 bp
Lane 3: 2466 bp
Lane 4: 2457 bp
Lane 5: 1158 bp

Δ*ciaR* (Right, 6-8)

Lane 6: 2688 bp
Lane 7: 2958 bp
Lane 8: 1158 bp

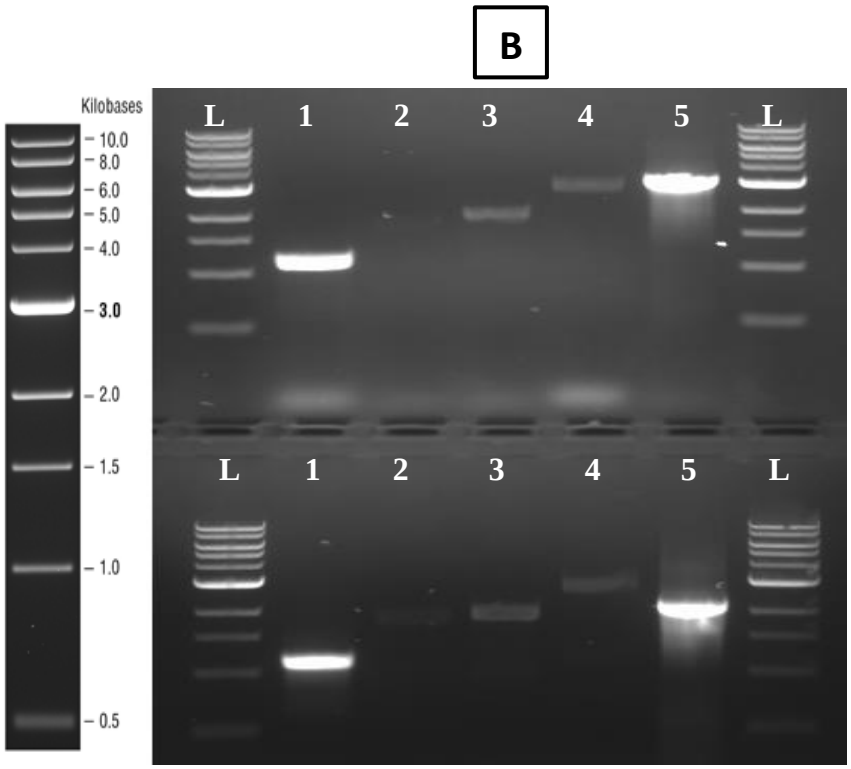

Δ*comD*

Lane 1: 1158 bp
Lane 2: 1866 bp
Lane 3: 2017 bp
Lane 4: 2966 bp
Lane 5: 3134 bp

Δ*SPD_0132/0133*

Lane 1: 1158 bp
Lane 2: 1929 bp
Lane 3: 2019 bp
Lane 4: 3031 bp
Lane 5: 2212 bp

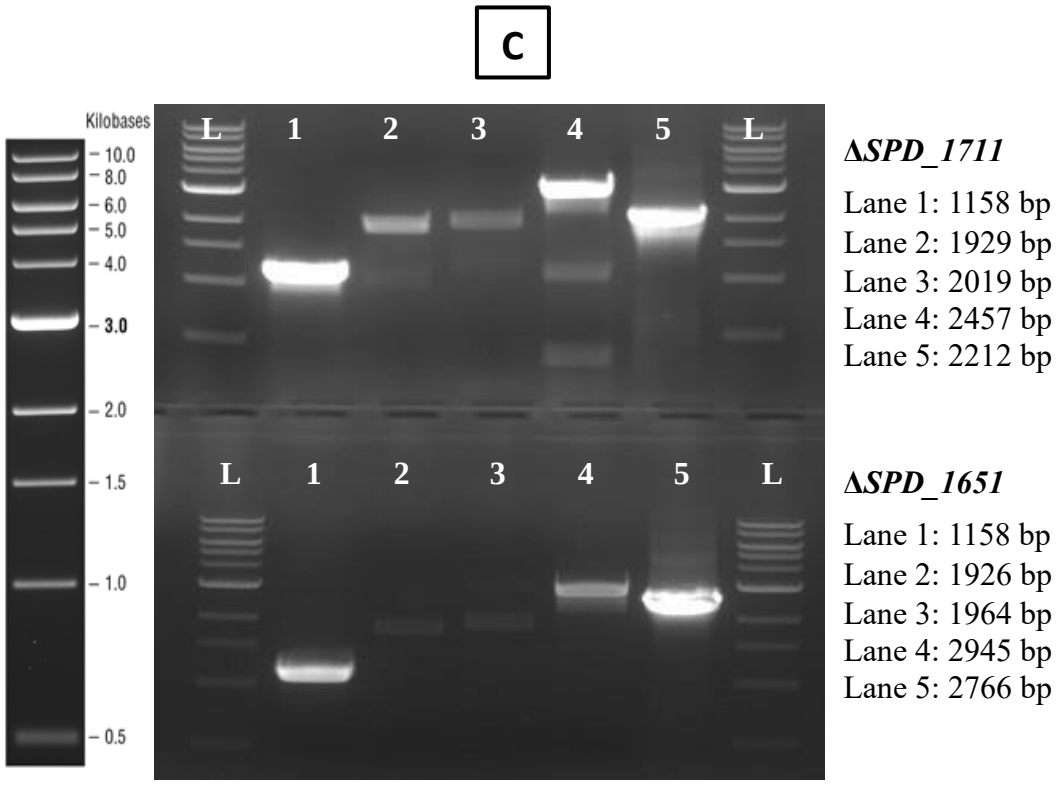

Figure 3.14. Successful integration of recombinant SOEing products into D39 genome.

Confirmations were done by using different primer sets and D39 DNA was used as a control. (Ext: External; Spec: Spectinomycin primer sets). In all panels, L represents 1 kb DNA maker (NEB). In panel A; Lane 1 and 6 contain amplicons obtained with Ext/LF/F-RF/R primers using wild type DNA; Lane 2 represents products entire mutagenized region using Ext/LF/F- Ext/RF/R primers; Lane 3 and 4 contain products using Ext/LF/F-Spec/R and Spec/F-Ext/RF/R, respectively. Lane 7 represents the product using Ext/LF/F-Spec/R. Lane 5 and 8 represent amplified products representing spectinomycin cassette. In panels B and C; Lane 1 contains amplified products representing spectinomycin cassette, obtained using Spec/F and Spec/R primers; Lane 2 represents products obtained with Ext/LF/F- Spec/R primers using mutant genomic DNA; Lane 3 represents products obtained with Spec/F-Ext/RF/R primers using mutant genomic DNA; Lane 4 contains the product for entire mutagenized region using Ext/LF/F-RF/R primers; Lane 5 contains amplicons obtained with Ext/LF/F-RF/R primers using wild type DNA. The sequences of primers have been given in Table 2.3 and 2.4.

3.14 Part D: Temperature-dependent phenotypic characterisation of pneumococcal mutant strains

The impact of temperature shifts on the mutants were investigated at different temperatures to identify their possible contribution to pneumococcal growth, production of virulence factors, capsular biosynthesis and biofilm formation as done for D39 wild type strain (Part A).

3.15 Growth behaviour of pneumococcal strains in CDM medium

Growth profile of pneumococcal strains was analysed in CDM supplemented with 55 mM glucose at 34°C, 37°C, or 40°C (Figure 3.15 A-C). There was no difference in the growth rate of all strains compare to the wild type at 37°C (Table 3.6) (p>0.05). However, the growth rates of Δ*comD*, Δ*SPD_1711*, and Δ*SPD_1651* (0.27 ± 0.01, 0.27 ± 0.01, and 0.26 ± 0.03 h^{-1}, respectively) were significantly lower than that of wild type strain (0.35 ± 0.00 h^{-1}) (p<0.05) at 34°C. This result indicated that mutations of ComD, SPD_1711, and SPD_1651 have temperature-dependent effects on pneumococcal growth. When incubation temperature shifted to 40°C, the growth rate of all the mutant strains were significantly attenuated compared to the wild type strain.

As for growth yield, the wild type strain had significantly higher growth yield than all other mutant strains at all temperature (Table 3.6).

Altogether, it can be concluded that high temperature has a major effect on pneumococcal growth phenotype and ComD, SPD_1711, and SPD_1651 are required for pneumococcal growth at different temperatures. Hence, further characterization is required to identify the role of these genes on pneumococcal virulence and survival under temperature shifts.

Table 3.6. Growth rate (h^{-1}) and yield (OD_{600nm}) of pneumococcal strains grown in CDM supplemented with 55 mM glucose at 34°C, 37°C, or 40°C.
Values are average of at least three independent experiments each with three replicates. '±'indicates standard error of means (SEM).

Strains	34°C		37°C		40°C	
	Growth rate $\mu(h^{-1})$	Growth yield (Max OD_{600})	Growth rate $\mu(h^{-1})$	Growth yield (Max OD_{600nm})	Growth rate $\mu(h^{-1})$	Growth yield (Max OD_{600nm})
D39 (wt)	0.35 ±0.00	1.38 ±0.00	0.39 ±0.00	1.48 ±0.00	0.30 ±0.01	1.19 ±0.01
Δ*gdhA*	0.30 ±0.02	1.20 ±0.03	0.33 ±0.01	1.22 ±0.08	0.21 ±0.02	0.80 ±0.02
Δ*ciaR*	0.34 ±0.00	1.22 ±0.01	0.39 ±0.06	1.22 ±0.06	0.22 ±0.04	0.76 ±0.08
Δ*comD*	0.27 ±0.01	0.97 ±0.10	0.34 ±0.00	1.38 ±0.01	0.23 ±0.02	0.74 ±0.07
Δ*merR*^{2}	0.34 ±0.01	1.24 ±0.01	0.34 ±0.01	1.24 ±0.00	0.23 ±0.02	0.78 ±0.04
Δ*SPD_0132/133*	0.38 ±0.00	0.88 ±0.01	0.34 ±0.01	1.03 ±0.08	0.23 ±0.03	0.77 ±0.03
Δ*SPD_1711*	0.27 ±0.01	0.97 ±0.09	0.38 ±0.06	1.06 ±0.07	0.22 ±0.02	0.66 ±0.04
Δ*SPD_1651*	0.26 ±0.03	0.86 ±0.00	0.46 ±0.00	0.93 ±0.02	0.21 ±0.06	0.56 ±0.04

A - 34°C

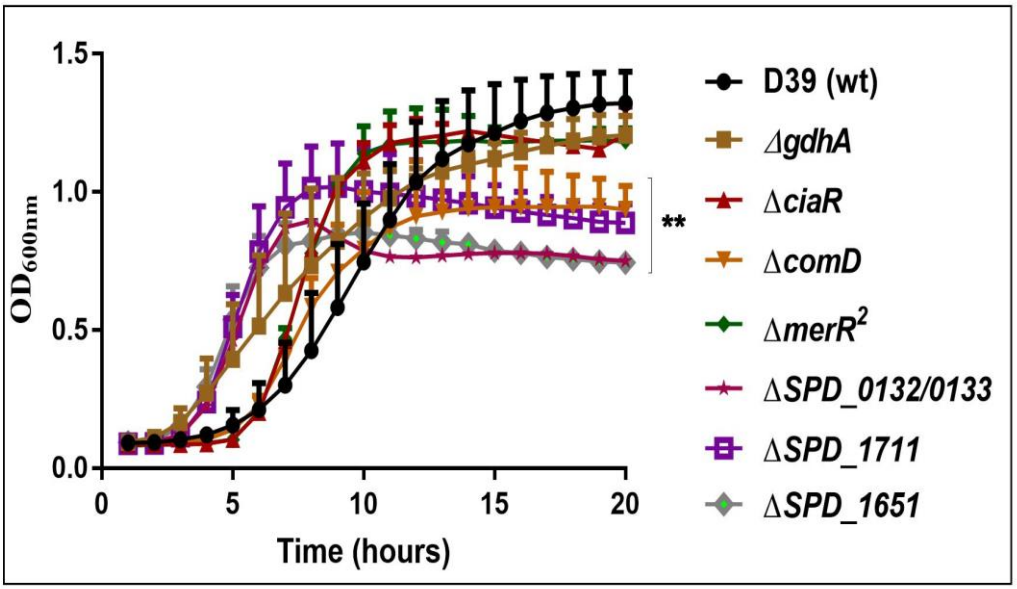
1.5
1.0
0.5
0.0
OD600nm
0
5
10
15
20
Time (hours)
**
D39 (wt)
ΔgdhA
ΔciaR
ΔcomD
ΔmerR2
ΔSPD_0132/0133
ΔSPD_1711
ΔSPD_1651

B - 37°C

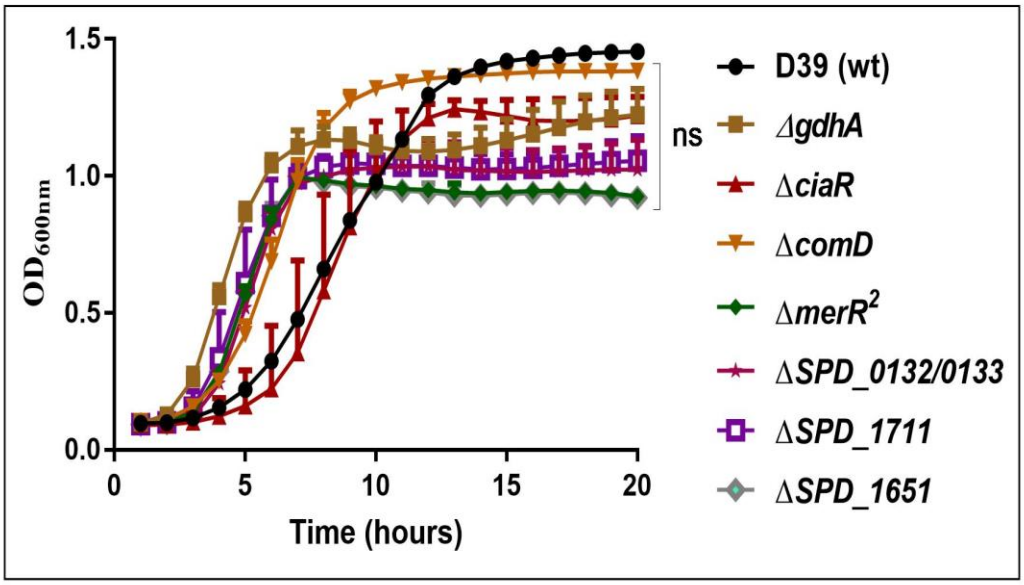
1.5
1.0
0.5
0.0
OD600nm
0
5
10
15
20
Time (hours)
ns
D39 (wt)
ΔgdhA
ΔciaR
ΔcomD
ΔmerR2
ΔSPD_0132/0133
ΔSPD_1711
ΔSPD_1651

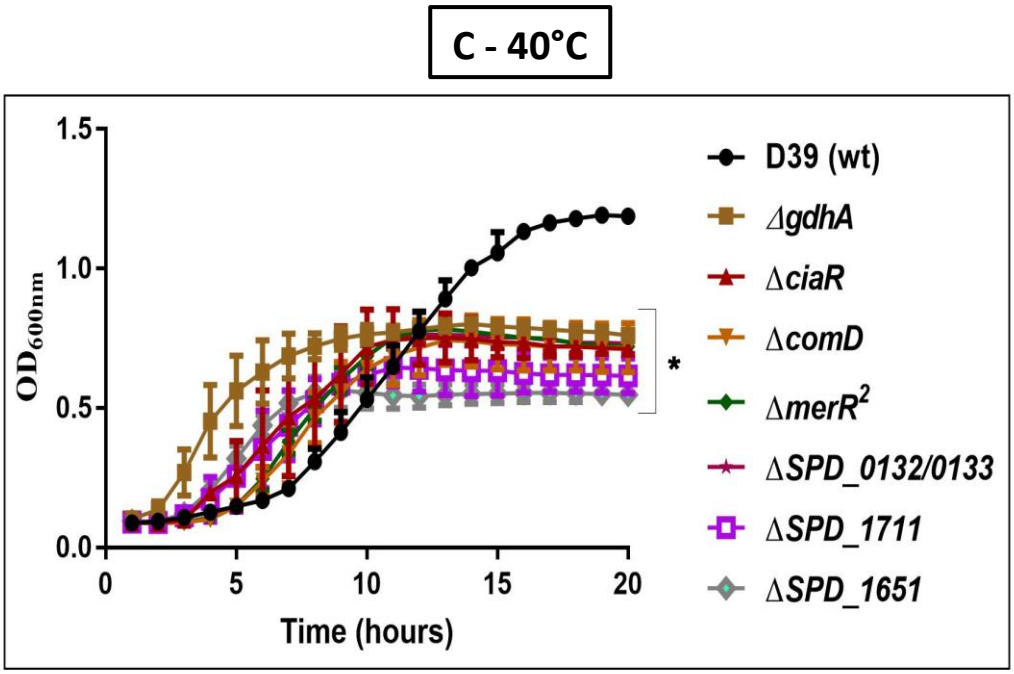

Figure 3.15. Pneumococcal growth curves performed in CDM supplemented with 55 mM glucose at 34°C (A), 37°C (B), or 40°C (C).
Error bars show the standard error of the mean for three individual measurements each with three replicates. No difference was seen between the growth rates of all mutant strains compared to wild type strain at 37°C. All mutants grew significantly less than wild type at 40°C. At 34°C, Δ*comD,* Δ*SPD_1711,* and Δ*SPD_1651* had lower growth rate relative to wild type. Significant differences were seen comparing the growth rates of mutant strains to the wild type D39 using two-way ANOVA. (* $p<0.05$, ** $p<0.01$, ns: not significant).

3.16 Cell size determination of pneumococcal strains in CDM medium

Bacterial cells have ability to synchronise growth pattern with the cell size, which require sensing temperature changes or nutrient availability (Chien *et al.*, 2012). To test how temperature shifts affect the morphology microscopically, the wild type and mutant strains were grown micro-aerobically in CDM supplemented with glucose at different temperatures until mid-log phase, Gram-stained, and the cell size was measured under the light microscopy as described in section 2.18.

The temperature shifts led to a statistically significant change in the cell size of mutants relative to the wild type strain D39. The results of the measurements of the cell dimensions are summarized in Table 3.7 and Figure 3.16. In particular, at 37°C, the cell size of Δ*SPD_0132/0133*, Δ*SPD_1711*, and Δ*SPD_1651* significantly reduced (p<0.05), while the rest of the mutants had similar size of cells compare to the wild type. This is likely due to the impact of these genes on cellular processes other than the thermal adaptation at 37°C. At 34°C, the size of all mutants, except Δ*merR*^{2} (0.40 ± 0.01 µm), was significantly lower than the wild type (0.44 ± 0.01 µm). Furthermore, incubation at 40°C reduced at least 20% of size for all the mutants compared to the wild type (p<0.05).

The results on cells size suggested that the inactivation of genes caused cells to reduce their size possibly by changing some cellular processes such as the length of time for DNA replication or volume of cell mass. In addition, it can be concluded that cell size of pneumococcus is controlled in a temperature-dependent manner.

Table 3.7. Cell sizes of pneumococcal strains grown in CDM supplemented with 55 mM glucose at 34°C, 37°C, or 40°C.
Values are average of at least 10 single cell each with three replicates. '±'indicates standard error of means (SEM).

	Cell size (µm)		
Strains	**34°C**	**37°C**	**40°C**
D39 (wt)	0.44 ± 0.01	0.48 ± 0.01	0.36 ± 0.00
Δ*gdhA*	0.39 ± 0.00	0.46 ± 0.00	0.25 ± 0.01
Δ*ciaR*	0.38 ± 0.01	0.45 ± 0.01	0.24 ± 0.01
Δ*comD*	0.38 ± 0.00	0.45 ± 0.01	0.26 ± 0.00
Δ*merR*^{2}	0.40 ± 0.01	0.47 ± 0.01	0.28 ± 0.01
Δ*SPD_0132/133*	0.39 ± 0.00	0.44 ± 0.02	0.23 ± 0.01
Δ*SPD_1711*	0.38 ± 0.00	0.43 ± 0.01	0.24 ± 0.01
Δ*SPD_1651*	0.38 ± 0.01	0.44 ± 0.00	0.25 ± 0.00

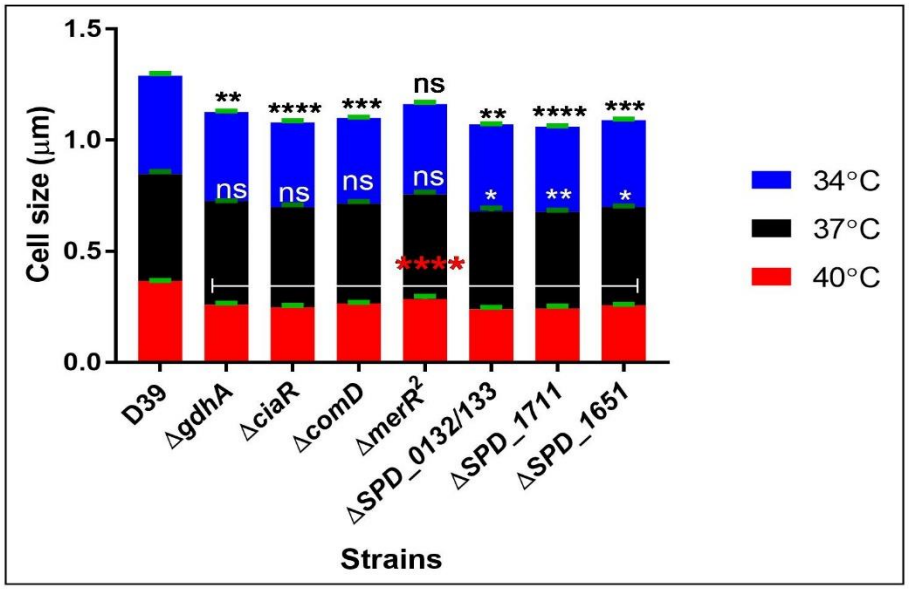

Figure 3.16. Cell sizes of pneumococcal strains grown in CDM supplemented with 55 mM glucose at different temperatures.
All the mutant strains reduced their size significantly compared to wild type D39 at 40°C. At 34°C, all the mutant cells, except Δ*merR*^{2}, had similar size relative to wild type. At 37°C, the cell size of Δ*SPD_0132/0133*, Δ*SPD_1711*, and Δ*SPD_1651* were significantly reduced (* p<0.05, ** p<0.01, *** p<0.001, **** p<0.0001, ns: not significant).

3.17 Involvement of selected genes on assessing of virulence factors

It was found that the growth and cell dimension of wild type and mutant strains were affected by temperature change. To further investigate the importance of these genes in pneumococcal metabolism and virulence, the neuraminidase and pneumolysin assays were performed under tested temperatures since these proteins are known to be widely studied pneumococcal virulence factors (Kadioglu *et al.*, 2008).

3.17.1 Determining the haemolytic activity

The pneumococcal haemolytic activity is assessed by the production of pneumolysin which is an important virulence protein (Shak *et al.*, 2013). The involvement of pneumococcal genes on the haemolytic activity was tested in the cell lysates harvested

from the cultures grown in CDM supplemented with 55 mM glucose at different temperatures.

The result showed that there was no difference in the haemolytic activity between all the mutant and wild type strains when bacteria were grown at 34°C and 37°C (data not shown) (p>0.05). In addition, the mutants produced between 25 to 50% significantly less pneumolysin than the wild type strain at 40°C (p<0.0001) (Figure 3.17). The highest level of reductions were observed for Δ*comD* and Δ*ciaR*, and Δ*SPD_0132/0133*.

Therefore, it can be concluded that the mutation does not affect the production of pneumolysin at nasopharyngeal and body temperatures (34°C and 37°C, respectively). At 40°C, significant level of reduction was likely due to restricted pneumolysin secretion or its activity at this high temperature.

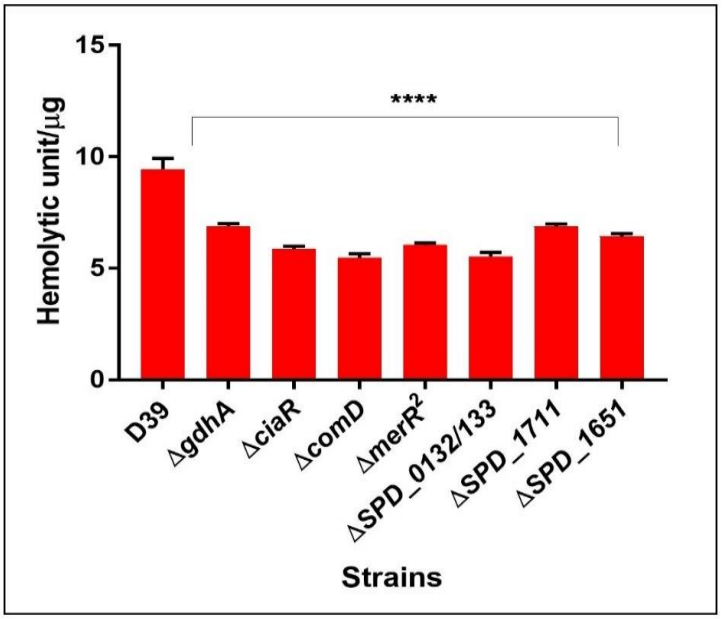

Figure 3.17. Determination of haemolytic activity of pneumococcal strains using cell lysate extracted from the strains grown in CDM supplemented with 55 mM glucose at 40°C.
Pneumolysin activity of all mutant strains reduced significantly at 40°C. No difference was observed at 34°C or 37°C (Data not shown). Average values shows the haemolytic unit per µg total protein, using triplicates of three independent biological samples (**** p<0.0001).

3.17.2 Determining the neuraminidase activity

Neuraminidases are the enzymes that cleave sialic acids from host glycoconjugates, and if the sialic acid is not cleaved, the other glycosidases are not able to recognize the specific cleavage sites (Terra *et al.*, 2010). Neuraminidase activity has a major impact on pneumococcal colonisation and virulence, and biofilm formation (Parker *et al.*, 2009), therefore, it is important to understand the influence of the temperature changes on the neuraminidase activity. The level of neuraminidases was measured using pneumococcal cell extracts harvested from the cultures grown in CDM supplemented with 55 mM glucose at different temperatures using the chromogenic pNP-NANA substrate as described in Section 2.15.4.

There was no difference in the neuraminidase activity of mutant strains compared to the wild type at 37°C (Figure 3.18 B) (p>0.05). At 34°C and 40°C, a significant reduction in neuraminidase activity was recorded in the mutants relative to the wild type (p<0.05). In detail, at 34°C, neuraminidase activity in the mutant strains decreased between 18 to 26% (Figure 3.18 A), while it was in between 15 to 40% for the wild type at 40°C (Figure 3.18 C).

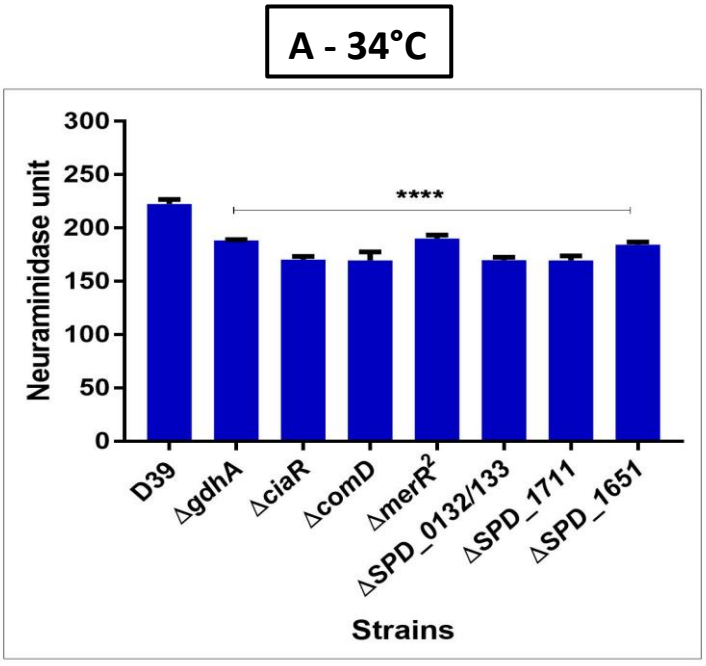

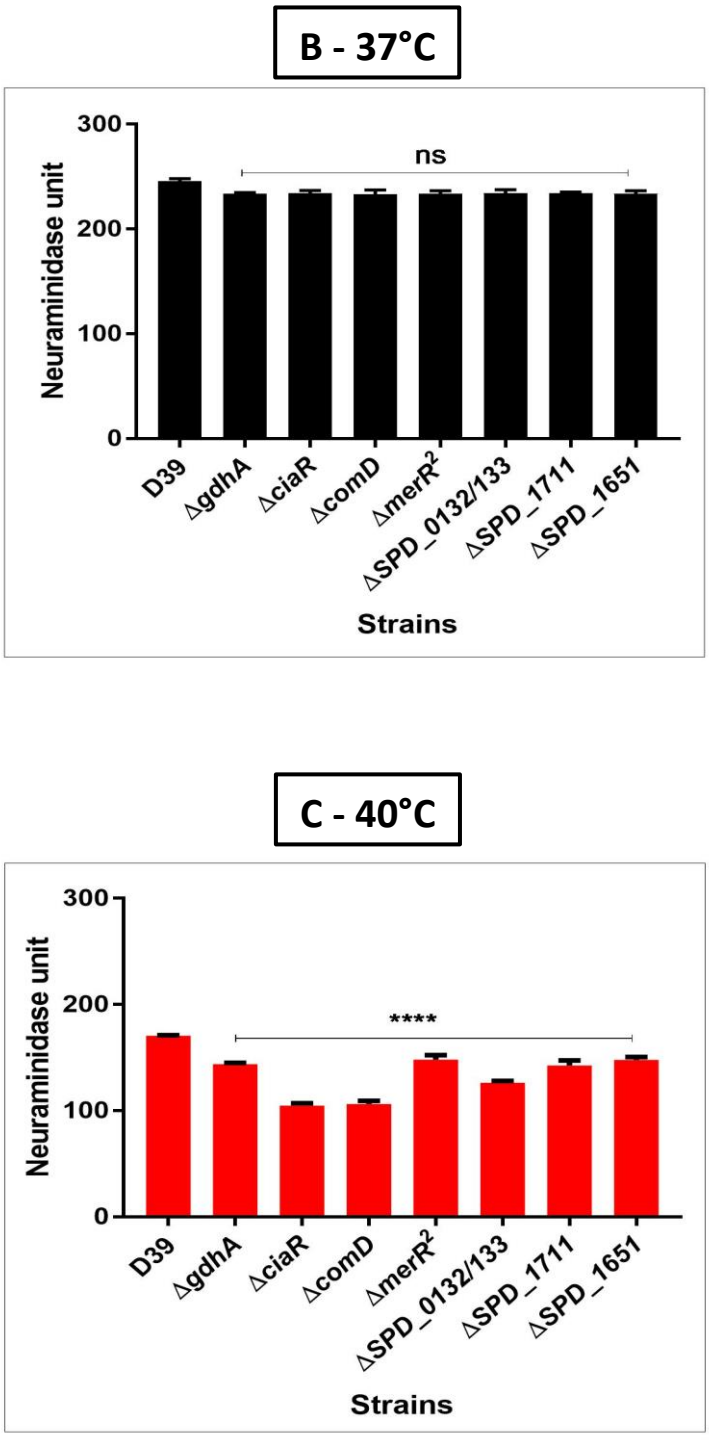

Figure 3.18. Determination of neuraminidase activity of pneumococcal strains grown in CDM supplemented with 55 mM glucose at 34°C (A), 37°C (B), or 40°C (B).

The values are expressed as neuraminidase unit (nmol p-NP released per minute/µg total protein) using triplicates of three independent biological samples. All mutants showed significantly reduced neuraminidase activity compared to the wild type D39 at 34°C or 40°C. No difference was observed at 37°C. (**** p<0.0001).

3.18 Biofilm formation of pneumococcal mutant strains

S. pneumoniae colonises the nasopharynx. Microbe forms biofilms on mucosal surfaces during infection of otitis media and pneumonia (Marks *et al.*, 2012a). It is generally agreed view that colonisation is the first step of invasive pneumococcal disease (Domenech *et al.*, 2012) and during colonisation and dispersion of pneumococcus, biofilm provides increased resistance to antimicrobial agents and adaptation to environmental stress (Chao *et al.*, 2014).

In order to determine the impact of selected genes on pneumococcal biofilm growth, the amount of biofilm formation was determined by crystal violet staining at different temperatures (Section 2.16). It can been seen in Figure 3.19 B, there was a clear reduction on biofilm produced by Δ*comD,* Δ*SPD_0132/133,* and Δ*merR*^{2} (0.15 ± 0.009, 0.2 ± 0.003, and 0.16 ± 0.015, cv/595nm, respectively) (p<0.05), suggesting that the absence of these genes affected the biofilm formation of pneumococcus at 37°C. In addition, no significant difference was observed between the other mutants and the wild type at 37°C (p>0.05). At 34°C, Δ*ciaR,* Δ*merR*^{2}*,* Δ*SPD_1711,* Δ*SPD_1651* (0.12 ± 0.002, 0.13 ± 0.033, 0.13 ± 0.019, 0.19 ± 0.013, cv/595nm, respectively) formed significantly less biofilm relative to the wild type (0.20 ± 0.016, cv/595nm) (p<0.05), confirming that these genes are important for pneumococcal biofilm and it is temperature-dependent (Figure 3.19 A). At 40°C, all mutant strains produced significantly less biofilm than the wild type (p<0.05), and the most reduction was observed for Δ*SPD_1711* and Δ*SPD_1651* (55%) (Figure 3.19 C). It can be concluded that temperature influences the pneumococcal biofilm formation and certain genes *ciaR*, *SPD_1711* (DNA-binding protein), and *SPD_1651* (iron-compound ABC transporter) understudy have a role on biofilm production.

A- 34°C

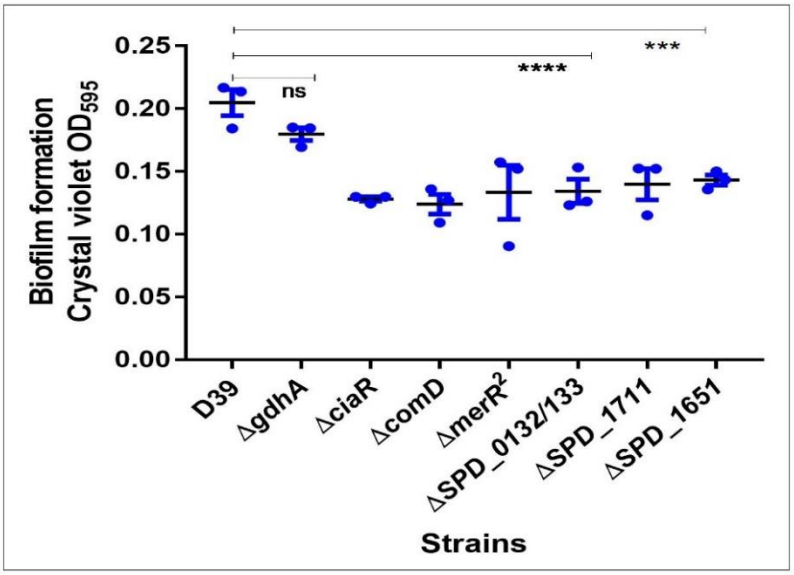
Biofilm formation
Crystal violet OD595
0.25
0.20
0.15
0.10
0.05
0.00
ns
****
***
D39
ΔgdhA
ΔciaR
ΔcomD
ΔmerR2
ΔSPD_0132/133
ΔSPD_1711
ΔSPD_1651
Strains

B - 37°C

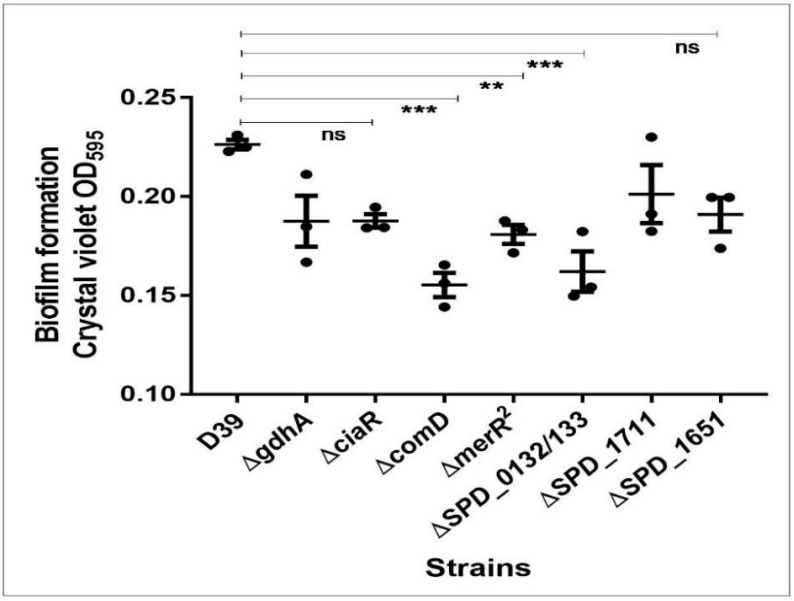
Biofilm formation
Crystal violet OD595
0.25
0.20
0.15
0.10
ns
***
**
***
ns
D39
ΔgdhA
ΔciaR
ΔcomD
ΔmerR2
ΔSPD_0132/133
ΔSPD_1711
ΔSPD_1651
Strains

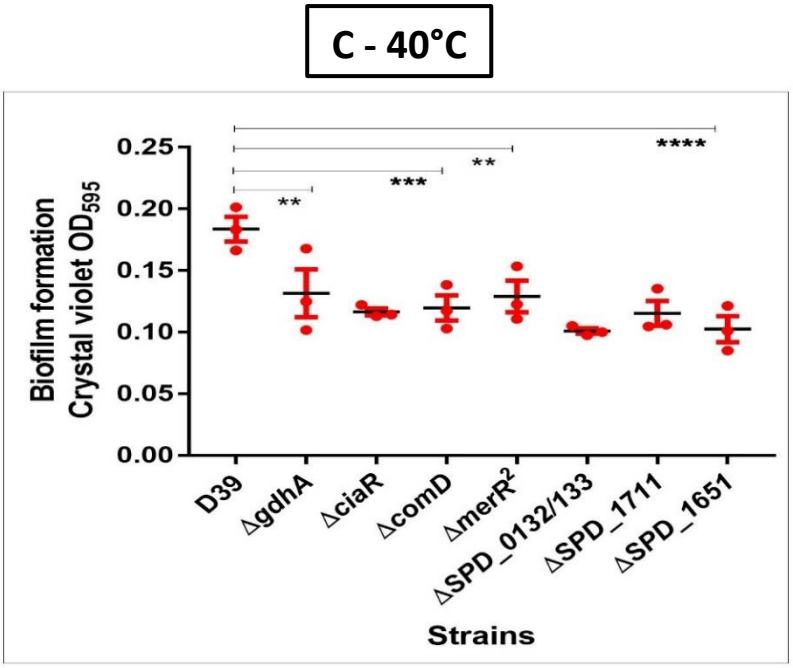

Figure 3.19. Biofilm formations of pneumococcal strains grown in THY medium at 34°C (A), 37°C (B), or 40°C (C).
Symbol represents the each biofilm density at 595nm. Experiments were repeated using triplicates of three independent biological samples. All the mutant strains formed significantly less biofilm than wild type D39 at 40°C. Certain genes had reduced biofilm formation compared to wild type D39 at 34°C or 37°C (*comD*, *merR*^{2}, and *SPD_0132/0133*) (** p<0.01, *** p<0.001, and **** p<0.0001, ns: not significant).

3.19 Determination of capsule level of pneumococcal mutant strains

Capsular polysaccharide (CPS) is known as the most important pneumococcal virulence factor, which plays role on protection of bacteria against phagocytosis, adhesion and biofilm formation, and survival in different environments (Morais *et al.*, 2018). The role of selected genes in capsule production at different temperatures was determined using glucuronic acid assay as described in Section 2.17.

As shown in Figure 3.20 B, only Δ*ciaR* and Δ*comD* strains produced significantly less glucuronic acid (25.01 ± 1.11 and 24.66 ± 1.75 µg/ml, respectively) relative to the wild type at 37°C (29.20 ± 1.22 µg/ml) (p<0.05). Interestingly, at 34°C, Δ*gdhA* and Δ*merR*^{2} strains had significantly more capsule (37.18 ± 1.88 and 37.23 ± 0.86 µg/ml respectively) at 34°C (33.81 ± 2.30 µg/ml), while other strains had less capsule relative to the wild type

(p<0.05) (Figure 3.20 A). Moreover, Δ*gdhA*, Δ*ciaR*, ΔcomD, and Δ*merR*^{2} strains did not show any difference on capsule synthesis compare to the wild type at 40°C (Figure 3.20 C) (p>0.05). These results suggested that *SPD_0132/133*, *SPD_1711*, and *SPD_1651* have temperature dependent role in capsule synthesis while other genes involve in capsule synthesis as independent of temperature.

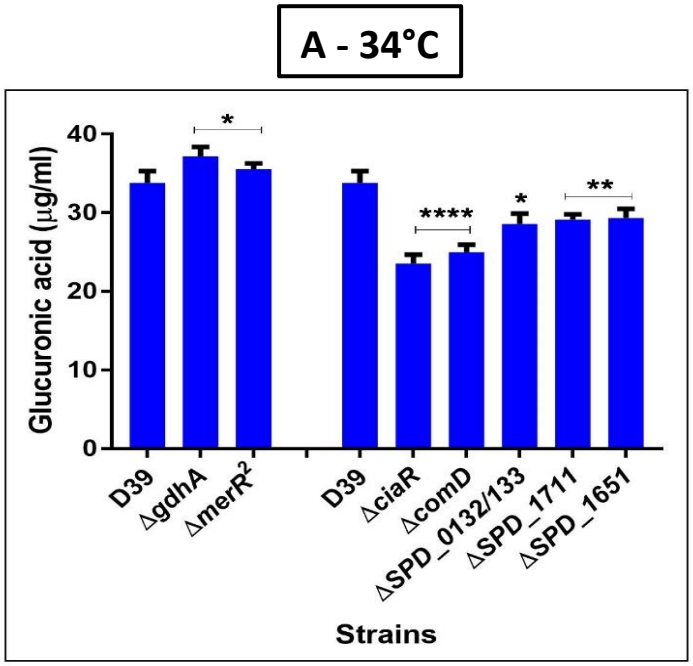

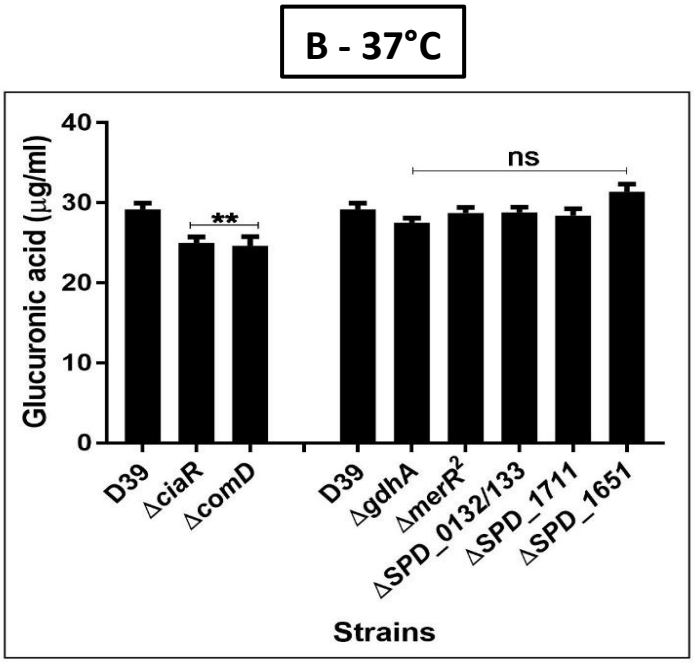

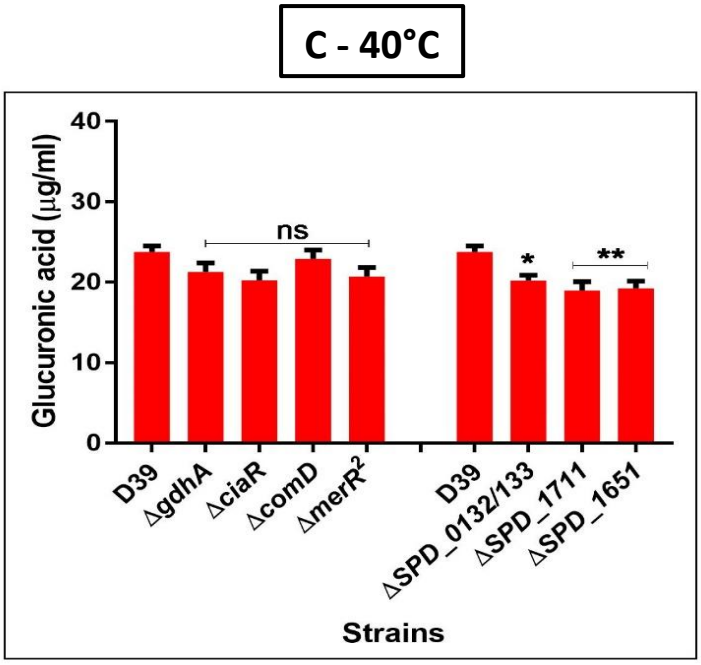

Figure 3.20. The glucuronic acid concentration from capsules of pneumococcal strains grown in CDM medium supplemented with glucose at 34°C (A), 37°C (B), or 40°C (C).
Certain genes had reduced capsule synthesis relative to wild type at 34°C, 37°C, or 40°C. Δ*gdhA* and Δ*ciaR* produced more capsule than the wild type strain at 34°C. Experiments were repeated using triplicates of three independent biological samples (* p<0.05, ** p<0.01, **** p<0.0001, ns: not significant).

3.20 Part E: Construction of reporter strains and temperature-dependent gene expression analysis (β-galactosidase assays)

3.21 Construction of reporter strain in proxy of *lacZ* gene

Reporter genes are routinely used genetic tools for investigating transcriptional or translational gene regulation. In this study, *E. coli* β-galactosidase gene *lacZ* was used to construct reporter strains to determine the gene expression at different temperatures (Miller, 1972). For this purpose, the integrative plasmid pPP2 was selected as a promoter probe vector (Figure 3.21). The pPP2 has a promoterless β-galactosidase gene (*lacZ*) to be driven by the putative promoter region of the target gene (Halfmann *et al.*, 2007a). The modified constructs carrying promoter-*lacZ* fusions were then transformed into *S. pneumoniae.* The pPP2 incorporates the *lacZ* fusions into *bgaA* locus (SPD_0562 encoding for β-galactosidase) in pneumococcal genome by homologues recombination

that eradicates the background of β-galactosidase activity without any effect on growth of the strain, and SPD_0564, which is probably playing role on secretion of BgaA enzyme to disrupt galactosides in carbon sources in the growth medium (Halfmann *et al.*, 2007a). Furthermore, the pPP2 contains tetracycline resistance gene *tetM* in *S. pneumoniae,* and beta-lactamase gene encoding ampicillin resistance *(bla)* in *E. coli*. These features are required for selection of desired constructs in both species. Once the transcriptional fusion strain is constructed, the promoterless *lacZ* gene is driven by the promoter of target gene and expression is measured at different temperatures.

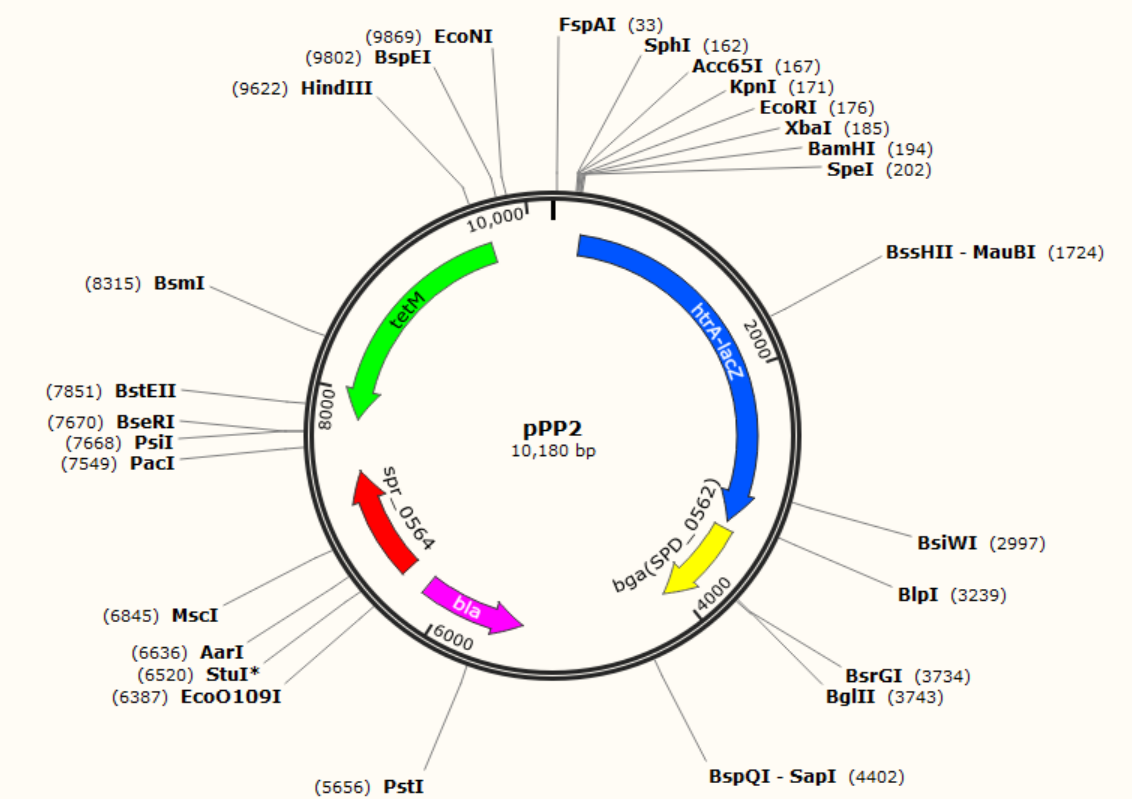

Figure 3.21. Illustration of the integrative promoter probe plasmid pPP2.
The recognition sites including different restriction endonucleases are indicated. The pneumococcal genes *SPD_0541* and *bgaA* serve as homologous sites for genomic integration of *tetM*-promoter-*lacZ* fusions. Figure is adapted from Halfmann *et al.* (2007a).

3.21.1 Identification of putative promoter regions of target genes

The putative promoter regions of selected genes were identified using BPROM (Softberry), which is a bacterial promoter prediction program. The software recognizes the upstream of ORF start and predicts the core promoter elements, -10 (marked in purple) and -35 (marked in red) boxes, as illustrated in Figure 3.22.

(1)

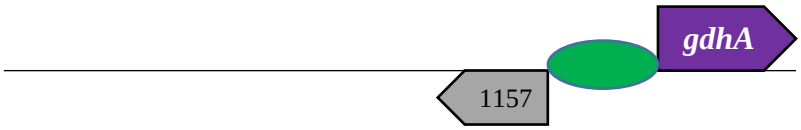

ATATGCATGGTTACGACCACCACGTGTTTC**TTGAAG**GAGAGAGTCGAGTCC
GAAC**TCCTCATAT**TTTTTTACATTTCGCTAAATCGTTGTTTGATTACAGTCT
AAAAGCTCTATAATCTCTTTATAAGATTTGCCCATCAGACGAAATATAGTAG
ATTGAAACTAGAATAGTACACCTCTACTTCTAAAACATTGTTAGAAATCGAT
TTGACTGTCCTGATCGATTTGCCCTGTTCTTGTTTCGTTTTACTATAGAACGA
TTTGAAGGCGTTTATGATATTTAGCTGTACGAGAGTCTTTTAAAAGTGTTTT
GATGGCTTGGATTTCTTCTTTAG**TTGATT**TCATATCACTA**TTATATAAT**GCT
TTTTGATTTTAGTCTGGTATAAATATTGCTTTCCTCCAAAATGGTCATAATTT
TACTAGCAAATCTAACATATCACGGATAAATTAACAAGTGATTTCTGAATTG
CTAAACATTTTCTTTTCTTATAGCATACCATACTTTAAGATTTTGTCTTTGAG
AAAGATATTTCCAAGAAAAACGTTCGTTTTTTTTATCTATTTTCAAAAAAAA
CCAAAAACTGAATTGAAAGAATTTTTAGAAAATTTCTGTTTTTTCTTTACAG
TGAAAAAAA**ATTCTG**CTATAATGTC**TTATGTAAT**AAAATATGACAATAAA
AGGAGAACGAT**ATG**ACATCTGC

(2)

ACTATTAGAAGGAAGAAAGTTTTGGAAATCGCTGTCCAATCCTTTTTTCTCA
AGCAAAATATGATATAATAAGTTTGT**TTGAAG**AAGAGCAGCAGC**TCTTAA**
ACTTAGAATAGGAGAAAACT**ATG**CAAGCAGT

(3)

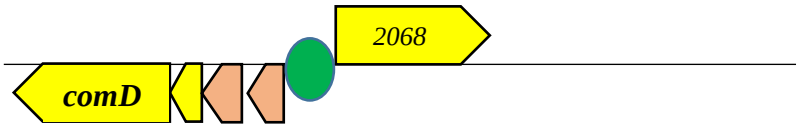

ATTTGCCTCCATATGTTTGAATTACTGAAAGTATAAACTGACTAGCTTAATT
ATAACTTAAACACAAAAGTTTTACACAAACTGTGGATAACTCTTTTGAAATT
GTGATTTTCTTAATTGAAATCTATTT**TTTATT**TTGTGAATAAGATG**TGAAAA**
AATAGAGAATATGTTAGAATAGAGTC**ATG**AAAATT

(4)

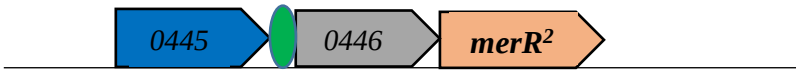

GATTTTATAAACAAATCAAAGAAGAGAGGGATGAGAGTTCCTCTTTTCTTTT
GCTTAAAATAAAAACGCTTCCTCTCAACT**ATTACT**CATAAAAATCACCG**AT**
TTATGATAAAATGGAAATAGAAAGTTGAGATT**ATG**AGTTATT

(5)

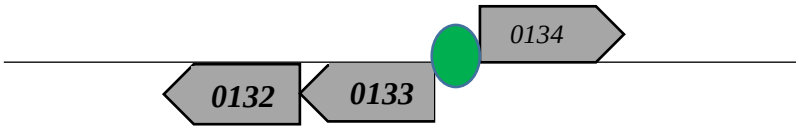

AACACATTCCTATCTTTTTGTCTGCTTACTATTATACTACAAAAGCTGGCAC
ATGGGAATTTTCTTTGCCCCCAGACAAGAGTGCCCTCACTTAACTAAAAATA
A**TTTAAA**AAAATGCTCAC**TTTTCCTTTT**CTTTTCCGAATATAAAAGTGAAC
AAGAAAAAAGGAGGAAAGTTCA**ATG**ACAAAT

(6)

TATTATCTGGCTTCATCAGGTAAGATGCTTCGCAATACCTACACACCTGATG
GTTACTACGTTGGCAACTTAGGTGCCTGGCAATAAGAATAATACTCTTTGAA
AATCTCTTCAAACCACGTCAGCTTCATCCACAACCTCAAAACAGTGTTTTGA
GCTGACTTCGTCAGTTCTATCTACAACCTCAAAGCAGTGCTTTGAGCAGCCT
GCGGCTAGCTTCCTAGTTTGGTCTTTGATTTTCATTGAGTATAAGAAGTCCT**T**
TTCCTTAAAGGAAGAGG**CTTTTTACT**TGCTTTTCTGCTGCTTCCTCATTTGT
CCTGAAGCCTTTTTTGTGTTAAA**ATG**AATGG

(7)

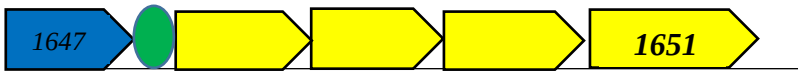

GCTCATGTTAAAGGAATGAACTACCTATTTCAAGAAGACAGTTCTTCTCAAA
TCTTTAACTTAGGAACTAAAAAAGGCTATACTATCAAAGAAATCTTTAAAA
CTGCTGAAGAATTACTAAATTAAAAAATCCCACACGAGATTGTTGCTCGAC

GTGCTAGTGACCCAGCCAGTGTCCTAGCAGATGCTTCAAAAGCTAAACAAT
ATCTTGATTGGACGGCTAGCTACTCCCTCGAAGATATTATTTTATCAGATTA
AGGTAAAAACATTTTAGAATAGG**ATAACA**AAGGAGAAAGTCT**TGTTGCTC**
TCTCCTTGTTGTATTTATTAAATTGTCAGAAATTTTATTGACAGATTAGAAA
AATAATGTTACATTTATATCCGCAGGTATCTTTCGATACCAAATCTACATGA
AAGGACGGGGT**ATG**AAACT

Figure 3.22. Intergenic region maps and upstream sequence of *GdhA* (1), *CiaR* (2), *ComD* (3), *MerR*^{2} (4), *SPD_0132/133* (5), *SPD_1711* (6), and *SPD_1651* (7).
The start codon of each gene is in bold blue, the putative -10 regions are in bold purple, and the -35 regions are in bold red. The promoter region of each gene is located in green circle. Colours are referring the codes for KEGG functional pathway categories; purple for energy metabolism, yellow for environmental information processing, blue for carbohydrate metabolism, light brown for genetic information processing, and grey for unclassified genes.

3.21.2 Preparation of insert/vector fragments for reporter constructs

The putative promoter region of target genes were amplified by PCR using the primer sets including *Sph*I and *Bam*HI restriction sites as listed in Table 2.6. All amplified products and the vector pPP2 which was extracted from *E. coli* were cleaned up, and the size of fragments were confirmed by agarose gel electrophoresis (Figure 3.23 A-B). The concentration of fragments were measured and then digested using the *Sph*I and *Bam*HI incorporated to the primers.

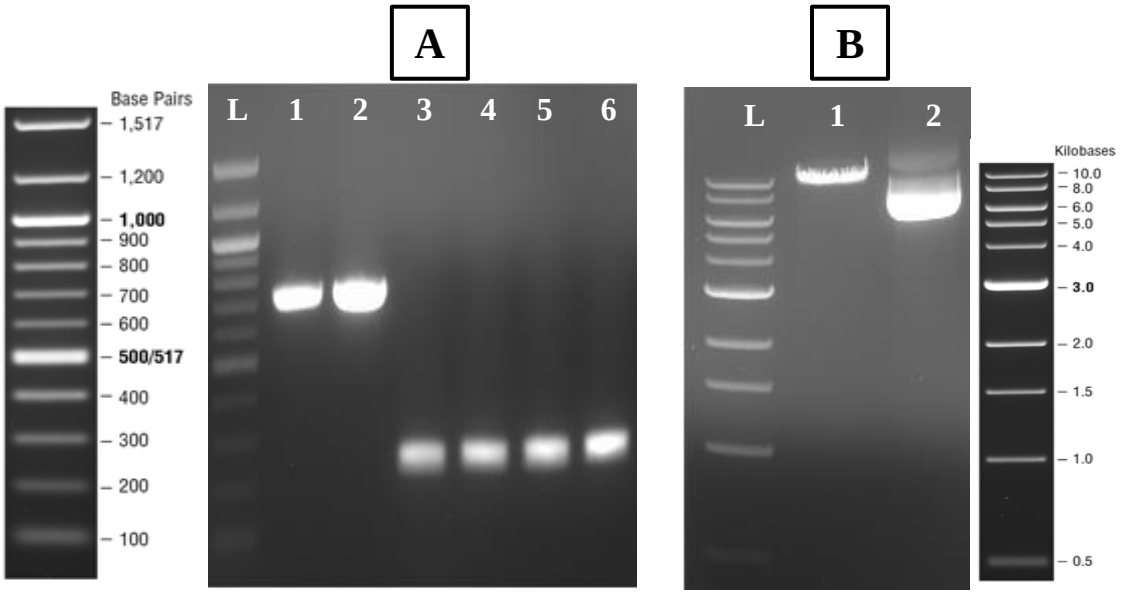

Figure 3.23. The images of agarose gel electrophoresis analysis showing the amplified promoter regions and pPP2 plasmid.
A: L- 500 ng of 100 bp DNA ladder (NEB); Lanes 1 and 2 - P*gdhA* (675 bp); Lane 3 - P*comD* (218 bp); Lane 4 -P*0132/133* (222 bp); Lane 5 - P*1711* (267 bp); Lane 6 -P*1651* (286 bp). P*ciaR* and P*merR*^{2} were constructed by former colleagues. **B**: L- 500 ng of 1 kb DNA ladder; Lane 1 - cut pPP2 plasmid; Lane 2 – uncut pPP2 plasmid.

3.21.3 Transformation of transcriptional reporter strain into *S. pneumoniae*

T4 DNA Ligase was used to ligate the each putative promoter region into the pPP2 plasmid. After 16 hours of ligation, the ligated construct was transformed into chemically competent *E. coli* Top10 cells, and ligation was confirmed by colony PCR using the primers Fusion-F and Fusion-R as described in Section 2.10. The results showed that putative promoter regions of target genes were fused to *lacZ* gene in the pPP2 plasmid.

The recombinant pPP2 plasmid was extracted from *E. coli* as mentioned in Section 2.6.2 and transformed into *S. pneumoniae* wild type D39 and the mutant strains as described in Section 2.11.2. The next day, the recombinant colonies were selected from the blood agar plate containing 3 µg/µl tetracycline, and colony PCR was done to confirm the successful integration of the reporter constructs using the primers Fusion-F and Fusion-R. Finally, PCR products were analysed on agarose gel electrophoresis (Figure 3.24). The expected

recombinant plasmid size was total of empty plasmid (200 bp) plus the size of each insert. In Figure 3.24, lanes 1, 2, and 3 confirm the desired amplification of promoter region (inserts) of *gdhA* fused with the cloning site in pPP2 (875 bp). Lanes 4, 5, 6, and 7 show the fusion constructs of P*1711* (467 bp), and P*1651* (486 bp), P*comD* (418 bp), P*0132/133* (422 bp), respectively. Lane 8 shows the amplification of a promoterless pPP2 (200 bp) as a negative control. The reporter strains were named as P*gdhA-lacZ*-wt, P*1711-lacZ*-wt, P*1651-lacZ*-wt, P*comDR-lacZ*-wt, and P*0132/133-lacZ*-wt (where P indicates promoter region in the wild type background). The transcriptional fusion constructs were also transformed into each of the seven mutant backgrounds and the transformants were selected in the presence of tetracycline (3 µg/ml).

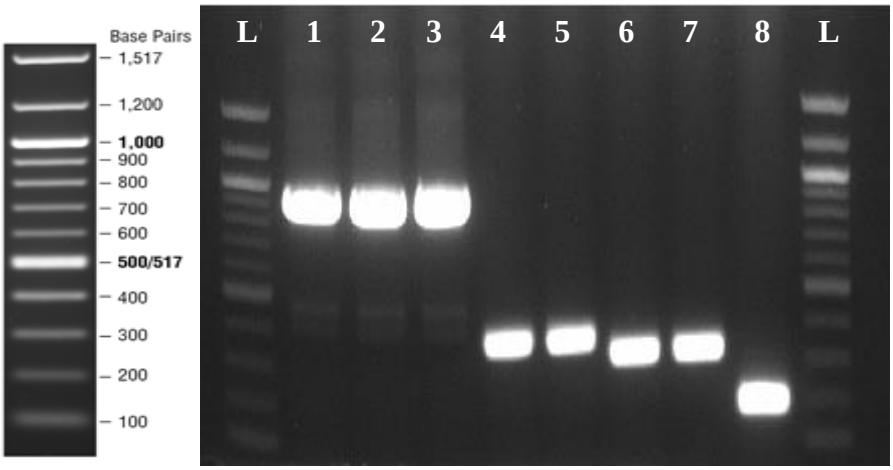

Figure 3.24. The images of agarose gel electrophoresis analysis confirming the successful transformation of reporter constructs into D39 wild type strain.
L- 500 ng of 100 bp DNA ladder (NEB); Lanes 1, 2 and 3 - P*gdhA* (875 bp); Lane 4 - P*1711* (467 bp); Lane 5 - P*1651* (486 bp); Lane 6 - P*comD* (418 bp); Lane 7 - P*0132/133* (422 bp); Lane 8 –promoterless pPP2 plasmid (200 bp). P*ciaR* and P*merR*^{2} in D39 were constructed from a former colleague.

3.21.4 Expression of transcriptional *lacZ*-fusions at different temperatures

The protocol to measure the expression of reporter constructs was previously published (Zhang and Bremer, 1995). The reporter strains were grown in CDM supplemented with glucose at tested temperatures and the level of β-galactosidase activity was determined by measuring the production of yellow colour over time due to hydrolysis of *O*-nitrophenyl-D-galactoside (ONPG, mimics the lactose) by β-galactosidase (Section 2.14.2).

Table 3.8 shows that the promoters are driven in the presence of glucose and most importantly, the induction of promoters at different temperatures confirmed our microarray data (Table 3.5). The highest induction of *lacZ* was obtained from P*0132/133-lacZ*-wt at 34°C (468.9 ± 10.3 MU, n=3) as the fold change of SPD_0132/133 was one of highest at 34°C (Table 3.5). The lowest induction was obtained with P*gdhA-lacZ*-wt and it was 37.7 ± 2.8 MU at 34°C, which is lower than at 37°C. In addition, the expression of P*merR*^{2}*-lacZ*-wt at 34°C was 151.5 ± 9 MU, which is lower than at 37°C. In the microarray data, GdhA and MerR^2 were downregulated at 34°C relative to at 37°C (Table 3.4). The activity of other strains were 232.9 ± 13.9, 254 ± 2.0, 209.3 ± 12.08, 183.96 ± 6.9, and 2.7 ± 0.1 MU for P*ciaR-lacZ*-wt, P*comD-lacZ*-wt, P*1711-lacZ*-wt, P*1651-lacZ*-wt, and Ppp2-*lacZ*-wt (negative control), respectively, and all expression levels were higher than at 37°C. As mentioned earlier, these pneumococcal genes were upregulated at 34°C relative to 37°C. P*merR*^{2}*-lacZ*-wt (389 ± 24.5 MU) was induced more than any other strains at 40°C, which was higher than at 37°C (218.2 ± 22.8 MU). In addition, the expression of P*gdhA-lacZ*-wt (68.8 ± 4.5 MU) was significantly higher than at 37°C (55.1 ± 2.7 MU). In conclusion, all expression results at different temperatures confirmed the microarray data (Table 3.5).

Reporter constructs	β-galactosidase activity (Miller Units/CFU/ml) in glucose (55mM)		
	34°C	**37°C**	**40°C**
P*gdhA*-*lacZ*-wt	37.7 ± 2.8	55.1 ± 2.7	68.8 ± 4.5
P*ciaR*-*lacZ*-wt	232.9 ± 13.9	188.9 ± 6.2	153.9 ± 11.8
P*comD*-*lacZ*-wt	254 ± 2.0	169.6 ± 2.3	125.9 ± 7.1
P*merR*^{2}-*lacZ*-wt	151.5 ± 9.0	218.2 ± 22.8	389 ± 24.5
P0*132/133*-*lacZ*-wt	468.9 ± 10.3	261.3 ± 36.8	161.9 ± 8.2
P*1711*-*lacZ*-wt	209.3 ± 12	310.6 ± 13.0	249.1 ± 17.5
P*1651*-*lacZ*-wt	183.9 ± 6.9	165.8 ± 2.1	124.8 ± 7.0
Ppp2-*lacZ*-wt	2.7 ± 0.1	4.7 ± 0.3	1.2 ± 0.2

Table 3.8. Expression levels of pneumococcal transcriptional *lacZ* fusions to the promoters of target genes grown in CDM supplemented with 55 mM of glucose at different temperatures.
The induction level is represented as Miller unit / CFU/ml. Values are average of at least three independent experiments each with three replicates. '±' indicates the standard error of means.

3.22 Part F: Glutamate dehydrogenase is required at high temperature

Sensing temperature changes within the host is frequently fulfilled by regulatory proteins and metabolic enzymes (Steinmann and Dersch, 2013). The function of selected genes and their possible involvement into pneumococcal adaptation to host environment were discussed in Part C. These genes are either transcriptional regulators or a part of pneumococcal regulatory systems (CiaR, MerR^2, and ComD), a DNA binding protein (SPD_1711), an iron-transporter (SPD_1651), or a hypothetical protein (SPD_0132/133). The growth studies indicated that the inactivation of genes led to decreased growth abilities in the presence of glucose and altered the profile of pneumococcal virulence determinants such as biofilm formation or capsule synthesis at different temperatures. To

characterize the extent of thermal adaptation of *S. pneumoniae*, glutamate dehydrogenase (GdhA) was selected for further study due to some reasons. GdhA is important for nitrogen metabolism of *S. pneumoniae* and a gdhA mutant strain displayed temperature dependent phenotypic differences compared to the wild type in this study. Moreover, gdh has been extensively studied in thermophilic bacteria in a temperature-dependent manner, suggesting that this gene may show similar characteristic in *S. pneumoniae*. Therefore, I hypothesized that GdhA is important for thermal adaptation of pneumococcus *in vitro* and *in vivo*.

3.23 Characterization of glutamate dehydrogenase

Glutamate dehydrogenases (GDHs, GdhA in *S. pneumoniae*) are a group of oxidoreductase enzymes that link carbon and nitrogen metabolism and catalyse the reversible oxidative deamination of L-glutamate to 2-oxoglutarate (α-ketoglutarate) by connecting amino-acid metabolism to tricarboxylic acid (TCA) cycle (Oliveira *et al.*, 2016). During the deamination reaction, nitrogen is used for numerous biosynthetic directions such as structure and function of the cells. The functionality of GDHs depends on the coenzyme preference; NAD^+ dependent (EC 1.4.1.2), $NADP^+$ dependent (EC 1.4.1.4) or dual specificity (NAD^+/$NADP^+$ dependent) (Choudhury and Punekar, 2007). In general, NAD^+ dependent GDHs are catabolic enzymes that degrades the glutamate for the reverse reaction, while $NADP^+$ dependent GDH involves anabolism by assimilation of ammonium to produce glutamate (Engel, 2014).

As mentioned previously, GDHs have active role on nitrogen metabolism, hence, detailed understanding of the network of nitrogen control is strictly important to figure out how bacteria adapt to the availability of nitrogen sources in the environment. Depending on the availability of nitrogen, bacteria can utilize a wide range of nitrogen-containing metabolites to uptake nitrogen (Amon *et al.*, 2010). Glutamine and glutamate are products of ammonium assimilation and preferred nitrogen sources for many bacteria. There are two pathways that are involved in formation of glutamate or glutamine: the glutamate dehydrogenase (GDH) and the glutamine synthetase/glutamate synthase (GS/GOGAT) (Figure 3.25).

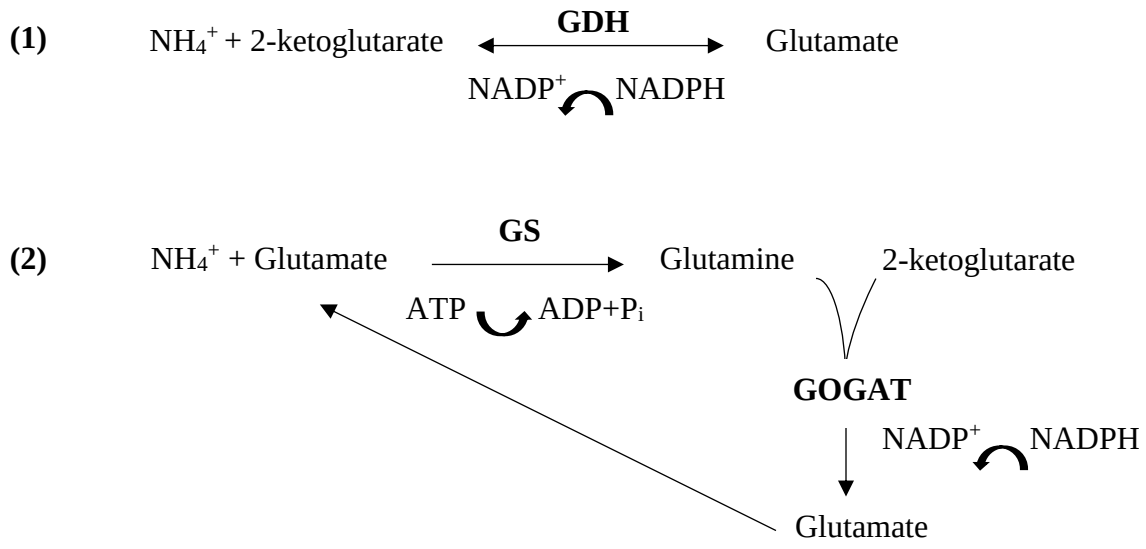

Figure 3.25. Nitrogen metabolism and the assimilation of ammonium.
Glutamine and glutamate are formed by two pathways. In the first reaction, glutamate is catalysed by glutamate dehydrogenase (GDH), and in the other coupled reaction, glutamine synthetase (GS) is involved in the production of glutamine and glutamate synthase (GOGAT) reacts with glutamine and 2-ketoglutarate to produce glutamate. In both reactions, transport and assimilation are regulated depending on the availability of ammonium. This scheme is adapted from Merrick and Edwards (1995).

3.24 Regulation of glutamine/glutamate metabolism in *S. pneumoniae*

Nitrogen assimilation in most Gram-positive bacteria is controlled by the transcriptional regulators GlnR, CodY and TnrA (Groot Kormelink *et al.*, 2012) . GlnR regulon represses *glnRA* and *glnPQ-zwf*, the *ureABC* operon (encode urease), and *gdhA* gene in the presence of nitrogen (Kloosterman *et al.*, 2006). CodY is a nutritional repressor, which represses the genes involved in amino acid metabolism, proteolytic proteins and some other genes, which play a role on glutamate biosynthesis (Hendriksen *et al.*, 2008).

In pneumococcus, the importance of GlnR on nitrogen metabolism has been reported. GlnRA encodes the glutamine synthesis from glutamate and ammonium, and required by GlnR to repress the target genes in the presence of nitrogen sources. The *glnPQ* encode the uptake and transportation of glutamine and glutamate, while *zwf* gene has a role on

pentose phosphate pathway (Kloosterman *et al.*, 2006). In addition, glutamate dehydrogenase (SPD_1158) is a $NADP^+$ dependent biosynthetic enzyme in *S. pneumoniae*. The regulation of these genes by GlnR is illustrated in Figure 3.26.

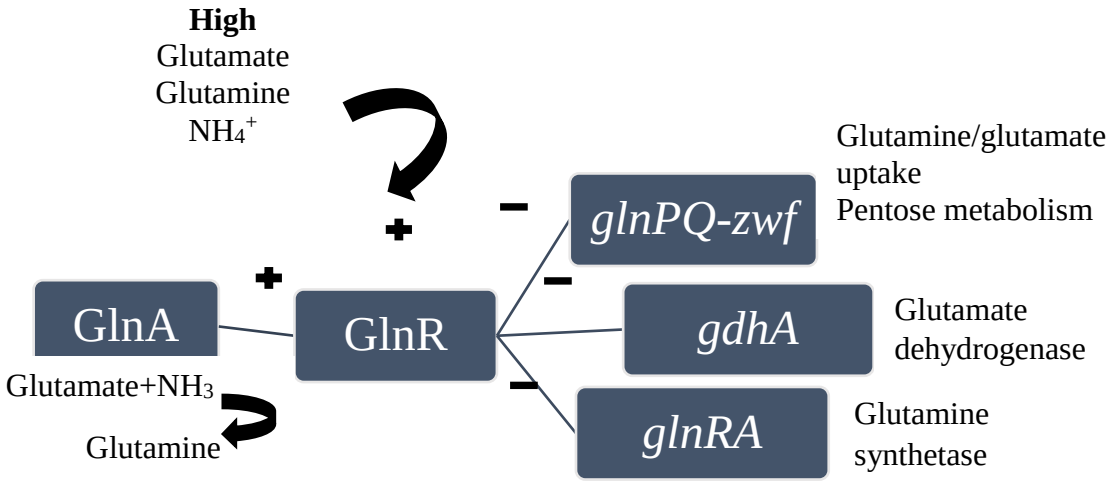

Figure 3.26. The pneumococcal GlnR regulon.
GlnR is responsive to high concentration of nitrogen sources and requires GlnA to repress the genes *glnPQ-zwf*, *gdh*, and *glnRA*. (+) defines the positive expression and (–) shows the repression of the target gene.

The network of GdhA with the transcriptional regulators GlnR and CodY suggested that GdhA plays a central role for a functional pneumococcal nitrogen control. Furthermore, recent studies on glutamate dehydrogenase demonstrated that it has additional roles in response to various nutritional signals. Girinathan et al. (2016) showed that uptake of glutamate is crucial for *C. difficile* to colonise in the host. In addition, the colonisation and pathogenicity of *C. difficile* in animal gut was inhibited in the absence of glutamate dehydrogenase (GDH) (Girinathan *et al.*, 2016). In *B. subtilis*, the growth of rocG (a homologue of GDH) mutant strain was restricted by a β-lactam antibiotic CEF (cefuroxime) when compared to the wild type strain. This suggested that glutamate dehydrogenase may get involved into cell envelop stress response. Moreover, it was also revealed that RocG has an impact on intracellular pH and may protect cells against growth arrest by CEF (Lee *et al.*, 2012).

In conclusion, the importance of GDH has been studied in many different organisms, however, its involvement into temperature adaptation has not been studied in detail, particularly in mesophiles. On the other hand, temperature-dependent GDH activity has been studied in hyperthermophiles, indicating that GDH is a thermostable protein (Bhuiya *et al.*, 2002). Hence, I hypothesized that the GdhA in the pneumococcus is a thermosensing protein to control the virulence.

3.25 Genetic complementation of *gdhA* mutant strain

Generation of insertion/deletion mutations often cause interruption known as polar effects in the expression of upstream or downstream genes of the targeted gene (Reyrat *et al.*, 1998). Complementation of Δ*gdhA* was done to exclude the chance of polar effect. In this study, Δ*gdhA* was genetically complemented because it plays an important role on nitrogen metabolism and phenotypic characterization and transcriptional *lacZ*-fusion analysis at different temperatures. For complementation, pCEP plasmid was used (Figure 3.27) (Guiral *et al.*, 2006). The multiple cloning site of pCEP, which is separated by maltose-inducible promoter and kanamycin resistance gene, is surrounded by 2 kb DNA homologous to pneumococcal genome allowing the homologues recombination in pneumococcus. Therefore, the intact copy of targeted gene is able to incorporate into the transcriptionally silent site *ami* to prevent the distressing of the cell physiology (Guiral *et al.*, 2006).

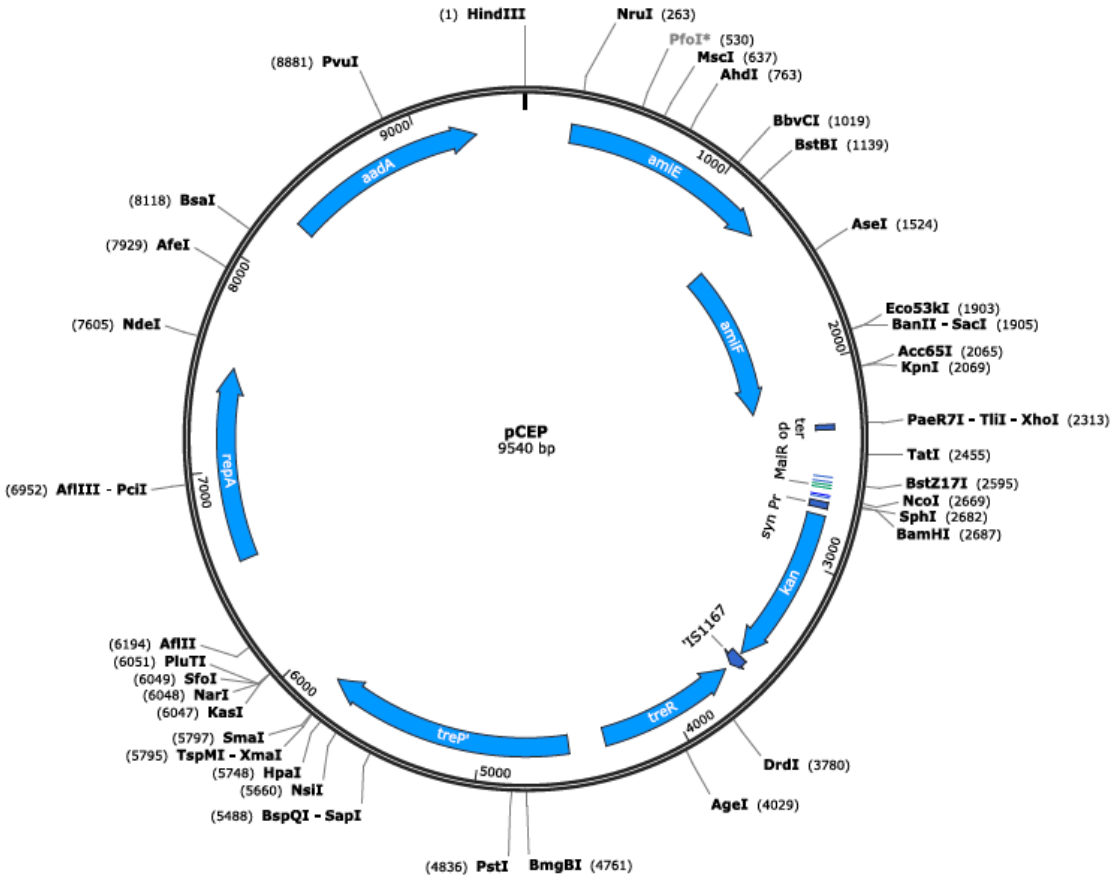

Figure 3.27. Genetic map of pCEP.
The multiple cloning site (MCS) consists of BstZ17I, *Nco*I, *Sph*I and *BamH*I restriction sites. *treR*: Trehalose operon repressor, *trePI*: PTS system, repA: replication site, *malR*: maltose-inducible promoter, *amiE*: oligopeptide ABC transporter, ATP-binding protein *amiE*, *kan*: kanamycin resistance cassette, *amiF*: oligopeptide ABC transporter ATP-binding protein AmiF. This figure is adapted from Guiral *et al.* (2006).

3.25.1 Preparation of pCEP for complementation

The pCEP plasmid was extracted from *E. coli* following the QIAprep spin Miniprep kit protocol (Sigma), and digested with *Nco*I-*Bam*HI restriction enzymes (Starlab, UK). The PCR product was purified using PCR Clean-Up System from Promega (UK) and digested plasmid was visualized by agarose gel electrophoresis.

3.25.2 Amplification of GdhA for complementation

The coding region of *gdhA* and its promoter site were amplified by PCR using the modified *gdhA*Comp/F and *gdhA*Comp/R primers incorporating *Nco*I and *Bam*HI restriction sites into the 5‘and 3‘ends of the amplicons (Table 2.5). PCR products were purified and digested with *Nco*I-*Bam*HI (Sigma, UK). The fragments were then ligated into with the compatible ends of pCEP by PCR (Section 2.13). An aliquot of ligation product was transformed into *E. coli* TOP10 cells for propagation. The next day, kanamycin resistant colonies carrying recombinant plasmid were collected. To confirm the successful recombination, colony PCR was done using the primers Mal/F and pCEP/R. The PCR products were analysed by agarose gel electrophoresis as shown in Figure 3.28. The amplicon shows successful cloning of the *gdhA* into pCEP. The expected amplicon size is 1799 bp (insert-1536 bp and vector-264 bp). The recombinant plasmid was designed as pCEP*gdhA*.

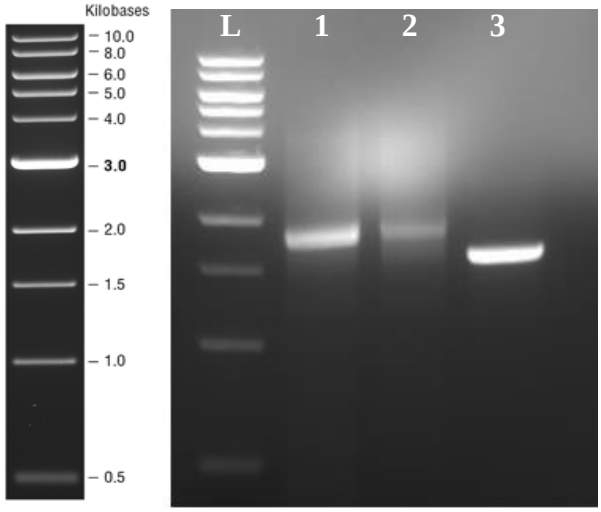

Figure 3.28. Agarose gel electrophoresis analysis showing the integration of *gdhA* with their putative promoter regions into pCEP.
L: 500 ng of 1 kb DNA ladder; Lanes 1 and 2 show the fusion of amplified target gene and its putative promoter region for *gdhA* (1536 bp) plus pCEP plasmid (263 bp), in total 1799 bp; Lane 3 shows the amplification of target gene with its putative promoter regions plus upstream and downstream of cloning site only.

3.25.3 Integration of recombinant pCEP construct into Δ*gdhA* strain

The recombinant pCEP plasmid (pCEP*gdhA*) was purified by using the Wizard SV Gel and PCR Clean-Up System from Promega, and tested by PCR using primers Mal/F and pCEP/R, whose recognition sites are localised up- and downstream of the cloning site, respectively. 100 ng of recombinant plasmid transformed into the *gdhA* mutant strain as described in Section 2.13.2. The transformants were selected on BAB plate supplemented with spectinomycin and kanamycin. Then, colony PCR was used to confirm the successful complementation using the primers Mal/F and pCEP/R. An illustration of this PCR strategy (Figure 3.29) and amplified positive transformant was confirmed by agarose gel electrophoresis (Figure 3.30) below. For the negative control, approximately 264 bp product was amplified in the empty vector. This plasmid has 2 kb homologous sequence to *S. pneumoniae* D39 genome, and these are located on a silent transcriptional site. The intact copy of the gene is integrated downstream of the *amiA* operon. Therefore, vector primers Mal/F and pCEP/R were used to confirm the complementation.

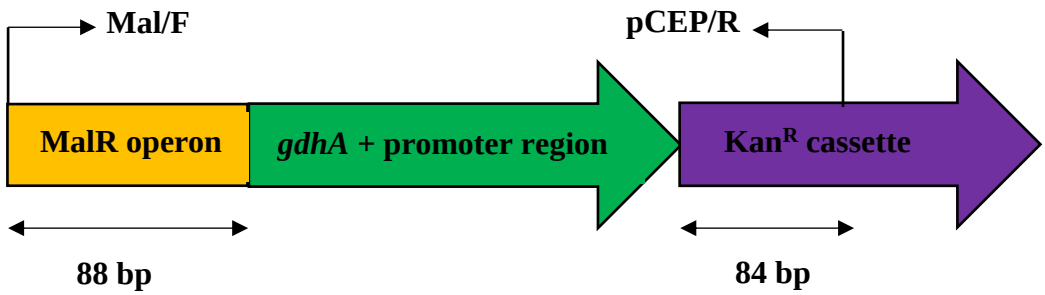

Figure 3.29. Illustration showing the strategy to confirm complementation.
The insert carrying the intact copy of *gdhA* with its putative promoter integrated into pneumococcal genome of Δ*gdhA.* Primers Mal/F and pCEP/R were used to amplify the target genes and the promoter region.

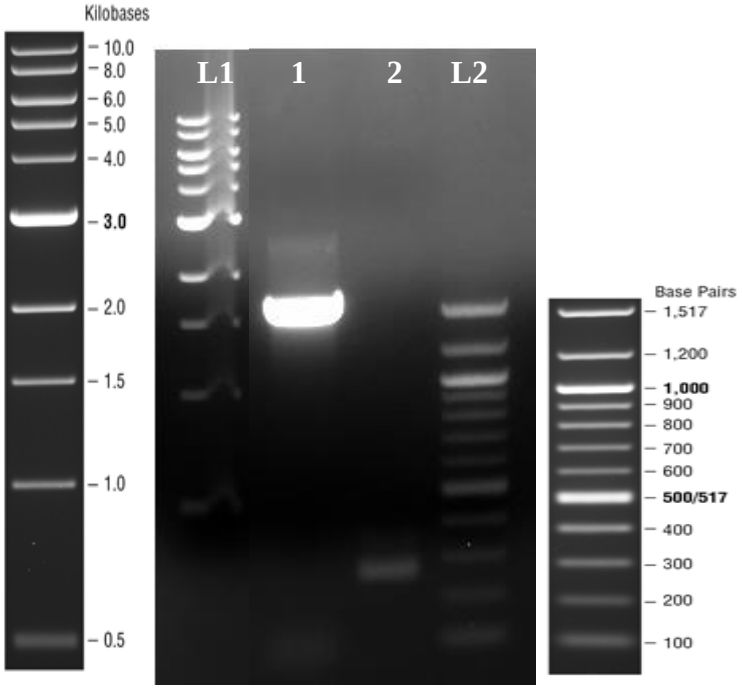

Figure 3.30. The image of agarose gel electrophoresis confirming the successful integration of insert carrying the intact copy of *gdhA* with its putative promoter within the pneumococcal genome of Δ*gdhA*.
L1: 500 ng of 1 kb DNA ladder (NEB); Lane 1 shows the integration of recombinant pCEP plasmid into the mutant strain. The final PCR product was identified as pCEP*gdhA* and 1799 bp in total. Lane 2 is PCR product approximately 264 bp obtained with pCEP without any insert as a negative control using the primers Mal/F and pCEP/R.

3.26 Additional phenotypic characterization of Δ*gdhA* mutant strain

3.26.1 Growth profile of GdhA is temperature- and nitrogen source-dependent

GdhA catalyses the reversible reaction of deamination of glutamate to α-ketoglutarate. To study the utilization of various nitrogen sources in a temperature-dependent manner, the wild type and Δ*gdhA* were grown in CDM supplemented with different concentration of L-glutamate and L-glutamine at 34°C, 37°C, or 40°C.

The growth rate and yield of the depicted strains are presented in Table 3.9 and Figure 3.31 A-B. On glutamate, the wild type and Δ*gdhA* strains were able to grow up to OD 0.7-0.8 at 600 nm with not-significant growth rate difference (0.37 ± 0.10 and 0.30 ± 0.03

h^{-1}) at 37°C (p>0.05). At 34°C, the growth rate of Δ*gdhA* (0.34 ± 0.00 h^{-1}) was reduced compared to 37°C on 5 mM glutamate, while D39 had similar rate at these temperatures. At 40°C, the wild type had the highest growth rate (0.35 ± 0.01 h^{-1}) in 10 mM glutamate, while the growth of Δ*gdhA* was abrogated (0.20 ± 0.01 h^{-1}).

The wild type strain grew better on glutamine compare to on glutamate and it reached approximately OD 1.0 at 600 nm in 10 mM glutamine at 34°C and 37°C. Δ*gdhA* had similar growth rate relative to the wild type at 37°C in 10 mM glutamine, however, it was significantly less (0.41 ± 0.01 h^{-1}) than the wild type (0.28 ± 0.00 h^{-1}) at 34°C. The growth rate and yield of both strains significantly attenuated at 40°C relative to other temperatures (p<0.05) and the reduction was more pronounced for Δ*gdhA*.

These results suggested that glutamate and glutamine play an important role on pneumococcal growth in N-limited host environment and *S. pneumoniae* prefers glutamine over glutamate. Furthermore, the growth rate and yield of the wild type and Δ*gdhA* vary with temperature changes (Table 3.9 A and B).

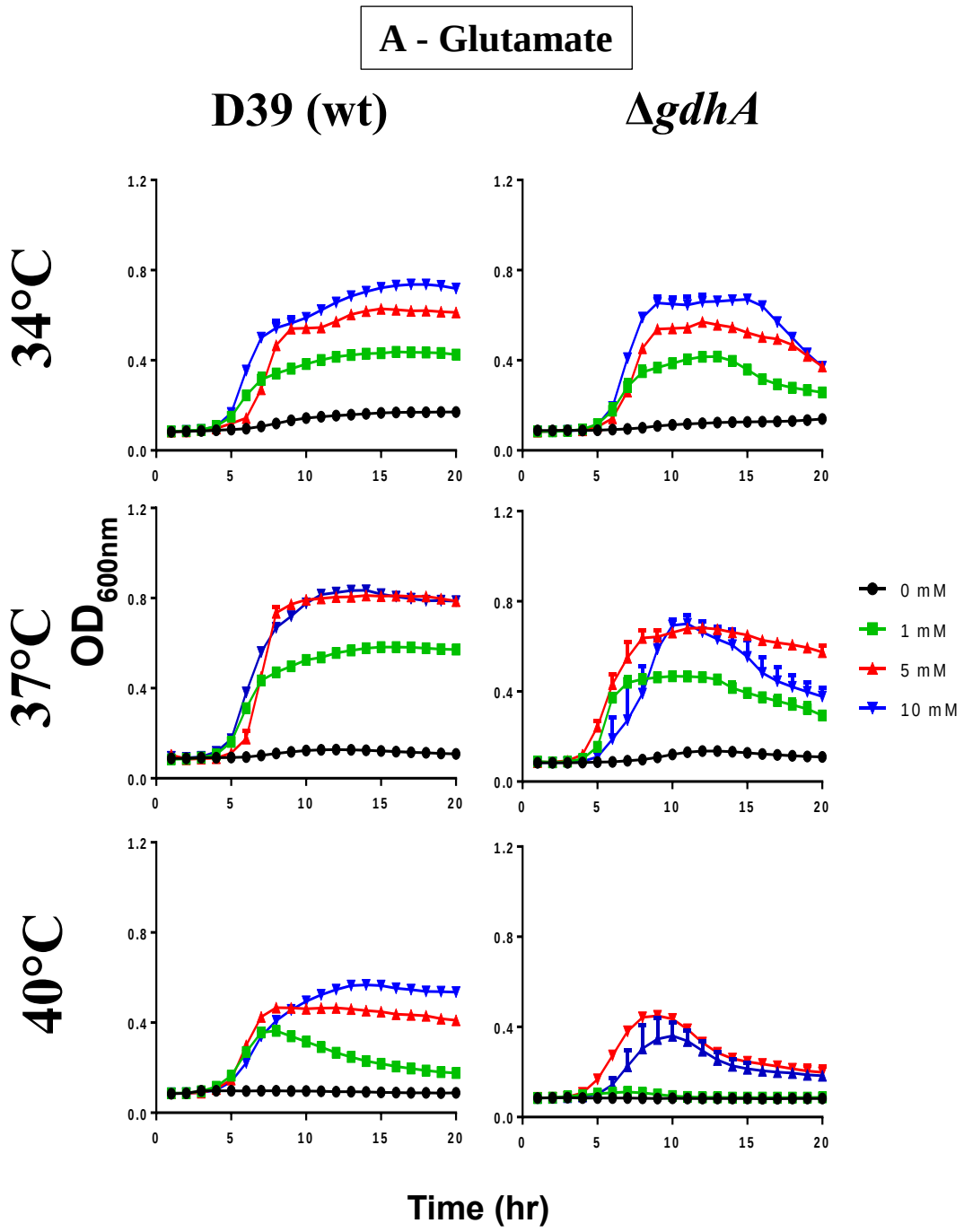
A - Glutamate
D39 (wt)
ΔgdhA
34°C
37°C
40°C
OD600nm
Time (hr)
0 mM
1 mM
5 mM
10 mM

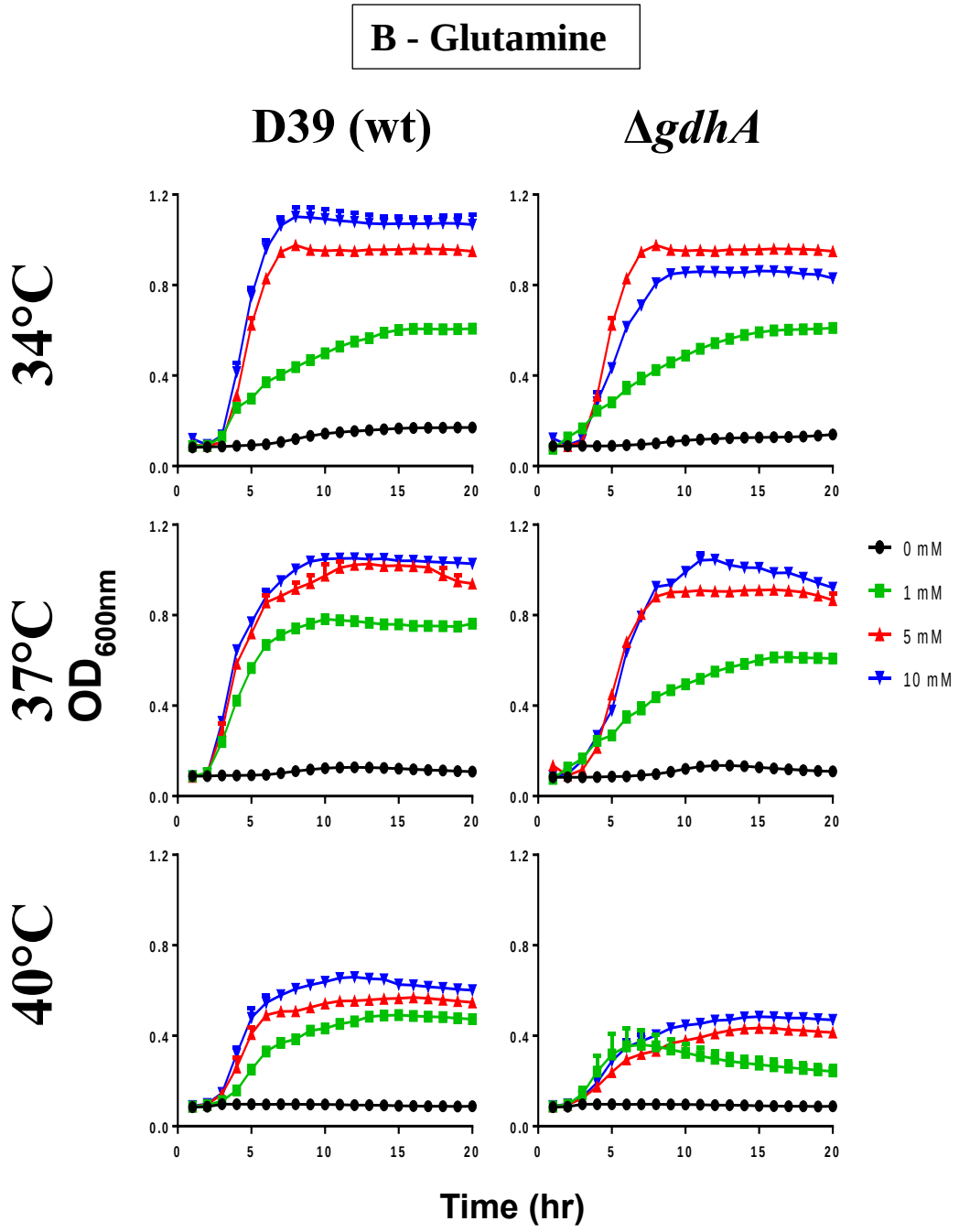

Figure 3.31. Temperature- and nitrogen source-dependent growth of pneumococcal strains.

The D39 (wt) and Δ*gdhA* were grown in 0 mM (black circle), 1 mM (green square), 5 mM (red reverse triangle), and 10 mM (blue reverse triangle) glutamate (**A**) and glutamine (**B**). Data represents the mean of three independent experiments each with three replicates.

A - Growth rate (h^{-1})

	34°C		37°C		40°C	
Glutamate (mM)	**D39 (wt)**	**Δ*gdhA***	**D39 (wt)**	**Δ*gdhA***	**D39 (wt)**	**Δ*gdhA***
0	0.06 ± 0.00	0.03 ± 0.02	0.04 ± 0.00	0.05 ± 0.01	0.01 ± 0.01	0.004 ± 0.00
1	0.16 ± 0.07	0.14 ± 0.03	0.32 ± 0.03	0.28 ± 0.01	0.34 ± 0.03	0.04 ± 0.02
5	0.34 ± 0.00	0.20 ± 0.01	0.37 ± 0.10	0.30 ± 0.03	0.20 ± 0.02	0.21 ± 0.07
10	0.22 ± 0.00	0.23 ± 0.03	0.31 ± 0.00	0.23 ± 0.04	0.35 ± 0.01	0.20 ± 0.02
Glutamine (mM)	**D39 (wt)**	**Δ*gdhA***	**D39 (wt)**	**Δ*gdhA***	**D39 (wt)**	**Δ*gdhA***
0	0.05 ± 0.01	0.04 ± 0.02	0.04 ± 0.00	0.08 ± 0.00	0.01 ± 0.02	0.01 ± 0.01
1	0.20 ± 0.04	0.11 ± 0.01	0.35 ± 0.02	0.10 ± 0.00	0.15 ± 0.01	0.20 ± 0.08
5	0.36 ± 0.01	0.19 ± 0.00	0.33 ± 0.02	0.22 ± 0.00	0.25 ± 0.03	0.14 ± 0.00
10	0.41 ± 0.01	0.28 ± 0.00	0.38 ± 0.03	0.33 ± 0.00	0.21 ± 0.01	0.26 ± 0.02

B - Growth yield (Max OD_{600})

Growth yield	34°C		37°C		40°C	
Glutamate (mM)	**D39 (wt)**	**Δ*gdhA***	**D39 (wt)**	**Δ*gdhA***	**D39 (wt)**	**Δ*gdhA***
0	0.17 ± 0.00	0.14 ± 0.01	0.12 ± 0.00	0.13 ± 0.01	0.09 ± 0.01	0.08 ± 0.00
1	0.43 ± 0.01	0.41 ± 0.01	0.58 ± 0.02	0.46 ± 0.01	0.36 ± 0.01	0.11 ± 0.00
5	0.63 ± 0.00	0.55 ± 0.01	0.81 ± 0.01	0.68 ± 0.00	0.46 ± 0.01	0.29 ± 0.01
10	0.73 ± 0.03	0.67 ± 0.01	0.83 ± 0.03	0.71 ± 0.05	0.57 ± 0.01	0.37 ± 0.00
Glutamine (mM)	**D39 (wt)**	**Δ*gdhA***	**D39 (wt)**	**Δ*gdhA***	**D39 (wt)**	**Δ*gdhA***
0	0.17 ± 0.00	0.13 ± 0.00	0.12 ± 0.06	0.14 ± 0.01	0.09 ± 0.03	0.09 ± 0.01
1	0.60 ± 0.03	0.61 ± 0.02	0.78 ± 0.00	0.61 ± 0.02	0.49 ± 0.01	0.37 ± 0.04
5	0.96 ± 0.01	0.96 ± 0.01	1.02 ± 0.02	0.92 ± 0.02	0.52 ± 0.03	0.43 ± 0.00
10	1.10 ± 0.06	0.87 ± 0.01	1.05 ± 0.01	1.04 ± 0.01	0.61 ± 0.01	0.48 ± 0.01

Table 3.9. Temperature- and nitrogen source-dependent growth rate (h^{-1}) (A) and growth yield (B) of the wild type and Δ*gdhA* strains.
The strains were grown in glutamate and glutamine at 34°C, 37°C, or 40°C. '±'indicates standard error of means.

3.26.2 Glutamate dehydrogenase is more active at higher temperature

Glutamate dehydrogenase activity of the wild type, Comp*ΔgdhA*, and Δ*gdhA* was measured using colorimetric assay kit (Biovision, USA). Bacterial cultures were grown overnight at 34°C, 37°C, or 40°C in CDM supplemented with 55 mM glucose. The culture was harvested by centrifugation, re-suspended in 1 ml ice-cold PBS (pH 7.0), and lysate were obtained by sonication. Afterwards, the concentration of lysate was determined using the Bradford assay (Section 2.15.2). GDH in lysate utilises glutamate as a substrate

and colour development is observed depending on the activity of the enzyme. In Figure 3.32, *gdhA* activity in D39 was the highest at 40°C (74.48 ± 0.83 mU), and the lowest at 34°C (16.51 ± 0.653 mU). The difference in enzyme activity between the temperatures was significant ($p<0.05$). The enzyme activity of the Comp*ΔgdhA* was similar to the wild type strain at all temperature. In addition, no enzymatic activity was detected in *ΔgdhA* at tested temperatures.

These results showed that the inactivation of GdhA abolished total glutamate dehydrogenase activity and the largest reduction of enzyme activity was observed at 40°C. Having the highest activity at this temperature in the wild type suggested that GdhA is a thermostable protein and involves thermal adaptation of pneumococcus at higher temperature.

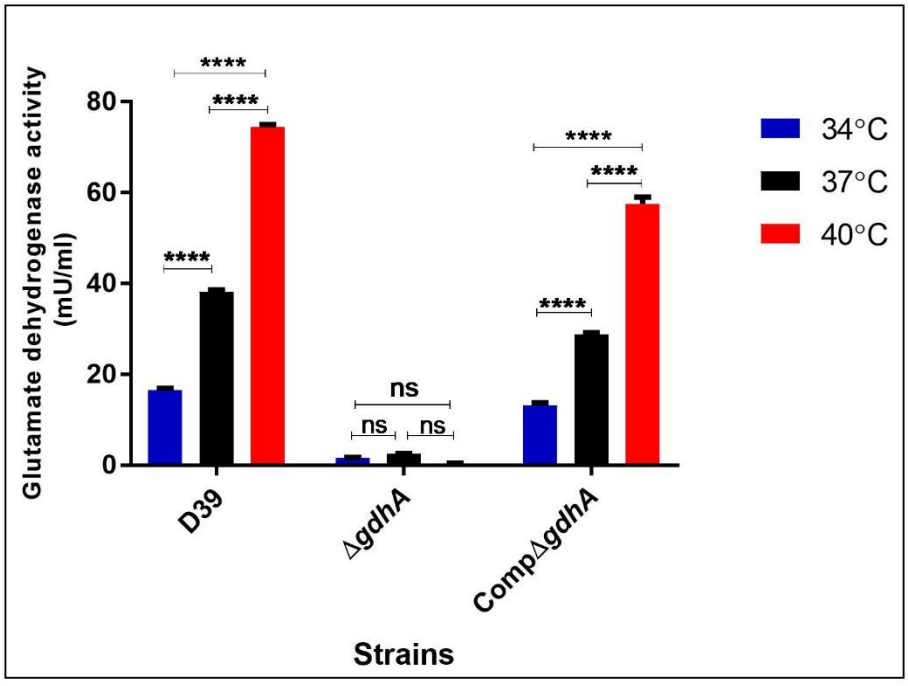

Figure 3.32. Glutamate dehydrogenase activity in D39, complemented mutant strain and its isogenic pneumococcal glutamate dehydrogenase mutants in D39 at 34°C, 37°C, or 40°C.
The enzyme activity is expressed as nmol/ml (mU/ml) of NADH released from the substrate per minute at pH 7.6. The highest induction of gdhA was obtained at 40°C in the wild type D39 and complemented mutant strain. No enzyme activity was recorded in *ΔgdhA* at all temperatures (**** $p<0.0001$, ns: not significant).

3.26.3 Inactivation of GdhA reduces the pH homeostasis in response to temperature shift

As mentioned earlier, GdhA plays a critical role in carbon-nitrogen metabolism in *S. pneumoniae* and the external pH could influence the transcriptional regulation of *gdhA* and acid-tolerance response controlled by F_1-ATPases (Kuhnert *et al.*, 2004). It is well known that the terminal pH value reflects the sensitivity of cells to acidification. To study the impact of temperature-pH effect on bacterial growth, pneumococcal strains were grown at different acidity levels at tested temperatures. In detail, the wild type and Δ*gdhA* strain were exposed to a range of pH (5.0, 5.4, 6.0, 6.4, 7.0, 7.4, and 8.0; table 2.7) at 34, 37, or 40°C for over 120 mins. Each 30 min interval, a sample if microbial suspension was plated out and CFU/ml was calculated.

The survival profiles of strains is presented in Figure 3.33. The acid tolerance of the wild type strain was lowest at pH 5.0 during incubation at 34°C and 37°C, and its growth reduced from $\log_{10}$ 8.4 to 5.2 CFU/ml in between 30 min to 120 min post-incubation. However, there were no significant differences on survival of wild type at pH 5.4 to 8.0. At 40°C, the reduction of CFU/ml is more pronounced at pH 5.0, 5.4, and 6.0 compared to at 37°C. The $\log_{10}$ CFU/ml is reduced from pH 8.0 to 5.0 after 120 at 40°C, suggesting that high temperature reduces the tolerance of wild type at acidic conditions.

The acid tolerance resistance of Δ*gdhA* was much lower than the wild type strain at all temperatures. For example, at 34°C and 37°C, the survival rate of Δ*gdhA* at pH 5.0 was $\log_{10}$ 3.92 and 4.7 CFU/ml, respectively, after 120 min incubation, whereas it was $\log_{10}$ 5.20 and 5.22 CFU/ml for the wild type in the same incubation period. At 40°C, the reduction on number of Δ*gdhA* cells was more pronounced. Under highest acidic pH (5.0), Δ*gdhA* could not survive after 90 min incubation. In addition, cell numbers were $\log_{10}$ 3.1, 5.2, and 6.9 CFU/ml at pH 5.4, 6, 6.4, respectively, after 120 min incubation at 40°C. At neutral pHs, the high temperature also attenuated the survival rate (Log_{10} 8.5 to 7.0 CFU/ml at pH 7, Log_{10} 8.4 to 7.2 CFU/ml at pH 7.4). Exposing to alkaline condition (pH 8.0) at 40°C also affected the survival of Δ*gdhA* as the cell numbers reduced from Log_{10} 8.4 to 6.3 CFU/ml after 120 min incubation. Taken together, the data suggested that environmental pH and temperature has synergistic adverse impact on the survival

ability of pneumococcus. Furthermore, GdhA may play an important role on pneumococcal survival at high temperature.

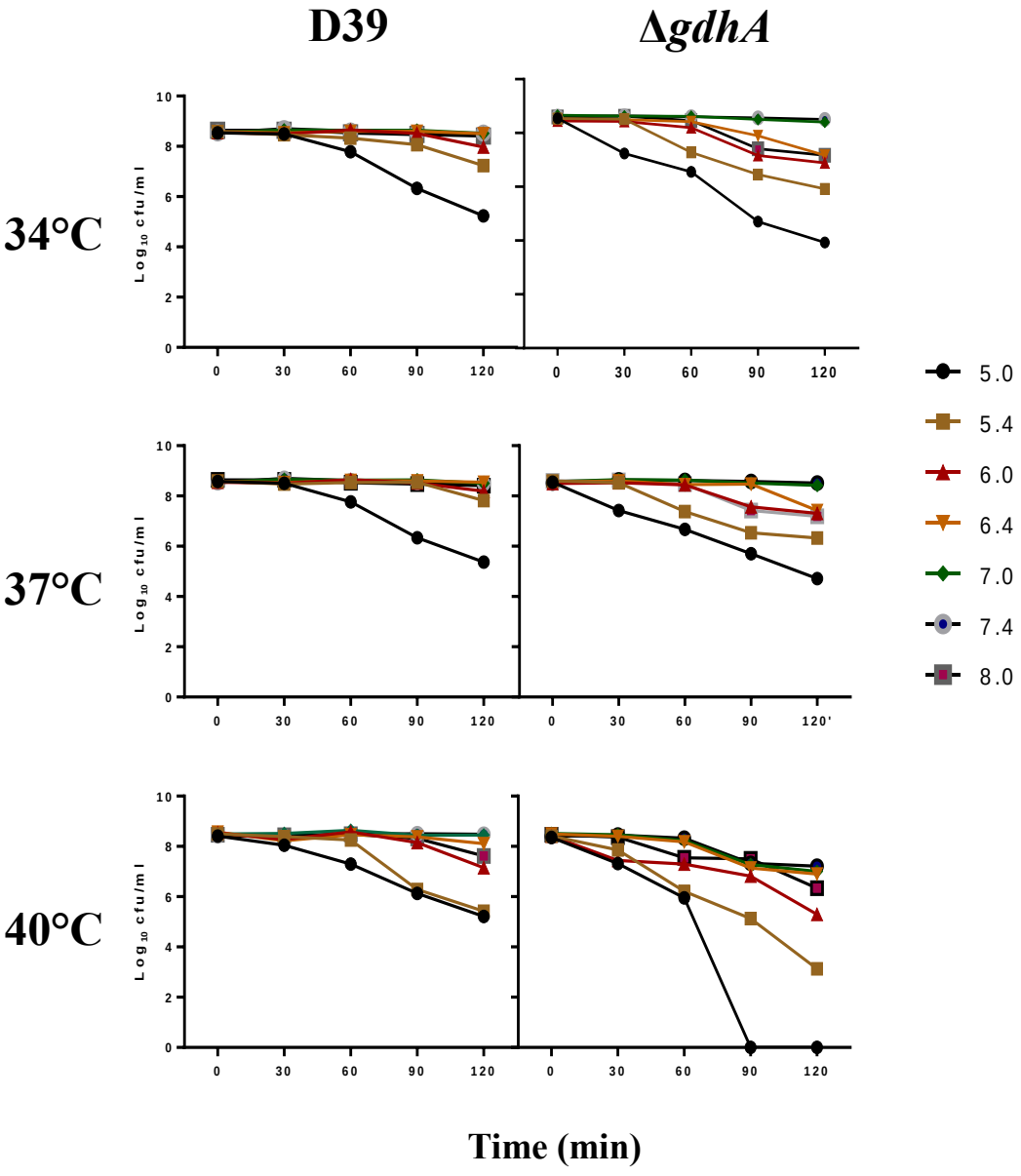

Figure 3.33. Acidity tolerance of D39 (wt) and Δ*gdhA* strains at 34°C, 37°C, or 40°C. The growth of both strains were expressed as log10 CFU/ml. The pH of buffers were adjusted from pH 5.0 to 8.0. At 40°C, the wild type D39 and Δ*gdhA* were more sensitive to acidic conditions compared to 34°C or 37°C. Data represent the mean of three independent experiments each with three replicates.

3.26.4 Temperature changes the formation of fermentation end products

The formation of metabolic end products including lactate, formate and acetate were quantified from pneumococcal strains using the commercial kits (Megazyme, Ireland) as previously described in Section 2.22. The wild type, Comp∆*gdhA* and ∆*gdhA* were grown in CDM supplemented with 55 mM glucose at different temperatures and the fermentative end products were measured upon extracting culture supernatants.

The amount of end products obtained from the supernatant are presented in Figure 3.34. There was no difference in between the wild type and complemented strain at all temperatures. On glucose, the lactate was the main fermentation end product for both strains. The lactate concentration was higher in the wild type (26.78 ± 0.58 mM) than in ∆*gdhA* strain (17.58 ± 1.12 mM). The lactate fluxes in the wild type and ∆*gdhA* were reduced when temperature was 34°C or 40°C.

It was observed that minor amounts of the formate and acetate were also formed with the temperature changes. Interestingly, the amount of formate produced in ∆*gdhA* was significantly higher compared to the wild type strain at all temperatures ($p<0.05$). The highest formate was recorded at 40°C (4.22 ± 0.08 mM). In addition, the amount of formate produced in this strain was significantly declined at 37°C and 34°C relative to 40°C (0.87 ± 0.03 mM and 0.74 ± 0.02 mM, respectively) ($p<0.05$). In the wild type, the amount of formate was 7.8-fold lower at 40°C (0.54 ± 0.00 mM), 4.1-fold lower at 37°C (0.87 ± 0.03 mM), and 4-fold lower at 34°C (0.74 ± 0.02 mM) compared to ∆*gdhA*. The amount of acetate production was the lowest among all tested fermentative end products for both strains and it was comparably lower at 34°C and 40°C relative to 37°C.

In conclusion, the lactate and acetate production in ∆*gdhA* was significantly lower than in the wild type at all temperatures ($p<0.001$). Another intriguing observation was the formate yield in ∆*gdhA* which was significantly higher than the wild type ($p<0.001$) and the highest formate production was recorded at 40°C.

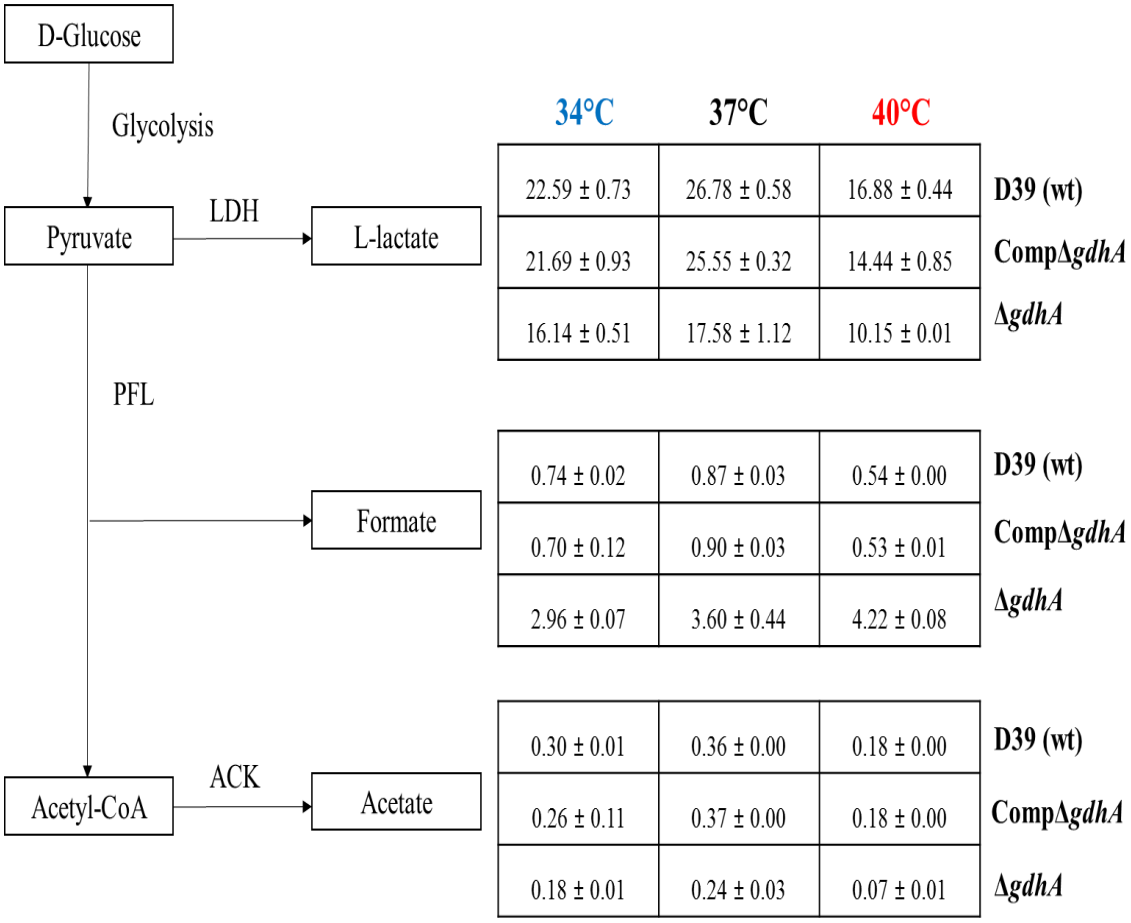

	34°C	37°C	40°C
D39 (wt)	22.59 ± 0.73	26.78 ± 0.58	16.88 ± 0.44
Comp*ΔgdhA*	21.69 ± 0.93	25.55 ± 0.32	14.44 ± 0.85
ΔgdhA	16.14 ± 0.51	17.58 ± 1.12	10.15 ± 0.01

D39 (wt)	0.74 ± 0.02	0.87 ± 0.03	0.54 ± 0.00
Comp*ΔgdhA*	0.70 ± 0.12	0.90 ± 0.03	0.53 ± 0.01
ΔgdhA	2.96 ± 0.07	3.60 ± 0.44	4.22 ± 0.08

D39 (wt)	0.30 ± 0.01	0.36 ± 0.00	0.18 ± 0.00
Comp*ΔgdhA*	0.26 ± 0.11	0.37 ± 0.00	0.18 ± 0.00
ΔgdhA	0.18 ± 0.01	0.24 ± 0.03	0.07 ± 0.01

Figure 3.34. The specific production rate of lactate, formate, and acetate in D39 (wt), Comp*ΔgdhA* and *ΔgdhA* strains at 34°C, 37°C, or 40°C.
Pneumococcal strains were grown in CDM supplemented with 55 mM glucose. The lactate is the main fermentation end product and lactate and acetate production in the wild type and Δ*gdhA* were reduced at 34°C or 40°C compared to 37°C. The formate production in Δ*gdhA* was significantly higher than the wild type and the highest formate production was recorded at 40°C. Values (mM) are mean of three independent experiments each with three replicates. '±' indicates standard error of means (SEM). LDH, lactate dehydrogenase; PFL, pyruvate-formate lyase; ACK, acetate kinase.

3.27 *In vivo* virulence studies

The experiments above demonstrated that GdhA is important for pneumococcal metabolism and production of virulence determinants *in vitro*. Hence, it was reasonable to test the involvement of GdhA in pneumococcal virulence *in vivo*. In this study, *Galleria mellonella* was used as a model to test virulence of the wild type, Comp∆*gdhA*, and ∆*gdhA* strains.

3.27.1 *Galleria mellonella* – a novel bacterial infection model

Galleria mellonella is an insect belonging to order *Lepidoptera* (Kwadha *et al.*, 2017). Numerous studies on this insect have been done to assess virulence of fungal species including *Aspergillus fumigatus* and *Candida albicans* (Li *et al.*, 2013; Slater *et al.*, 2011), and various Gram-positive and Gram-negative bacterial pathogens (Desbois and Coote, 2011; Evans and Rozen, 2012; Koch *et al.*, 2014), and even of viruses (Champion *et al.*, 2016). Comparing to other traditional mammalian host models, *G. mellonella* provides technical and logical advantages. The insect is large enough (last instar larvae are about 2 cm long and weight 250 mg) to be injected with defined doses of microbes. It is significantly cheaper than rodent models and *G. mellonella* is easy to maintain with a short life span for quick experiments. *G. mellonella*, can be kept at 20°C to 30°C and infection studies can be performed at below room temperature and over 37°C (mimics human body temperature), which makes it ideal to test the hypotheses of this study. Moreover, work with *G. mellonella* does not require ethical approval (Ignasiak and Maxwell, 2017). Regarding the infection with pathogens, the immune system of *Galleria* uses protection system such as enzymes, reactive oxygen species, melanin, antimicrobial peptides, and receptor proteins for germs as other mammalian models (Tsai *et al.*, 2016). Previously, a health index score for *G. mellonella* was established from an uninfected healthy worm (cream colour) to infected dead worm (black colour) (Tsai *et al.*, 2016). In this study, I scored the larvae from 1 to 5 assessing alive to dead status as consequence of inoculation with infective *S. pneumoniae* as shown in Figure 3.35.

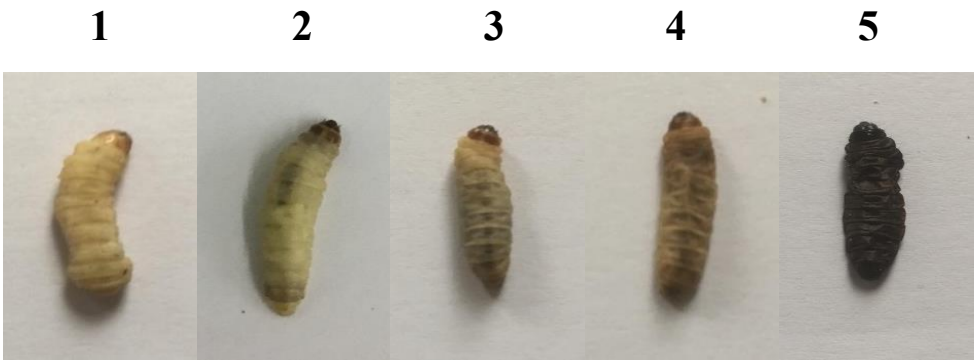

Figure 3.35. Photographic image of larvae and health score.
1. Alive, active; 2. Alive, move without stimulation; 3. Alive, move with stimulation; 4. Alive, no movement; 5. Dead, melanisation.

3.27.2 Determination of median lethal dose (LD_{50}) of *S. pneumoniae*

The LD_{50} test was developed to assess the median number of chemical or infection agent required to kill at least 50% of a test group (Rowan and Rollin, 1983).

In the dose-response experiments, infective doses of pneumococcus, which were prepared in BHI supplemented with 20% serum at 34°C, 37°C, or 40°C (Section 2.23.1), were determined by injecting groups of ten larvae with the suspensions of $1x10^4$, $1x10^5$, $5x10^5$, and $1x10^6$ CFU/larvae in 10 µl PBS. The larvae were then incubated and monitored for 4 days at exactly the same temperature in which bacteria were grown. The lethal dose to kill 50% of larvae (LD_{50}) was calculated for each strain at 24 h and the results were plotted in Figure 3.36. For example, the entire plates of larvae injected with $5x10^5$ CFU/larvae were imaged in Figure 3.37. 1×10^7 CFU/larvae of wild type or the mutant were 100% lethal at all temperatures within 6 hours. The exact LD_{50} of all strains was calculated by recording the number of dead larvae obtained from the used dosages at tested temperatures and expressed as $Log_{10}LD_{50}$, and statistically analysed by two-way ANOVA.

There was no significant difference in mortality rate of larvae infected either with the wild type or mutant that had been cultured at 37°C. In addition, the virulence of the wild type and complemented strain were similar at all temperatures. However, the results showed that Δ*gdhA* was significantly less virulent (5.31 ± 0.07 CFU/larvae) than the wild type and CompΔ*gdhA* (5.05 ± 0.06 and 5.11 ± 0.03 CFU/larvae) when cultured at 34°C ($p<0.05$). At 40°C, the virulence of all strains decreased compared to other temperatures. $Log_{10}LD_{50}$ of Δ*gdhA* (6.32 ± 0.04 CFU/larvae) was significantly higher, indicating that it is less virulent than wild type (5.26 ± 0.01 CFU/larvae) and CompΔ*gdhA* (5.23 ± 0.04 CFU/larvae) ($p<0.05$) (Figure 3.36).

In vivo results strongly suggest that Δ*gdhA* contribute to pneumococcal virulence in a temperature dependent manner. The results obtained with the complemented strain ruled out the possibility of polar effect of mutation. However, it was not clear whether the temperature effect on virulence was due to the incubation temperature of bacteria or larvae. To understand this, the wild type and Δ*gdhA* were grown in one temperature (37°C or 40°C), and the infected larvae were incubated at another temperature (37°C or 40°C). The results showed that the virulence is dependent on the incubation temperature of pneumococci (Figure 3.38). When D39 was grown at 37°C and the larvae were incubated either 37°C or 40°C, no difference on mortality was observed ($p>0.05$). However, when growth temperature of the wild type was 40°C, the virulence of the wild type reduced at larvae incubation temperature of 40°C ($p<0.05$). On the other hand, when these conditions were applied, the virulence of Δ*gdhA* was reduced at both conditions, suggesting that pneumococcal virulence is related to growth temperature of microbe rather than incubation temperature of larvae.

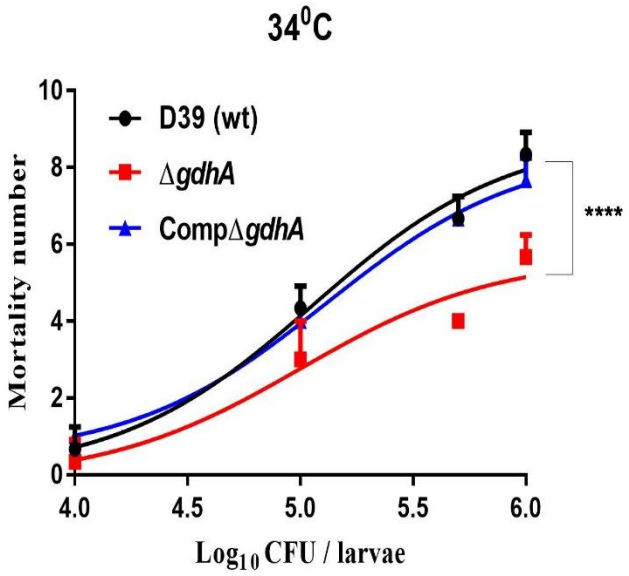

	34°C (Log_{10} CFU/larvae)
D39	5.05 ± 0.06
Δ*gdhA*	5.31 ± 0.07
Comp Δ*gdhA*	5.11 ± 0.03

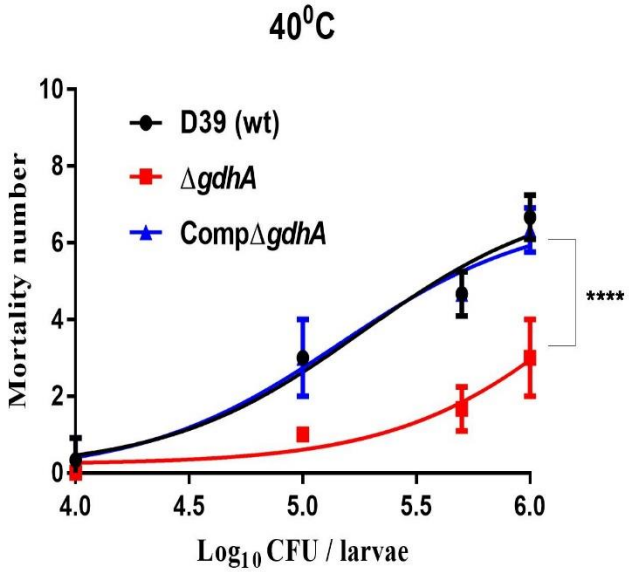

	40°C (Log_{10} CFU/larvae)
D39	5.26 ± 0.01
Δ*gdhA*	6.32 ± 0.04
Comp Δ*gdhA*	5.23 ± 0.04

Figure 3.36. Log10 LD_{50} for *G. mellonella* after 24 hr post infection.
Larvae were injected with $1x10^6$, $5x10^5$, $1x10^5$, and $1x10^4$ CFU/larvae of D39 (wt), Δ*gdhA*, CompΔ*gdhA* at 34°C and 40°C. No significant difference was observed between each strain at 37°C. Error bars represent the standard error of mean of triplicate experiments (10 larvae per each) (**** $p<0.0001$).

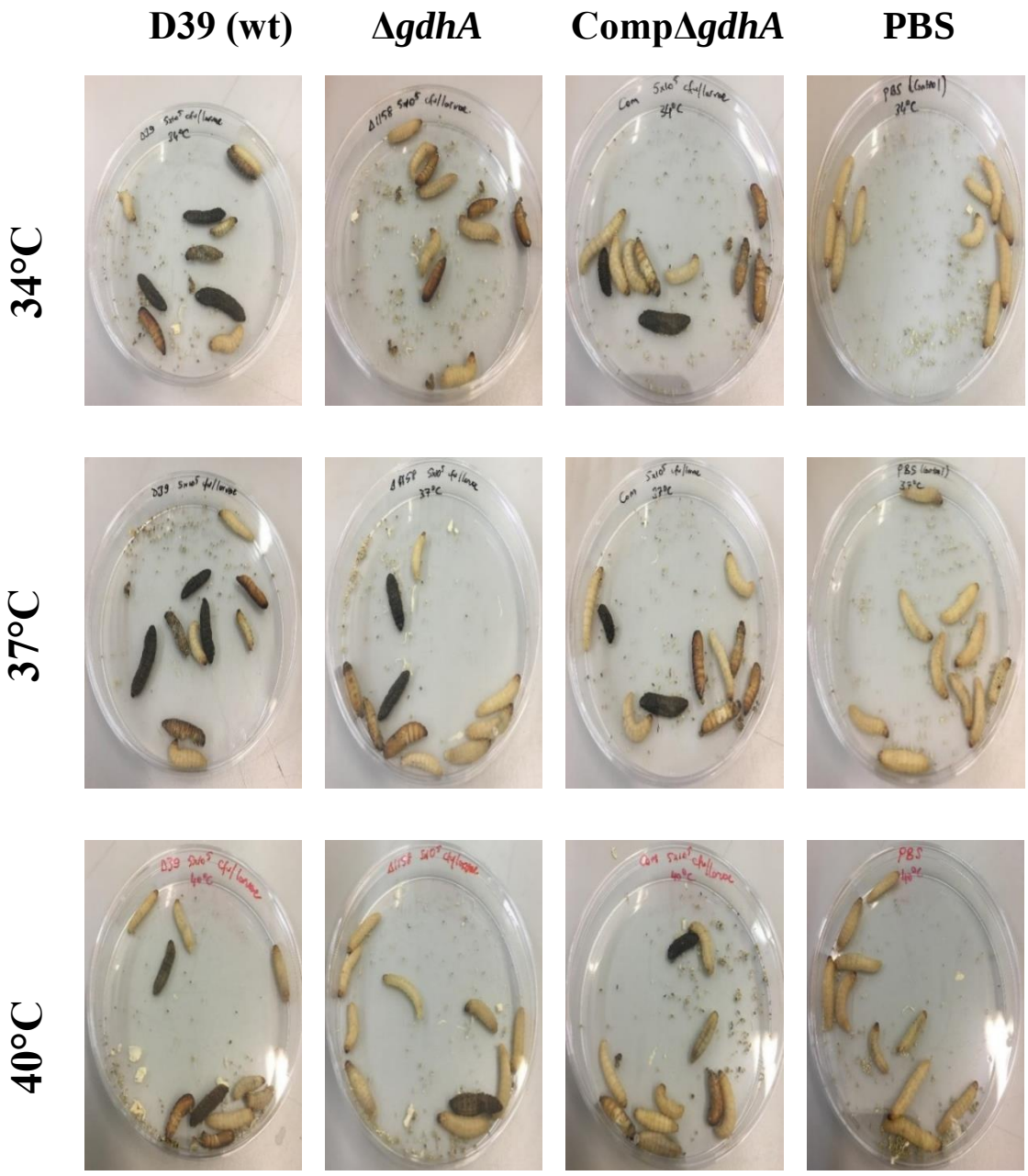

Figure 3.37. Images of *G. mellonella* after 24 hr post infection.
Larvae were injected with 5x10^5 CFU/larvae of D39 (wt), Δ*gdhA*, CompΔ*gdhA* grown at 34°C, 37°C, or 40°C. PBS was injected as a negative control and no dead larvae were recorded at these temperatures. For each strain, 10 larvae were sampled and incubated at growth temperature of pneumococcus.

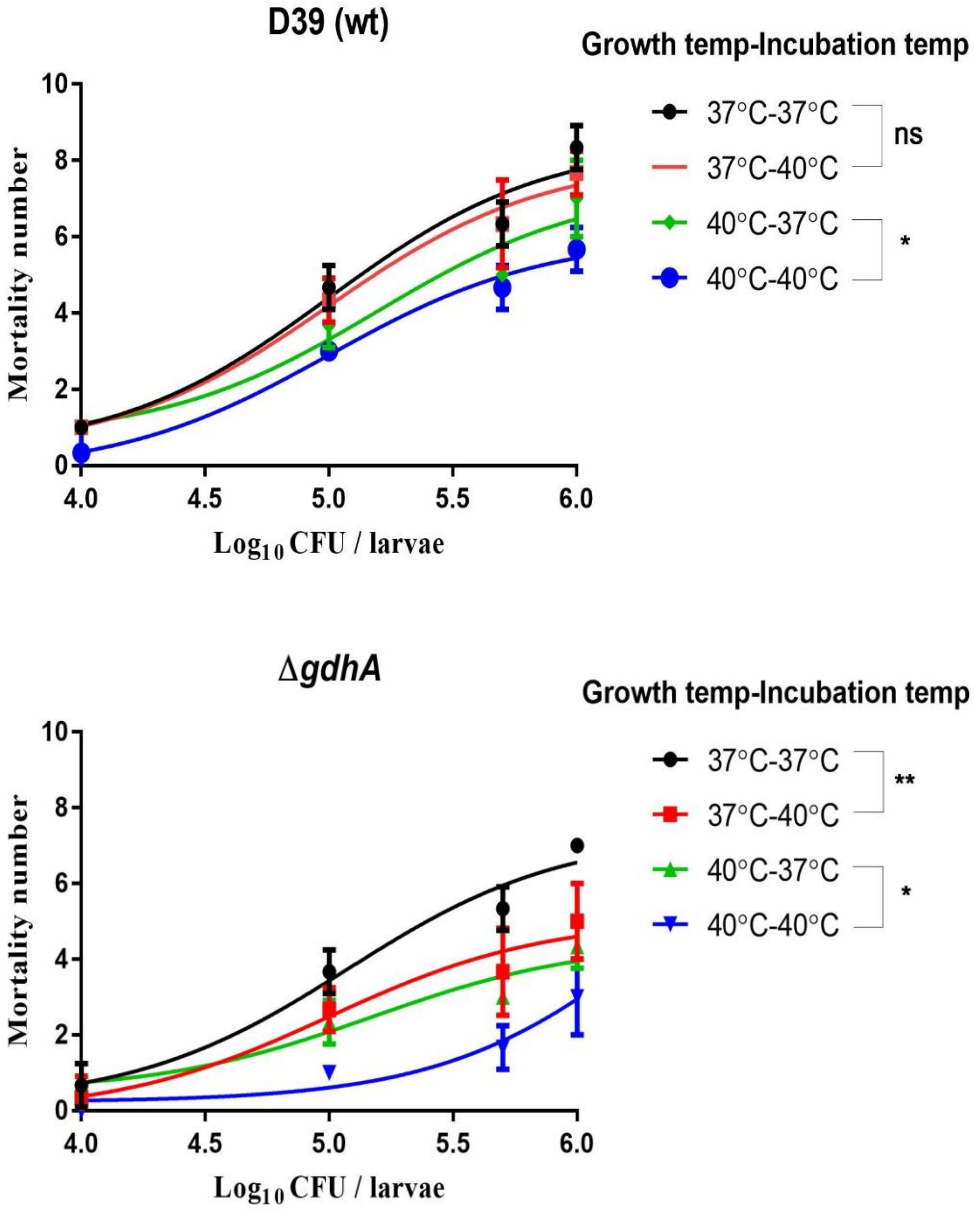

Figure 3.38. Mortality number of *G. mellonella*.
D39 (wt) and Δ*gdhA* were grown at 37°C or 40°C and larvae were incubated at either pneumococcal growth temperature or at the other temperature as a control after injection. Error bars represent the standard error of mean of triplicate experiments (10 larvae/experiment) (* $p<0.05$, ** $p<0.01$).

Chapter 4 Discussion

Streptococcus pneumoniae asymptomatically colonises the nasopharynx. However, under favourable conditions, it spreads to different human tissues and causes pneumonia, sepsis, meningitis, and otitis media (Henriques-Normark and Tuomanen, 2013). The diversity of diseases the microbe causes implies the success of pneumococcus to sense and adapt to variable environmental conditions in different host tissues, and its ability to alter phenotype from commensal to invasive pathogen. The environments encountered by the pneumococcus vary in terms of different levels of oxygen and metals, availability of nutrients, and fluctuating temperature in health and disease (Charpentier *et al.*, 2000). The pneumococcus has a high level of adaptive capacity and I described pneumococcal response to some well-known stress conditions in section 1.6. In this study, I hypothesised that temperature has impact on pneumococcal phenotype *in vitro* and thermal adaptation is critical for pneumococcal virulence *in vivo*.

In different anatomical sites within the human host, the pneumococcus encounters with fluctuating temperatures. In the nasopharynx, as the main niche where the microbe resides, the temperature is around 33°C-34°C (Pandya *et al.*, 2005). The core body temperature is 37°C. In the lungs, temperature is generally lower than 37°C due to inhaled air. During infection with pneumococci or viral co-infection such as influenza, both external and internal body temperature increases up to 40°C-42°C (Pandya *et al.*, 2005).

Nucleic acids, proteins, lipids and membrane fluidity are affected by the environmental temperature changes, therefore, they are known as thermosensors (Shapiro and Cowen, 2012). Thermosensors involve in the regulation of cellular processes such as transcription, translation, and signal transduction (Sengupta and Garrity, 2013). Of these, small non-coding RNAs (sRNAs) have been studied in many microbes with pathogenic potential including *S. pneumoniae* (Patenge *et al.*, 2015). Bacterial sRNAs are multifunctional as they regulate the many stress-response genes involving DNA damage, nutrient starvation, envelope stress, sugar metabolism, biofilm formation, and virulence (Holmqvist and Wagner, 2017; Patenge *et al.*, 2015). In pneumococcus, CiaRH two-component regulatory pathway, which was one of the target gene in this study, involving

competence and virulence was shown to be first identified regulator of sRNAs (*cia*-dependent sRNAs) and at least 15 sRNAs controlled by CiaR were found using motif analysis of repeat sequence (TTTAAG-N5-TTTAAG) in the promoter regions of certain pneumococcal genes (Patenge *et al.*, 2015). Functional csRNAs in the genome of other streptococci including *S. mitis* and *S. sanguinis* were also identified (Halfmann *et al.*, 2007b). However, our knowledge with how the pneumococcus adjusts itself to fluctuating temperature within the dynamic host niches is limited.

To understand how pneumococci successfully colonise the host and transition to disease, it is important to identify how microbe responds to fluctuating temperature within the host. Therefore, the effect of temperature on the selected phenotypes of *S. pneumoniae* D39 and its isogenic mutants were systematically explored.

4.1 Temperature alters phenotype of *S. pneumoniae* D39

Bacterial cells have to maintain homeostatic functions at different temperatures to sustain their normal growth. *S. pneumoniae* can grow at a wide range of temperature (25°C-42°C). As the nasopharynx is the main niche of pneumococcus, I hypothesized that the nasopharyngeal temperature (34°C) would be ideal for growth and creates similar phenotype that is obtained at optimal growth temperature (37°C) *in vitro*. Indeed, the wild type pneumococcus had maximal growth at both temperatures in BHI, which is a complex medium. In addition, increase in temperature (40°C) did not affect the growth in BHI, suggesting that temperature fluctuations *in vitro* does not adversely affect pneumococcal growth in nutrient-rich environment, very likely the pneumococcus has adaptive capability to deal with the unfavourable conditions created by the temperature changes in the presence of complex nutrients. A previous study reported that the growth rate of D39 and TIGR4 wild type strains at 37°C and 40°C were similar in BHI, however D39 grew less well at 30°C, possibly due to non-optimal growth temperature, whereas TIGR4 was not affected (Ibrahim *et al.*, 2005). This shows that temperature adaptive mechanisms may vary from one strain to the next. Therefore, it would be interesting to investigate if there is any difference in adaptive potential of colonising and invasive strains in the future.

I also investigated the impact of temperature on growth profile of the wild type in CDM supplemented with glucose (55 mM) as a nutrient-limited medium, where the microbe is expected to be under more stress than in complex medium. At 34°C and 37°C, D39 had similar growth rate, but it had a reduced rate of growth at 40°C. These findings suggested that nutrient composition does not affect the growth of pneumococcus at lower temperature but adversely affects at higher temperature. This also suggest that the maintenance of normal pneumococcal growth requires the activation of certain metabolic pathways.

In this study, I studied the impact of seven pneumococcal genes on thermal adaptation. I selected these genes based on their differential expressions at different temperatures and literature searches that showed their possible role on pneumococcal virulence, survival, or stress-response. On glucose, the mutant strains grew as well as the wild type at 37°C, but SPD_0132/0133, SPD_1711, and SPD_1651 mutants had reduced in cell size, Δ*comD*, Δ*merR*^{2}, and Δ*SPD_0132/0133* strains had attenuated in biofilm formation, and Δ*comD* and Δ*ciaR* attenuated in capsule production at 37°C compared to the wild type, implying that these genes have additional roles than thermal adaptation in pneumococcal biology.

When temperature was lowered to 34°C or raised to 40°C, the growth of Δ*comD*, Δ*SPD_1711*, and Δ*SPD_1651* were attenuated relative to the wild type, suggesting that these genes are required for growth at these temperatures. ComD is a part of *comCDE* operon encoding two-component signal transduction system, which controls the competence development during colonisation of upper respiratory tract (Kowalko and Sebert, 2008). Given that competence system allows synchronisation of DNA uptake at community level, competence system`s involvement in thermal adaptation suggests that temperature fluctuations exert population wide phenotypic changes via their impact on DNA uptake, which may lead to changes in DNA topography or alterations in gene expression. The role of competence system on pneumococcal growth at different temperature has not been studied in detail, however the involvement of competence systems in thermal adaptive response in other Gram-positive bacteria has been documented. For example, MecB, a member of the ClpC ATPase family in *B. subtilis*,

controls the competence development and it is required for growth at high temperature (Msadek *et al.*, 1994). Members of the Clp subfamily are heat shock proteins whose expressions are controlled by the CtsR, which is a global transcriptional regulator of stress-response genes in various bacteria (Frees *et al.*, 2004; Msadek *et al.*, 1994). In *S. pneumoniae*, *clpPE* regulon controls the competence development for DNA uptake, which is similar to *B. subtilis* (Chastanet *et al.*, 2001).

The role of SPD_1711 (DNA-binding protein) and SPD_1651 (iron-compound ABC transporter ATP-binding protein) on bacterial growth at different temperatures have not been studied. However, I speculate that SPD_1711 exerts its influence on growth through modulation of DNA binding, which affects gene expression. SPD_1651, on the other hand, may influence the level of intracellular iron, which is important for optimal growth of *S. pneumoniae* (Brown *et al.*, 2002).

In this study, I hypothesized that temperature may alter the cell size of *S. pneumoniae*. Adjusting cell size in a given environmental condition is important to ensure that cells are able to coordinate division with growth and have the appropriate size to survive. It is also well known fact that cell size is an important component for modulation of surface to volume ratio, which is critical parameter for growth rate (Harris and Theriot, 2018). Schaechter et al. (1958) found that *Salmonella* cell size is linked to growth rate, as the cells were two-fold larger when grown in nutrient-rich medium compared to growth in nutrient-limited medium with lower growth rate (Schaechter *et al.*, 1958). In addition, nutrient availability has impact on cell shape as *B. subtilis* cells increased their length (Sargent, 1975), while *E. coli* cells were longer and wider (Zaritsky *et al.*, 1993), in nutrient-rich medium. Chien *et al.* (2012) also reviewed that microbial cell size is responsive to nutrient availability (Chien *et al.*, 2012).

The pneumococcal cells reduced their size when grown at 40°C compared to their size at 37°C, while the cell size at 34°C was similar to that at 37°C in BHI. These results contradict with the nutrient availability-growth rate-cell size linkage, as no difference on growth rate of pneumococcus could be observed at 40°C relative to 37°C in nutrient-rich environment. The reason for this is currently unknown. Moreover, cell size at 34°C and

40°C significantly decreased when grown in CDM relative to 37°C. Although the growth rates of pneumococcus at 34°C and 37°C were similar in CDM, the cells were smaller at 34°C. Therefore, my results show that although temperature affects cell size, there is not a consistent pattern to explain a link between growth rate-cell size and growth temperature.

The mutant analysis showed that *gdhA, comD,* and *ciaR* play a role in altering the phenotype of pneumococcus in response to temperature fluctuation. Their involvement in thermal adaptation may be due to their role in cell division. The regulation of cell division is a key process of cell size control to ensure microbial growth. In most bacteria, cell division is controlled by FtzZ, which assembles the cell division mechanism into ring-like structure Z-ring, and acts as a scaffold to express cell division proteins (Chien *et al.*, 2012). It has been shown that the cell division in a α-proteobacterium *Caulobacter crescentus* is mediated by NAD-dependent glutamate dehydrogenase GdhZ. GdhZ initiates the release of progeny cells by stimulating the disassembly of Z-ring and GTPase activity of FtsZ, and coordinates the cell cycle with nutrient availability (Beaufay *et al.*, 2015). Based on this, it can be hypothesized that pneumococcal GdhA may involve into cell division network. It should be noted however that microarray data did not indicate significant change in the transcript level of FtsZ (SPD_1479) at tested temperatures. Hence, further work is required to establish how GdhA may involve in cell size determination.

Protein kinases and phosphatases are known to transmit signals in response to environmental factors and this is mainly controlled by two-component systems (TCS). In *S. pneumoniae*, a protein kinase StkP and its cognate phosphatase PhpP are involved in such a function. StkP is a conserved Ser/Thr kinase and involved in regulation of cell division proteins including FtsZ when phosphorylated. It was reported that CiaRH TCS, which is found to be differentially regulated at different temperatures in this study, was positively regulated by overexpressed phosphorylated StkP. Ibrahim *et al.* (2005) suggested that CiaRH regulon induces HtrA (high temperature requirement A), which degrades phosphorylated StkP to control the cell division in *S. pneumoniae* (Ibrahim *et al.*, 2005). This suggests that CiaR is involved in regulation of cell division. Moreover,

HtrA is also functional in controlling of competence development. Hence, ComD (histidine kinase) in Com regulon has an input in regulation of cell division. As discussed above, while GdhA, CiaR, and ComD may influence cell size by their impact on the cascades involved in this specific process, it is also possible that they may have an indirect role in cell division control when exposed to different temperatures.

In *S. pneumoniae,* biofilm formation occurs during colonisation of the nasopharynx (Chao *et al.*, 2014). This niche has a lower temperature (34°C) than the core body temperature and has a low nutrient availability. The results of this study showed that biofilm biosynthesis is not influenced at 34°C relative to 37°C when the pneumococcus is propagated in THY, which is a nutrient-rich medium. However, I found that high temperature (40°C) attenuated the biofilm formation. Attenuated biofilm at this temperature may be related to changes in cell surface architecture (Kostakioti *et al.*, 2013), which may affect the aggregation of pneumococcal cells (Sanchez *et al.*, 2010). Chao *et al.* (2014) reported that *S. pneumoniae* forms denser and functional biofilms at 34°C than at 37°C *in vivo*. This *in vitro* and *in vivo* phenotypic difference may indicate that abiotic surfaces are insufficient to provide *in vivo* features to support pneumococcal biofilm formation. In most cases, pneumococcal infection precedes with viral infection that increases bacterial growth (Chao *et al.*, 2014). Influenza A virus (IAV) has been found to increase susceptibility to pneumococcal pneumonia (Morens *et al.*, 2008) through suppression of immune responses and increasing the attachment of pneumococcal cells to respiratory epithelial cells (McCullers and Bartmess, 2003). It was also mentioned that IAV infection causes transmission of dispatched biofilms between individuals (Diavatopoulos *et al.*, 2010). The viral infection elevates the host temperature (38.5°C) and effects the biofilm formation as it causes dispersal of bacteria from the biofilm *ex-vivo* (Chao *et al.*, 2014).

The mutant analysis showed that Δ*ciaR,* Δ*SPD*_1711, and Δ*SPD_1651* strains formed significantly less biofilm than the wild type at 34°C and 40°C, suggesting that these genes are required for biofilm formation of *S. pneumoniae*. In addition, biofilm formation of *comD, SPD_0132/133,* and *merR*^{2} mutants attenuated at all temperatures, indicating that

these strains are involved in biofilm formation but their involvement in biofilm synthesis may not be temperature-dependent.

In *S. pneumoniae*, biofilm formation during colonisation of nasopharynx is regulated by two-component systems including CiaRH regulon (Chao *et al.*, 2014). Using *in vivo* model, Blanchette-Cain *et al.* (2013) found that inactivation of CiaRH resulted in decrease in colonisation (Blanchette-Cain *et al.*, 2013). CiaR (SPD_0701) is the response regulator of CiaRH regulon and it has been reported that induction of CiaR enhances the expression of stress-response genes (Dagkessamanskaia *et al.*, 2004). At lower temperature (34°C), biofilm formation of *ciaR* mutant was significantly lower than the wild type. Moreover, the reduction of biofilm biosynthesis in the mutant was more pronounced at higher temperature (40°C) where the microbe is under more stress. It can be concluded that CiaR is required for regulation of biofilm at different temperatures.

The role of SPD_1711 (single stranded-DNA binding protein) on bacterial biofilm has not been studied. Zweig et al. (2013) reported that extracellular DNA plays an important role in biofilm formation of *N. gonorrhoeae.* The T4SS (type IV secretion system) secretes ssDNA, which initiates the biofilm formation. The involvement of ssDNA in biofilm biosynthesis was measured using fluorescently labelled ssDNA and ss/dsDNA binding proteins on confocal microscopy (Zweig *et al.*, 2014). It is also well known that temperature is a critical factor for interaction between binding proteins and DNA as DNA structure and flexibility are affected by temperature fluctuation (Driessen *et al.*, 2014). For example, binding of RecA protein to ssDNA in *E. coli* and a thermophilic bacteria *Thermus thermophilus* is temperature-dependent. In *E. coli,* RecA binding decreases with elevated temperature and irreversible unbounded state occurs at 42°C, which is possibly due to uncorrelated domain structures. However, this transition state is not observed in *T. thermophilus* RecA as it is more thermostable (Merrin *et al.*, 2011). I speculate that binding capability of SPD_1711 in *S. pneumoniae* is also modulated by temperature as its expression went up 59.25-fold at 34°C and went down 36.58-fold at 40°C relative to 37°C.

The role of iron transporters on bacterial biofilm at different temperatures has not been studied. However, importance of iron for biofilm biosynthesis in mesophilic bacteria such as *Pseudomonas aeruginosa*, *Bacillus subtilis*, and *Staphylococcus aureus* (Hayrapetyan *et al.*, 2016; Kang and Kirienko, 2018; Lin *et al.*, 2012) and in thermophilic bacteria *Thermotoga maritima* (Pysz *et al.*, 2004) has been extensively studied. Iron is an essential nutrient for bacterial growth, energy production, and nucleotide synthesis, but availability of iron is limited in host environment (Ratledge and Dover, 2000). Hence, iron acquisition is critical for bacterial viability. A study with transcriptional analysis of biofilm formation in *T. maritima* found that iron-transport proteins are significantly upregulated in biofilm (Pysz *et al.*, 2004). Given this information, there may be a positive correlation between iron transporters and biofilm formation. In pneumococcus, biofilm formation is initiated in the nasopharynx (Domenech *et al.*, 2012). SPD_1651 may influence the level of iron in this niche, which may be required for pneumococcal biofilm as its expression is upregulated at 34°C relative to 37°C.

In this study, I also investigated the impact of temperature on activity of two major virulence factors, neuraminidase and pneumolysin, of *S. pneumoniae*. Neuraminidases cleave the terminal sialic acid residues from host glycans including mucin, glycolipids, and glycoproteins, which are used as carbon and nitrogen source by bacteria (Hentrich *et al.*, 2016). Furthermore, it was reported that neuraminidase plays an important role on pneumococcal pathogenesis via its role in nutrient metabolism, biofilm production, adhesion, and immune protection (Parker *et al.*, 2009). The cleavage of sialic acids is mediated by neuraminidases, which are encoded by *nanABC* genes (Hentrich *et al.*, 2016). NanA has been shown to promote biofilm formation during colonisation of nasopharynx and lungs, and activation of innate immune system (Blanchette *et al.*, 2016). NanB is important for pneumococcal survival in upper respiratory tract and sepsis (Manco *et al.*, 2006), and NanC works synergistically with NanA and NanB, allowing pneumococcus to access glycoconjugates (Janesch *et al.*, 2018).

Neuraminidase activity of D39 at 34°C and 40°C was similar to that observed at 37°C in BHI, suggesting that temperature has no adverse effect in the activity of neuraminidase in a complex medium. On glucose, on the other hand, D39 had attenuated neuraminidase

activity at 34°C and 40°C. Mutant analysis showed that all selected genes have no impact on neuraminidase activity of pneumococcus at 37°C. However, neuraminidase activity of mutant strains was significantly reduced by temperature changes, which might be related to insufficient utilisation of free sugars. Therefore, these genes may involve in regulation of neuraminidase activity in a temperature-dependent manner. In future, the neuraminidase activity determination should be made in the presence of complex host glycans such as mucin, which has high levels of bound sialic acid.

Recently, CiaR was shown to be upregulated in response to sialic acid. It was also reported that CiaR controls the transcription of NanA and sialic acid transporter SatABC (Hentrich *et al.*, 2016). Therefore, the activation of CiaR is important for pneumococcal growth on sialic acid. In addition, Neu5Ac increases pneumococcal resistance to oxidative stress through HtrA (high temperature requirement A) that is controlled by CiaR. Hentrich et al. (2016) reported that N-acetyl neuraminic acid (Neu5Ac) is important for CiaR activation and CiaR mediated colonisation was mediated by the presence of Neu5Ac as the CiaR-null strain showed a decrease in nasopharyngeal colonization in both wild type and *Cmah* $^{-/-}$ mice (Hentrich *et al.*, 2016). These results indicate the complexity of pneumococcal thermal adaptive response, and its link to pneumococcal survival in host tissues.

Pneumolysin (Ply) is a cholesterol-dependent cytolytic pore-forming toxin, and expressed during the late log phase of growth (Mitchell and Mitchell, 2010). Ply promotes pneumococcal adhesion to epithelial cells in the host by blocking the ciliary motion of the epithelium in the respiratory tract (Steinfort *et al.*, 1989). Furthermore, Ply is able to break the barrier of the alveolar capillary bed and allows pneumococcus to spread into blood stream resulting in bacteraemia (Rubins *et al.*, 1996). The production of pneumolysin at different temperatures was measured via haemolytic activity assay using the same concentration of cell lysates. The wild type strain had similar haemolytic activity at 34°C and 37°C both in rich and defined medium. At 40°C, on the other hand, haemolytic activity attenuated when microbe was grown in CDM with glucose. Several studies reported that haemolytic activity is temperature-dependent. For example, Poole and Braun (1988) showed that haemolysin gene expression is higher at 30°C than at 37°C

in *Serratia marcescens*, and the impact of temperature was growth phase dependent, because more hemolysin was recorded at early log phase at 30°C (Poole and Braun, 1988). In another study, the binding of a pore-forming peptide toxin (tolaasin) produced by *Pseudomonas tolaasii*, to red blood cells (RBC) was temperature sensitive. Tolaasin has poor binding to RBC at 4°C when compared to binding at 37°C. When temperature decreases to 4°C once toolasin bound to RBC at 37°C, complete haemolysis was observed, suggesting that this toxin may have a role in virulence linked to thermal adaptation (Cho *et al.*, 2010). Based on to these observations, it can be speculated that the reduced haemolytic activity of D39 at 40°C may be related to expression of *ply* (SPD_1726) at 40°C, and the structural changes that effect Ply binding RBC.

The mutant studies showed that the haemolytic activity of the mutant strains was not different from the wild type at 34°C or 37°C. At 40°C, haemolysis was significantly reduced for all the strains. Inactivation of these selected genes may affect the tolerance of microbe to high temperature, which results in decreased production of pneumolysin.

In this study, I also investigated the amount of capsule produced at different temperatures because pneumococcal polysaccharide capsule is the major virulence factor and microbial capsules are affected by environmental factors such as oxygen concentration and sugar (Rendueles *et al.*, 2017). The capsule is an adhesin involved in initial colonisation of nasopharynx, and provides protection against phagocytosis during invasive infection (Hathaway *et al.*, 2012). The capsule amount produced by the wild type strain was not different in BHI medium at tested temperatures. In line with this observation, in *S. pyogenes*, the wild type strains HSC5 and MGAS315 were found to produce capsule at basal level with no significant difference when grown in THY medium at 25°C, 30°C, or 37°C (Kang *et al.*, 2012). In addition, the wild type strain produced significantly more capsule at 34°C than at 37°C in CDM supplemented with glucose in this study. This result is very interesting because the expression of *cps* locus (SPD_0315 to SPD_0327) was below 2-fold in the microarray at 34°C relative to 37°C. The capsule of D39 is formed of repeating units of glucose (Glc), glucuronic acid (GlcUA) and rhamnose (Rha) (Iannelli *et al.*, 1999) and its synthesis is linked to sugar metabolism (Bentley *et al.*, 2006). Sugar constituents are activated by uridine 5'-triphosphate (UTP), yielding uridine diphosphate

glucose (UDP-Glc) and uridine diphosphate glucuronic acid (UDP-GlcUA), and deoxythymidine triphosphate (dTTP) (Iannelli *et al.*, 1999). In many Gram-positive bacteria, pyrimidine synthesis is linked to the production of uridine monophosphate (UMP) and a connection between capsule production and pyrimidine-uracil metabolism has also been shown in *S. pneumoniae* (Carvalho *et al.*, 2018), suggesting that sugar catabolism and pyrimidine-uracil metabolism may play role on capsule synthesis. However, the expression of genes that are involved in these pathways was below 2-fold. It is therefore possible that the temperature impact on capsule synthesis may be occurring currently by undiscovered pneumococcal pathways.

To investigate the role of selected genes on capsule production, the mutant strains were incubated at 34°C, 37°C, or 40°C in CDM with glucose. The results showed that *SPD_0132/133*, *SPD_1711*, and *SPD_1651* mutant strains involved in capsule synthesis in pneumococcus in a temperature-dependent manner. Interestingly, I observed that *CiaR* and *ComD* mutants produced less capsule than the wild type at 37°C, while they had similar amount of capsule at 40°C. The reason for this observation is unclear but it may be due to *ciaR* and *comD* downregulation or transcript degradation at this temperature.

SPD_0132/0133 is a hypothetical protein coding for bacteriocin synthesis (Kanehisa et al., 2015). Its direct role on capsule production has not been studied yet, however, it was shown that competence and bacteriocin locus are in cross-talk in encapsulated D39. Recently, Zheng *et al.* (2017) showed that Com regulon plays a role in transcriptional regulation of *cps* locus in *S. pneumoniae* (Zheng *et al.*, 2017). Therefore, it can be hypothesized that the synergistic talk between *com* and bacteriocin locus regulate the capsule synthesis in pneumococcus (Wang *et al.*, 2018). On the other hand, SPD_1711 (DNA-binding protein) may affect the capsule synthesis through its impact on growth, and SPD_1651 (iron-compound ABC transporter ATP-binding protein) plays a role in capsule synthesis through modulation of intracellular level of iron, which is an important nutrient for growth of pneumococcus.

4.2 Temperature alters the pneumococcal transcriptome

In this study, I analysed the transcript level of D39 grown at 34°C and 40°C relative to 37°C at mid-logarithmic phase and found that *S. pneumoniae* profoundly changes gene expression in response to temperature shift. A 2-fold difference in relative gene expression is considered to be highly significant and leads to biological effect (Ferguson *et al.*, 2010). Hence, I focused only transcripts whose expression at this level of fold-change at different temperatures. Out of 2085 pneumococcal genes, 132 genes at 34°C (6.3%) and 120 genes at 40°C (5.7%) were differentially expressed relative to their expression at 37°C. At 34°C, 97 genes were upregulated whereas 35 genes were downregulated. This may indicate that these genes play a role in nasopharyngeal colonisation as the temperature in this niche is reported to be 34°C. On the other hand, 34 genes were upregulated whereas 76 genes were downregulated at 40°C that mimicked the high fever during pneumococcal infection. Pandya *et al.* (2005) studied the gene expression of *S. pneumoniae* TIGR4 at 21, 29, 33, 37, or 40°C. Unlike to my study, threshold level was 1.5-fold in that study. The results showed that 29% of 1717 TIGR4 genes were differentially regulated in at least one temperature relative to 37°C (Pandya *et al.*, 2005). The highest number of differentially expressed genes was found at 21°C (425 genes), which is thought to be related to adaptation progress to non-optimal growth temperature. In addition, the number of genes induced at 33°C (158) was lower than at 40°C (Pandya *et al.*, 2005), which conflicted with my data as the number of differentially expressed genes were higher at 34°C than at 40°C. Moreover, similar to my data, there were overlapping genes that were induced differently at different temperatures. Temperature-induced gene expression analysis in Gram-negative bacteria has also been studied. In *E. coli* K12, 401 (~9% of the genome) genes were found to be differentially expressed at 28°C and 389 (~9% of the genome) genes at 33°C relative to 37°C (Gadgil *et al.*, 2005). These results suggest that the fluctuations in temperature lead to major differences in gene expression both in Gram-negative and positive bacteria.

As shown in Figure 3.9, I analysed differentially expressed genes by functional categories. Uncharacterized hypothetical proteins represented the largest group of genes at least in one temperature. This group of genes have also been found to be highly responsive to temperature shift in group A Streptococcus (GAS) (Smoot *et al.*, 2001).

Smoot *et al.* (2001) reported that these genes were highly downregulated at 29°C relative to 37°C, whereas in my data, this category mostly upregulated at 34°C relative to 37°C. This shows that different species of bacteria use unique mechanisms for temperature adaptation. The second largest group of genes was those encoding for cellular metabolism related to genetic information processing. Most of these genes were upregulated at 34°C, while downregulated at 40°C. In line with my data, Mereghetti *et al.* (2008) reported that genes involved in cellular processes in *S. agalactiae* were upregulated at 30°C relative to 40°C, suggesting that these genes are important for thermal adaptation (Mereghetti *et al.*, 2008). In addition, carbohydrate and lipid metabolism genes were the least affected by the temperature fluctuations. This shows that these pathways are constitutively expressed due to their essential functions in pneumococcal biology.

In the microarray data, one of the prominent findings was genes encoding for proteins involved in purine metabolism (SPD_0051 to SPD_0060) was upregulated at 34°C whereas they were downregulated at 40°C relative to 37°C. In contrast to my findings, transcriptomic studies in *S. pneumoniae* TIGR4 and *S. agalactiae* showed that purine metabolism genes were downregulated at lower temperature (33°C and 30°C, respectively) and upregulated at higher temperature (40°C for both strains) (Mereghetti *et al.*, 2008; Pandya *et al.*, 2005). It is intriguing to point out that the expression of purine-metabolism genes are different in two pneumococcal species D39 and TIGR4 (Pandya *et al.*, 2005) possibly due to having different genomic background. This may explain the differences in expression patterns of these genes at different temperatures. I speculate that increase in expression of purine metabolism genes at 34°C affects competence state, which occurs more efficiently at 34°C and requires DNA synthesis (Tavares *et al.*, 2018).

The expression of genes coding for iron transport proteins (SPD_1650, SPD_1651, and SPD_1652) were upregulated at 34°C and downregulated at 40°C relative to 37°C. Iron is an important metal as it is required as a cofactor for many proteins such as cytochrome or ferredoxin and plays a role on redox reactions. Moreover, free iron is limited in mammalian host, therefore limitation of metal availability is known to be a defence mechanism against bacterial invasion (Kang and Kirienko, 2018). Smoot *et al.* (2001) reported that the temperature of patients infected with group A Streptococcus exceeds

40°C. As an initial host response, the host restricts free iron available to the microbe. These investigators found that the expression of genes encoding iron transport was upregulated at elevated temperature to survive in limited iron environment (Smoot *et al.*, 2001). In addition, Mereghetti *et al.* (2008) also observed that iron transport genes were upregulated at high temperature in a group B Streptococcus, *S. agalactiae* (Mereghetti *et al.*, 2008). In my data, *SPD_1650*, *SPD_1651*, and *SPD_1652* were the only differentially expressed iron-transport genes. In D39 genome, many other iron-transport genes were upregulated at 40°C whereas downregulated at 34°C, however, their expressions were below 2-fold. Therefore, the significance of differential expression of genes below 2-fold should be experimentally verified in pneumococcal thermoregulation.

Regulatory proteins are extremely important because changes in their transcription may have pleiotropic effects that may significantly influence the genes required for bacterial metabolism, virulence, and survival. In my data, ten regulatory genes were differentially transcribed (Appendix A). These include two-component regulatory pathway and competence-related genes (*com*, *cgl*, and *ciaRH*); *blp* operon encoding bacteriocin synthesis (SPD_0046 and SPD_0047); *codY* (SPD_1412), a global nutritional regulator mainly involved in amino acid metabolism; SPD_2068, encoding chaperon system; and chromosome partitioning protein SpoJ (SPD_2069). These loci were upregulated at 34ºC, while downregulated at 40ºC. Furthermore, MerR family protein (SPD_0447) controlling nitrogen metabolism, SPD_1524 (GntR) involved in polysaccharide synthesis, and SPD_1645 (MarR) encoding aromatic catabolism genes, were downregulated at 34ºC. Interestingly, no difference in expression of *codY*, *gntR*, and *marR* could be seen at 40ºC.

Competence-related genes and *ciaRH* have been extensively studied in pneumococcus (Dagkessamanskaia *et al.*, 2004; Prudhomme *et al.*, 2016). These studies have shown that *com* and *ciaRH* work co-ordinately, hence their differential transcriptions imply the existence of a broader gene regulatory network on various cellular processes (Prudhomme *et al.*, 2016). For example, competence-induced cell lysis was shown to be important for release of pneumococcal virulence factors pneumolysin, and teichoic and lipoteichoic acid (Guiral *et al.*, 2005). In addition, competence for DNA transformation is crucial for pneumococcal virulence as Kowalko and Sebert (2008) reported that inactivation of

comD, codes for a histidine kinase, attenuated the pneumonia and bacteraemia in mice (Kowalko and Sebert, 2008). This result was also confirmed by another study (Zhu and Lau, 2011). CiaRH mediates the regulation of competence development, autolysis, bacteriocin production, biofilm formation, colonisation and virulence, and stress-response mechanisms in *S. pneumoniae* (Blanchette-Cain *et al.*, 2013).

The impact of temperature on the expression of transcriptional regulators has also been studied in other *streptococci.* Interestingly, the expression of two-component systems of *S. agalactiae*, CovS/CovR controlling the virulence genes (gbs1671 and gbs1672), Stp1/Stk1 which is a serine/threonine phosphatase (gbs0306 and gbs0307), CiaRH (gbs1019 and gbs1020), and VicRK encoding the division protein, and surface virulence factors (gbs0741 and gbs0742) did not show any difference between 30ºC and 40ºC. On the other hand, other regulatory genes mediating carbohydrate metabolism, ion uptake, and cell envelope synthesis were upregulated at 30ºC, while regulators controlling DNA replication (gbs0048 and a putative Cro/CI family regulator), or binding (gbs0618 and a putative TetR family regulator), gbs0685 (an uncharacterized DNA-binding response regulator), were upregulated at 40ºC (Mereghetti *et al.*, 2008).

4.3 GdhA is required for high temperature adaptation of *S. pneumoniae* D39

Glutamate is an important metabolite that plays a role in carbon and nitrogen metabolism (Feehily and Karatzas, 2013), and numerous studies have shown that glutamate metabolism is closely connected with the virulence of various microbes including *S. pneumoniae* (Kloosterman *et al.*, 2006; Somerville and Proctor, 2009). Glutamate dehydrogenase catalyses reversible reaction of glutamate to α-ketoglutarate (α-KG) with the reduction of $NADP^+$ to NADPH (Kloosterman *et al.*, 2006). In *S. pneumoniae* D39, *gdhA* is NADPH-dependent which likely contributes to the biosynthesis of glutamate from α-KG (Kloosterman *et al.*, 2006).

The microarray data showed that *gdhA* transcripts increased at 40°C, while the expression went down at 34°C relative to 37°C. This conclusion was also further confirmed by

transcriptional *lacZ*-fusion where P*gdhA*-*lacZ*-wt showed highest induction of *lacZ* on glucose at 40°C and the lowest at 34°C. It has been shown that GlnR (Kloosterman *et al.*, 2006) and CodY (Hendriksen *et al.*, 2008) regulate GdhA. Kaspar *et al.* (2014) suggested that transcription of *gdh* is lower at 24°C than at 37°C in *L. monocytogenes* (Kaspar *et al.*, 2014).

Loss of *gdhA* did not alter the growth profiles of the mutant strain at 34°C and 37°C comparing to the wild type when grown in CDM supplemented with glucose. At 40°C, the growth of *gdhA* mutant strain is abrogated relative to 34°C. Transcriptional activation and growth characteristic of *gdhA* at 40°C raised the hypothesis that GdhA enzyme is functional at high temperature. The results of enzyme activity assay showed that GdhA has the highest activity at 40°C, while it has the lowest activity at 34°C relative to 37°C, suggesting that GdhA is a thermostable protein and may contribute to high-temperature adaptation of *S. pneumoniae*. To prove this, protein-engineering and structural techniques can be applied to characterize its thermostability in the future. The stability of GdhA is possibly related to loss of nitrogen control under temperature stress, leading to overexpression of *gdhA* or increased glutamate catabolism under high temperatures in response to nitrogen availability. Contrary to this prediction, Kloosterman *et al.* (2006) suggested that GdhA of *S. pneumoniae* is involved in the production of glutamate from α-KG, and plays a role as an emergency measure under nitrogen poor conditions (Kloosterman *et al.*, 2006).

The role of GdhA on pH homeostasis at different temperatures was also studied. I found that under pH 5.0 at 40°C, Δ*gdhA* strain could not survive after 90 min incubation. It is probably due to acidic deactivation of enzyme and inactivation of deamination of ammonium. The similar results were observed in *Candida utilis* (Neumann *et al.*, 1976). Enzymatic activity of Gdh was also tested on lactic acid bacteria and was found that the activity increases with the elevated pH and temperature (De Angelis *et al.*, 2010). Hence, I conclude that pH influences the thermodynamics and kinetics of GdhA and GdhA is important for *S. pneumoniae* when the microbe is exposed to high temperature.

Temperature has also effect on the metabolic end product profile in D39 wild type and Δ*gdhA*. Both strains had homolactic metabolite profiles at all temperatures in CDM-glucose medium. Al-Bayati *et al.* (2017) reported that D39 has a homolactic profile at 37°C and lactate was the main end product, while Δ*ccpA* (catabolite control protein) produced mixed acid profile on glucose (Al-Bayati *et al.*, 2017). In this study, D39 and Δ*gdhA* strains produced mainly lactate at 40°C, which was significantly more than the production at 37°C, suggesting that a metabolic reprogramming occurs at elevated temperature. On the other hand, the loss of *gdhA* resulted in increased production of formate (the highest was observed at 40°C), which was also observed in Δ*ccpA* (Al-Bayati *et al.*, 2017). *In silico* analysis showed that the *cre* consensus sequence, where CcpA binds, is in the promoter region of *gdhA*. Hence, I conclude that CcpA regulates *gdhA* in a temperature-dependent manner.

In this study, I investigated the virulence of D39 and Δ*gdhA* strains at different temperatures in *Galleria mellonella*. The results showed that the loss of *gdhA* decreases the virulence at least 40% after 24 hr post-infection with $1x10^6$ CFU/larvae at 40°C relative to 37°C, indicating that *gdhA* is required for virulence of pneumococcus at high temperature. Moreover, the virulence of wild type D39 attenuated 20% at the same dose and temperature. Previous studies demonstrated that LD_{50} of D39 was $1.1x10^6$ CFU/larvae at 37°C (Evans and Rozen, 2012), which is ten times more virulent than LD_{50} of D39 in my study ($1.01 x10^5$). One possible reason for this difference in the same strains may be the growth medium, which was TY in Evans and Rozen (2012) study, while it was BHI supplemented with serum (20%) in my study. Another possibility is that there may be differences in the lineages of *G. mellonella* used in these studies, which can affect the susceptibility to pneumococcal infections.

G. mellonella is an outstanding infection model to evaluate the virulence of microbial species, as they are inexpensive to buy and provides rapid results. However, this model has also limitations. The genome of this insect has not been fully sequenced, therefore, accessible microarrays or RNA library is limited (Tsai *et al.*, 2016). In addition, researchers cannot purchase desired genotype due to absence of stock centers for *G. mellonella*. The larvae are purchased from independent breeders where genotypes,

breeding conditions, or maintenance of the animals shows differences. These variations influence their susceptibility to infections, which may affect the mortality rates after injection of pathogens (Tsai *et al.*, 2016).

G. mellonella larvae can survive between 25°C and 37°C. It was also mentioned that larvae can tolerate up to 42°C (Barnoy *et al.*, 2017). A previous study showed that pre-exposure of larvae to heat induces their immune system and survival. Exposure of larvae to 4°C or 37°C led to increased production of haemocytes and antimicrobial peptides such as gallerimycin and transferrin compared to incubation at 30°C. This mild-heat shock increased the resistance to infection by *Candida albicans* (Mowlds and Kavanagh, 2008). It can be concluded that temperature has strong effect on larval immune system, therefore, variations in experimental temperatures should be minimal to ensure the consistency of results. In my study, I tested 34°C, 37°C, or 40°C to reduce the impact of temperature on larval immune system, which allowed me to investigate the temperature-pathogen interaction only.

Final remarks

In this study, it was shown that temperature has a crucial impact on pneumococcal transcriptome and phenotype. Through transcriptional analysis, it was determined that 6% and 5% of genes were differentially expressed at 34ºC and 40ºC, respectively, at mid-exponential growth phase relative to 37ºC. Moreover, there were overlapping genes that were expressed at both temperatures. This suggested that overlapped genes are likely involved in thermal adaptation of *S. pneumoniae*. It was shown in this study that pneumococcal phenotype is influenced by the growth medium because the pneumococcus did not show any phenotype when it was grown in a complex medium at different temperatures, but the phenotype changed in CDM. The mutant analysis showed that selected genes involve in specific phenotypes in a temperature-dependent manner. It was also observed that higher temperature (40ºC) attenuated the fitness of wild type and its isogenic mutants more severely compared to lower temperature (34ºC).

In this study, it was found that GdhA is a thermostable enzyme and may play an important role on high temperature adaptation of *S. pneumoniae*. It was also shown that loss of *gdhA* leads to significant attenuation in pneumococcal virulence at 40ºC in *G. mellonella* model.

Future plan

The adaptation to fluctuating environmental temperatures is one of the crucial responses for bacterial fitness. When bacteria enter into mammalian host, they employ a wide range of adaptive mechanisms to acquire a phenotype that allows efficient survival at different temperatures by inducing changes in their metabolic, proteomic and transcriptomic profiles. In this study, I characterized seven pneumococcal genes that were expressed differentially at different temperatures. GdhA was one of the proteins required for high temperature survival of *S. pneumoniae*. *In vitro* studies showed that GdhA is enzymatically active at high temperature (40°C) and loss of this gene resulted in attenuated pneumococcal fitness in various experimental platforms at 40°C. Moreover, GdhA is required for pneumococcal virulence at high temperature *in vivo*. Therefore, I hypothesise that GdhA is a thermostable protein. Hence, in the future, protein engineering strategies, biochemical, and structural characterization of this enzyme can be done to analyse the thermostability of pneumococcal GdhA. To start analysis, GdhA, consisting of 448 amino acid, can be cloned into an expression vector in *E. coli* for overexpression and purification. The recombinant GdhA can be exposed to different temperatures, and the activity of enzyme will be tested. Half-life of the enzyme and kinetic properties will be measured at a range of temperature between 37°C to 42°C using NADP as a cofactor because *S. pneumoniae* D39 GdhA is a NADP-dependent (Kanehisa *et al.*, 2016). In addition, the K_m of the enzyme for ammonia can also be identified which may show that the enzyme is active in the deamination, indicating the glutamate catabolic direction, but not glutamate biosynthesis in a temperature-dependent manner.

It has been shown that glutamate dehydrogenase derivatives can be multifunctional. In *B. subtilis*, the glutamate dehydrogenase RocG, which involves in glutamate synthesis, was found to have a role in antibiotic resistance such as cefuroxime and fosfomycin resistance (Lee *et al.*, 2012). In another study with *C. difficile* reported that glutamate dehydrogenase plays a role in amino acid metabolism, which promotes bacterial colonisation in hamster model (Girinathan *et al.*, 2016). The same authors also showed that glutamate dehydrogenase is functional on resistance of *C. difficile* to H_2O_2 (Girinathan *et al.*, 2014). Therefore, I hypothesized that GdhA might have additional roles in *S. pneumoniae* D39.

To study this, transcriptional profile of *gdhA*-null mutant and wild type strain can be tested at different temperatures by RNAseq analysis.

Previously, it was shown that transcriptional regulators GlnR (MerR[2] in D39, SPD_0447) and CodY (SPD_1412) independently repress *gdhA* and control its transcription (Kloosterman *et al.*, 2006). In addition, CcpA regulates RocG (homologue of glutamate dehydrogenase) in *B. subtilis* (Belitsky *et al.*, 2004). CcpA controls CCR (carbon catabolite repression) that represses the expression of genes that are specific to utilise non-preferred sugars until the cell has consumed the preferred sugar (Deutscher, 2008). Belitsky et al. (2004) identified a putative CcpA binding site (*cre*) in *B. subtilis* (Belitsky *et al.*, 2004). The *cre* consensus sequence is TGWAARCGYTWNCW (where N is any base, W is A or T, R is A or G, Y is C or T) (Stulke and Hillen, 2000). *In silico* analysis showed that *gdhA* contains two-*cre* like sequences, AGAAAAACGTTCGT and TGAAAAAAAATTCT located on upstream of starting codons, suggesting CcpA might control *gdhA* by binding to the *cre* site. Hence, it might be interesting to determine the interaction of CcpA and GdhA in *S. pneumoniae* using EMSA assay. It is also worthy to investigate which *cre*-like sequences in GdhA are functional using truncation studies followed by *lacZ* reporter assays in the wild type and mutant backgrounds (strain mutated in *cre* site).

Although, the regulatory role of GlnR, CodY, and potentially CcpA (as shown in *B. subtilis*) on *gdhA* have been studied, it is still unknown whether these regulators mediate the expression of *gdhA* at different temperatures. This can be done by *lacZ* reporter assay. To do this, *glnR, codY,* and *ccpA* mutants can be constructed by SOEing PCR. Then, the promoter of *gdhA* can be fused to a *lacZ* gene (P*gdhA-lacZ*). The reporter construct can be transformed into the wild type and Δ*glnR,* Δ*codY,* and Δ*ccpA*. The β-galactosidase activity can be tested for the new reporter strains grown at 34°C, 37°C, or 40°C.

Appendix A

STable1. Microarray analysis of gene expression in wild type D39 grown at 34°C and 40°C relative to 37°C. Fold changes are approximately ≥2 or ≤−2. All *p* values are < 0.001.

Tags	Name	Fold (34/37)	Fold (40/37)	Product
SPD_0014	*comX1*	9.68	-5.94	transcriptional regulator ComX1
SPD_0017		-4.06	4.48	hypothetical protein
SPD_0023		14.6	-12.26	hypothetical protein
SPD_0024	*purA*	1.97	1.97	adenylosuccinate synthetase
SPD_0035		3	-1.93	hypothetical protein
SPD_0036		2.32	-2.18	hypothetical protein
SPD_0037			-1.91	hypothetical protein
SPD_0046	*blpU*	9.33	-7.89	bacteriocin BlpU
SPD_0047		9.35	-7.69	hypothetical protein
SPD_0049	*comA*	14.81	-9.74	competence factor transporting ATP-binding protein/permease ComA
SPD_0050	*comB*	7.92	-5.97	competence factor transport protein ComB
SPD_0051	*purC*	4.73	-4.41	phosphoribosylaminoimidazole-succinocarboxamide synthase
SPD_0052		2.58	-1.95	phosphoribosylformylglycinamidine synthase
SPD_0053	*purF*	3.05	-2.36	amidophosphoribosyltransferase
SPD_0054	*purM*	3.42	-2.26	phosphoribosylaminoimidazole synthetase
SPD_0055	*purN*	3.22	-2.5	phosphoribosylglycinamide formyltransferase
SPD_0056		4.45	-3.42	vanZ protein
SPD_0057	*purH*	2.51		bifunctional phosphoribosylaminoimidazolecarboxamide formyltransferase/IMP cyclohydrolase
SPD_0058	*purD*	2.99	-3.85	phosphoribosylamine--glycine ligase
SPD_0059	*purE*	1.92		phosphoribosylaminoimidazole carboxylase catalytic subunit
SPD_0060	*purK*	2.79	-2.89	phosphoribosylaminoimidazole carboxylase ATPase subunit
SPD_0091		2.44		hypothetical protein
SPD_0093		-2.07		hypothetical protein
SPD_0094		-3.02		hypothetical protein
SPD_0095		-2.92		hypothetical protein
SPD_0096		-2.54		hypothetical protein
SPD_0113		-4.01	23.88	hypothetical protein
SPD_0114		-3.58	19.9	hypothetical protein
SPD_0115		-3.46	21.52	hypothetical protein
SPD_0116		-2.9	32.51	hypothetical protein

SPD_0117		-2.05	10.65	hypothetical protein
SPD_0118		-2.38	6.8	hypothetical protein
SPD_0119			4.41	hypothetical protein
SPD_0120			4.28	hypothetical protein
SPD_0121		-2.44	23.86	hypothetical protein
SPD_0122			4.39	hypothetical protein
SPD_0123			3.59	hypothetical protein
SPD_0124			4.1	hypothetical protein
SPD_0132		6.23	-5.8	hypothetical protein
SPD_0133		52.94	-31.81	hypothetical protein
SPD_0277	*celA*	1.93		6-phospho-beta-glucosidase
SPD_0279	*celB*	2.67	-2.22	PTS system cellobiose transporter subunit IIB
SPD_0334	*aliA*	-1.93		oligopeptide ABC transporter oligopeptide-binding protein AliA
SPD_0381	*acpP*	-1.9		acyl carrier protein
SPD_0391		9.83		hypothetical protein
SPD_0392		8.48	-7.83	hypothetical protein
SPD_0447	*merR*^{2}	-3.66	2.96	transcriptional regulator, MerR family protein
SPD_0448	*glnA*	-4.66	4.12	glutamine synthetase, type I
SPD_0449		-2.23		hypothetical protein
SPD_0451		2.15	-2.47	type I restriction-modification system subunit S
SPD_0452		-2.35		integrase/recombinase, phage integrase family protein
SPD_0453	*hsdS*	-2.37	2.14	type I restriction-modification system subunit S
SPD_0466		7.01	-6.49	hypothetical protein
SPD_0467	*blpS*	3.21	-2.84	BlpS protein
SPD_0468	*blpR*	2.49	-2.41	response regulator BlpR
SPD_0470	*blpC*	3.38	-2.02	peptide pheromone BlpC
SPD_0471	*blpB*	6.85	-4.88	pseudogene
SPD_0472	*blpA*	7.53	-5.72	pseudogene
SPD_0473	*blpY*	16.54	-9.59	immunity protein BlpY
SPD_0474		10.44	-7.41	hypothetical protein
SPD_0475		10.18	-6.43	CAAX amino terminal protease family protein
SPD_0546	*brnQ*	3.52		branched-chain amino acid transport system II carrier protein
SPD_0701	*ciaR*	2.06	-2.59	DNA-binding response regulator CiaR
SPD_0702	*ciaH*	1.96	-2.24	sensor histidine kinase CiaH
SPD_0723	*rpiA*		-1.99	ribose-5-phosphate isomerase A
SPD_0724	*deoB*		-1.9	phosphopentomutase
SPD_0735			-1.9	methyltransferase small subunit
SPD_0756			2.6	tRNA-Gln
SPD_0769	*ssrA*		2.12	transfer-messenger RNA
SPD_0771	*lacR1*	2.02	-3.04	lactose phosphotransferase system repressor

SPD_0772		1.91	-3.01	1-phosphofructokinase
SPD_0773		2.12	-2.46	PTS system fructose specific transporter subunit IIABC
SPD_0775		2.35		hypothetical protein
SPD_0803		2.05		hypothetical protein
SPD_0811	*speE*		-2.27	spermidine synthase
SPD_0845		3.66	-3.62	ABC transporter ATP-binding protein
SPD_0846		2.04		hypothetical protein
SPD_0898			1.93	hypothetical protein
SPD_0913		3.21	-2.75	hypothetical protein
SPD_0975	*radC*	2.26		DNA repair protein RadC
SPD_1098		-3.44	2.79	amino acid ABC transporter amino acid-binding protein/permease
SPD_1099		-2.9	2.68	amino acid ABC transporter ATP-binding protein
SPD_1122		8.13	-6.99	DNA processing protein DprA
SPD_1131	*carB*	1.9		carbamoyl phosphate synthase large subunit
SPD_1158	*gdhA*	-2.21	2.11	glutamate dehydrogenase
SPD_1167		1.97		ABC transporter ATP-binding protein
SPD_1172	*nanE-2*	2.12		N-acetylmannosamine-6-phosphate 2-epimerase
SPD_1175			2.48	hypothetical protein
SPD_1176			2.16	ABC transporter ATP-binding protein
SPD_1177			2.19	drug efflux ABC transporter ATP-binding protein/permease
SPD_1179			1.97	hypothetical protein
SPD_1286		1.99		TrmH family RNA methyltransferase group 3
SPD_1296		1.93		glutamine amidotransferase subunit PdxT
SPD_1310			-1.95	hypothetical protein
SPD_1340	*atpB*		1.96	F0F1 ATP synthase subunit A
SPD_1380		1.98		hypothetical protein
SPD_1381	*def-2*	2.35		peptide deformylase
SPD_1382		2.02		glutathione S-transferase
SPD_1408		2.23	-1.93	hypothetical protein
SPD_1409			-2.25	sugar ABC transporter ATP-binding protein
SPD_1412	*codY*	2.1		transcriptional repressor CodY
SPD_1463		-1.98		ABC transporter substrate-binding protein
SPD_1464	*tpx*		1.93	thiol peroxidase
SPD_1497	*nanE-1*	2.38		N-acetylmannosamine-6-phosphate 2-epimerase
SPD_1514			2.74	ABC transporter ATP-binding protein
SPD_1515			2.86	hypothetical protein
SPD_1516			2.99	hypothetical protein
SPD_1517			3.39	hypothetical protein
SPD_1524		-2.56		GntR family transcriptional regulator protein
SPD_1527		2.9	-2.29	hypothetical protein

SPD_1528		2.06	-2.02	ABC transporter ATP-binding protein
SPD_1593		2.9	-2.24	type IV prepilin peptidase
SPD_1628	*xpt*	2.04	-2.77	xanthine phosphoribosyltransferase
SPD_1645		-2.22		transcriptional regulator, MarR family protein
SPD_1650		2.61		iron-compound ABC transporter permease
SPD_1651		3.83	-1.96	iron-compound ABC transporter ATP-binding protein
SPD_1652		4.01		iron-compound ABC transporter iron-compound-binding protein
SPD_1682		-3.49		tRNA-Ser
SPD_1683			2.41	tRNA-Ile
SPD_1685			2.63	tRNA-Phe
SPD_1690		-2.01	2.15	tRNA-Pro
SPD_1691		-2.22	2.21	tRNA-Arg
SPD_1694		-2.83	2.57	tRNA-Thr
SPD_1695		-2.04	2.79	tRNA-Leu
SPD_1696		-2.42	2.62	tRNA-Lys
SPD_1697		-2.58	3.41	tRNA-Asp
SPD_1698		-2.58	2.77	tRNA-Val
SPD_1711		59.25	-36.58	single-stranded DNA-binding protein
SPD_1729		2.15		hypothetical protein
SPD_1738	*dinF*	2.14		MATE efflux family protein DinF
SPD_1739	*recA*		-1.97	recombinase A
SPD_1740	*cinA*	5.84	-5.37	competence damage-inducible protein A
SPD_1744		3.1	-3.22	hypothetical protein
SPD_1826	*nadC*	2.52		nicotinate-nucleotide pyrophosphorylase
SPD_1828		2.83	-2.94	hypothetical protein
SPD_1830		1.97		glycosyl hydrolase family protein
SPD_1831		2.21		PTS system transporter subunit IIC
SPD_1834		10.54	-8.83	bifunctional acetaldehyde-CoA/alcohol dehydrogenase
SPD_1855		3.71	-2.42	hypothetical protein
SPD_1856		6.18	-5.38	hypothetical protein
SPD_1857		7.65	-5.64	hypothetical protein
SPD_1858		20.86	-13.85	hypothetical protein
SPD_1859		16.21	-9.63	hypothetical protein
SPD_1860	*clgD*	20.13	-16.37	competence protein CglD
SPD_1861	*cglC*	22.59	-20.39	competence protein CglC
SPD_1862	*cglB*	37.39	-19.58	competence protein CglB
SPD_1863	*cglA*	29.51	-19.6	competence protein CglA
SPD_1882			2.42	tRNA-Trp
SPD_1956	*ilvD*	-1.98		dihydroxy-acid dehydratase
SPD_1984		3.14	-1.92	hypersensitive-induced reaction protein 4
SPD_2006		2.52		hypothetical protein
SPD_2017	*cbpA*		1.93	choline binding protein A
SPD_2028	*cbpD*	4.19		choline binding protein D
SPD_2033	*yfiA*	3.55	-2.24	ribosomal subunit interface protein

SPD_2034		3.31	-2.51	competence protein ComF
SPD_2035		2.82		helicase
SPD_2063	*comE*	39.75	-25.36	response regulator
SPD_2064	*comD*	53.65	-44.92	sensor histidine kinase ComD
SPD_2065	*comC1*	35.18	-23.95	competence-stimulating peptide type 1
SPD_2068		6.38	-3.73	serine protease
SPD_2069		4.4	-3.5	SpoJ protein

Bibliography

Al-Bayati, F. A., Kahya, H. F., Damianou, A., Shafeeq, S., Kuipers, O. P., Andrew, P. W., and Yesilkaya, H. (2017). Pneumococcal galactose catabolism is controlled by multiple regulators acting on pyruvate formate lyase. *Sci Rep, 7*, 43587. doi:10.1038/srep43587

Alloing, G., Trombe, M. C., and Claverys, J. P. (1990). The ami locus of the gram-positive bacterium *Streptococcus pneumoniae* is similar to binding protein-dependent transport operons of gram-negative bacteria. *Mol Microbiol, 4*(4), 633-644. doi:10.1111/j.1365-2958.1990.tb00632.x

Amon, J., Titgemeyer, F., and Burkovski, A. (2010). Common patterns - unique features: nitrogen metabolism and regulation in Gram-positive bacteria. *FEMS Microbiol Rev, 34*(4), 588-605. doi:10.1111/j.1574-6976.2010.00216.x

Andisi, V. F., Hinojosa, C. A., de Jong, A., Kuipers, O. P., Orihuela, C. J., and Bijlsma, J. J. (2012). Pneumococcal gene complex involved in resistance to extracellular oxidative stress. *Infect Immun, 80*(3), 1037-1049. doi:10.1128/IAI.05563-11

Andre, G. O., Converso, T. R., Politano, W. R., Ferraz, L. F., Ribeiro, M. L., Leite, L. C., and Darrieux, M. (2017). Role of *Streptococcus pneumoniae* Proteins in Evasion of Complement-Mediated Immunity. *Front Microbiol, 8*, 224. doi:10.3389/fmicb.2017.00224

Arbique, J. C., Poyart, C., Trieu-Cuot, P., Quesne, G., Carvalho Mda, G., Steigerwalt, A. G., Morey, R. E., Jackson, D., Davidson, R. J., and Facklam, R. R. (2004). Accuracy of phenotypic and genotypic testing for identification of *Streptococcus pneumoniae* and description of *Streptococcus pseudopneumoniae* sp. nov. *J Clin Microbiol, 42*(10), 4686-4696. doi:10.1128/JCM.42.10.4686-4696.2004

Attaiech, L., Olivier, A., Mortier-Barriere, I., Soulet, A. L., Granadel, C., Martin, B., Polard, P., and Claverys, J. P. (2011). Role of the single-stranded DNA-binding protein SsbB in pneumococcal transformation: maintenance of a reservoir for genetic plasticity. *PLoS Genet, 7*(6), e1002156. doi:10.1371/journal.pgen.1002156

Auzat, I., Chapuy-Regaud, S., Le Bras, G., Dos Santos, D., Ogunniyi, A. D., Le Thomas, I., Garel, J. R., Paton, J. C., and Trombe, M. C. (1999). The NADH oxidase of *Streptococcus pneumoniae*: its involvement in competence and virulence. *Mol Microbiol, 34*(5), 1018-1028. doi:10.1046/j.1365-2958.1999.01663.x

Ayala, J. C., Silva, A. J., and Benitez, J. A. (2017). H-NS: an overarching regulator of the *Vibrio cholerae* life cycle. *Res Microbiol, 168*(1), 16-25. doi:10.1016/j.resmic.2016.07.007

Backhaus, E., Berg, S., Andersson, R., Ockborn, G., Malmstrom, P., Dahl, M., Nasic, S., and Trollfors, B. (2016). Epidemiology of invasive pneumococcal infections: manifestations, incidence and case fatality rate correlated to age, gender and risk factors. *BMC Infect Dis, 16*, 367. doi:10.1186/s12879-016-1648-2

Balachandran, P., Brooks-Walter, A., Virolainen-Julkunen, A., Hollingshead, S. K., and Briles, D. E. (2002). Role of pneumococcal surface protein C in nasopharyngeal carriage and pneumonia and its ability to elicit protection against carriage of *Streptococcus pneumoniae*. *Infect Immun, 70*(5), 2526-2534. doi:10.1128/iai.70.5.2526-2534.2002

Barnoy, S., Gancz, H., Zhu, Y., Honnold, C. L., Zurawski, D. V., and Venkatesan, M. M. (2017). The Galleria mellonella larvae as an in vivo model for evaluation of Shigella virulence. *Gut Microbes, 8*(4), 335-350. doi:10.1080/19490976.2017.1293225

Bartilson, M., Marra, A., Christine, J., Asundi, J. S., Schneider, W. P., and Hromockyj, A. E. (2001). Differential fluorescence induction reveals *Streptococcus pneumoniae* loci regulated by competence stimulatory peptide. *Mol Microbiol, 39*(1), 126-135. doi:10.1046/j.1365-2958.2001.02218.x

Basak, S., and Jiang, R. (2012). Enhancing *E. coli* tolerance towards oxidative stress via engineering its global regulator cAMP receptor protein (CRP). *PLoS One, 7*(12), e51179. doi:10.1371/journal.pone.0051179

Beaufay, F., Coppine, J., Mayard, A., Laloux, G., De Bolle, X., and Hallez, R. (2015). A NAD-dependent glutamate dehydrogenase coordinates metabolism with cell division in *Caulobacter crescentus*. *EMBO J, 34*(13), 1786-1800. doi:10.15252/embj.201490730

Belitsky, B. R., Kim, H. J., and Sonenshein, A. L. (2004). CcpA-dependent regulation of *Bacillus subtilis* glutamate dehydrogenase gene expression. *J Bacteriol, 186*(11), 3392-3398. doi:10.1128/JB.186.11.3392-3398.2004

Ben Belgacem, Z., Rehaiem, A., Fajardo Bernardez, P., Manai, M., and Pastrana Castro, L. (2012). Interactive effects of pH and temperature on the bacteriocin stability by response surface analysis. *Mikrobiologiia, 81*(2), 214-219.

Bentley, S. D., Aanensen, D. M., Mavroidi, A., Saunders, D., Rabbinowitsch, E., Collins, M., Donohoe, K., Harris, D., Murphy, L., Quail, M. A., Samuel, G., Skovsted, I. C., Kaltoft, M. S., Barrell, B., Reeves, P. R., Parkhill, J., and Spratt, B. G. (2006). Genetic analysis of the capsular biosynthetic locus from all 90 pneumococcal serotypes. *PLoS Genet, 2*(3), e31. doi:10.1371/journal.pgen.0020031

Berry, A. M., Ogunniyi, A. D., Miller, D. C., and Paton, J. C. (1999). Comparative virulence of *Streptococcus pneumoniae* strains with insertion-duplication, point, and deletion mutations in the pneumolysin gene. *Infect Immun, 67*(2), 981-985.

Bhuiya, M. W., Sakuraba, H., and Ohshima, T. (2002). Temperature dependence of kinetic parameters for hyperthermophilic glutamate dehydrogenase from *Aeropyrum pernix* K1. *Biosci Biotechnol Biochem, 66*(4), 873-876. doi:10.1271/bbb.66.873

Bidossi, A., Mulas, L., Decorosi, F., Colomba, L., Ricci, S., Pozzi, G., Deutscher, J., Viti, C., and Oggioni, M. R. (2012). A functional genomics approach to establish the complement of carbohydrate transporters in *Streptococcus pneumoniae*. *PLoS One, 7*(3), e33320. doi:10.1371/journal.pone.0033320

Biswas-Fiss, E. E., Kukiratirat, J., and Biswas, S. B. (2012). Thermodynamic analysis of DNA binding by a Bacillus single stranded DNA binding protein. *BMC Biochem, 13*, 10. doi:10.1186/1471-2091-13-10

Blanchette-Cain, K., Hinojosa, C. A., Akula Suresh Babu, R., Lizcano, A., Gonzalez-Juarbe, N., Munoz-Almagro, C., Sanchez, C. J., Bergman, M. A., and Orihuela, C. J. (2013). *Streptococcus pneumoniae* biofilm formation is strain dependent, multifactorial, and associated with reduced invasiveness and immunoreactivity during colonization. *MBio, 4*(5), e00745-00713. doi:10.1128/mBio.00745-13

Blanchette, K. A., Shenoy, A. T., Milner, J., 2nd, Gilley, R. P., McClure, E., Hinojosa, C. A., Kumar, N., Daugherty, S. C., Tallon, L. J., Ott, S., King, S. J., Ferreira, D. M., Gordon, S. B., Tettelin, H., and Orihuela, C. J. (2016). Neuraminidase A-Exposed Galactose Promotes *Streptococcus pneumoniae* Biofilm Formation during Colonization. *Infect Immun, 84*(10), 2922-2932. doi:10.1128/IAI.00277-16

Bogaert, D., De Groot, R., and Hermans, P. W. (2004). *Streptococcus pneumoniae* colonisation: the key to pneumococcal disease. *Lancet Infect Dis, 4*(3), 144-154. doi:10.1016/S1473-3099(04)00938-7

Bogaert, D., Weinberger, D., Thompson, C., Lipsitch, M., and Malley, R. (2009). Impaired innate and adaptive immunity to *Streptococcus pneumoniae* and its effect on colonization in an infant mouse model. *Infect Immun, 77*(4), 1613-1622. doi:10.1128/IAI.00871-08

Bradford, M. M. (1976). A rapid and sensitive method for the quantitation of microgram quantities of protein utilizing the principle of protein-dye binding. *Anal Biochem, 72*, 248-254. doi:10.1006/abio.1976.9999

Bricker, A. L., and Camilli, A. (1999). Transformation of a type 4 encapsulated strain of *Streptococcus pneumoniae*. *FEMS Microbiol Lett, 172*(2), 131-135. doi:10.1111/j.1574-6968.1999.tb13460.x

Brooks, L. R. K., and Mias, G. I. (2018). *Streptococcus pneumoniae*'s Virulence and Host Immunity: Aging, Diagnostics, and Prevention. *Front Immunol, 9*, 1366. doi:10.3389/fimmu.2018.01366

Brown, J. S., Gilliland, S. M., Ruiz-Albert, J., and Holden, D. W. (2002). Characterization of pit, a *Streptococcus pneumoniae* iron uptake ABC transporter. *Infect Immun, 70*(8), 4389-4398. doi:10.1128/iai.70.8.4389-4398.2002

Brown, N. L., Stoyanov, J. V., Kidd, S. P., and Hobman, J. L. (2003). The MerR family of transcriptional regulators. *FEMS Microbiol Rev, 27*(2-3), 145-163. doi:10.1016/S0168-6445(03)00051-2

Brueggemann, A. B., Griffiths, D. T., Meats, E., Peto, T., Crook, D. W., and Spratt, B. G. (2003). Clonal relationships between invasive and carriage *Streptococcus pneumoniae* and serotype- and clone-specific differences in invasive disease potential. *J Infect Dis, 187*(9), 1424-1432. doi:10.1086/374624

Brunworth, J. D., Garg, R., Mahboubi, H., Johnson, B., and Djalilian, H. R. (2012). Detecting nasopharyngeal reflux: a novel pH probe technique. *Ann Otol Rhinol Laryngol, 121*(7), 427-430. doi:10.1177/000348941212100701

Bryant, K. A., Block, S. L., Baker, S. A., Gruber, W. C., Scott, D. A., and Group, P. C. V. I. S. (2010). Safety and immunogenicity of a 13-valent pneumococcal conjugate vaccine. *Pediatrics, 125*(5), 866-875. doi:10.1542/peds.2009-1405

Burghout, P., Cron, L. E., Gradstedt, H., Quintero, B., Simonetti, E., Bijlsma, J. J., Bootsma, H. J., and Hermans, P. W. (2010). Carbonic anhydrase is essential for *Streptococcus pneumoniae* growth in environmental ambient air. *J Bacteriol, 192*(15), 4054-4062. doi:10.1128/JB.00151-10

Burnaugh, A. M., Frantz, L. J., and King, S. J. (2008). Growth of *Streptococcus pneumoniae* on human glycoconjugates is dependent upon the sequential activity of bacterial exoglycosidases. *J Bacteriol, 190*(1), 221-230. doi:10.1128/JB.01251-07

Carvalho, S. M., Kloosterman, T. G., Manzoor, I., Caldas, J., Vinga, S., Martinussen, J., Saraiva, L. M., Kuipers, O. P., and Neves, A. R. (2018). Interplay Between Capsule Expression and Uracil Metabolism in *Streptococcus pneumoniae* D39. *Front Microbiol, 9*, 321. doi:10.3389/fmicb.2018.00321

Champion, O. L., Wagley, S., and Titball, R. W. (2016). *Galleria mellonella* as a model host for microbiological and toxin research. *Virulence, 7*(7), 840-845. doi:10.1080/21505594.2016.1203486

Chao, Y., Marks, L. R., Pettigrew, M. M., and Hakansson, A. P. (2014). *Streptococcus pneumoniae* biofilm formation and dispersion during colonization and disease. *Front Cell Infect Microbiol, 4*, 194. doi:10.3389/fcimb.2014.00194

Charpentier, E., Novak, R., and Tuomanen, E. (2000). Regulation of growth inhibition at high temperature, autolysis, transformation and adherence in *Streptococcus pneumoniae* by clpC. *Mol Microbiol, 37*(4), 717-726. doi:10.1046/j.1365-2958.2000.02011.x

Chastanet, A., Prudhomme, M., Claverys, J. P., and Msadek, T. (2001). Regulation of *Streptococcus pneumoniae* clp genes and their role in competence development and stress survival. *J Bacteriol, 183*(24), 7295-7307. doi:10.1128/JB.183.24.7295-7307.2001

Chien, A. C., Hill, N. S., and Levin, P. A. (2012). Cell size control in bacteria. *Curr Biol, 22*(9), R340-349. doi:10.1016/j.cub.2012.02.032

Cho, K. H., Wang, H. S., and Kim, Y. K. (2010). Temperature-dependent hemolytic activity of membrane pore-forming peptide toxin, tolaasin. *J Pept Sci, 16*(2), 85-90. doi:10.1002/psc.1199

Choi, I. H., Shim, J. H., Kim, S. W., Kim, S. N., Pyo, S. N., and Rhee, D. K. (1999). Limited stress response in *Streptococcus pneumoniae*. *Microbiol Immunol, 43*(8), 807-812.

Choudhury, R., and Punekar, N. S. (2007). Competitive inhibition of glutamate dehydrogenase reaction. *FEBS Lett, 581*(14), 2733-2736. doi:10.1016/j.febslet.2007.05.032

Clatworthy, A. E., Pierson, E., and Hung, D. T. (2007). Targeting virulence: a new paradigm for antimicrobial therapy. *Nat Chem Biol, 3*(9), 541-548. doi:10.1038/nchembio.2007.24

Claverys, J. P., Prudhomme, M., and Martin, B. (2006). Induction of competence regulons as a general response to stress in gram-positive bacteria. *Annu Rev Microbiol, 60*, 451-475. doi:10.1146/annurev.micro.60.080805.142139

Clutterbuck, E. A., Lazarus, R., Yu, L. M., Bowman, J., Bateman, E. A., Diggle, L., Angus, B., Peto, T. E., Beverley, P. C., Mant, D., and Pollard, A. J. (2012). Pneumococcal conjugate and plain polysaccharide vaccines have divergent effects on antigen-specific B cells. *J Infect Dis, 205*(9), 1408-1416. doi:10.1093/infdis/jis212

Cockeran, R., Durandt, C., Feldman, C., Mitchell, T. J., and Anderson, R. (2002). Pneumolysin activates the synthesis and release of interleukin-8 by human neutrophils in vitro. *J Infect Dis, 186*(4), 562-565. doi:10.1086/341563

Coico, R. (2005). Gram staining. *Curr Protoc Microbiol, Appendix 3*, Appendix 3C. doi:10.1002/9780471729259.mca03cs00

Cornick, J. E., and Bentley, S. D. (2012). *Streptococcus pneumoniae*: the evolution of antimicrobial resistance to beta-lactams, fluoroquinolones and macrolides. *Microbes Infect, 14*(7-8), 573-583. doi:10.1016/j.micinf.2012.01.012

Cortes, P. R., Pinas, G. E., Cian, M. B., Yandar, N., and Echenique, J. (2015). Stress-triggered signaling affecting survival or suicide of *Streptococcus pneumoniae*. *Int J Med Microbiol, 305*(1), 157-169. doi:10.1016/j.ijmm.2014.12.002

Cotter, P. D., Ross, R. P., and Hill, C. (2013). Bacteriocins - a viable alternative to antibiotics? *Nat Rev Microbiol, 11*(2), 95-105. doi:10.1038/nrmicro2937

Crooks, G. E., Hon, G., Chandonia, J. M., and Brenner, S. E. (2004). WebLogo: a sequence logo generator. *Genome Res, 14*(6), 1188-1190. doi:10.1101/gr.849004

Cybulski, L. E., Ballering, J., Moussatova, A., Inda, M. E., Vazquez, D. B., Wassenaar, T. A., de Mendoza, D., Tieleman, D. P., and Killian, J. A. (2015). Activation of the bacterial thermosensor DesK involves a serine zipper dimerization motif that is modulated by bilayer thickness. *Proc Natl Acad Sci U S A, 112*(20), 6353-6358. doi:10.1073/pnas.1422446112

da Silva Neto, J. F., Braz, V. S., Italiani, V. C., and Marques, M. V. (2009). Fur controls iron homeostasis and oxidative stress defense in the oligotrophic alpha-proteobacterium *Caulobacter crescentus*. *Nucleic Acids Res, 37*(14), 4812-4825. doi:10.1093/nar/gkp509

Dagkessamanskaia, A., Moscoso, M., Henard, V., Guiral, S., Overweg, K., Reuter, M., Martin, B., Wells, J., and Claverys, J. P. (2004). Interconnection of competence, stress and CiaR regulons in *Streptococcus pneumoniae*: competence triggers stationary phase autolysis of ciaR mutant cells. *Mol Microbiol, 51*(4), 1071-1086. doi:10.1111/j.1365-2958.2003.03892.x

Dave, S., Brooks-Walter, A., Pangburn, M. K., and McDaniel, L. S. (2001). PspC, a pneumococcal surface protein, binds human factor H. *Infect Immun, 69*(5), 3435-3437. doi:10.1128/IAI.69.5.3435-3437.2001

Davey, L., Halperin, S. A., and Lee, S. F. (2016). Mutation of the *Streptococcus gordonii* Thiol-Disulfide Oxidoreductase SdbA Leads to Enhanced Biofilm Formation Mediated by the CiaRH Two-Component Signaling System. *PLoS One, 11*(11), e0166656. doi:10.1371/journal.pone.0166656

Davidson, A. L., Dassa, E., Orelle, C., and Chen, J. (2008). Structure, function, and evolution of bacterial ATP-binding cassette systems. *Microbiol Mol Biol Rev, 72*(2), 317-364, table of contents. doi:10.1128/MMBR.00031-07

Dawid, S., Roche, A. M., and Weiser, J. N. (2007). The blp bacteriocins of *Streptococcus pneumoniae* mediate intraspecies competition both in vitro and in vivo. *Infect Immun, 75*(1), 443-451. doi:10.1128/IAI.01775-05

De Angelis, M., Calasso, M., Di Cagno, R., Siragusa, S., Minervini, F., and Gobbetti, M. (2010). NADP-glutamate dehydrogenase activity in nonstarter lactic acid bacteria: effects of temperature, pH and NaCl on enzyme activity and expression. *J Appl Microbiol, 109*(5), 1763-1774. doi:10.1111/j.1365-2672.2010.04804.x

Desbois, A. P., and Coote, P. J. (2011). Wax moth larva (*Galleria mellonella*): an in vivo model for assessing the efficacy of antistaphylococcal agents. *J Antimicrob Chemother, 66*(8), 1785-1790. doi:10.1093/jac/dkr198

Deutscher, J. (2008). The mechanisms of carbon catabolite repression in bacteria. *Curr Opin Microbiol, 11*(2), 87-93. doi:10.1016/j.mib.2008.02.007

Diavatopoulos, D. A., Short, K. R., Price, J. T., Wilksch, J. J., Brown, L. E., Briles, D. E., Strugnell, R. A., and Wijburg, O. L. (2010). Influenza A virus facilitates *Streptococcus pneumoniae* transmission and disease. *FASEB J, 24*(6), 1789-1798. doi:10.1096/fj.09-146779

Dickey, T. H., Altschuler, S. E., and Wuttke, D. S. (2013). Single-stranded DNA-binding proteins: multiple domains for multiple functions. *Structure, 21*(7), 1074-1084. doi:10.1016/j.str.2013.05.013

Ding, L., Wang, Y., Hu, Y., Atkinson, S., Williams, P., and Chen, S. (2009). Functional characterization of FlgM in the regulation of flagellar synthesis and motility in *Yersinia pseudotuberculosis*. *Microbiology, 155*(Pt 6), 1890-1900. doi:10.1099/mic.0.026294-0

Dirmesropian, S., Wood, J. G., MacIntyre, C. R., and Newall, A. T. (2015). A review of economic evaluations of 13-valent pneumococcal conjugate vaccine (PCV13) in adults and the elderly. *Hum Vaccin Immunother, 11*(4), 818-825. doi:10.1080/21645515.2015.1011954

Domenech, M., Garcia, E., and Moscoso, M. (2012). Biofilm formation in *Streptococcus pneumoniae*. *Microb Biotechnol, 5*(4), 455-465. doi:10.1111/j.1751-7915.2011.00294.x

Donati, C., Hiller, N. L., Tettelin, H., Muzzi, A., Croucher, N. J., Angiuoli, S. V., Oggioni, M., Dunning Hotopp, J. C., Hu, F. Z., Riley, D. R., Covacci, A., Mitchell, T. J., Bentley, S. D., Kilian, M., Ehrlich, G. D., Rappuoli, R., Moxon, E. R., and Masignani, V. (2010). Structure and dynamics of the pan-genome of *Streptococcus pneumoniae* and closely related species. *Genome Biol, 11*(10), R107. doi:10.1186/gb-2010-11-10-r107

Dong, T. G., and Mekalanos, J. J. (2012). Characterization of the RpoN regulon reveals differential regulation of T6SS and new flagellar operons in *Vibrio cholerae* O37 strain V52. *Nucleic Acids Res, 40*(16), 7766-7775. doi:10.1093/nar/gks567

Dowell, S. F., Whitney, C. G., Wright, C., Rose, C. E., Jr., and Schuchat, A. (2003). Seasonal patterns of invasive pneumococcal disease. *Emerg Infect Dis, 9*(5), 573-579. doi:10.3201/eid0905.020556

Driessen, R. P., Sitters, G., Laurens, N., Moolenaar, G. F., Wuite, G. J., Goosen, N., and Dame, R. T. (2014). Effect of temperature on the intrinsic flexibility of DNA and its interaction with architectural proteins. *Biochemistry, 53*(41), 6430-6438. doi:10.1021/bi500344j

Dumas, Z., Ross-Gillespie, A., and Kummerli, R. (2013). Switching between apparently redundant iron-uptake mechanisms benefits bacteria in changeable environments. *Proc Biol Sci, 280*(1764), 20131055. doi:10.1098/rspb.2013.1055

Duong, N., Osborne, S., Bustamante, V. H., Tomljenovic, A. M., Puente, J. L., and Coombes, B. K. (2007). Thermosensing coordinates a cis-regulatory module for transcriptional activation of the intracellular virulence system in *Salmonella enterica* serovar Typhimurium. *J Biol Chem, 282*(47), 34077-34084. doi:10.1074/jbc.M707352200

Elsholz, A. K., Michalik, S., Zuhlke, D., Hecker, M., and Gerth, U. (2010). CtsR, the Gram-positive master regulator of protein quality control, feels the heat. *EMBO J, 29*(21), 3621-3629. doi:10.1038/emboj.2010.228

Engel, P. C. (2014). Glutamate dehydrogenases: the why and how of coenzyme specificity. *Neurochem Res, 39*(3), 426-432. doi:10.1007/s11064-013-1089-x

Eshwar, A. K., Guldimann, C., Oevermann, A., and Tasara, T. (2017). Cold-Shock Domain Family Proteins (Csps) Are Involved in Regulation of Virulence, Cellular Aggregation, and Flagella-Based Motility in *Listeria monocytogenes*. *Front Cell Infect Microbiol, 7*, 453. doi:10.3389/fcimb.2017.00453

Evans, B. A., and Rozen, D. E. (2012). A *Streptococcus pneumoniae* infection model in larvae of the wax moth *Galleria mellonella*. *Eur J Clin Microbiol Infect Dis, 31*(10), 2653-2660. doi:10.1007/s10096-012-1609-7

Feehily, C., and Karatzas, K. A. (2013). Role of glutamate metabolism in bacterial responses towards acid and other stresses. *J Appl Microbiol, 114*(1), 11-24. doi:10.1111/j.1365-2672.2012.05434.x

Felmingham, D., Reinert, R. R., Hirakata, Y., and Rodloff, A. (2002). Increasing prevalence of antimicrobial resistance among isolates of *Streptococcus pneumoniae* from the PROTEKT surveillance study, and compatative in vitro activity of the ketolide, telithromycin. *J Antimicrob Chemother, 50 Suppl S1*, 25-37. doi:10.1093/jac/dkf808

Feoktistova, M., Geserick, P., and Leverkus, M. (2016). Crystal Violet Assay for Determining Viability of Cultured Cells. *Cold Spring Harb Protoc, 2016*(4), pdb prot087379. doi:10.1101/pdb.prot087379

Ferguson, B. S., Nam, H., Hopkins, R. G., and Morrison, R. F. (2010). Impact of reference gene selection for target gene normalization on experimental outcome using real-time qRT-PCR in adipocytes. *PLoS One, 5*(12), e15208. doi:10.1371/journal.pone.0015208

Frees, D., Chastanet, A., Qazi, S., Sorensen, K., Hill, P., Msadek, T., and Ingmer, H. (2004). Clp ATPases are required for stress tolerance, intracellular replication and biofilm formation in *Staphylococcus aureus*. *Mol Microbiol, 54*(5), 1445-1462. doi:10.1111/j.1365-2958.2004.04368.x

Gadgil, M., Kapur, V., and Hu, W. S. (2005). Transcriptional response of *Escherichia coli* to temperature shift. *Biotechnol Prog, 21*(3), 689-699. doi:10.1021/bp049630l

Gao, H., Zhang, Y., Han, Y., Yang, L., Liu, X., Guo, Z., Tan, Y., Huang, X., Zhou, D., and Yang, R. (2011). Phenotypic and transcriptional analysis of the osmotic regulator OmpR in *Yersinia pestis*. *BMC Microbiol, 11*, 39. doi:10.1186/1471-2180-11-39

Geno, K. A., Gilbert, G. L., Song, J. Y., Skovsted, I. C., Klugman, K. P., Jones, C., Konradsen, H. B., and Nahm, M. H. (2015). Pneumococcal Capsules and Their Types: Past, Present, and Future. *Clin Microbiol Rev, 28*(3), 871-899. doi:10.1128/CMR.00024-15

Girinathan, B. P., Braun, S., Sirigireddy, A. R., Espinola-Lopez, J., and Govind, R. (2016). Correction: Importance of Glutamate Dehydrogenase (GDH) in *Clostridium difficile* Colonization In Vivo. *PLoS One, 11*(10), e0165579. doi:10.1371/journal.pone.0165579

Girinathan, B. P., Braun, S. E., and Govind, R. (2014). *Clostridium difficile* glutamate dehydrogenase is a secreted enzyme that confers resistance to H2O2. *Microbiology, 160*(Pt 1), 47-55. doi:10.1099/mic.0.071365-0

Gorke, B., and Stulke, J. (2008). Carbon catabolite repression in bacteria: many ways to make the most out of nutrients. *Nat Rev Microbiol, 6*(8), 613-624. doi:10.1038/nrmicro1932

Graumann, P., Wendrich, T. M., Weber, M. H., Schroder, K., and Marahiel, M. A. (1997). A family of cold shock proteins in *Bacillus subtilis* is essential for cellular growth and for efficient protein synthesis at optimal and low temperatures. *Mol Microbiol, 25*(4), 741-756. doi:10.1046/j.1365-2958.1997.5121878.x

Groot Kormelink, T., Koenders, E., Hagemeijer, Y., Overmars, L., Siezen, R. J., de Vos, W. M., and Francke, C. (2012). Comparative genome analysis of central nitrogen metabolism and its control by GlnR in the class Bacilli. *BMC Genomics, 13*, 191. doi:10.1186/1471-2164-13-191

Grove, D. E., Willcox, S., Griffith, J. D., and Bryant, F. R. (2005). Differential single-stranded DNA binding properties of the paralogous SsbA and SsbB proteins from *Streptococcus pneumoniae*. *J Biol Chem, 280*(12), 11067-11073. doi:10.1074/jbc.M414057200

Gualdi, L., Hayre, J. K., Gerlini, A., Bidossi, A., Colomba, L., Trappetti, C., Pozzi, G., Docquier, J. D., Andrew, P., Ricci, S., and Oggioni, M. R. (2012). Regulation of neuraminidase expression in *Streptococcus pneumoniae*. *BMC Microbiol, 12*, 200. doi:10.1186/1471-2180-12-200

Guiral, S., Henard, V., Laaberki, M. H., Granadel, C., Prudhomme, M., Martin, B., and Claverys, J. P. (2006). Construction and evaluation of a chromosomal expression platform (CEP) for ectopic, maltose-driven gene expression in *Streptococcus pneumoniae*. *Microbiology, 152*(Pt 2), 343-349. doi:10.1099/mic.0.28433-0

Guiral, S., Mitchell, T. J., Martin, B., and Claverys, J. P. (2005). Competence-programmed predation of noncompetent cells in the human pathogen *Streptococcus pneumoniae*: genetic requirements. *Proc Natl Acad Sci U S A, 102*(24), 8710-8715. doi:10.1073/pnas.0500879102

Gunka, K., Stannek, L., Care, R. A., and Commichau, F. M. (2013). Selection-driven accumulation of suppressor mutants in *bacillus subtilis*: the apparent high mutation frequency of the cryptic gudB gene and the rapid clonal expansion of gudB(+) suppressors are due to growth under selection. *PLoS One, 8*(6), e66120. doi:10.1371/journal.pone.0066120

Halfmann, A., Hakenbeck, R., and Bruckner, R. (2007a). A new integrative reporter plasmid for *Streptococcus pneumoniae*. *FEMS Microbiol Lett, 268*(2), 217-224. doi:10.1111/j.1574-6968.2006.00584.x

Halfmann, A., Kovacs, M., Hakenbeck, R., and Bruckner, R. (2007b). Identification of the genes directly controlled by the response regulator CiaR in *Streptococcus pneumoniae:* five out of 15 promoters drive expression of small non-coding RNAs. *Mol Microbiol, 66*(1), 110-126. doi:10.1111/j.1365-2958.2007.05900.x

Hammerschmidt, S. (2006). Adherence molecules of pathogenic pneumococci. *Curr Opin Microbiol, 9*(1), 12-20. doi:10.1016/j.mib.2005.11.001

Harris, L. K., and Theriot, J. A. (2018). Surface Area to Volume Ratio: A Natural Variable for Bacterial Morphogenesis. *Trends Microbiol, 26*(10), 815-832. doi:10.1016/j.tim.2018.04.008

Harrison, C. (2003). GrpE, a nucleotide exchange factor for DnaK. *Cell Stress Chaperones, 8*(3), 218-224. doi:10.1379/1466-1268(2003)008<0218:ganeff>2.0.co;2

Hathaway, L. J., Brugger, S. D., Morand, B., Bangert, M., Rotzetter, J. U., Hauser, C., Graber, W. A., Gore, S., Kadioglu, A., and Muhlemann, K. (2012). Capsule type of *Streptococcus pneumoniae* determines growth phenotype. *PLoS Pathog, 8*(3), e1002574. doi:10.1371/journal.ppat.1002574

Hatta, M., Hatta, Y., Kim, J. H., Watanabe, S., Shinya, K., Nguyen, T., Lien, P. S., Le, Q. M., and Kawaoka, Y. (2007). Growth of H5N1 influenza A viruses in the upper respiratory tracts of mice. *PLoS Pathog, 3*(10), 1374-1379. doi:10.1371/journal.ppat.0030133

Hayrapetyan, H., Siezen, R., Abee, T., and Nierop Groot, M. (2016). Comparative Genomics of Iron-Transporting Systems in *Bacillus cereus* Strains and Impact of Iron Sources on Growth and Biofilm Formation. *Front Microbiol, 7*, 842. doi:10.3389/fmicb.2016.00842

Henderson, F. W., Gilligan, P. H., Wait, K., and Goff, D. A. (1988). Nasopharyngeal carriage of antibiotic-resistant pneumococci by children in group day care. *J Infect Dis, 157*(2), 256-263. doi:10.1093/infdis/157.2.256

Hendriksen, W. T., Bootsma, H. J., Estevao, S., Hoogenboezem, T., de Jong, A., de Groot, R., Kuipers, O. P., and Hermans, P. W. (2008). CodY of *Streptococcus pneumoniae*: link between nutritional gene regulation and colonization. *J Bacteriol, 190*(2), 590-601. doi:10.1128/JB.00917-07

Henriques-Normark, B., and Tuomanen, E. I. (2013). The pneumococcus: epidemiology, microbiology, and pathogenesis. *Cold Spring Harb Perspect Med, 3*(7). doi:10.1101/cshperspect.a010215

Hentrich, K., Lofling, J., Pathak, A., Nizet, V., Varki, A., and Henriques-Normark, B. (2016). *Streptococcus pneumoniae* Senses a Human-like Sialic Acid Profile via the Response Regulator CiaR. *Cell Host Microbe, 20*(3), 307-317. doi:10.1016/j.chom.2016.07.019

Hirst, R. A., Kadioglu, A., O'Callaghan, C., and Andrew, P. W. (2004). The role of pneumolysin in pneumococcal pneumonia and meningitis. *Clin Exp Immunol, 138*(2), 195-201. doi:10.1111/j.1365-2249.2004.02611.x

Hogberg, L., Geli, P., Ringberg, H., Melander, E., Lipsitch, M., and Ekdahl, K. (2007). Age- and serogroup-related differences in observed durations of nasopharyngeal carriage of penicillin-resistant pneumococci. *J Clin Microbiol, 45*(3), 948-952. doi:10.1128/JCM.01913-06

Holmqvist, E., and Wagner, E. G. H. (2017). Impact of bacterial sRNAs in stress responses. *Biochem Soc Trans, 45*(6), 1203-1212. doi:10.1042/BST20160363

Honsa, E. S., Johnson, M. D., and Rosch, J. W. (2013). The roles of transition metals in the physiology and pathogenesis of *Streptococcus pneumoniae*. *Front Cell Infect Microbiol, 3*, 92. doi:10.3389/fcimb.2013.00092

Horton, R. M. (1995). PCR-mediated recombination and mutagenesis. SOEing together tailor-made genes. *Mol Biotechnol, 3*(2), 93-99. doi:10.1007/BF02789105

Hurme, R., and Rhen, M. (1998). Temperature sensing in bacterial gene regulation--what it all boils down to. *Mol Microbiol, 30*(1), 1-6. doi:10.1046/j.1365-2958.1998.01049.x

Hyams, C., Camberlein, E., Cohen, J. M., Bax, K., and Brown, J. S. (2010). The *Streptococcus pneumoniae* capsule inhibits complement activity and neutrophil phagocytosis by multiple mechanisms. *Infect Immun, 78*(2), 704-715. doi:10.1128/IAI.00881-09

Iannelli, F., Pearce, B. J., and Pozzi, G. (1999). The type 2 capsule locus of *Streptococcus pneumoniae*. *J Bacteriol, 181*(8), 2652-2654.

Ibrahim, Y. M., Kerr, A. R., McCluskey, J., and Mitchell, T. J. (2004a). Control of virulence by the two-component system CiaR/H is mediated via HtrA, a major virulence factor of *Streptococcus pneumoniae*. *J Bacteriol, 186*(16), 5258-5266. doi:10.1128/JB.186.16.5258-5266.2004

Ibrahim, Y. M., Kerr, A. R., McCluskey, J., and Mitchell, T. J. (2004b). Role of HtrA in the virulence and competence of *Streptococcus pneumoniae*. *Infect Immun, 72*(6), 3584-3591. doi:10.1128/IAI.72.6.3584-3591.2004

Ibrahim, Y. M., Kerr, A. R., Silva, N. A., and Mitchell, T. J. (2005). Contribution of the ATP-dependent protease ClpCP to the autolysis and virulence of *Streptococcus pneumoniae*. *Infect Immun, 73*(2), 730-740. doi:10.1128/IAI.73.2.730-740.2005

Ignasiak, K., and Maxwell, A. (2017). *Galleria mellonella* (greater wax moth) larvae as a model for antibiotic susceptibility testing and acute toxicity trials. *BMC Res Notes, 10*(1), 428. doi:10.1186/s13104-017-2757-8

Janesch, P., Rouha, H., Badarau, A., Stulik, L., Mirkina, I., Caccamo, M., Havlicek, K., Maierhofer, B., Weber, S., Gross, K., Steinhauser, J., Zerbs, M., Varga, C., Dolezilkova, I., Maier, S., Zauner, G., Nielson, N., Power, C. A., and Nagy, E. (2018). Assessing the function of pneumococcal neuraminidases NanA, NanB and NanC in in vitro and in vivo lung infection models using monoclonal antibodies. *Virulence, 9*(1), 1521-1538. doi:10.1080/21505594.2018.1520545

Jedrzejas, M. J. (2001). Pneumococcal virulence factors: structure and function. *Microbiol Mol Biol Rev, 65*(2), 187-207 ; first page, table of contents. doi:10.1128/MMBR.65.2.187-207.2001

Jin, S., Song, Y. N., Deng, W. Y., Gordon, M. P., and Nester, E. W. (1993). The regulatory VirA protein of *Agrobacterium tumefaciens* does not function at elevated temperatures. *J Bacteriol, 175*(21), 6830-6835. doi:10.1128/jb.175.21.6830-6835.1993

Johnsborg, O., and Havarstein, L. S. (2009). Regulation of natural genetic transformation and acquisition of transforming DNA in *Streptococcus pneumoniae*. *FEMS Microbiol Rev, 33*(3), 627-642. doi:10.1111/j.1574-6976.2009.00167.x

Kadioglu, A., Coward, W., Colston, M. J., Hewitt, C. R., and Andrew, P. W. (2004). CD4-T-lymphocyte interactions with pneumolysin and pneumococci suggest a crucial protective role in the host response to pneumococcal infection. *Infect Immun, 72*(5), 2689-2697. doi:10.1128/iai.72.5.2689-2697.2004

Kadioglu, A., Taylor, S., Iannelli, F., Pozzi, G., Mitchell, T. J., and Andrew, P. W. (2002). Upper and lower respiratory tract infection by *Streptococcus pneumoniae* is affected by pneumolysin deficiency and differences in capsule type. *Infect Immun, 70*(6), 2886-2890. doi:10.1128/iai.70.6.2886-2890.2002

Kadioglu, A., Weiser, J. N., Paton, J. C., and Andrew, P. W. (2008). The role of *Streptococcus pneumoniae* virulence factors in host respiratory colonization and disease. *Nat Rev Microbiol, 6*(4), 288-301. doi:10.1038/nrmicro1871

Kahya, H. F., Andrew, P. W., and Yesilkaya, H. (2017). Deacetylation of sialic acid by esterases potentiates pneumococcal neuraminidase activity for mucin utilization, colonization and virulence. *PLoS Pathog, 13*(3), e1006263. doi:10.1371/journal.ppat.1006263

Kamp, H. D., and Higgins, D. E. (2011). A protein thermometer controls temperature-dependent transcription of flagellar motility genes in *Listeria monocytogenes*. *PLoS Pathog, 7*(8), e1002153. doi:10.1371/journal.ppat.1002153

Kanehisa, M., Sato, Y., Kawashima, M., Furumichi, M., and Tanabe, M. (2016). KEGG as a reference resource for gene and protein annotation. *Nucleic Acids Res, 44*(D1), D457-462. doi:10.1093/nar/gkv1070

Kang, D., and Kirienko, N. V. (2018). Interdependence between iron acquisition and biofilm formation in *Pseudomonas aeruginosa*. *J Microbiol, 56*(7), 449-457. doi:10.1007/s12275-018-8114-3

Kang, S. O., Wright, J. O., Tesorero, R. A., Lee, H., Beall, B., and Cho, K. H. (2012). Thermoregulation of capsule production by *Streptococcus pyogenes*. *PLoS One, 7*(5), e37367. doi:10.1371/journal.pone.0037367

Kaplan, S. L., Barson, W. J., Lin, P. L., Romero, J. R., Bradley, J. S., Tan, T. Q., Hoffman, J. A., Givner, L. B., and Mason, E. O., Jr. (2013). Early trends for invasive pneumococcal infections in children after the introduction of the 13-valent pneumococcal conjugate vaccine. *Pediatr Infect Dis J, 32*(3), 203-207. doi:10.1097/INF.0b013e318275614b

Kaspar, D., Auer, F., Schardt, J., Schindele, F., Ospina, A., Held, C., Ehrenreich, A., Scherer, S., and Muller-Herbst, S. (2014). Temperature- and nitrogen source-dependent regulation of GlnR target genes in *Listeria monocytogenes*. *FEMS Microbiol Lett, 355*(2), 131-141. doi:10.1111/1574-6968.12458

Kerr, A. R., Paterson, G. K., McCluskey, J., Iannelli, F., Oggioni, M. R., Pozzi, G., and Mitchell, T. J. (2006). The contribution of PspC to pneumococcal virulence varies between strains and is accomplished by both complement evasion and complement-independent mechanisms. *Infect Immun, 74*(9), 5319-5324. doi:10.1128/IAI.00543-06

Kim, D. Y., Kim, D. R., Ha, S. C., Lokanath, N. K., Lee, C. J., Hwang, H. Y., and Kim, K. K. (2003). Crystal structure of the protease domain of a heat-shock protein HtrA from *Thermotoga maritima*. *J Biol Chem, 278*(8), 6543-6551. doi:10.1074/jbc.M208148200

Kim, L., McGee, L., Tomczyk, S., and Beall, B. (2016). Biological and Epidemiological Features of Antibiotic-Resistant *Streptococcus pneumoniae* in Pre- and Post-Conjugate Vaccine Eras: a United States Perspective. *Clin Microbiol Rev, 29*(3), 525-552. doi:10.1128/CMR.00058-15

King, Q. O., Lei, B., and Harmsen, A. G. (2009). Pneumococcal surface protein A contributes to secondary *Streptococcus pneumoniae* infection after influenza virus infection. *J Infect Dis, 200*(4), 537-545. doi:10.1086/600871

King, S. J. (2010). Pneumococcal modification of host sugars: a major contributor to colonization of the human airway? *Mol Oral Microbiol, 25*(1), 15-24. doi:10.1111/j.2041-1014.2009.00564.x

King, S. J., Hippe, K. R., and Weiser, J. N. (2006). Deglycosylation of human glycoconjugates by the sequential activities of exoglycosidases expressed by *Streptococcus pneumoniae*. *Mol Microbiol, 59*(3), 961-974. doi:10.1111/j.1365-2958.2005.04984.x

Kirstein, J., Dougan, D. A., Gerth, U., Hecker, M., and Turgay, K. (2007). The tyrosine kinase McsB is a regulated adaptor protein for ClpCP. *EMBO J, 26*(8), 2061-2070. doi:10.1038/sj.emboj.7601655

Klein, B. S., and Tebbets, B. (2007). Dimorphism and virulence in fungi. *Curr Opin Microbiol, 10*(4), 314-319. doi:10.1016/j.mib.2007.04.002

Klinkert, B., and Narberhaus, F. (2009). Microbial thermosensors. *Cell Mol Life Sci, 66*(16), 2661-2676. doi:10.1007/s00018-009-0041-3

Kloosterman, T. G., Hendriksen, W. T., Bijlsma, J. J., Bootsma, H. J., van Hijum, S. A., Kok, J., Hermans, P. W., and Kuipers, O. P. (2006). Regulation of glutamine and glutamate metabolism by GlnR and GlnA in *Streptococcus pneumoniae*. *J Biol Chem, 281*(35), 25097-25109. doi:10.1074/jbc.M601661200

Kloosterman, T. G., van der Kooi-Pol, M. M., Bijlsma, J. J., and Kuipers, O. P. (2007). The novel transcriptional regulator SczA mediates protection against Zn2+ stress by activation of the Zn2+-resistance gene czcD in *Streptococcus pneumoniae*. *Mol Microbiol, 65*(4), 1049-1063. doi:10.1111/j.1365-2958.2007.05849.x

Koch, G., Nadal-Jimenez, P., Cool, R. H., and Quax, W. J. (2014). Assessing Pseudomonas virulence with nonmammalian host: *Galleria mellonella*. *Methods Mol Biol, 1149*, 681-688. doi:10.1007/978-1-4939-0473-0_52

Konkel, M. E., Kim, B. J., Klena, J. D., Young, C. R., and Ziprin, R. (1998). Characterization of the thermal stress response of *Campylobacter jejuni*. *Infect Immun, 66*(8), 3666-3672.

Konkel, M. E., and Tilly, K. (2000). Temperature-regulated expression of bacterial virulence genes. *Microbes Infect, 2*(2), 157-166.

Kostakioti, M., Hadjifrangiskou, M., and Hultgren, S. J. (2013). Bacterial biofilms: development, dispersal, and therapeutic strategies in the dawn of the postantibiotic era. *Cold Spring Harb Perspect Med, 3*(4), a010306. doi:10.1101/cshperspect.a010306

Kowalko, J. E., and Sebert, M. E. (2008). The *Streptococcus pneumoniae* competence regulatory system influences respiratory tract colonization. *Infect Immun, 76*(7), 3131-3140. doi:10.1128/IAI.01696-07

Koziolek, M., Grimm, M., Becker, D., Iordanov, V., Zou, H., Shimizu, J., Wanke, C., Garbacz, G., and Weitschies, W. (2015). Investigation of pH and Temperature Profiles in the GI Tract of Fasted Human Subjects Using the Intellicap((R)) System. *J Pharm Sci, 104*(9), 2855-2863. doi:10.1002/jps.24274

Krajewski, S. S., and Narberhaus, F. (2014). Temperature-driven differential gene expression by RNA thermosensors. *Biochim Biophys Acta, 1839*(10), 978-988. doi:10.1016/j.bbagrm.2014.03.006

Kruger, E., Zuhlke, D., Witt, E., Ludwig, H., and Hecker, M. (2001). Clp-mediated proteolysis in Gram-positive bacteria is autoregulated by the stability of a repressor. *EMBO J, 20*(4), 852-863. doi:10.1093/emboj/20.4.852

Kuhnert, W. L., Zheng, G., Faustoferri, R. C., and Quivey, R. G., Jr. (2004). The F-ATPase operon promoter of *Streptococcus mutans* is transcriptionally regulated in response to external pH. *J Bacteriol, 186*(24), 8524-8528. doi:10.1128/JB.186.24.8524-8528.2004

Kwadha, C. A., Ong'amo, G. O., Ndegwa, P. N., Raina, S. K., and Fombong, A. T. (2017). The Biology and Control of the Greater Wax Moth, *Galleria mellonella*. *Insects, 8*(2). doi:10.3390/insects8020061

Kwon, H. Y., Kim, S. W., Choi, M. H., Ogunniyi, A. D., Paton, J. C., Park, S. H., Pyo, S. N., and Rhee, D. K. (2003). Effect of heat shock and mutations in ClpL and ClpP on virulence gene expression in *Streptococcus pneumoniae*. *Infect Immun, 71*(7), 3757-3765. doi:10.1128/iai.71.7.3757-3765.2003

Kwon, H. Y., Ogunniyi, A. D., Choi, M. H., Pyo, S. N., Rhee, D. K., and Paton, J. C. (2004). The ClpP protease of *Streptococcus pneumoniae* modulates virulence gene expression and protects against fatal pneumococcal challenge. *Infect Immun, 72*(10), 5646-5653. doi:10.1128/IAI.72.10.5646-5653.2004

Kyaw, M. H., Rose, C. E., Jr., Fry, A. M., Singleton, J. A., Moore, Z., Zell, E. R., Whitney, C. G., and Active Bacterial Core Surveillance Program of the Emerging Infections Program, N. (2005). The influence of chronic illnesses on the incidence of invasive pneumococcal disease in adults. *J Infect Dis, 192*(3), 377-386. doi:10.1086/431521

Laakso, K., Koskenniemi, K., Koponen, J., Kankainen, M., Surakka, A., Salusjarvi, T., Auvinen, P., Savijoki, K., Nyman, T. A., Kalkkinen, N., Tynkkynen, S., and Varmanen, P. (2011). Growth phase-associated changes in the proteome and transcriptome of *Lactobacillus rhamnosus* GG in industrial-type whey medium. *Microb Biotechnol, 4*(6), 746-766. doi:10.1111/j.1751-7915.2011.00275.x

Lam, O., Wheeler, J., and Tang, C. M. (2014). Thermal control of virulence factors in bacteria: a hot topic. *Virulence, 5*(8), 852-862. doi:10.4161/21505594.2014.970949

LaPlante, K. L., Rybak, M. J., Tsuji, B., Lodise, T. P., and Kaatz, G. W. (2007). Fluoroquinolone resistance in *Streptococcus pneumoniae*: area under the concentration-time curve/MIC ratio and resistance development with gatifloxacin, gemifloxacin, levofloxacin, and moxifloxacin. *Antimicrob Agents Chemother, 51*(4), 1315-1320. doi:10.1128/AAC.00646-06

Lee, Y. H., Kingston, A. W., and Helmann, J. D. (2012). Glutamate dehydrogenase affects resistance to cell wall antibiotics in *Bacillus subtilis*. *J Bacteriol, 194*(5), 993-1001. doi:10.1128/JB.06547-11

Leoni, L., Orsi, N., de Lorenzo, V., and Visca, P. (2000). Functional analysis of PvdS, an iron starvation sigma factor of *Pseudomonas aeruginosa*. *J Bacteriol, 182*(6), 1481-1491. doi:10.1128/jb.182.6.1481-1491.2000

Levesque, C. M., Mair, R. W., Perry, J. A., Lau, P. C., Li, Y. H., and Cvitkovitch, D. G. (2007). Systemic inactivation and phenotypic characterization of two-component systems in expression of *Streptococcus mutans* virulence properties. *Lett Appl Microbiol, 45*(4), 398-404. doi:10.1111/j.1472-765X.2007.02203.x

Li, D. D., Deng, L., Hu, G. H., Zhao, L. X., Hu, D. D., Jiang, Y. Y., and Wang, Y. (2013). Using *Galleria mellonella-Candida albicans* infection model to evaluate antifungal agents. *Biol Pharm Bull, 36*(9), 1482-1487. doi:10.1248/bpb.b13-00270

Li, J. S., Bi, Y. T., Dong, C., Yang, J. F., and Liang, W. D. (2011). Transcriptome analysis of adaptive heat shock response of *Streptococcus thermophilus*. *PLoS One, 6*(10), e25777. doi:10.1371/journal.pone.0025777

Li, W., Zhao, X., Zou, S., Ma, Y., Zhang, K., and Zhang, M. (2012). Scanning assay of beta-galactosidase activity. *Prikl Biokhim Mikrobiol, 48*(6), 668-672.

Liao, J., and Sauer, K. (2012). The MerR-like transcriptional regulator BrlR contributes to *Pseudomonas aeruginosa* biofilm tolerance. *J Bacteriol, 194*(18), 4823-4836. doi:10.1128/JB.00765-12

Lin, M. H., Shu, J. C., Huang, H. Y., and Cheng, Y. C. (2012). Involvement of iron in biofilm formation by *Staphylococcus aureus*. *PLoS One, 7*(3), e34388. doi:10.1371/journal.pone.0034388

Liu, C., Niu, Y., Zhou, X., Zheng, X., Wang, S., Guo, Q., Li, Y., Li, M., Li, J., Yang, Y., Ding, Y., Lamont, R. J., and Xu, X. (2015). *Streptococcus mutans* copes with heat stress by multiple transcriptional regulons modulating virulence and energy metabolism. *Sci Rep, 5*, 12929. doi:10.1038/srep12929

Liu, Y., and Burne, R. A. (2009). Multiple two-component systems modulate alkali generation in *Streptococcus gordonii* in response to environmental stresses. *J Bacteriol, 191*(23), 7353-7362. doi:10.1128/JB.01053-09

Lu, D., and Keck, J. L. (2008). Structural basis of *Escherichia coli* single-stranded DNA-binding protein stimulation of exonuclease I. *Proc Natl Acad Sci U S A, 105*(27), 9169-9174. doi:10.1073/pnas.0800741105

Lux, T., Nuhn, M., Hakenbeck, R., and Reichmann, P. (2007). Diversity of bacteriocins and activity spectrum in *Streptococcus pneumoniae*. *J Bacteriol, 189*(21), 7741-7751. doi:10.1128/JB.00474-07

Manco, S., Hernon, F., Yesilkaya, H., Paton, J. C., Andrew, P. W., and Kadioglu, A. (2006). Pneumococcal neuraminidases A and B both have essential roles during infection of the respiratory tract and sepsis. *Infect Immun, 74*(7), 4014-4020. doi:10.1128/IAI.01237-05

Mansilla, M. C., Cybulski, L. E., Albanesi, D., and de Mendoza, D. (2004). Control of membrane lipid fluidity by molecular thermosensors. *J Bacteriol, 186*(20), 6681-6688. doi:10.1128/JB.186.20.6681-6688.2004

Margolis, E. (2009). Hydrogen peroxide-mediated interference competition by *Streptococcus pneumoniae* has no significant effect on *Staphylococcus aureus* nasal colonization of neonatal rats. *J Bacteriol, 191*(2), 571-575. doi:10.1128/JB.00950-08

Marion, C., Burnaugh, A. M., Woodiga, S. A., and King, S. J. (2011). Sialic acid transport contributes to pneumococcal colonization. *Infect Immun, 79*(3), 1262-1269. doi:10.1128/IAI.00832-10

Marion, C., Limoli, D. H., Bobulsky, G. S., Abraham, J. L., Burnaugh, A. M., and King, S. J. (2009). Identification of a pneumococcal glycosidase that modifies O-linked glycans. *Infect Immun, 77*(4), 1389-1396. doi:10.1128/IAI.01215-08

Marion, C., Stewart, J. M., Tazi, M. F., Burnaugh, A. M., Linke, C. M., Woodiga, S. A., and King, S. J. (2012). *Streptococcus pneumoniae* can utilize multiple sources of hyaluronic acid for growth. *Infect Immun, 80*(4), 1390-1398. doi:10.1128/IAI.05756-11

Marks, L. R., Parameswaran, G. I., and Hakansson, A. P. (2012a). Pneumococcal interactions with epithelial cells are crucial for optimal biofilm formation and colonization in vitro and in vivo. *Infect Immun, 80*(8), 2744-2760. doi:10.1128/IAI.00488-12

Marks, L. R., Reddinger, R. M., and Hakansson, A. P. (2012b). High levels of genetic recombination during nasopharyngeal carriage and biofilm formation in *Streptococcus pneumoniae*. *MBio, 3*(5). doi:10.1128/mBio.00200-12

Martin-Galiano, A. J., Ferrandiz, M. J., and de la Campa, A. G. (2001). The promoter of the operon encoding the F0F1 ATPase of *Streptococcus pneumoniae* is inducible by pH. *Mol Microbiol, 41*(6), 1327-1338. doi:10.1046/j.1365-2958.2001.02597.x

Mascher, T., Zahner, D., Merai, M., Balmelle, N., de Saizieu, A. B., and Hakenbeck, R. (2003). The *Streptococcus pneumoniae* cia regulon: CiaR target sites and transcription profile analysis. *J Bacteriol, 185*(1), 60-70. doi:10.1128/jb.185.1.60-70.2003

McCullers, J. A., and Bartmess, K. C. (2003). Role of neuraminidase in lethal synergism between influenza virus and *Streptococcus pneumoniae*. *J Infect Dis, 187*(6), 1000-1009. doi:10.1086/368163

McEwan, A. G., Djoko, K. Y., Chen, N. H., Counago, R. L., Kidd, S. P., Potter, A. J., and Jennings, M. P. (2011). Novel bacterial MerR-like regulators their role in the response to carbonyl and nitrosative stress. *Adv Microb Physiol, 58*, 1-22. doi:10.1016/B978-0-12-381043-4.00001-5

Mehr, S., and Wood, N. (2012). *Streptococcus pneumoniae*--a review of carriage, infection, serotype replacement and vaccination. *Paediatr Respir Rev, 13*(4), 258-264. doi:10.1016/j.prrv.2011.12.001

Mereghetti, L., Sitkiewicz, I., Green, N. M., and Musser, J. M. (2008). Remodeling of the *Streptococcus agalactiae* transcriptome in response to growth temperature. *PLoS One, 3*(7), e2785. doi:10.1371/journal.pone.0002785

Merrick, M. J., and Edwards, R. A. (1995). Nitrogen control in bacteria. *Microbiol Rev, 59*(4), 604-622.

Merrin, J., Kumar, P., and Libchaber, A. (2011). Effects of pressure and temperature on the binding of RecA protein to single-stranded DNA. *Proc Natl Acad Sci U S A, 108*(50), 19913-19918. doi:10.1073/pnas.1112646108

Meyer, S., Carlson, P. D., and Lucks, J. B. (2017). Characterizing the Structure-Function Relationship of a Naturally Occurring RNA Thermometer. *Biochemistry, 56*(51), 6629-6638. doi:10.1021/acs.biochem.7b01170

Miles, A. A., Misra, S. S., and Irwin, J. O. (1938). The estimation of the bactericidal power of the blood. *J Hyg (Lond), 38*(6), 732-749. doi:10.1017/s002217240001158x

Millar, E. V., Watt, J. P., Bronsdon, M. A., Dallas, J., Reid, R., Santosham, M., and O'Brien, K. L. (2008). Indirect effect of 7-valent pneumococcal conjugate vaccine on pneumococcal colonization among unvaccinated household members. *Clin Infect Dis, 47*(8), 989-996. doi:10.1086/591966

Mishra, S., and Imlay, J. (2012). Why do bacteria use so many enzymes to scavenge hydrogen peroxide? *Arch Biochem Biophys, 525*(2), 145-160. doi:10.1016/j.abb.2012.04.014

Mitchell, A. M., and Mitchell, T. J. (2010). *Streptococcus pneumoniae*: virulence factors and variation. *Clin Microbiol Infect, 16*(5), 411-418. doi:10.1111/j.1469-0691.2010.03183.x

Modell, J. W., Kambara, T. K., Perchuk, B. S., and Laub, M. T. (2014). A DNA damage-induced, SOS-independent checkpoint regulates cell division in *Caulobacter crescentus*. *PLoS Biol, 12*(10), e1001977. doi:10.1371/journal.pbio.1001977

Morais, V., Dee, V., and Suarez, N. (2018). Purification of Capsular Polysaccharides of *Streptococcus pneumoniae*: Traditional and New Methods. *Front Bioeng Biotechnol, 6*, 145. doi:10.3389/fbioe.2018.00145

Morens, D. M., Taubenberger, J. K., and Fauci, A. S. (2008). Predominant role of bacterial pneumonia as a cause of death in pandemic influenza: implications for pandemic influenza preparedness. *J Infect Dis, 198*(7), 962-970. doi:10.1086/591708

Morita, M. T., Tanaka, Y., Kodama, T. S., Kyogoku, Y., Yanagi, H., and Yura, T. (1999). Translational induction of heat shock transcription factor sigma32: evidence for a built-in RNA thermosensor. *Genes Dev, 13*(6), 655-665. doi:10.1101/gad.13.6.655

Morozov, G. I., Porat, N., Kushnir, T., Najmuldeen, H., Adawi, A., Chalifa-Caspi, V., Benisty, R., Ohayon, A., Liron, O., Azriel, S., Malka, I., Dotan, S., Portnoi, M., Piotrowski, A. A., Kafka, D., Hajaj, B., Fishilevich, T., Shagan, M., Tal, M., Ellis, R., Morrison, D. A., Mitchell, A. M., Mitchell, T. J., Dagan, R., Yesilkaya, H., and Nebenzahl, Y. M. (2018). Flavin Reductase Contributes to Pneumococcal Virulence by Protecting from Oxidative Stress and Mediating Adhesion and Elicits Protection Against Pneumococcal Challenge. *Sci Rep, 8*(1), 314. doi:10.1038/s41598-017-18645-8

Mowlds, P., and Kavanagh, K. (2008). Effect of pre-incubation temperature on susceptibility of Galleria mellonella larvae to infection by Candida albicans. *Mycopathologia, 165*(1), 5-12. doi:10.1007/s11046-007-9069-9

Msadek, T., Kunst, F., and Rapoport, G. (1994). MecB of *Bacillus subtilis*, a member of the ClpC ATPase family, is a pleiotropic regulator controlling competence gene expression and growth at high temperature. *Proc Natl Acad Sci U S A, 91*(13), 5788-5792. doi:10.1073/pnas.91.13.5788

Munoz-Almagro, C., Jordan, I., Gene, A., Latorre, C., Garcia-Garcia, J. J., and Pallares, R. (2008). Emergence of invasive pneumococcal disease caused by nonvaccine serotypes in the era of 7-valent conjugate vaccine. *Clin Infect Dis, 46*(2), 174-182. doi:10.1086/524660

Najmuldeen, H., Alghamdi, R., Alghofaili, F., and Yesilkaya, H. (2019). Functional assessment of microbial superoxide dismutase isozymes suggests a differential role for each isozyme. *Free Radic Biol Med, 134*, 215-228. doi:10.1016/j.freeradbiomed.2019.01.018

Namkoong, H., Ishii, M., Funatsu, Y., Kimizuka, Y., Yagi, K., Asami, T., Asakura, T., Suzuki, S., Kamo, T., Fujiwara, H., Tasaka, S., Betsuyaku, T., and Hasegawa, N. (2016). Theory and strategy for Pneumococcal vaccines in the elderly. *Hum Vaccin Immunother, 12*(2), 336-343. doi:10.1080/21645515.2015.1075678

Narberhaus, F., Waldminghaus, T., and Chowdhury, S. (2006). RNA thermometers. *FEMS Microbiol Rev, 30*(1), 3-16. doi:10.1111/j.1574-6976.2005.004.x

Nelson, A. L., Roche, A. M., Gould, J. M., Chim, K., Ratner, A. J., and Weiser, J. N. (2007). Capsule enhances pneumococcal colonization by limiting mucus-mediated clearance. *Infect Immun, 75*(1), 83-90. doi:10.1128/IAI.01475-06

Neumann, P., Markau, K., and Sund, H. (1976). Studies of glutamate dehydrogenase. Regulation of glutamate dehydrogenase from *Candida utilis* by a pH and temperature-dependent conformational transition. *Eur J Biochem, 65*(2), 465-472. doi:10.1111/j.1432-1033.1976.tb10362.x

Obert, C., Sublett, J., Kaushal, D., Hinojosa, E., Barton, T., Tuomanen, E. I., and Orihuela, C. J. (2006). Identification of a Candidate *Streptococcus pneumoniae* core genome and regions of diversity correlated with invasive pneumococcal disease. *Infect Immun, 74*(8), 4766-4777. doi:10.1128/IAI.00316-06

Ogunniyi, A. D., LeMessurier, K. S., Graham, R. M., Watt, J. M., Briles, D. E., Stroeher, U. H., and Paton, J. C. (2007). Contributions of pneumolysin, pneumococcal surface protein A (PspA), and PspC to pathogenicity of *Streptococcus pneumoniae* D39 in a mouse model. *Infect Immun, 75*(4), 1843-1851. doi:10.1128/IAI.01384-06

Ojha, A., Anand, M., Bhatt, A., Kremer, L., Jacobs, W. R., Jr., and Hatfull, G. F. (2005). GroEL1: a dedicated chaperone involved in mycolic acid biosynthesis during biofilm formation in mycobacteria. *Cell, 123*(5), 861-873. doi:10.1016/j.cell.2005.09.012

Oliveira, T., Sharkey, M. A., Engel, P. C., and Khan, A. R. (2016). Crystal structure of a chimaeric bacterial glutamate dehydrogenase. *Acta Crystallogr F Struct Biol Commun, 72*(Pt 6), 462-466. doi:10.1107/S2053230X16007305

Olszewski, M., Grot, A., Wojciechowski, M., Nowak, M., Mickiewicz, M., and Kur, J. (2010). Characterization of exceptionally thermostable single-stranded DNA-binding proteins from *Thermotoga maritima* and *Thermotoga neapolitana*. *BMC Microbiol, 10*, 260. doi:10.1186/1471-2180-10-260

Ong, C. L., Potter, A. J., Trappetti, C., Walker, M. J., Jennings, M. P., Paton, J. C., and McEwan, A. G. (2013). Interplay between manganese and iron in pneumococcal pathogenesis: role of the orphan response regulator RitR. *Infect Immun, 81*(2), 421-429. doi:10.1128/IAI.00805-12

Ortega, J., Iwanczyk, J., and Jomaa, A. (2009). *Escherichia coli* DegP: a structure-driven functional model. *J Bacteriol, 191*(15), 4705-4713. doi:10.1128/JB.00472-09

Owen, R. H., Boulnois, G. J., Andrew, P. W., and Mitchell, T. J. (1994). A role in cell-binding for the C-terminus of pneumolysin, the thiol-activated toxin of *Streptococcus pneumoniae*. *FEMS Microbiol Lett, 121*(2), 217-221. doi:10.1111/j.1574-6968.1994.tb07101.x

Paixao, L., Caldas, J., Kloosterman, T. G., Kuipers, O. P., Vinga, S., and Neves, A. R. (2015a). Transcriptional and metabolic effects of glucose on *Streptococcus pneumoniae* sugar metabolism. *Front Microbiol, 6*, 1041. doi:10.3389/fmicb.2015.01041

Paixao, L., Oliveira, J., Verissimo, A., Vinga, S., Lourenco, E. C., Ventura, M. R., Kjos, M., Veening, J. W., Fernandes, V. E., Andrew, P. W., Yesilkaya, H., and Neves, A. R. (2015b). Host

glycan sugar-specific pathways in *Streptococcus pneumoniae*: galactose as a key sugar in colonisation and infection [corrected]. *PLoS One, 10*(3), e0121042. doi:10.1371/journal.pone.0121042

Pandya, U., Allen, C. A., Watson, D. A., and Niesel, D. W. (2005). Global profiling of *Streptococcus pneumoniae* gene expression at different growth temperatures. *Gene, 360*(1), 45-54. doi:10.1016/j.gene.2005.06.023

Parker, D., Soong, G., Planet, P., Brower, J., Ratner, A. J., and Prince, A. (2009). The NanA neuraminidase of *Streptococcus pneumoniae* is involved in biofilm formation. *Infect Immun, 77*(9), 3722-3730. doi:10.1128/IAI.00228-09

Paster, E., and Ryu, W. S. (2008). The thermal impulse response of *Escherichia coli*. *Proc Natl Acad Sci U S A, 105*(14), 5373-5377. doi:10.1073/pnas.0709903105

Patenge, N., Pappesch, R., Khani, A., and Kreikemeyer, B. (2015). Genome-wide analyses of small non-coding RNAs in streptococci. *Front Genet, 6*, 189. doi:10.3389/fgene.2015.00189

Paterson, G. K., and Orihuela, C. J. (2010). Pneumococci: immunology of the innate host response. *Respirology, 15*(7), 1057-1063. doi:10.1111/j.1440-1843.2010.01814.x

Pericone, C. D., Overweg, K., Hermans, P. W., and Weiser, J. N. (2000). Inhibitory and bactericidal effects of hydrogen peroxide production by *Streptococcus pneumoniae* on other inhabitants of the upper respiratory tract. *Infect Immun, 68*(7), 3990-3997. doi:10.1128/iai.68.7.3990-3997.2000

Peterson, S. N., Sung, C. K., Cline, R., Desai, B. V., Snesrud, E. C., Luo, P., Walling, J., Li, H., Mintz, M., Tsegaye, G., Burr, P. C., Do, Y., Ahn, S., Gilbert, J., Fleischmann, R. D., and Morrison, D. A. (2004). Identification of competence pheromone responsive genes in *Streptococcus pneumoniae* by use of DNA microarrays. *Mol Microbiol, 51*(4), 1051-1070. doi:10.1046/j.1365-2958.2003.03907.x

Pettigrew, M. M., Fennie, K. P., York, M. P., Daniels, J., and Ghaffar, F. (2006). Variation in the presence of neuraminidase genes among *Streptococcus pneumoniae* isolates with identical sequence types. *Infect Immun, 74*(6), 3360-3365. doi:10.1128/IAI.01442-05

Phadtare, S., and Inouye, M. (2004). Genome-wide transcriptional analysis of the cold shock response in wild-type and cold-sensitive, quadruple-csp-deletion strains of *Escherichia coli*. *J Bacteriol, 186*(20), 7007-7014. doi:10.1128/JB.186.20.7007-7014.2004

Pinas, G. E., Reinoso-Vizcaino, N. M., Yandar Barahona, N. Y., Cortes, P. R., Duran, R., Badapanda, C., Rathore, A., Bichara, D. R., Cian, M. B., Olivero, N. B., Perez, D. R., and Echenique, J. (2018). Crosstalk between the serine/threonine kinase StkP and the response regulator ComE controls the stress response and intracellular survival of *Streptococcus pneumoniae*. *PLoS Pathog, 14*(6), e1007118. doi:10.1371/journal.ppat.1007118

Plaitakis, A., Kalef-Ezra, E., Kotzamani, D., Zaganas, I., and Spanaki, C. (2017). The Glutamate Dehydrogenase Pathway and Its Roles in Cell and Tissue Biology in Health and Disease. *Biology (Basel), 6*(1). doi:10.3390/biology6010011

Plecha, S. C., and Withey, J. H. (2015). Mechanism for inhibition of *Vibrio cholerae* ToxT activity by the unsaturated fatty acid components of bile. *J Bacteriol, 197*(10), 1716-1725. doi:10.1128/JB.02409-14

Poole, K., and Braun, V. (1988). Influence of growth temperature and lipopolysaccharide on hemolytic activity of *Serratia marcescens*. *J Bacteriol, 170*(11), 5146-5152. doi:10.1128/jb.170.11.5146-5152.1988

Porcheron, G., Garenaux, A., Proulx, J., Sabri, M., and Dozois, C. M. (2013). Iron, copper, zinc, and manganese transport and regulation in pathogenic Enterobacteria: correlations between strains, site of infection and the relative importance of the different metal transport systems for virulence. *Front Cell Infect Microbiol, 3*, 90. doi:10.3389/fcimb.2013.00090

Price, K. E., and Camilli, A. (2009). Pneumolysin localizes to the cell wall of *Streptococcus pneumoniae*. *J Bacteriol, 191*(7), 2163-2168. doi:10.1128/JB.01489-08

Price, P. B., and Sowers, T. (2004). Temperature dependence of metabolic rates for microbial growth, maintenance, and survival. *Proc Natl Acad Sci U S A, 101*(13), 4631-4636. doi:10.1073/pnas.0400522101

Prudhomme, M., Berge, M., Martin, B., and Polard, P. (2016). Pneumococcal Competence Coordination Relies on a Cell-Contact Sensing Mechanism. *PLoS Genet, 12*(6), e1006113. doi:10.1371/journal.pgen.1006113

Pysz, M. A., Conners, S. B., Montero, C. I., Shockley, K. R., Johnson, M. R., Ward, D. E., and Kelly, R. M. (2004). Transcriptional analysis of biofilm formation processes in the anaerobic, hyperthermophilic bacterium *Thermotoga maritima*. *Appl Environ Microbiol, 70*(10), 6098-6112. doi:10.1128/AEM.70.10.6098-6112.2004

Qi, F., Merritt, J., Lux, R., and Shi, W. (2004). Inactivation of the ciaH Gene in *Streptococcus mutans* diminishes mutacin production and competence development, alters sucrose-dependent biofilm formation, and reduces stress tolerance. *Infect Immun, 72*(8), 4895-4899. doi:10.1128/IAI.72.8.4895-4899.2004

Quin, L. R., Onwubiko, C., Moore, Q. C., Mills, M. F., McDaniel, L. S., and Carmicle, S. (2007). Factor H binding to PspC of *Streptococcus pneumoniae* increases adherence to human cell lines in vitro and enhances invasion of mouse lungs in vivo. *Infect Immun, 75*(8), 4082-4087. doi:10.1128/IAI.00474-07

Ramakrishnan, B., Boeggeman, E., and Qasba, P. K. (2012). Binding of N-acetylglucosamine (GlcNAc) beta1-6-branched oligosaccharide acceptors to beta4-galactosyltransferase I reveals a new ligand binding mode. *J Biol Chem, 287*(34), 28666-28674. doi:10.1074/jbc.M112.373514

Ramos-Sevillano, E., Ercoli, G., and Brown, J. S. (2019). Mechanisms of Naturally Acquired Immunity to *Streptococcus pneumoniae*. *Front Immunol, 10*, 358. doi:10.3389/fimmu.2019.00358

Ratledge, C., and Dover, L. G. (2000). Iron metabolism in pathogenic bacteria. *Annu Rev Microbiol, 54*, 881-941. doi:10.1146/annurev.micro.54.1.881

Reinert, R. R. (2009). The antimicrobial resistance profile of *Streptococcus pneumoniae*. *Clin Microbiol Infect, 15 Suppl 3*, 7-11. doi:10.1111/j.1469-0691.2009.02724.x

Rendueles, O., Garcia-Garcera, M., Neron, B., Touchon, M., and Rocha, E. P. C. (2017). Abundance and co-occurrence of extracellular capsules increase environmental breadth: Implications for the emergence of pathogens. *PLoS Pathog, 13*(7), e1006525. doi:10.1371/journal.ppat.1006525

Restrepo, A. V., Salazar, B. E., Agudelo, M., Rodriguez, C. A., Zuluaga, A. F., and Vesga, O. (2005). Optimization of culture conditions to obtain maximal growth of penicillin-resistant *Streptococcus pneumoniae*. *BMC Microbiol, 5*, 34. doi:10.1186/1471-2180-5-34

Reyes-Caballero, H., Guerra, A. J., Jacobsen, F. E., Kazmierczak, K. M., Cowart, D., Koppolu, U. M., Scott, R. A., Winkler, M. E., and Giedroc, D. P. (2010). The metalloregulatory zinc site in *Streptococcus pneumoniae* AdcR, a zinc-activated MarR family repressor. *J Mol Biol, 403*(2), 197-216. doi:10.1016/j.jmb.2010.08.030

Reyrat, J. M., Pelicic, V., Gicquel, B., and Rappuoli, R. (1998). Counterselectable markers: untapped tools for bacterial genetics and pathogenesis. *Infect Immun, 66*(9), 4011-4017.

Rezaei Javan, R., van Tonder, A. J., King, J. P., Harrold, C. L., and Brueggemann, A. B. (2018). Genome Sequencing Reveals a Large and Diverse Repertoire of Antimicrobial Peptides. *Front Microbiol, 9*, 2012. doi:10.3389/fmicb.2018.02012

Rinnenthal, J., Klinkert, B., Narberhaus, F., and Schwalbe, H. (2011). Modulation of the stability of the Salmonella fourU-type RNA thermometer. *Nucleic Acids Res, 39*(18), 8258-8270. doi:10.1093/nar/gkr314

Rodgers, G. L., Arguedas, A., Cohen, R., and Dagan, R. (2009). Global serotype distribution among *Streptococcus pneumoniae* isolates causing otitis media in children: potential

implications for pneumococcal conjugate vaccines. *Vaccine, 27*(29), 3802-3810. doi:10.1016/j.vaccine.2009.04.021

Roncarati, D., and Scarlato, V. (2017). Regulation of heat-shock genes in bacteria: from signal sensing to gene expression output. *FEMS Microbiol Rev, 41*(4), 549-574. doi:10.1093/femsre/fux015

Rosenow, C., Ryan, P., Weiser, J. N., Johnson, S., Fontan, P., Ortqvist, A., and Masure, H. R. (1997). Contribution of novel choline-binding proteins to adherence, colonization and immunogenicity of *Streptococcus pneumoniae*. *Mol Microbiol, 25*(5), 819-829. doi:10.1111/j.1365-2958.1997.mmi494.x

Rowan, A. N., and Rollin, B. E. (1983). Animal research--for and against: a philosophical, social, and historical perspective. *Perspect Biol Med, 27*(1), 1-17.

Rubins, J. B., Charboneau, D., Fasching, C., Berry, A. M., Paton, J. C., Alexander, J. E., Andrew, P. W., Mitchell, T. J., and Janoff, E. N. (1996). Distinct roles for pneumolysin's cytotoxic and complement activities in the pathogenesis of pneumococcal pneumonia. *Am J Respir Crit Care Med, 153*(4 Pt 1), 1339-1346. doi:10.1164/ajrccm.153.4.8616564

Russell, F. M., Licciardi, P. V., Balloch, A., Biaukula, V., Tikoduadua, L., Carapetis, J. R., Nelson, J., Jenney, A. W., Waqatakirewa, L., Colquhoun, S., Cheung, Y. B., Tang, M. L., and Mulholland, E. K. (2010). Safety and immunogenicity of the 23-valent pneumococcal polysaccharide vaccine at 12 months of age, following one, two, or three doses of the 7-valent pneumococcal conjugate vaccine in infancy. *Vaccine, 28*(18), 3086-3094. doi:10.1016/j.vaccine.2010.02.065

Saito, H., and Miura, K. I. (1963). Preparation of Transforming Deoxyribonucleic Acid by Phenol Treatment. *Biochim Biophys Acta, 72*, 619-629.

Salerno, B., Anne, G., and Bryant, F. R. (2011). DNA binding compatibility of the *Streptococcus pneumoniae* SsbA and SsbB proteins. *PLoS One, 6*(9), e24305. doi:10.1371/journal.pone.0024305

Salvadori, G., Junges, R., Morrison, D. A., and Petersen, F. C. (2019). Competence in *Streptococcus pneumoniae* and Close Commensal Relatives: Mechanisms and Implications. *Front Cell Infect Microbiol, 9*, 94. doi:10.3389/fcimb.2019.00094

Sanchez-Alberola, N., Campoy, S., Barbe, J., and Erill, I. (2012). Analysis of the SOS response of Vibrio and other bacteria with multiple chromosomes. *BMC Genomics, 13*, 58. doi:10.1186/1471-2164-13-58

Sanchez, C. J., Shivshankar, P., Stol, K., Trakhtenbroit, S., Sullam, P. M., Sauer, K., Hermans, P. W., and Orihuela, C. J. (2010). The pneumococcal serine-rich repeat protein is an intra-species bacterial adhesin that promotes bacterial aggregation in vivo and in biofilms. *PLoS Pathog, 6*(8), e1001044. doi:10.1371/journal.ppat.1001044

Sargent, M. G. (1975). Control of cell length in *Bacillus subtilis*. *J Bacteriol, 123*(1), 7-19.

Schaechter, M., Maaloe, O., and Kjeldgaard, N. O. (1958). Dependency on medium and temperature of cell size and chemical composition during balanced grown of *Salmonella typhimurium*. *J Gen Microbiol, 19*(3), 592-606. doi:10.1099/00221287-19-3-592

Sengupta, P., and Garrity, P. (2013). Sensing temperature. *Curr Biol, 23*(8), R304-307. doi:10.1016/j.cub.2013.03.009

Shafeeq, S., Yesilkaya, H., Kloosterman, T. G., Narayanan, G., Wandel, M., Andrew, P. W., Kuipers, O. P., and Morrissey, J. A. (2011). The cop operon is required for copper homeostasis and contributes to virulence in *Streptococcus pneumoniae*. *Mol Microbiol, 81*(5), 1255-1270. doi:10.1111/j.1365-2958.2011.07758.x

Shainheit, M. G., Mule, M., and Camilli, A. (2014). The core promoter of the capsule operon of *Streptococcus pneumoniae* is necessary for colonization and invasive disease. *Infect Immun, 82*(2), 694-705. doi:10.1128/IAI.01289-13

Shak, J. R., Ludewick, H. P., Howery, K. E., Sakai, F., Yi, H., Harvey, R. M., Paton, J. C., Klugman, K. P., and Vidal, J. E. (2013). Novel role for the *Streptococcus pneumoniae* toxin

pneumolysin in the assembly of biofilms. *MBio, 4*(5), e00655-00613. doi:10.1128/mBio.00655-13

Shapiro, R. S., and Cowen, L. E. (2012). Thermal control of microbial development and virulence: molecular mechanisms of microbial temperature sensing. *MBio, 3*(5). doi:10.1128/mBio.00238-12

Shelburne, S. A., Davenport, M. T., Keith, D. B., and Musser, J. M. (2008). The role of complex carbohydrate catabolism in the pathogenesis of invasive streptococci. *Trends Microbiol, 16*(7), 318-325. doi:10.1016/j.tim.2008.04.002

Shen, A., and Higgins, D. E. (2006). The MogR transcriptional repressor regulates nonhierarchal expression of flagellar motility genes and virulence in *Listeria monocytogenes*. *PLoS Pathog, 2*(4), e30. doi:10.1371/journal.ppat.0020030

Shereda, R. D., Kozlov, A. G., Lohman, T. M., Cox, M. M., and Keck, J. L. (2008). SSB as an organizer/mobilizer of genome maintenance complexes. *Crit Rev Biochem Mol Biol, 43*(5), 289-318. doi:10.1080/10409230802341296

Singh, A. K., Pluvinage, B., Higgins, M. A., Dalia, A. B., Woodiga, S. A., Flynn, M., Lloyd, A. R., Weiser, J. N., Stubbs, K. A., Boraston, A. B., and King, S. J. (2014). Unravelling the multiple functions of the architecturally intricate *Streptococcus pneumoniae* beta-galactosidase, BgaA. *PLoS Pathog, 10*(9), e1004364. doi:10.1371/journal.ppat.1004364

Slater, J. L., Gregson, L., Denning, D. W., and Warn, P. A. (2011). Pathogenicity of *Aspergillus fumigatus* mutants assessed in *Galleria mellonella* matches that in mice. *Med Mycol, 49 Suppl 1*, S107-113. doi:10.3109/13693786.2010.523852

Smoot, L. M., Smoot, J. C., Graham, M. R., Somerville, G. A., Sturdevant, D. E., Migliaccio, C. A., Sylva, G. L., and Musser, J. M. (2001). Global differential gene expression in response to growth temperature alteration in group A Streptococcus. *Proc Natl Acad Sci U S A, 98*(18), 10416-10421. doi:10.1073/pnas.191267598

Solovyev, V. V., Shahmuradov, I. A., and Salamov, A. A. (2010). Identification of promoter regions and regulatory sites. *Methods Mol Biol, 674*, 57-83. doi:10.1007/978-1-60761-854-6_5

Somerville, G. A., and Proctor, R. A. (2009). At the crossroads of bacterial metabolism and virulence factor synthesis in Staphylococci. *Microbiol Mol Biol Rev, 73*(2), 233-248. doi:10.1128/MMBR.00005-09

Song, J. H., Ko, K. S., Lee, J. Y., Baek, J. Y., Oh, W. S., Yoon, H. S., Jeong, J. Y., and Chun, J. (2005). Identification of essential genes in *Streptococcus pneumoniae* by allelic replacement mutagenesis. *Mol Cells, 19*(3), 365-374.

Song, J. Y., Nahm, M. H., and Moseley, M. A. (2013). Clinical implications of pneumococcal serotypes: invasive disease potential, clinical presentations, and antibiotic resistance. *J Korean Med Sci, 28*(1), 4-15. doi:10.3346/jkms.2013.28.1.4

Steinfort, C., Wilson, R., Mitchell, T., Feldman, C., Rutman, A., Todd, H., Sykes, D., Walker, J., Saunders, K., Andrew, P. W., and et al. (1989). Effect of *Streptococcus pneumoniae* on human respiratory epithelium in vitro. *Infect Immun, 57*(7), 2006-2013.

Steinmann, R., and Dersch, P. (2013). Thermosensing to adjust bacterial virulence in a fluctuating environment. *Future Microbiol, 8*(1), 85-105. doi:10.2217/fmb.12.129

Steinmoen, H., Teigen, A., and Havarstein, L. S. (2003). Competence-induced cells of *Streptococcus pneumoniae* lyse competence-deficient cells of the same strain during cocultivation. *J Bacteriol, 185*(24), 7176-7183. doi:10.1128/jb.185.24.7176-7183.2003

Stulke, J., and Hillen, W. (2000). Regulation of carbon catabolism in *Bacillus species*. *Annu Rev Microbiol, 54*, 849-880. doi:10.1146/annurev.micro.54.1.849

Swaggerty, C. L., Genovese, K. J., He, H., Byrd, J. A., Jr., and Kogut, M. H. (2018). Editorial: Mechanisms of Persistence, Survival, and Transmission of Bacterial Foodborne Pathogens in Production Animals. *Front Vet Sci, 5*, 139. doi:10.3389/fvets.2018.00139

Swiatlo, E., Champlin, F. R., Holman, S. C., Wilson, W. W., and Watt, J. M. (2002). Contribution of choline-binding proteins to cell surface properties of *Streptococcus pneumoniae*. *Infect Immun, 70*(1), 412-415. doi:10.1128/iai.70.1.412-415.2002

Tai, S. S., Yu, C., and Lee, J. K. (2003). A solute binding protein of *Streptococcus pneumoniae* iron transport. *FEMS Microbiol Lett, 220*(2), 303-308. doi:10.1016/S0378-1097(03)00135-6

Takaya, A., Tomoyasu, T., Matsui, H., and Yamamoto, T. (2004). The DnaK/DnaJ chaperone machinery of *Salmonella enterica* serovar Typhimurium is essential for invasion of epithelial cells and survival within macrophages, leading to systemic infection. *Infect Immun, 72*(3), 1364-1373. doi:10.1128/iai.72.3.1364-1373.2004

Tanaka, K. J., Song, S., Mason, K., and Pinkett, H. W. (2018). Selective substrate uptake: The role of ATP-binding cassette (ABC) importers in pathogenesis. *Biochim Biophys Acta Biomembr, 1860*(4), 868-877. doi:10.1016/j.bbamem.2017.08.011

Tavares, G. C., Carvalho, A. F., Pereira, F. L., Rezende, C. P., Azevedo, V. A. C., Leal, C. A. G., and Figueiredo, H. C. P. (2018). Transcriptome and Proteome of Fish-Pathogenic *Streptococcus agalactiae* Are Modulated by Temperature. *Front Microbiol, 9*, 2639. doi:10.3389/fmicb.2018.02639

Terra, V. S., Homer, K. A., Rao, S. G., Andrew, P. W., and Yesilkaya, H. (2010). Characterization of novel beta-galactosidase activity that contributes to glycoprotein degradation and virulence in *Streptococcus pneumoniae*. *Infect Immun, 78*(1), 348-357. doi:10.1128/IAI.00721-09

Tettelin, H., Nelson, K. E., Paulsen, I. T., Eisen, J. A., Read, T. D., Peterson, S., Heidelberg, J., DeBoy, R. T., Haft, D. H., Dodson, R. J., Durkin, A. S., Gwinn, M., Kolonay, J. F., Nelson, W. C., Peterson, J. D., Umayam, L. A., White, O., Salzberg, S. L., Lewis, M. R., Radune, D., Holtzapple, E., Khouri, H., Wolf, A. M., Utterback, T. R., Hansen, C. L., McDonald, L. A., Feldblyum, T. V., Angiuoli, S., Dickinson, T., Hickey, E. K., Holt, I. E., Loftus, B. J., Yang, F., Smith, H. O., Venter, J. C., Dougherty, B. A., Morrison, D. A., Hollingshead, S. K., and Fraser, C. M. (2001). Complete genome sequence of a virulent isolate of *Streptococcus pneumoniae*. *Science, 293*(5529), 498-506. doi:10.1126/science.1061217

Tin Tin Htar, M., Christopoulou, D., and Schmitt, H. J. (2015). Pneumococcal serotype evolution in Western Europe. *BMC Infect Dis, 15*, 419. doi:10.1186/s12879-015-1147-x

Tong, H. H., Li, D., Chen, S., Long, J. P., and DeMaria, T. F. (2005). Immunization with recombinant *Streptococcus pneumoniae* neuraminidase NanA protects chinchillas against nasopharyngeal colonization. *Infect Immun, 73*(11), 7775-7778. doi:10.1128/IAI.73.11.7775-7778.2005

Trappetti, C., Kadioglu, A., Carter, M., Hayre, J., Iannelli, F., Pozzi, G., Andrew, P. W., and Oggioni, M. R. (2009). Sialic acid: a preventable signal for pneumococcal biofilm formation, colonization, and invasion of the host. *J Infect Dis, 199*(10), 1497-1505. doi:10.1086/598483

Tsai, C. J., Loh, J. M., and Proft, T. (2016). *Galleria mellonella* infection models for the study of bacterial diseases and for antimicrobial drug testing. *Virulence, 7*(3), 214-229. doi:10.1080/21505594.2015.1135289

Tsai, M. J., Wang, J. R., Yang, C. D., Kao, K. C., Huang, W. L., Huang, H. Y., Tseng, C. P., Huang, H. D., and Ho, S. Y. (2018). PredCRP: predicting and analysing the regulatory roles of CRP from its binding sites in *Escherichia coli*. *Sci Rep, 8*(1), 951. doi:10.1038/s41598-017-18648-5

Usuf, E., Bottomley, C., Adegbola, R. A., and Hall, A. (2014). Pneumococcal carriage in sub-Saharan Africa--a systematic review. *PLoS One, 9*(1), e85001. doi:10.1371/journal.pone.0085001

Voss, S., Hallstrom, T., Saleh, M., Burchhardt, G., Pribyl, T., Singh, B., Riesbeck, K., Zipfel, P. F., and Hammerschmidt, S. (2013). The choline-binding protein PspC of *Streptococcus*

pneumoniae interacts with the C-terminal heparin-binding domain of vitronectin. *J Biol Chem, 288*(22), 15614-15627. doi:10.1074/jbc.M112.443507

Walker, M. C., and van der Donk, W. A. (2016). The many roles of glutamate in metabolism. *J Ind Microbiol Biotechnol, 43*(2-3), 419-430. doi:10.1007/s10295-015-1665-y

Wang, C. Y., Patel, N., Wholey, W. Y., and Dawid, S. (2018). ABC transporter content diversity in *Streptococcus pneumoniae* impacts competence regulation and bacteriocin production. *Proc Natl Acad Sci U S A, 115*(25), E5776-E5785. doi:10.1073/pnas.1804668115

Weinberger, D. M., Harboe, Z. B., Viboud, C., Krause, T. G., Miller, M., Molbak, K., and Konradsen, H. B. (2014). Pneumococcal disease seasonality: incidence, severity and the role of influenza activity. *Eur Respir J, 43*(3), 833-841. doi:10.1183/09031936.00056813

Weiser, J. N., Ferreira, D. M., and Paton, J. C. (2018). *Streptococcus pneumoniae*: transmission, colonization and invasion. *Nat Rev Microbiol, 16*(6), 355-367. doi:10.1038/s41579-018-0001-8

White-Ziegler, C. A., Angus Hill, M. L., Braaten, B. A., van der Woude, M. W., and Low, D. A. (1998). Thermoregulation of *Escherichia coli* pap transcription: H-NS is a temperature-dependent DNA methylation blocking factor. *Mol Microbiol, 28*(6), 1121-1137. doi:10.1046/j.1365-2958.1998.00872.x

Winardhi, R. S., Yan, J., and Kenney, L. J. (2015). H-NS Regulates Gene Expression and Compacts the Nucleoid: Insights from Single-Molecule Experiments. *Biophys J, 109*(7), 1321-1329. doi:10.1016/j.bpj.2015.08.016

Worsham, P. L., and Konisky, J. (1984). Effect of growth temperature on the acquisition of iron by *Salmonella typhimurium* and *Escherichia coli*. *J Bacteriol, 158*(1), 163-168.

Wosten, M. M., van Dijk, L., Veenendaal, A. K., de Zoete, M. R., Bleumink-Pluijm, N. M., and van Putten, J. P. (2010). Temperature-dependent FlgM/FliA complex formation regulates *Campylobacter jejuni* flagella length. *Mol Microbiol, 75*(6), 1577-1591. doi:10.1111/j.1365-2958.2010.07079.x

Wren, J. T., Blevins, L. K., Pang, B., Basu Roy, A., Oliver, M. B., Reimche, J. L., Wozniak, J. E., Alexander-Miller, M. A., and Swords, W. E. (2017). Pneumococcal Neuraminidase A (NanA) Promotes Biofilm Formation and Synergizes with Influenza A Virus in Nasal Colonization and Middle Ear Infection. *Infect Immun, 85*(4). doi:10.1128/IAI.01044-16

Wu, C., Ayala, E. A., Downey, J. S., Merritt, J., Goodman, S. D., and Qi, F. (2010). Regulation of ciaXRH operon expression and identification of the CiaR regulon in *Streptococcus mutans*. *J Bacteriol, 192*(18), 4669-4679. doi:10.1128/JB.00556-10

Wu, K., Xu, H., Zheng, Y., Wang, L., Zhang, X., and Yin, Y. (2016). CpsR, a GntR family regulator, transcriptionally regulates capsular polysaccharide biosynthesis and governs bacterial virulence in *Streptococcus pneumoniae*. *Sci Rep, 6*, 29255. doi:10.1038/srep29255

Yang, D. C., Blair, K. M., and Salama, N. R. (2016). Staying in Shape: the Impact of Cell Shape on Bacterial Survival in Diverse Environments. *Microbiol Mol Biol Rev, 80*(1), 187-203. doi:10.1128/MMBR.00031-15

Yang, S. C., Lin, C. H., Sung, C. T., and Fang, J. Y. (2014). Corrigendum: Antibacterial activities of bacteriocins: application in foods and pharmaceuticals. *Front Microbiol, 5*, 683. doi:10.3389/fmicb.2014.00683

Yesilkaya, H., Andisi, V. F., Andrew, P. W., and Bijlsma, J. J. (2013). *Streptococcus pneumoniae* and reactive oxygen species: an unusual approach to living with radicals. *Trends Microbiol, 21*(4), 187-195. doi:10.1016/j.tim.2013.01.004

Yesilkaya, H., Kadioglu, A., Gingles, N., Alexander, J. E., Mitchell, T. J., and Andrew, P. W. (2000). Role of manganese-containing superoxide dismutase in oxidative stress and virulence of *Streptococcus pneumoniae*. *Infect Immun, 68*(5), 2819-2826. doi:10.1128/iai.68.5.2819-2826.2000

Yesilkaya, H., Spissu, F., Carvalho, S. M., Terra, V. S., Homer, K. A., Benisty, R., Porat, N., Neves, A. R., and Andrew, P. W. (2009). Pyruvate formate lyase is required for pneumococcal

fermentative metabolism and virulence. *Infect Immun, 77*(12), 5418-5427. doi:10.1128/IAI.00178-09

Yildirim, I., Hanage, W. P., Lipsitch, M., Shea, K. M., Stevenson, A., Finkelstein, J., Huang, S. S., Lee, G. M., Kleinman, K., and Pelton, S. I. (2010). Serotype specific invasive capacity and persistent reduction in invasive pneumococcal disease. *Vaccine, 29*(2), 283-288. doi:10.1016/j.vaccine.2010.10.032

Yu, J., Bryant, A. P., Marra, A., Lonetto, M. A., Ingraham, K. A., Chalker, A. F., Holmes, D. J., Holden, D., Rosenberg, M., and McDevitt, D. (2001). Characterization of the *Streptococcus pneumoniae* NADH oxidase that is required for infection. *Microbiology, 147*(Pt 2), 431-438. doi:10.1099/00221287-147-2-431

Yuste, J., Botto, M., Paton, J. C., Holden, D. W., and Brown, J. S. (2005). Additive inhibition of complement deposition by pneumolysin and PspA facilitates *Streptococcus pneumoniae* septicemia. *J Immunol, 175*(3), 1813-1819. doi:10.4049/jimmunol.175.3.1813

Yuste, J., Sen, A., Truedsson, L., Jonsson, G., Tay, L. S., Hyams, C., Baxendale, H. E., Goldblatt, F., Botto, M., and Brown, J. S. (2008). Impaired opsonization with C3b and phagocytosis of *Streptococcus pneumoniae* in sera from subjects with defects in the classical complement pathway. *Infect Immun, 76*(8), 3761-3770. doi:10.1128/IAI.00291-08

Zambelli, F., Pesole, G., and Pavesi, G. (2013). Motif discovery and transcription factor binding sites before and after the next-generation sequencing era. *Brief Bioinform, 14*(2), 225-237. doi:10.1093/bib/bbs016

Zaritsky, A., Woldringh, C. L., Helmstetter, C. E., and Grover, N. B. (1993). Dimensional rearrangement of *Escherichia coli* B/r cells during a nutritional shift-down. *J Gen Microbiol, 139*(11), 2711-2714. doi:10.1099/00221287-139-11-2711

Zhang, L., Li, Z., Wan, Z., Kilby, A., Kilby, J. M., and Jiang, W. (2015). Humoral immune responses to *Streptococcus pneumoniae* in the setting of HIV-1 infection. *Vaccine, 33*(36), 4430-4436. doi:10.1016/j.vaccine.2015.06.077

Zhang, S., Wilson, F., and Pace, L. (2006). *Streptococcus pneumoniae*-associated cellulitis in a two-month-old Domestic Shorthair kitten. *J Vet Diagn Invest, 18*(2), 221-224. doi:10.1177/104063870601800217

Zhang, X., and Bremer, H. (1995). Control of the *Escherichia coli* rrnB P1 promoter strength by ppGpp. *J Biol Chem, 270*(19), 11181-11189. doi:10.1074/jbc.270.19.11181

Zheng, Y., Zhang, X., Wang, X., Wang, L., Zhang, J., and Yin, Y. (2017). ComE, an Essential Response Regulator, Negatively Regulates the Expression of the Capsular Polysaccharide Locus and Attenuates the Bacterial Virulence in *Streptococcus pneumoniae*. *Front Microbiol, 8*, 277. doi:10.3389/fmicb.2017.00277

Zhi, X., Abdullah, I. T., Gazioglu, O., Manzoor, I., Shafeeq, S., Kuipers, O. P., Hiller, N. L., Andrew, P. W., and Yesilkaya, H. (2018). Rgg-Shp regulators are important for pneumococcal colonization and invasion through their effect on mannose utilization and capsule synthesis. *Sci Rep, 8*(1), 6369. doi:10.1038/s41598-018-24910-1

Zhu, L., and Lau, G. W. (2011). Inhibition of competence development, horizontal gene transfer and virulence in *Streptococcus pneumoniae* by a modified competence stimulating peptide. *PLoS Pathog, 7*(9), e1002241. doi:10.1371/journal.ppat.1002241

Zweig, M., Schork, S., Koerdt, A., Siewering, K., Sternberg, C., Thormann, K., Albers, S. V., Molin, S., and van der Does, C. (2014). Secreted single-stranded DNA is involved in the initial phase of biofilm formation by *Neisseria gonorrhoeae*. *Environ Microbiol, 16*(4), 1040-1052. doi:10.1111/1462-2920.12291